



University of
Stavanger

Faculty of Science and Technology

MASTER'S THESIS

Study program/Specialization: Petroleum Geology	Spring semester, 2017 Open
Author: Alexandra Elisabeth Myhre	 (Writer's signature)
Faculty supervisor: Udo Zimmerman	
External supervisor(s): n/a	
Thesis title: High-resolution heavy mineral stratigraphy of selected Precambrian successions underlying the Nama Group in Namibia	
Credits (ECTS): 30	
Key words: <ul style="list-style-type: none">- Heavy Minerals- SEM-CL-EDS- MLA- XRD- Zircon- Neoproterozoic- Mesoproterozoic- Namibia- Klein Aub Fm- Aubures Fm- Matchless Amphibolite- Numees Diamictite- Holgat Fm- Kuibis Fm- Blaubeker Diamictite- EMPA	Pages: 93 + enclosure: 53 Stavanger, 12.7.2017 Date/year

A.E. Myhre

**High-resolution heavy mineral stratigraphy of selected Precambrian successions
underlying the Nama Group in Namibia**

Copyright

by

Alexandra Elisabeth Myhre

2017

Acknowledgement

Primarily I want to thank my supervisor Dr. Udo Zimmermann for this opportunity, as well as your guidance and inspiration. As well as guidance from PhD student Mona Minde, thank you for all your help in the SEM, and Caroline Ruud for assisting preparing samples.

Moreover, Dr. Zimmermann also arranged for a trip to go to TU Bergakademie in Freiberg, Germany. At TU Bergakademie Sabine Haser deserves a huge thanks as she sat by our sides everyday helping with the MLA, and sample preparation for the EMPA analyses. Moreover, Prof. Bernhard Schultz assisted in EMPA analyses and preparing data after our stay.

I would also like to acknowledge everyone at UiS and CSUB who have been a part of my life during this master's degree. A special thanks to Sigrid Øxnevad who I have had great discussions and she has been a great support throughout my time at UIS, as well as André Solvang for exchanging knowledge. Further, Thomas Meldahl Olsen and Sofie Knutdatter Arntzen carried out U-Pb dating at Institute for Mineralogy at the University of Münster, Germany, and I am very grateful for your time doing this.

Lastly, I want to thank you family and friends, especially Kristine Cummins Walløe for always being there for extra encouragement, and my boyfriend Øystein Storaas for his love and support.

Abstract

This project research the provenance of Precambrian formations: Kuibis Formation, Holgat Formation, Numees Formation, Blaubeker Formation, Matchless Amphibolite, Aubures Formation, and Klein Aub Formation from Namibia. The aim is to enhance provenance understanding, as detrital zircons from previously studies on the Ediacaran rocks show zircon ages older than 1.0 Ga; with a basis in high-resolution heavy mineral studies using different techniques; Scanning Electron Microscope, X-Ray Diffraction (XRD), uranium-lead zircon dating (U-Pb), Mineral Liberation Analyzer (MLA), and Electron Microprobe (EMPA).

Results show that the Klein Aub Formation is dominated by magnetite, mica, quartz, and titanites. The Aubures Formation is dominated by magnetite, ulvöspinel, and quartz. The Blaubeker Formation is dominated by quartz, magnetite, carbonates and chamosite. Quartz, mica, rutile, and magnetite dominate the Numees Formation. Quartz, carbonates, and rutile dominate the Holgat Formation. The Kuibis Formation is dominated by quartz, rutile, and apatite. The EMPA results for tourmalines and garnets were plotted in ternary diagrams to evaluate potential source areas, in combination with XRD results that showed evidence of minerals associated with the Pilanesberg Complex in NW South Africa, Northern Kalahari Manganese Field, Irumide belt in Zambia, and Limpopo belt. Moreover, terminal velocity was calculated from the MLA results. The Matchless Amphibolite show evidence from amphiboles, pyroxenes, and garnets of a Fe-Mn-Ca-Al-rich protolith.

This work show the importance of microprobe analysis in combination with MLA, among using other methodologies when U-Pb analysis is insufficient. Lastly, the methodology is relevant in all stages of the hydrocarbon industry; exploration to production; analyzing reservoir characteristics; understanding and predicting reservoir distribution and quality; and geosteering.

Table of Contents

Acknowledgement.....	iii
Abstract.....	iv
Table of Contents	v
List of Figures.....	vii
List of Tables	ix
List of Graphs.....	xi
Often used abbreviations.....	xiii
Introduction.....	1
Previous work.....	1
Sampling.....	2
Geological Setting.....	4
Klein Aub Formation, Sinclair Group.....	6
Klein Aub Formation	8
Aubures Formation	9
Matchless Amphibolite.....	12
Blaubeker Formation	14
Port Nolloth Group.....	16
Numees Formation	17
Holgat Formation	19
Kuibis Subgroup.....	20
Ediacaran fossils.....	23
Methodology	25
Sample preparation	25
Scanning Electron Microscope.....	25
Optical Analysis	29
X-Ray Diffraction	29
Mineral Liberation Analyzer (MLA).....	30
Electron Microprobe Analysis (EMPA)	32
Geochemistry: U-Pb dating.....	33
U-Pb dating of Zircon	35
Heavy Mineral Studies – Single grain.....	38
Results	41
Semi-quantification	41
MLA.....	43
XRD	48
Optical Analysis	50
Geochemistry - Isotope dating.....	52
Klein Aub Formation - Sinclair Group	52
Aubures Formation.....	53
Blaubeker Formation.....	54
Blaubeker Clast	55
Kuibis Formation	56

EMPA	57
Klein Aub Formation	57
Aubures Formation.....	58
Matchless Amphibolite	60
Blaubeker Formation.....	62
Numees Formation	63
Holgat Formation	65
Kuibis Formation	66
Interpretation	67
SEM & MLA.....	67
U-Pb Dating.....	77
XRD	77
EMPA	79
Tourmaline	79
Pyroxene.....	81
Garnet.....	81
Amphibole.....	82
Hydrocarbon industry	83
Conclusions.....	84
Further Work.....	86
References.....	87
Appendix A – Full Semi-Quantification of Heavy Minerals using SEM	94
Appendix B – Full MLA distribution.....	96
Magnetic Fraction.....	96
Apatite Fraction.....	97
Zircon Fraction	99
Appendix C – Particle Density Distribution.....	101
Appendix D – Particle Size Distribution.....	103
Appendix E – U-Pb dating	104
Klein Aub Formation	104
Aubures Formation	112
Blaubeker Formation	120
Blaubeker Clast	124
Kuibis Formation.....	127
Appendix F – EMPA data	130
Holgat Fm.....	144

List of Figures

Figure 1: (top) Google Earth (2017) map of Namibia with outcrop locations on a regional scale, (bottom) Google Earth (2017) map of Namibia with outcrop locations (scale bar=50 km)....	3
Figure 2: Rifting and collision events, top: rifting and subduction under South America, middle: hot pot volcanism, bottom: continent-continent collision due to closing of the ocean (Gresse et al., 2006 adapted from Frimmel et al., 1996).....	4
Figure 3: Regional geology of southern Africa, Garzanti et al. 2014 and references therein	5
Figure 4: Cycles of the Sinclair Group with lithology proposed by Watters 1978.....	6
Figure 5: Map of Proto-Kalahari at 1200 Ma, northern part marked by a passive margin (black line), whereas the rest of the craton is marked by island arcs and active continental margins (green lines) G: Grunehogna Craton, DML: Dronning Maud Land K: Kaapvaal Craton, Moz: northern Mozambique; R: Rehoboth, S: Sinclair, Z: Zimbabwe Craton. Created by Jacobs et al., 2008 and references therein.	7
Figure 6: Regional map with tectonic framework, including outcrop area of Sinclair Supergroup, by Mapani et al. 2014.....	7
Figure 7:Map showing the distribution of the Tsumis Group in the Rehoboth area in Namibia (Becker & Schalk, 2008).....	8
Figure 8: Stratigraphy of Klein Aub Formation, Dikdoorn Member to the right (Becker & Schalk, 2008)	9
Figure 9: Outcrops pictures at sampling site, taken by Dr. Udo Zimmermann (2006)	9
Figure 10: Distribution of Aubures Formation(pink section) (Miller, 2008)	10
Figure 11: Matchless Amphibolite sampling site, taken by Dr. Udo Zimmermann (2006)	12
Figure 12: Matchless Amphibolite within the Damara Orogen (Killick, 2000)	12
Figure 13: Matchless Amphibolite sampling site, taken by Dr. Udo Zimmermann (2006)	13
Figure 14: Evolution of the Kalahari and Congo cratons with the opening and closure of the Khomas Sea and Adamastor Ocean (Stanistreet et al., 1991; Germs, 1995).....	14
Figure 15: Blaubeker Formation sampling site (left) and Blaubeker Formation clast for isotope and heavy minerals (right), taken by Dr. Udo Zimmermann (2006).....	14
Figure 16: Stratigraphy of the Witvlei Group in the Nama Basin, Namibia (Gorjan et al., 2003 after Hegenberger, 1993).....	15

Figure 17: Stratigraphy by Zimmermann et al. 2011, after Germs (1995) and Gresse et al. (2005) of Port Nolloth and Nama Group.....	16
Figure 18: Different interpretations of correlations of tillites between Congo craton and Kalahari craton, Kaufman et al., 1990	17
Figure 19: Numees Formation sampling site, taken by Dr. Udo Zimmermann (2006).....	17
Figure 20: The contact between the Numees (below) and Holgat (above), taken by Dr. Udo Zimmermann (2006)	18
Figure 21: Holgat Formation sampling site, taken by Dr. Udo Zimmermann (2006)	19
Figure 22: Folding found in the Holgat Formation, taken by Dr. Udo Zimmermann (2006)	19
Figure 23: Stratigraphy of the Port Nolloth Group and Nama Group, Praekelt et al., 2008 modified after Gaucher et al., 2005 and Grötzingen et al., 1995	21
Figure 24: Overview of stratigraphy of the Nama Group with depositional environment at Zaris subbasin (left) and Witputz subbasin (right) in the Nama Basin (Grotzinger & Miller, 2008 and citation therein).	22
Figure 25: Cloudina found in Mooifontein Member, Kuibis Subgroup. Scale bar: 100microns (Brain, 2001).....	24
Figure 26: Possible Spriggina ovata (Germs, 1973)	24
Figure 27: Signals detectable in a SEM (after Hjelen, 1986)	25
Figure 28: Signals' depth of investigation in SEM (Hjelen, 1986)	26
Figure 29: Schematic Diagram of a SEM by Hjelen (1986).....	26
Figure 30: Distribution of backscatter electrons with atomic number and voltage (Duncumb & Shields, 1963; Theisen, 1965; Hjelen, 1986).....	27
Figure 31: Schematic illustration of electron beam ionizing an atom, and characteristic x-ray (Theisen, 1965)	28
Figure 32: Zeiss Supra 35-VP FE-SEM-EDS at UIS	29
Figure 33: Bruker D8 Advance eco, at University of Stavanger	30
Figure 34: FEI Quanta 600 F SEM with Bruker XFlash 6130 EDS at Technische Universität Bergakademie Freiberg, Germany	31
Figure 35: (left) Leica EM MED020 Carbon Coater (right) samples in sample holder with tape	32
Figure 36: JEOL microprobe JXA 8900 at Technische Universität Bergakademie Freiberg, Germany.....	33

Figure 37: Processes affecting the geochemical signature for igneous rocks, modified after Rollinson (1993)	34
Figure 38: Processes affecting the geochemical signature for metamorphic rocks, modified after Rollinson (1993)	34
Figure 39: Processes affecting the geochemical signature for sedimentary rocks, modified after Rollinson (1993)	35
Figure 40: Example of Concordia-discordia diagram with $^{206}\text{Pb}/^{238}\text{U}$ vs $^{207}\text{Pb}/^{235}\text{U}$ (Rollinson (1993) after Kröner et al. (1987))	36
Figure 41: (top left) Galena found in the Kuibis Formation, (top right) Rutile needles in quartz in the Kuibis Formation, (mid left) Quartz with rutile, zircon and xenotime found in the Kuibis Formation, (mid right) Apatite grains with monazite and zircons in the Numees Formation, (bottom left) Hastingsite-Mn with quartz and epidote in the Matchless Amphibolite, and (bottom right) iron oxide, potentially mineralized fossil in the Blaubeker Formation.....	45
Figure 42: XRD results of (top left) Klein Aub Formation Magnetic and Apatite Fractions; (top right) Aubures Formation Magnetic and Apatite Fractions; (bottom left) Matchless Amphibolite Magnetic and Apatite Fractions; and (bottom right) Blaubeker Formation Magnetic and Apatite Fractions	48
Figure 43: XRD results of (top left) Holgat Magnetic Fraction; (top right) Numees Formation Magnetic Fraction; (bottom) Kuibis Magnetic and Apatite Fractions.....	49
Figure 44: (1) F-Apatite, Kuibis Formation, (2) Cl-Apatite, Kuibis Formation, (3) Dolomite, Holgat Formation, (4) F-Apatite, Numees Formation, (5) Monazite, Blaubeker Formation, (6) Dolomite, Blaubeker Formation, (7) Zircon, Blaubeker Formation, (8) Zircon, Aubures Formation, (9) 2xF-Apatite, Aubures Formation, (10) F-Apatite, Klein Aub Formation, (11) Amphibole, Matchless, (12) Epidote, Matchless	51
Figure 45: The Hjulstrom Diagram (Nichols, 2012)	76

List of Tables

Table 1: Sample summary	2
Table 2: Comparison of interpretation of the Sinclair Group (Hoal, 1989) AMT: Awasib Mountain Terrain.....	11
Table 3: Stratigraphy of the southern part of the Damara Orogen, after Killick, 2000	13

Table 4: Parent-daughter relationship of uranium and thorium, after Jaffey et al. (1971). U: uranium, Pb: lead, Th: thorium, t: time, Byr: billion years, yr: years.....	36
Table 5: Overview of a selection of minerals with chemical formula, occurrence and other remarks. (1) Deer et al., 1992 (2) Nesse, 2012	38
Table 6: Mineral Distribution of magnetic, apatite, and zircon fractions for all formations from SEM	41
Table 7: Mineral Distribution of magnetic fraction for all formations from MLA	43
Table 8: Mineral Distribution of magnetic fraction for all formations from MLA with a density filter of >2.95	44
Table 9: Mineral Distribution of apatite and zircon fractions for all formations from MLA.....	44
Table 10: Mineral Distribution of apatite and zircon fractions for all formations from MLA with a density filter of 2.7-3.3 g/cm ³ for apatite and >3.37 g/cm ³	44
Table 11: EMPA data for Klein Aub Formation with mean value and standard deviation for each measured grain - Magnetic Fraction. *Boron cannot be measured by this technique, so a standard of 10.5 wt% must be added to the total, given by Prof. Bernhard Schulz at Institut für Mineralogie der TU Freiberg	57
Table 12: EMPA data for Aubures Formationwith mean value and standard deviation for each measured grain - Magnetic Fraction. *Boron cannot be measured by this technique, so a standard of 10.5 wt% must be added to the total, given by Prof. Bernhard Schulz at Institut für Mineralogie der TU Freiberg	58
Table 13: EMPA data for Aubures Formationwith mean value and standard deviation for each measured grain - Zircon Fraction.....	59
Table 14: EMPA data for Matchless Amphibolite with mean value and standard deviation for each measured grain - Magnetic Fraction	60
Table 15: EMPA data for Matchless Amphibolite with mean value and standard deviation for each measured grain - Zircon Fraction.....	61
Table 16: EMPA data for Blaubeker Formationwith mean value and standard deviation for each measured grain - Magnetic Fraction	62
Table 17: EMPA data for Numees Formationwith mean value and standard deviation for each measured grain - Magnetic Fraction	63

Table 18: EMPA data for Holgat Formation with mean value and standard deviation for each measured grain - Magnetic Fraction. *Boron cannot be measured by this technique, so a standard of 10.5 wt% must be added to the total, given by Prof. Bernhard Schulz at Institut für Mineralogie der TU Freiberg	65
Table 18: EMPA data for Kuibis Formation with mean value and standard deviation for each measured grain - Magnetic Fraction	66
Table 19: Terminal settling velocity	76

List of Graphs

Graph 1: Grain size distribution from MLA measurements for magnetic fraction of all formations	46
Graph 2: Grain size distribution from MLA measurements for apatite and zircon fractions of all formations	47
Graph 3: Probability Density Plot showing the distribution of zircon ages of the Klein Aub Formation	52
Graph 4: Concordia Plots of Klein Aub Formation	53
Graph 5: Probability Density plot showing the distribution of zircon ages of Aubures Formation	53
Graph 6: Concordia Plots of Aubures Formation	54
Graph 7: Probability Density plot showing the distribution of zircon ages of Blaubeker Formation	54
Graph 8: Concordia Plot of Blaubeker Formation	55
Graph 9: Probability Density plot showing the distribution of zircon ages of Blaubeker Clast	55
Graph 10: Concordia Plots of a clast sampled in the Blaubeker Formation	56
Graph 11: (left) Probability Density plot showing the distribution of zircon ages of Kuibis Formation (right) Concordia Plot of Kuibis Formation	56
Graph 12: Semi-quantification of Magnetic Fraction	68
Graph 13: Semi-quantification of Apatite Fraction	69
Graph 14: Semi-quantification of Zircon Fraction	70
Graph 15: Mineral distribution from MLA measurements for magnetic fraction of all formations, filtered with density requirement > 2.95	71

Graph 16: Mineral distribution from MLA measurements for zircon fraction of all formations, filtered with density requirement > 3.3	72
Graph 17: Mineral distribution from MLA measurements for apatite fraction of all formations, filtered with density requirement >2.95 and < 3.3.....	73
Graph 18: Particle Size Distribution of apatite and zircon fractions for all formations, full spreadsheet can be found in Appendix D	75
Graph 19: Particle Size Distribution of magnetic fractions for all formations, full spreadsheet can be found in Appendix D.....	75
Graph 20: Ternary diagram of tourmalines for Kuibis Formation after Henry & Guidotti (1985)	79
Graph 21: Ternary diagram of tourmalines for Holgat Formation, after Henry & Guidotti (1985)	79
Graph 22: Ternary diagram of tourmalines for Numees Formation after Henry & Guidotti (1985)	80
Graph 23: Ternary diagram of tourmalines for Aubures Formation after Henry & Guidotti (1985)	80
Graph 24: Ternary diagram of tourmalines for Klein Aub Formation after Henry & Guidotti (1985)	81
Graph 25: Ternary diagram of pyroxenes from Matchless Amphibolite, plotting after Marshall (1996) and composition names according to Morimoto (1989)	81
Graph 26: Ternary diagram of garnet from the Numees Formation, plotting after plotting after Marshall (1996) and endmembers after Morton et al. (2004).....	82
Graph 27: Ternary diagram of garnet from the Matchless Amphibolite, plotting after plotting after Marshall (1996) and endmembers after Morton et al. (2004).....	82

Often used abbreviations		P:	Pressure
Am:	Amphibole	Pl:	Plagioclase
Ap:	Apatite	Px:	Pyroxene
Aub:	Aubures Formation	Pb:	Lead
BBCL:	Blaubeker Formation	Qtz:	Quartz
Chr:	Chromite	Rt:	Rutile
En:	Enstatite	SEM:	Scanning Electron Microscope
Ep:	Epidote	Sin:	Sinclair Group
EMPA:	Electron Microprobe Analysis	Spl:	Spinel
Fsp:	Feldspar	T:	Temperature
FeO:	Iron oxide	Ttn:	Titanite
Fm:	Formation	Tur:	Tourmaline
Ga:	Billion years ago	U:	Uranium
Grt:	Garnet	UiS:	University of Stavanger
Gp:	Group	Usp:	Ulvospinel
Grs:	Grossular	XRD:	X-Ray Diffraction
HC:	Hydrocarbon	Xtm:	Xenotime
Hs:	Hastingsite	Zrn:	Zirc
Hbl:	Hornblende		
Hol:	Holgat Formation		
Ilm:	Ilmenite		
Krs:	Kaersutite		
Kui:	Kuibis Formation		
Ma:	Million years ago		
MLA:	Mineral Liberation Analysis		
Mn:	Manganese		
Mnz:	Monazite		
Ms:	Muscovite		
Num:	Numees Formation		
Or:	Orthoclase		

Introduction

Understanding the Precambrian Earth has fascinated scientists for decades. However, few rock exposures and limited research material exist to enhance this understanding. By determining provenance of these old rocks, more information about the Early Earth can be analyzed. Therefore, this project will include a provenance study of different rock formations in Namibia; i.e. the Kuibis Subgroup (sandstone), Numees Formation (diamictite), Holgat Formation (sandstone), Blaubeker Formation (diamictite), Aubures Formation (sandstone), Klein Aub Formation (sandstone), and Matchless Amphibolite. The main objective of this study is to gain more information about the provenance of these rocks. For example, detrital zircons from previously studies on the Ediacaran rocks (Kuibis Formation, Numees Formation, Holgat Formation, and Blaubeker Formation) show zircon ages older than 1.0 Ga. Moreover, the Klein Aub Formation is part of the Sinclair Group, which is either Neoproterozoic or Mesoproterozoic. There is also some discussion whether the Aubures Formation, which overlies the Klein Aub Formation, is part of the Sinclair Group or not. Lastly, the project involves a discussion on the parent rock of the Matchless Amphibolite. These discussions are based on high-resolution heavy mineral studies carried out for each formation by using different techniques; such as Field Emission Scanning Electron Microscope with Backscattered Electrons, Cathodoluminescence and Energy Quantification of heavy minerals, X-Ray Diffraction, Mineral Liberation Analyzer, and Electron Microprobe.

Previous work

Precambrian research has been studied in detail, although great uncertainties and discussions still exist. For example, scientists cannot agree on the number and magnitude of the glaciations that occurred during the Neoproterozoic. Some suggest at least two glaciations (e.g. Kennedy et al., 2001b; reviewed in Zimmermann et al., 2010), whereas others suggest five (e.g. Eerola, 2001). Even though there is an overall agreement on glacial events during the Neoproterozoic, many debates still exist concerning the evidence of Neoproterozoic glaciations in sedimentary rocks. For example, diamictites are often used as evidence of glacial events, whereas others find such evidence to be insufficient (e.g. Eerola, 2001).

Geological dating of rocks can be done in different ways, using for example biostratigraphy, mineral dating, or lithostratigraphy. Zircon dating indicate Archean to Mesoproterozoic ages for all formations. As a result, zircon dating has not provided sufficient data for dating the formations. Moreover, as these are very old rocks, few fossils are present at

the time or are preserved in the rock record, except for the Kuibis Formation in which *Cloudina* has been found. Therefore, previous work has raised more questions than answers. This project will therefore use different techniques to study the provenance of these different formations.

Sampling

Dr. Udo Zimmermann (University of Stavanger) and his team collected the samples for this project in 2006 in Namibia, figure 1. The following formations will be analyzed in this project: Numees Formation, Holgat Formation, Kuibis Formation, Aubures Formation, Blaubeker Formation, Klein Aub Formation (Sinclair Group), and Matchless Amphibolite.

Geotrack International Pty Ltd has separated these samples into the following four different fractions:

- 1) magnetic fraction ($>2.7\text{ g/cm}^3$),
- 2) non-magnetic apatite fraction ($2.7\text{-}3.3\text{ g/cm}^3$),
- 3) non-magnetic zircon ($>3.37\text{ g/cm}^3$) and
- 4) zircon concentrate.

Table 1: Sample summary

Sample	Formation	Location	Magnetic fraction	Non-magnetic apatite fraction	Non-magnetic zircon	Zircon concentrate	U-Pb dating
08022-13	Numees Formation	S27°35'15.1'' E16°41'27.3''	X	X	X		
08022-12	Holgat Formation	S27°35'15.1'' E16°41'27.3''	X	X			
GS08022-9	Kuibis Formation	S27°35'15.1'' E16°41'27.3''	X	X			X
GS12104-17 AUB	Aubures Formation	S25°16'24.47'' E 16°37'28.63''	X	X	X	X	X
GS12104-18 BBCL	Blaubeker Formation	S23°54'16.8'' E16°28'24.4''	X	X	X	X	X
GS12104-16 SIN	Sinclair Group; Klein Aub Formation; Dikdoorn Member	S23°51'17.39'' E16°31'56.53''	X	X	X	X	X
GS12104-21 MATCH	Matchless Amphibolite	S23°18'19.4'' E15°45'04.4''	X	X	X	X	



Figure 1: (top) Google Earth (2017) map of Namibia with outcrop locations on a regional scale, (bottom) Google Earth (2017) map of Namibia with outcrop locations (scale bar=50 km)

Geological Setting

The Kaapvaal Craton, Zimbabwe Craton, and Limpopo Belt contain most of the Archean rock exposures in southern Africa and are linked, in the west, by the Paleoproterozoic Magondi-Okwa-Kheis Belt and, in the south, by the Mesoproterozoic Namaqua-Natal Belt (figure 3) (Garzanti et al., 2014). The Neoproterozoic section is marked by the Congo Craton in the north, which amalgamates the southern African cratons, and by the Damara-Gariep belt (figure 3) (Garzanti et al., 2014). Lastly, the assemblage of Rodinia caused the Kalahari Craton to stabilize by 1.0 Ga (Jacobs et al., 2008; Garzanti et al., 2014). Rocks found in southern Zambia show evidence of granitoid intrusions and amphibolite-facies metasediments, whereas the volcano-sedimentary rocks of southern Namibia (Sinclair Group) show evidence of mild to low-grade deformation with granitoid intrusions (Becker et al., 2006; Garzanti et al., 2014). The Neoproterozoic successions in Namibia are marked by post-Rodinia rifting and drifting events, which include fluvial to eolian siliciclastic rock exposures (Garzanti et al., 2014).

The late Proterozoic to early Paleozoic successions are characterized by collisional tectonics and subduction zone processes (figure 2) (Gresse et al., 2006). Strontium and carbon isotope studies show evidence of particularly high erosion rates during late Proterozoic to early Cambrian (Kaufman et al., 1993; Derry et al., 1994). This could suggest extensive uplift and erosion of Pan-African belts, such as the Damara-Gariep belt in Namibia (Braiser & Lindsay, 2001). Moreover, the Damara Orogen is marked by Neoproterozoic metasedimentary rocks underlain by basement gneiss dated to 2.0-1.2 Ga, as well as intrusive granitoids dated to 570-460 Ma (Miller, 2008; Garzanti et al., 2014).

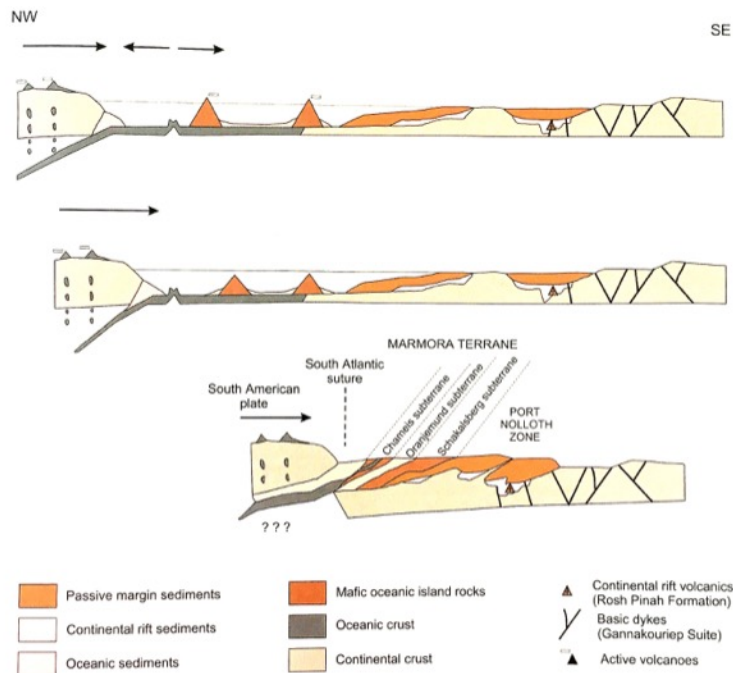


Figure 2: Rifting and collision events, top: rifting and subduction under South America, middle: hot pot volcanism, bottom: continent-continent collision due to closing of the ocean (Gresse et al., 2006 adapted from Frimmel et al., 1996)

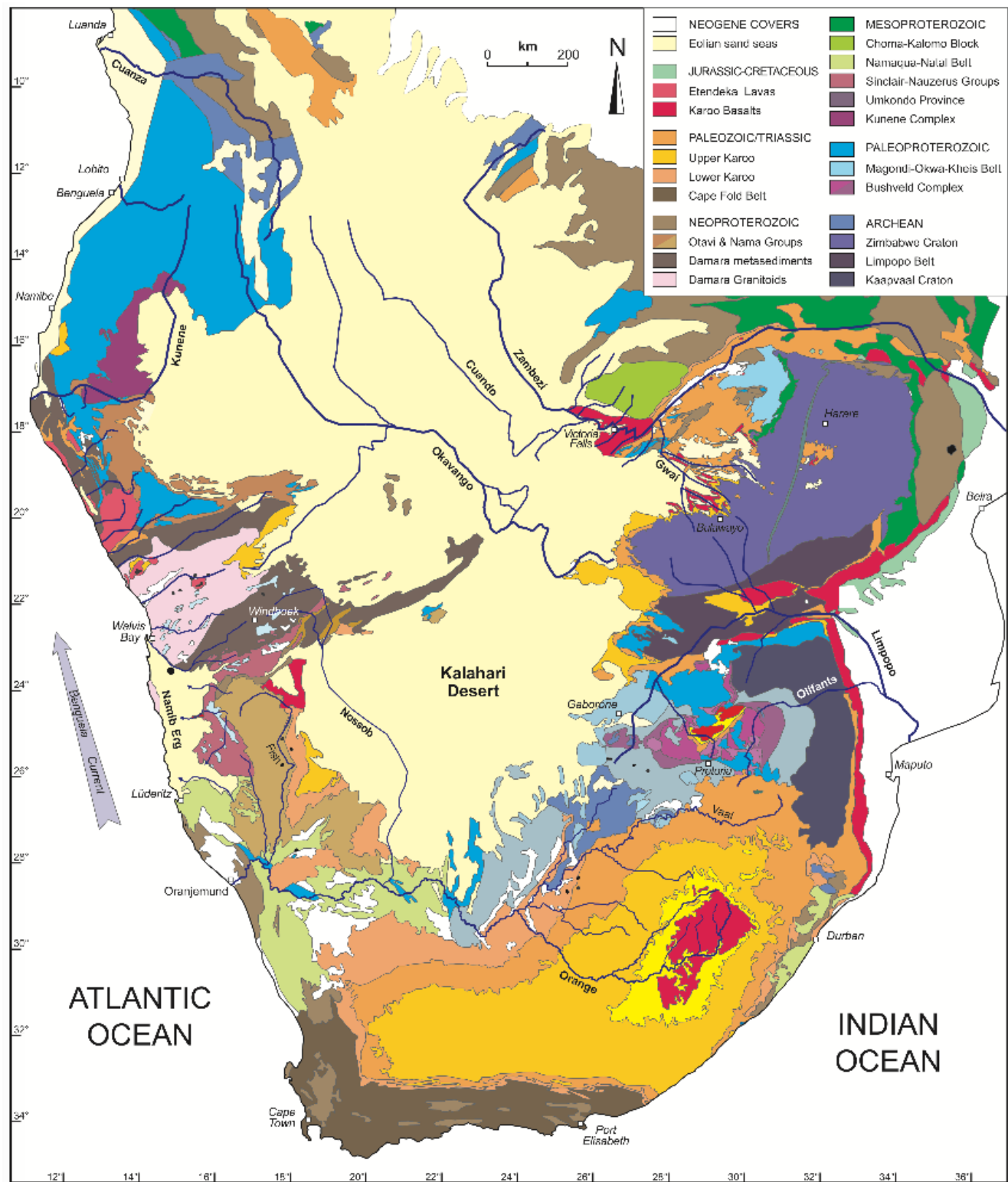


Figure 3: Regional geology of southern Africa, Garzanti et al. 2014 and references therein

Klein Aub Formation, Sinclair Group

The Mesoproterozoic Sinclair Group (ca. 1.4-1.0 Ga, Miller, 2008) was first identified as three main cycles, as seen in figure 4 (Watters, 1978), although four main sequences have been identified later (e.g. Miller, 2008; Jacobs et al., 2008).

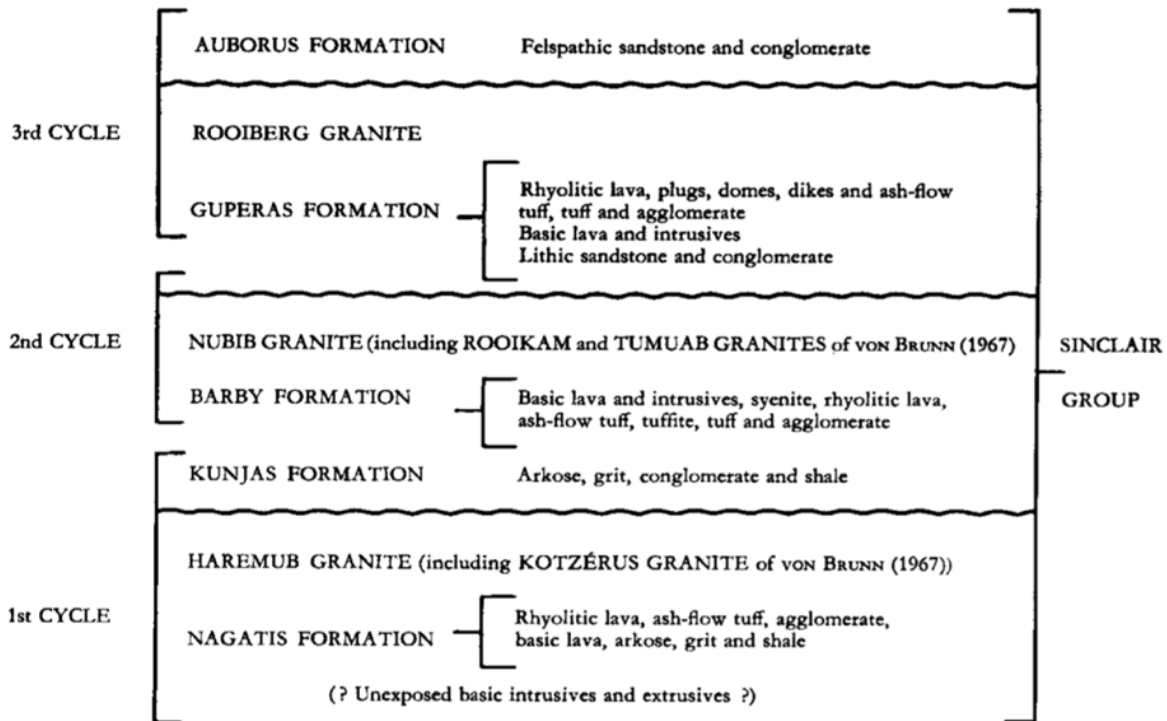


Figure 4: Cycles of the Sinclair Group with lithology proposed by Watters 1978

The Sinclair Group in Namibia is part of low-grade Mesoproterozoic sedimentary and volcanic rocks deposited along the north-west and western margins of the Proto-Kalahari Craton, joined by the Nauzerus Group in Namibia and Kgwebe Formation in Botswana (figure 5,6) (Becker et al., 2006; Jacobs et al., 2008).

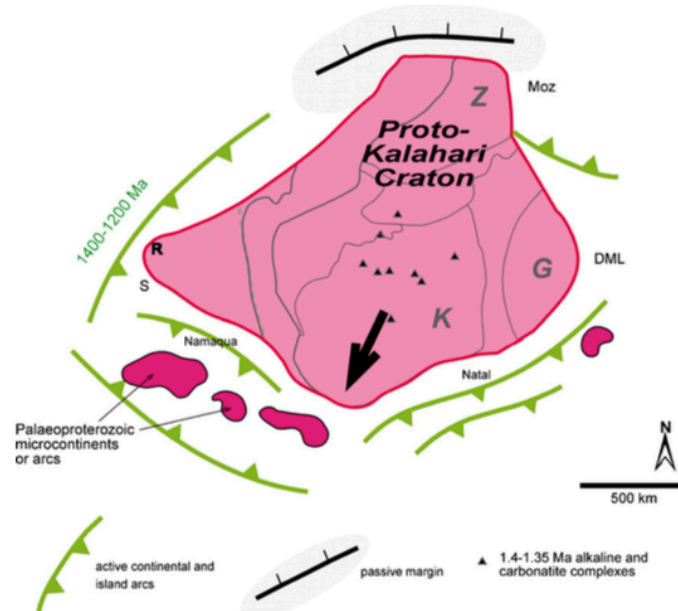


Figure 5: Map of Proto-Kalahari at 1200 Ma, northern part marked by a passive margin (black line), whereas the rest of the craton is marked by island arcs and active continental margins (green lines) G: Grunehogna Craton, DML: Dronning Maud Land K: Kaapvaal Craton, Moz: northern Mozambique; R: Rehoboth, S: Sinclair, Z: Zimbabwe Craton. Created by Jacobs et al., 2008 and references therein.

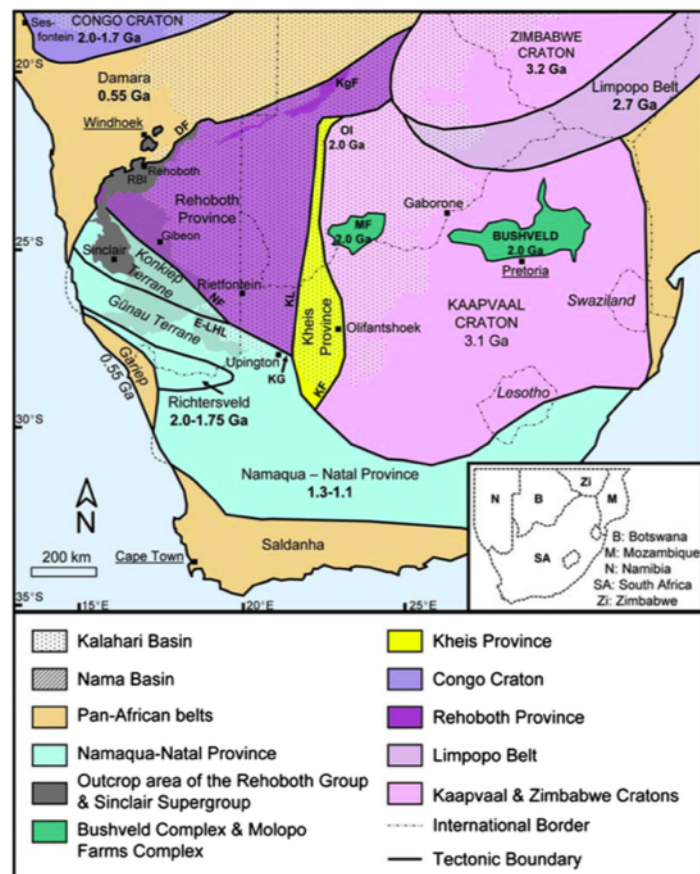


Figure 6: Regional map with tectonic framework, including outcrop area of Sinclair Supergroup, by Mapani et al. 2014

Klein Aub Formation

The Klein Aub Formation is part of the Tsumis Group with the Doornpoort and Eskadron Formation. Deposition is analyzed to be post-uplift with igneous activity in the Rehoboth area (Becker & Schalk, 2008). The study of the Tsumis Group is divided in two: regional mapping (e.g. Handley, 1965; Borg, 1988) and Klein Aub mineralization (e.g. Borg and Maiden, 1987; Borg, 1995). Figure 7 shows a map with the distribution of the Tsumis Group.

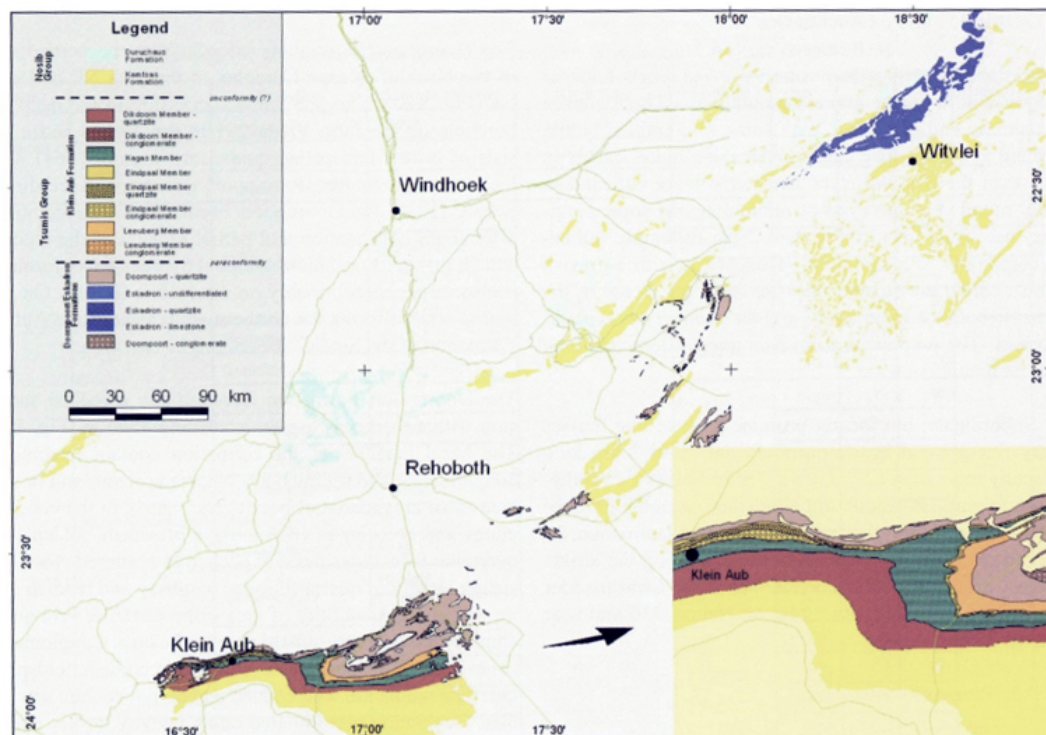


Figure 7: Map showing the distribution of the Tsumis Group in the Rehoboth area in Namibia (Becker & Schalk, 2008)

The Klein Aub Formation outcrops by Kareeboomkolk 424 (east) and continuously between Lepel 339 and Auchas 347 (west) (Becker & Schalk, 2008) (figure 7). The Formation consists only of sedimentary rocks that are weakly deformed, by SE tilting and not folding. The Leeuberg, Eindpaal, Kargas and Dikdoorn Members make up the Klein Aub Formation (Becker & Schalk, 2008), shown in figure 8.

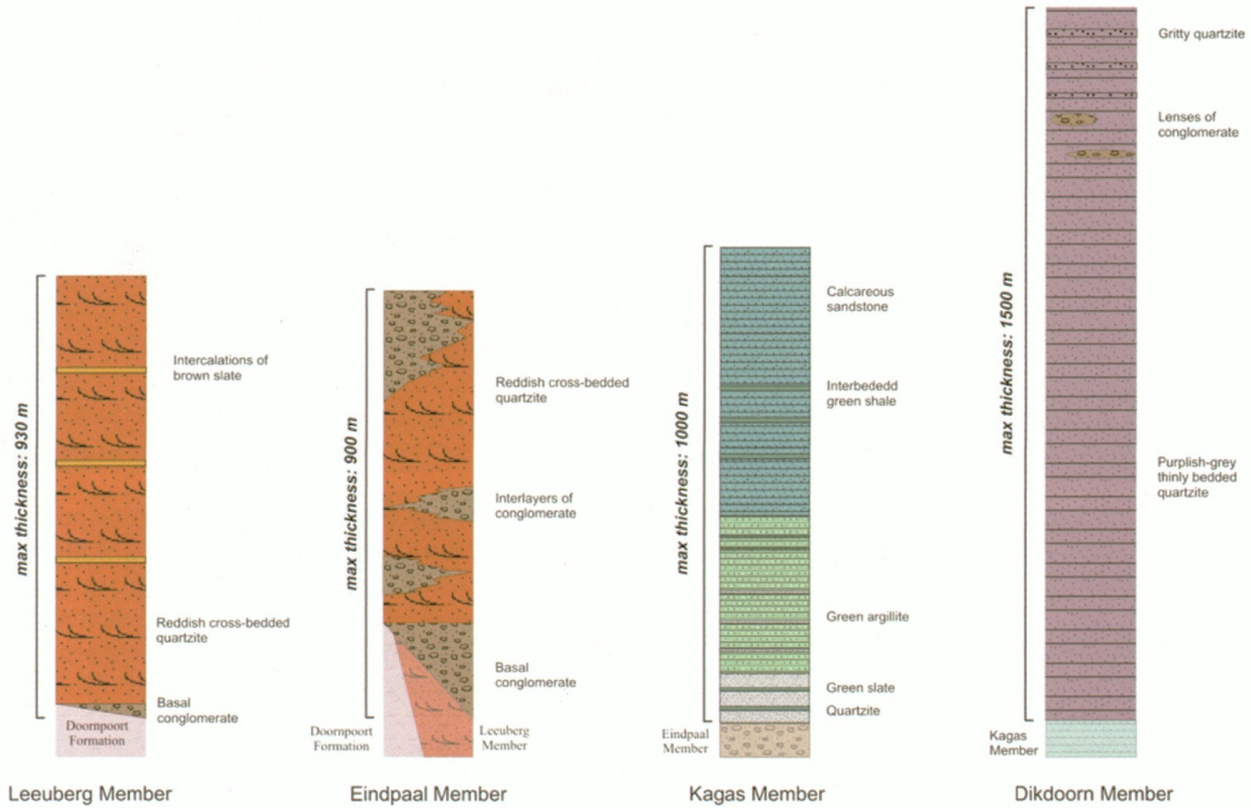


Figure 8: Stratigraphy of Klein Aub Formation, Dikdoorn Member to the right (Becker & Schalk, 2008)
Dikdoorn Member

Fine-grained, purple-gray quartzite make up the Dikdoorn Member, with a maximum thickness of approximately 1500 m, and a south dip (Becker & Schalk, 2008). Generally, the rocks show layering, from finely laminated to well layered.

Aubures Formation



Figure 9: Outcrops pictures at sampling site, taken by Dr. Udo Zimmermann (2006)

The Aubures Formation is made up of redbed successions of shales, sandstones, conglomerates, and granite with a maximum thickness of 2590 m (Miller, 2008). Figure 10 shows the distribution of the Aubures Formation in Namibia, marked by deposition in two

halfgraben basins with an elongated NNW orientations; the Dabis-Naus-Kronenhof-Blutpütz Ost area and Duwisib to Zwartmodder (Miller, 2008).

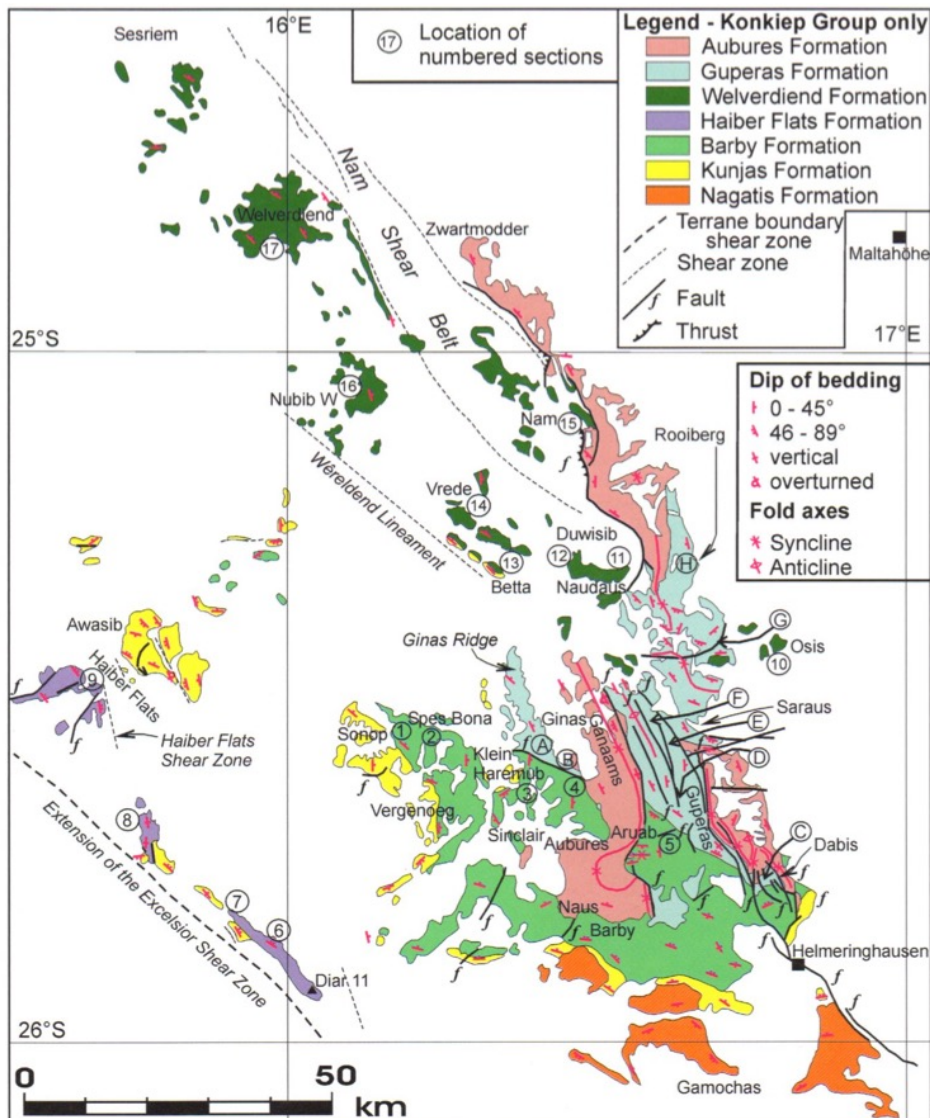


Figure 10: Distribution of Aubures Formation (pink section) (Miller, 2008)

There is a debate whether the Aubures Formation is part of the Sinclair Group or not. For example, Miller (1969; 2008) and Watters (1974) consider the Aubures Formation to represent the uppermost part of the Sinclair Group, whereas Hoal (1989) suggest that the Aubures is post-Sinclair. Hoal (1989) argues evidence for this by the fault dependent NNW orientation, it was deposited post-volcano-sedimentary episodes found in the Sinclair Group, and Kröner (1977) suggest post-Sinclair because of a paleomagnetic age of ~1 Ga. A summary of different interpretation of the age of the Aubures Formation can be seen in table 2 by Hoal (1989).

Table 2: Comparison of interpretation of the Sinclair Group (Hoal, 1989) AMT: Awasib Mountain Terrain

Proposed Evolution of the Sinclair Sequence (Watters, 1974)			Observed Evolution of the Sinclair Sequence (SACS, 1980; this study)			Proposed Evolution of late-stage crust in the AMT(this study)		
3rd cycle	Auborus Formation	<i>sandstone, conglomerate</i>	Post-Sinclair (early Damara?)					
	Rooiberg granite (now Sonntag Granite)		3rd cycle	Sonntag/Gamsberg Granite and dyke swarms		3rd cycle	Chowachasib Granite and dyke swarms	
	Guperas Formation	<i>rhyolitic intrusives and extrusives basic lava and intrusives</i>		Guperas Formation	<i>rhyolitic extrusives basic lava</i>			
2nd cycle	Guperas Formation	<i>sandstone, conglomerate</i>	2nd cycle		<i>sandstone, conglomerate</i>	2nd cycle	Awasib Granite Saffier Intrusive Suite, Haisib Intrusive Suite, Bushman Hill Quartz Diorite.	
	Nubib/Rooikam/Tumuab Granite Spes Bona syenite			Nubib/Rooikam/Haremub Granite Saffier Intrusive Suite	<i>gabbro, norite, monzonite, diorite, syenite</i>		Barby Formation and Haiber Flats Formation	
	Barby Formation	<i>basic lava and intrusives, rhyolitic extrusives</i>		Barby Formation	<i>basic lava and rhyolitic extrusives</i>		Urusib Formation	
1st cycle	Kunjas Formation	<i>arkose, grit shale</i>	1st cycle	Kunjas Formation	<i>arkose, grit shale</i>	1st cycle		
	Haremub/Kotzerus Granite			Tumuab/Kotzerus Granite				
	Nagatis Formation	<i>rhyolitic extrusives and minor basic lava, arkose, grit, shale</i> (?Unexposed basic intrusives and extrusives)		Nagatis Formation	<i>rhyolitic extrusives and minor basic lava arkose, grit, shale</i>			

The base of the Aubures Formation is marked by a <1 m breccia that overlies the Barby or Guperas Formations. The breccia is overlain by conglomerates of a maximum thickness of 1000 m which thins towards the north, further overlain by conglomerate lenses interbedded in feldspathic sandstones. Studies of the conglomerates lenses and the basal conglomerate show similar characteristics, although the lenses are thinner. The sandstone succession fines upwards to shales and siltstones. The total succession of sandstones, shales, and siltstones extends to a thickness of 1250 m in the northern section. Characteristically, of the sandstones are generally well compacted, non-porous, feldspathic with minor quartz and calcite cement. Studies presented by Miller (2008) show a content of 18-26 % feldspar, 3-17 % lithic fragments (felsites and quartzites), 1-10 % hematite, 1-4 % opaque ore, >4.6 % mica, and <1-4.4 % heavy minerals. However, some layers show evidence of mica, opaque, and heavy mineral content up to 9 %. Miller (2008) identifies the depositional environment as “initial rapid fluvial deposition into a shallow, pear-shaped basin under highly oxidizing conditions from various nearby basin-margin sources, but mainly from the south (...).” Moreover, diagenesis includes compaction (porosity loss), minor cement (calcite and silica), and hematite recrystallization.

Matchless Amphibolite



Figure 11: Matchless Amphibolite sampling site, taken by Dr. Udo Zimmermann (2006)

The Matchless Amphibolite Member is represented by two northeast trending intracontinental zones separated by 1-3 km and extending for 350 km, in the late Proterozoic Damara Orogen (figure 12) (Killick, 2000; Miller, 2008).

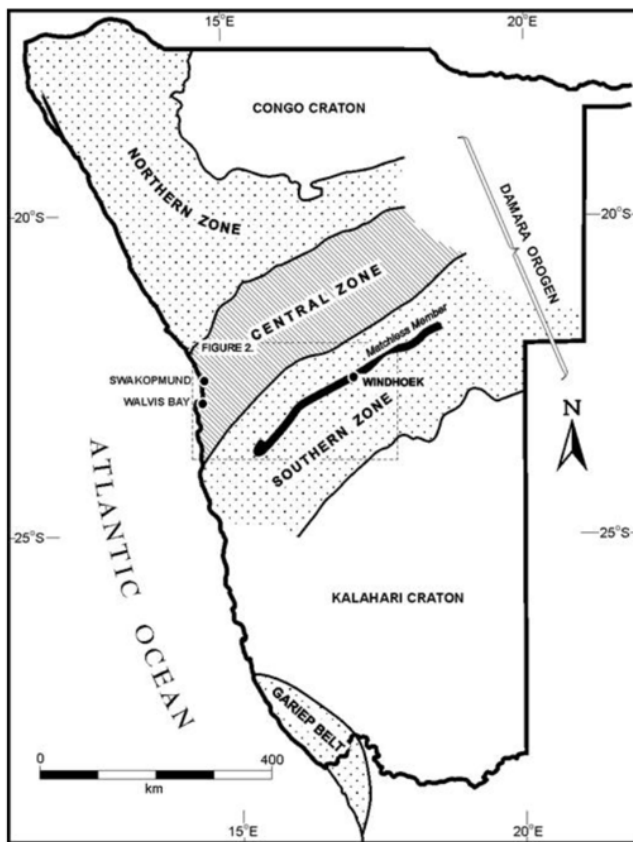


Figure 12: Matchless Amphibolite within the Damara Orogen (Killick, 2000)



Figure 13: Matchless Amphibolite sampling site, taken by Dr. Udo Zimmermann (2006)

The Damara Orogen is divided into Nosib Group underlying the Swakop Group (table 3) (Killick, 2000). The Matchless Amphibolite is part of the lower part of the Kuiseb Formation, characterized by amphibolite, amphibolite schists, and quartz-mica schists (Killick, 2000) in the Southern Zone of the Damara Orogen (Miller, 1979). The rocks consist mostly of hornblende and plagioclase, with minor occurrences of quartz, chlorite epidote, talc, and tremolite-actinolite; as well as accessory minerals, such as carbonate, pyrite, apatite, ilmenite, and rutile (Killick, 2000).

Table 3: Stratigraphy of the southern part of the Damara Orogen, after Killick, 2000

Group	Subgroup	Formation	Lithology
Swakop	Khomas	Kuiseb	Quartz-mica schist with minor intercalations of carbonaceous schist and amphibolite (Matchless Member)
		Auas	Quartzite, schist, dolomite and amphibolite
		Chuos	Mixtite, schist, amphibolite and itabirite
	Kudis		Dolomite, mica schist, carbonaceous schist and quartzite
Nosib			Quartzite, phyllite and conglomerate

The Matchless amphibolite has a minimum age of 765+37 Ma according to Rb/Sr whole-rock by Hawkesworth et al. (1981). Martin (1965) identified a volcanic origin, which was further analyzed by Sawyer (1981) and Miller (1983), who presented preserved textural evidence suggesting that pillow lava and gabbroic intrusions were the parent rocks of the Matchless amphibolite. Moreover, studies done by Breitkopf (1989) suggest plume-type MORB. The amphibolite is therefore a mid-ocean ridge of the sea between the Congo Craton and the Kalahari Craton; the Khomas Sea (Miller, 2008) (figure 14).

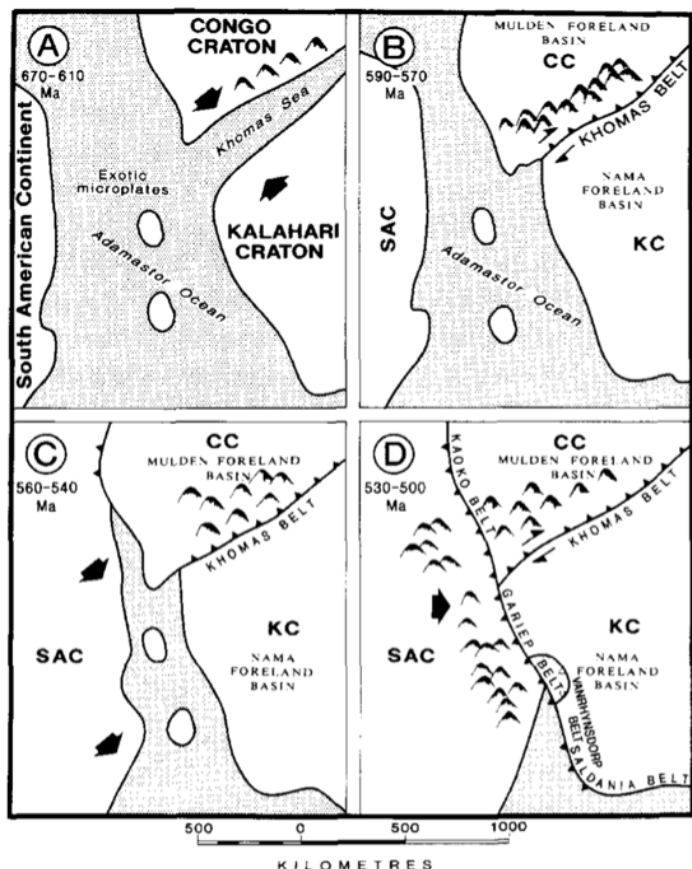


Figure 14: Evolution of the Kalahari and Congo cratons with the opening and closure of the Khomas Sea and Adamastor Ocean (Stanistreet et al., 1991; Germs, 1995)

Blaubeker Formation



Figure 15: Blaubeker Formation sampling site (left) and Blaubeker Formation clast for isotope and heavy minerals (right), taken by Dr. Udo Zimmermann (2006)

The Blaubeker Formation is considered to be the oldest Neoproterozoic glacial deposit in the Nama Basin, which has been interpreted to stem from Sturtian glaciation (Hegenberger, 1993; Gorjan et al., 2003). Overlying the Blaubeker Formation is the post-glacial carbonate-rich Gobabis Member of the Court Formation (figure 16) (Gorjan et al., 2003). The Court Formation was first included in the Nosib Group, but was later reclassified as the base of the Witvlei Group by Hoffnan (1989b) (Miller, 2008). Due to the presence of diamictite with heterolithic boulders, Hoffman (1989b) and Hegenberger (1993) interpreted the Blaubeker Formation to be of glacial origin and has been correlated to the Chous Formation (Miller, 2008). The Blaubeker Formation outcrops in the Nina area, located south west of Witvlei, close to the Naukluft Nappe Complex on the northern Kalahari Craton (Gorjan et al., 2003; Miller, 2008).

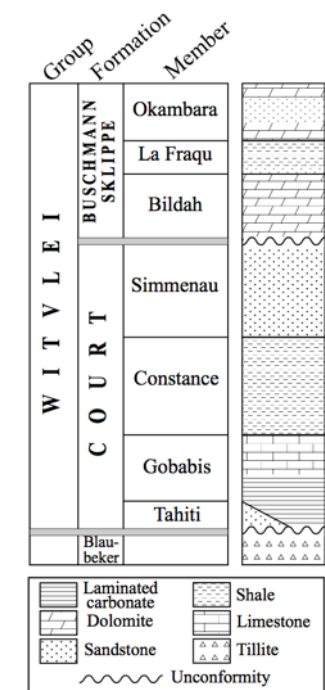


Figure 16:
Stratigraphy of the
Witvlei Group in the
Nama Basin, Namibia
(Gorjan et al., 2003)

after Hegenberger, 1993)

Port Nolloth Group

The Port Nolloth Group consists of the following formations: Lekkersing Formation, Vredefontein Formation, Kaigas Formation, Rosh Pinah Formation, Dabie River Formation, Numees Formation, and Holgat Formation (figure 17). Two diamictite units have been identified; Kaigas Formation and Numees Formation.

age	Port Nolloth Zone			at Witputs
< 555 Ma	Nama Group Port Nolloth Group	Kuibis Subgroup	Dabis Formation <i>Kanis Member</i>	quartzites
< 570 Ma		Holgat Formation	Sanddrif Member Holgat Formation	metagreywackes metacarbonate quartzites
		Bloeddrif Member		carbonates
741-754 Ma		Numees Formation <i>Jakkelsberg Member</i>		diamictite
		Dabie River Formation		Felsic pelites
717+/-11 Ma		Rosh Pinah Fm	Pickelhaube Fm	carbonates
		Wallekraal Fm		rhodochrosite magmatic veins
		Kaigas Formation		diamictite metaromite
771+/-6 Ma		Vredefontein Formation		metarhomictic rocks quartzite
		Lekkersing Formation	Gomondwana Suite	metavolcanic metasedimentary rocks quartzite metavolcanic metasedimentary rocks
	NAMAQUA BASEMENT			NAMAQUA BASEMENT

Figure 17: Stratigraphy by Zimmermann et al. 2011, after Germs (1995) and Gresse et al. (2005) of Port Nolloth and Nama Group

The Port Nolloth Group is marked by sedimentary heterogeneous sequences with few volcanic deposits (Frimmel, 2008). Generally, the Stinkfonten Subgroup (Lekkersing Formation and Vredefontein Formation) consists of siliciclastic rocks deposited in a rift graben with two felsic volcanic depositions. The Stinkfonten Subgroup is followed by the Kaigas Formation, the proximal glacial deposition locally found in the Port Nolloth zone. The glacial deposit is followed by the Hilda Subgroup, which consist of carbonate sediments, volcanic rocks, and siliciclastic rocks. Following the Hilda Subgroup, a new glacial event is deposited; the diamictite of the Numees Formation. The cap-carbonate of the Numees Formation is marked by the Bloeddrift Member of the Holgat Formation, which is the uppermost formation of the Port Nolloth Group. Turbiditic metasedimentary rocks of the Bloeddrift Member overlie these carbonates (Frimmel, 2008). However, age constraints are given by Gaucher et al. (2005) using non-biostratigraphic achritarchs in the Holgat Formation, which overlies the Bloeddrift Member. The contact in the specific exposure where the fossils have been found is controversial as some authors assign a concordant contact and interpret the Numees Formation as Late

Ediacaran (Gaucher *et al.* 2005), others interpret as discordant and deny a chronostratigraphic determination (Zimmermann *et al.*, 2010).

The Kaigas and Numees glacial horizons have been correlated to different parts of Southern Africa, although their origin is disputed (Eyvles and Januscak, 2004). For example, the Chuos glacial horizon in the Congo Craton has been correlated to three different glacial horizons found in the Kalahari Craton; as seen in figure 18 by Kaufman *et al.* (1990). Moreover, the Numees Formation has also been correlated to the Gaskiers and Moelv global glaciations (590 and 565 Ma), as well as the Dernburg Formation in the Marmora Terrane, which is of oceanic origin (Frimmel, 2008).

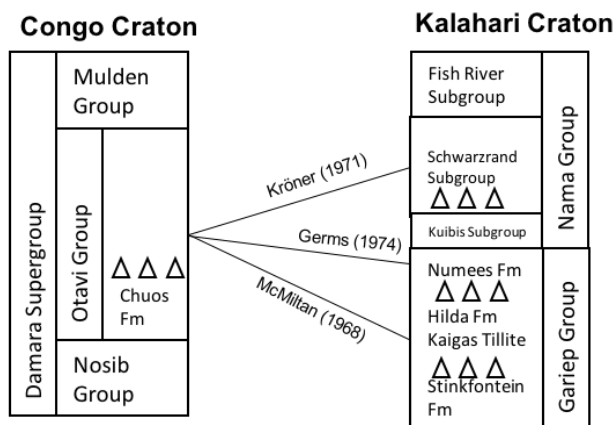


Figure 18: Different interpretations of correlations of tillites between Congo craton and Kalahari craton, Kaufman *et al.*, 1990

Numees Formation



Figure 19: Numees Formation sampling site, taken by Dr. Udo Zimmermann (2006)

The Numees Formation is reported to be of glacial origin, because of well-preserved dropstones (Frimmel, 2008 and citation therein). During the first reports of the Numees, confusion existed regarding the stratigraphic position, as two diamictite zones were found in

some outcrops. The Numees Formation is the younger diamictite in the Gariep Group, where the Kaigas Formation is the older (Frimmel, 2008). Generally, the Numees Formation is locally overlain by the Hilda Subgroup (Kröner, 1974), where the maximum thickness is estimated to be 500 m, which thins out towards the east where it directly onlaps onto the basement (Frimmel, 2008). Furthermore, there is a general trend of fining upwards into a clast and matrix grain size. In South Africa, the Jakkalsberg Member, a ferruginous unit, is found near the base of the Numees Formation. This Member only outcrops in a few sites west of Dreigrathberg, close to the Orange River (Frimmel, 2008). The diamictite is overlain by the cap-carbonates found in the lowermost part of the Holgat Formation, i.e. the Bloeddrift member. The contact between the Numees (below) and Holgat (above) can be seen on figure 20.



Figure 20: The contact between the Numees (below) and Holgat (above), taken by Dr. Udo Zimmermann (2006)

Holgat Formation



Figure 21: Holgat Formation sampling site, taken by Dr. Udo Zimmermann (2006)

The Holgat Formation is part of the Port Nolloth Group, as the youngest formation. The Formation consists mainly of metamorphosed parasequences of arenites, which show a trend of fining upwards, interbedded with argillite and conglomerates. Evidence of turbiditic origin is found in the arenitic beds of the Holgat Formation (Frimmel, 2008). Due to extensive folding and thrusting, determination of thickness is difficult. However, it is suggested that the Holgat Formation is a few hundred meters and thins towards the east to less than 100 m (Frimmel, 2008).



Figure 22: Folding found in the Holgat Formation, taken by Dr. Udo Zimmermann (2006)

The base of Holgat Formation is marked by a finely laminated limestone; the Bloeddrif Member. The thickness of the Bloeddrif Member varies, although it is approximately 100 m in Port Nolloth Zone, but it thins towards the east. The Bloeddrif Member conformably overlays the Numees Formation. Due to this, the Bloeddrif Member is considered to be the cap carbonate over the Numees glacial rocks. Moreover, tube-like structures can be found in the limestone, which some suggest are of microbial origin (Hegenberger, 1993; Hoffman et al., 1998a), and others suggest that these tube-like structures could originate from gas escape as a result of the

warming of permafrost (Kennedy et al, 2001a). Although open to discussion, microbial evidence supported by stromatolites deposits suggest the origin of the tube-like structure (Frimmel, 2008).

Kuibis Subgroup

The Nama Group (figure 23) is divided into Kuibis, Schwarzrand, and Fish River Subgroups of Neoproterozoic to early Paleozoic age (Germs, 1983; Praekely et al., 2008). Moreover, the Kuibis Subgroup clastic sedimentary rocks are mostly quartz-arenitic and gray in color, whereas the Schwarzrand Subgroup has less quartz content and green in color. Both the Kuibis and Schwarzrand Subgroups contain local carbonate deposits. The Fish River Subgroup, however, is locally feldspar rich and red in color, but have no carbonate deposits. The base of the Kuibis Subgroup, the base of Nomtasa Formation (Schwarzrand Subgroup), and the near base of the Fish River Subgroup are representative of major unconformities (Praekely et al., 2008). Local paleovalleys filled with basal conglomerates have been identified, where evidence in the Kuibis quartzite suggest glacial origin (e.g. Schwellnus, 1941; Germs, 1974, 1983; Praekely et al., 2008).

Radiometric dating by Grötzingen et al. (1995) suggest a radiometric age of the upper Kuibis Subgroup to be 548 ± 1 Ma. The upper Kuibis Subgroup is distinct by a volcanic ash bed, which has 545 ± 1 Ma and 543 ± 1 Ma U/Pb single zircon ages (Grötzingen et al., 1995). Furthermore, body fossils, trace fossils, and microfossils are found in the Nama Group (Germs, 1995). Fossils, such as Ediacaran fossils, organic-walled microfossils, trace fossils, and *Cloudina*, are found in the Kuibis Subgroup and lower-middle Schwarzrand Subgroups and suggest a late Neoproterozoic age (Praekely et al., 2008; Grotzinger & Miller, 2008). The upper Nama Group, including the uppermost Schwarzrand and Fish River Subgroups, show evidence of the tracefossils *Trepticnus pedum* and *Diplichnites* and therefore possibly is of Cambrian age (Germs, 1974, 1983; Geyer, 2005; Praekely et al., 2008). Maximum thickness of the Kuibis Subgroup ranges from 225 m in the Witputz subbasin and thickens towards the Zris subbasin with a thickness of 500-600 m. In the Zaris subbasin and Witputs subbasin, thrombolite-stromatolite reefs have developed in the Kuibis Subgroup (Grötzingen, 2000).

B. NAMIBIA			
NAMA GROUP	SCHWARZ-RAND SUBGROUP	Urusis Formation	Nasep Member
		Nudaus Formation	Vingerbreek Member
	KUIBIS SUBGROUP	Zaris Formation	Urikos Member Mooifontein Mb.
		Dabis Formation	Kliphoek Member Mara Member Kanies Member
PORT NOLLOTH GROUP		Holgat Formation	548±1 Ma*
		Bloeddrif Formation	558±28 Ma**
		Numees Formation	
		Dabie River Fm	
		Pickelhaube Formation	

Figure 23: Stratigraphy of the Port Nolloth Group and Nama Group, Praekelt et al., 2008 modified after Gaucher et al., 2005 and Grötzinger et al., 1995

Moreover, a minimum of four depositional sequences have been identified (Grötzinger & Miller, 2008), see figure 24. Grötzinger (2000) identified these sequences and noted that the two lowermost (K1 and K2, figure 24) are present throughout the Nama basin, whereas the two uppermost (K3 and K4, figure 24) are only present in the Zaris subbasin. The Kanies and Kliphoek Members, show evidence of deposition of coarse siliciclastic rocks during a lowstand system. These coarse siliciclastic rocks are overlain by Mara and Mooifontein members (respectively), which are depositions of carbonates deposited during a transgressive system to a highstand system (Grötzinger & Miller, 2008). Moreover, Grötzinger (2000) reported evidence of local erosion between the sequences. Shales deposited in the mid and outer ramp facies indicate an increase in water depth and includes the maximum flooding surface. Further up the succession, the Omkyk Member is marked by a third sequence with depositions of inner ramp grainstones. The fourth sequence is marked by deposition of calcarenites deposited in lagoon, barriers, fore-reef, and patch reef environments, found in the Hoogland Member. Lastly, a fifth sequence (K5, figure 24) is suggested and represents the uppermost of the Kuibis Subgroup with shale deposits (Grötzinger & Miller, 2008).

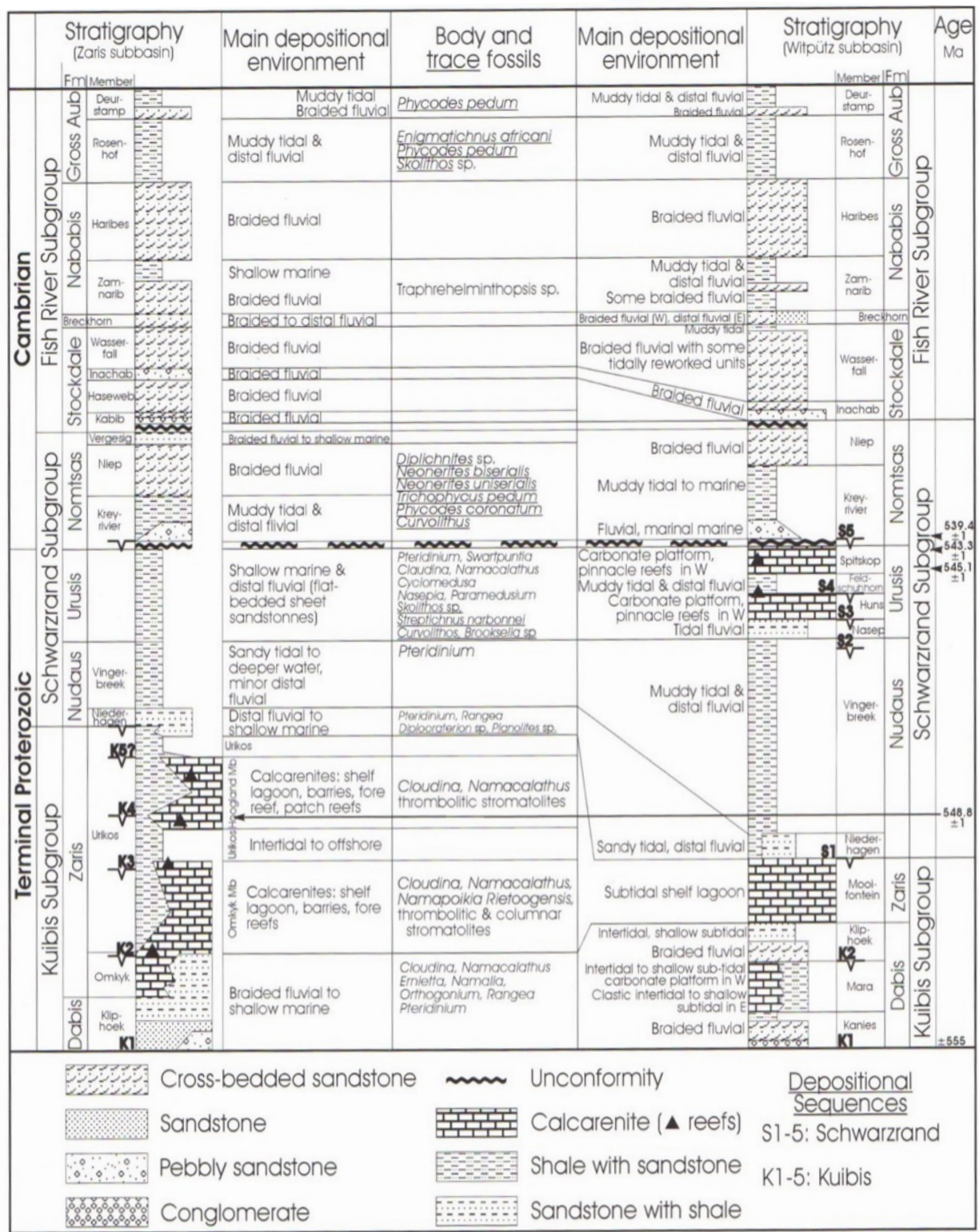


Figure 24: Overview of stratigraphy of the Nama Group with depositional environment at Zaris subbasin (left) and Witputz subbasin (right) in the Nama Basin (Grotzinger & Miller, 2008 and citation therein).

Ediacaran fossils

The origin of life has been subject to great debate (Lowe, 1994; Lazcano, 1994; Doolittle, 1999, to name a few). Initially, it was believed that life emerged at the Precambrian/Cambrian boundary (Margulies & Dolan, 2002). R. C. Sprigg reported in 1947 his findings of well-preserved impressions of soft-body organisms in various shapes and sizes underneath the Cambrian rocks. These fossils are now considered to be the Ediacaran Biota, although Brain (2001) suggests a Naman fauna because German geologists P. Range, H. Schneiderhöhn and H. Von Staff already had identified impressions in Nama quartzites between 1908 and 1914. Moreover, the term Vendobionta was introduced by Seilacher (1989; 1992), which is a group of Ediacaran biotas that are not animals but foliate organisms (Seilacher, 1993; Runnegar, 1993). Nevertheless, these fossils have been found in numerous places around the world, including Siberia, Southern Africa, Canada, Greenland, etc. The emerging of Precambrian life might be due to soft-bodies preserving less frequently than hard parts, where the hard parts occur in the Cambrian (Margulies & Dolan, 2002).

Seilacher (1989) suggested that the Ediacaran biota is an extinct group of animals that had a revolutionary body shape and methods of feeding not found in the Phanerozoic animal life. Moreover, the Ediacaran biota can be separated into two groups described by Runnegar (1994: p. 295): “(1) core members of the Ediacara fauna or Seilacher’s Vendobionta – creatures that are sizable, foliate, and composed of “segments” or “modules” arranged in a serial or fractal fashion (*Charnia*, *Charniodiscus*, *Dickinsonia*, *Ernietta*, *Phyllozoon*, *Pteridinium*, *Rangea*, etc.); and (2) smaller, bilaterally symmetrical forms having anterior-posterior asymmetry (*Marywadea*, *Onega*, *Parvancorina*, *Spriggina*, etc.)”.

Even though most of the Ediacaran biota were soft-bodied, a few exceptions have been found, such as *Cloudina* (Bengston, 1993). Although *Cloudina* has been found in numerous places, it was originally found in the Nama Group (Germs, 1972; Conway Morris et al., 1990; Grant, 1990), and in images of *Cloudina* found in the Mooifontein Member. Kuibis Subgroup can be seen in figure 25 (Brain, 2001). Moreover, the worldwide occurrence suggests that bio-mineralization during the Neoproterozoic was a global phenomenon (Weiguo, 1993). *Cloudina* commonly has a tubular cone-in-cone shell structure, which has been interpreted as dwelling tubes. These tubes were formed by small worm-like suspension feeders (Weiguo, 1993).

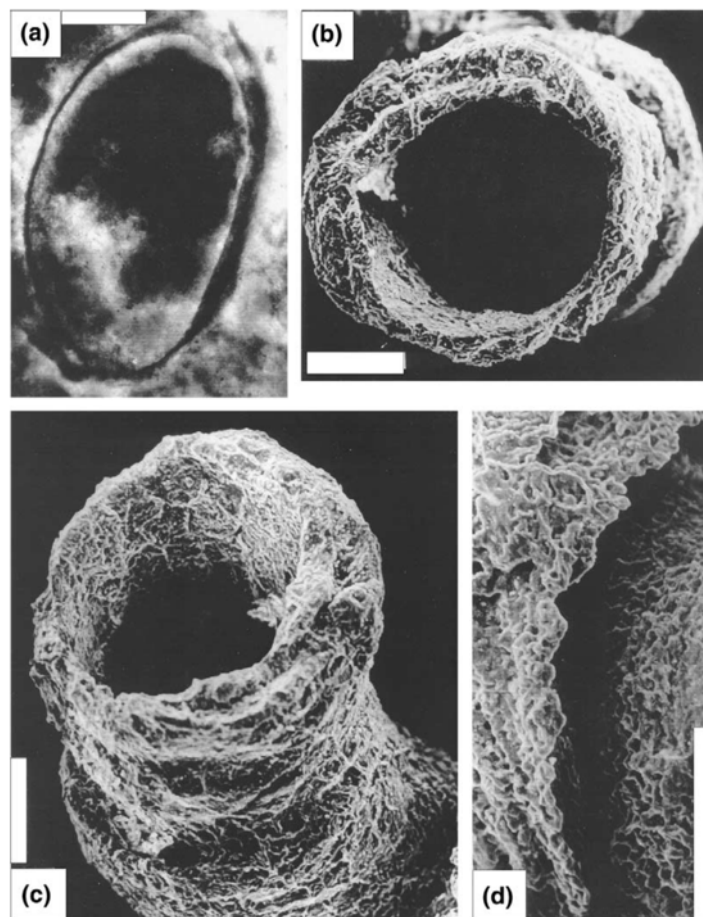


Figure 25: *Cloudina* found in Mooifontein Member, Kuibis Subgroup. Scale bar: 100microns (Brain, 2001)

Another important finding in the Kuibis Subgroup, is the possible discovery of *Spriggina ovata* Worm presented by Germs (1973) (figure 26). This possible discovery supports the relationship between the Ediacara fauna found in Australia and in South West Africa (Germs, 1973).



Figure 26: Possible *Spriggina ovata* (Germs, 1973)

Methodology

Various methods will be used for the high-resolution provenance study, which includes: Field Emission Scanning Electron Microscope with Backscattered Electrons; Cathodoluminescence and Energy Quantification; X-Ray Diffraction; Mineral Liberation Analyzer; and Electron Microprobe. An optical analysis using Scanning Electron Microscope with Secondary Electrons is also included.

Sample preparation

The samples were provided in Frantz Separated fractions and therefore, limited sample preparation was carried out. For all analyses, heavy mineral mounds were prepared by adding a random selection of grains to a tape. Further, a circular mould was placed on the tape. An epoxy resin was prepared from EpoFix Resin and EpoFix Hardener. The resinous glue was added to the mould under vacuum conditions to reduce bubbles. Then the mixture was allowed to dry under vacuum conditions for 2-3 hours and 24 hours at room temperature. Moreover, the mounds were polished using grinding paper, glass plates with powder of 1000 µm, to remove bubbles and create a polished and smooth surface. Lastly, the mounds were polished using Struers Tega Force -5 and Terga Doser -5 with Pan 3 µm and Nap 1 µm cloths for ca. 10 minutes.

Scanning Electron Microscope

A scanning electron microscope (SEM) produces an image by scanning the sample with a focused electron beam. The electrons interact with atoms in the sample and produce multiple signals (figure 27). These signals are detected and provide information about the sample's topography and chemical composition (Hjelen, 1986). The signals detectable in a SEM have different depth of investigation, which therefore must be considered when evaluating which signal to use for a research project (figure 28).

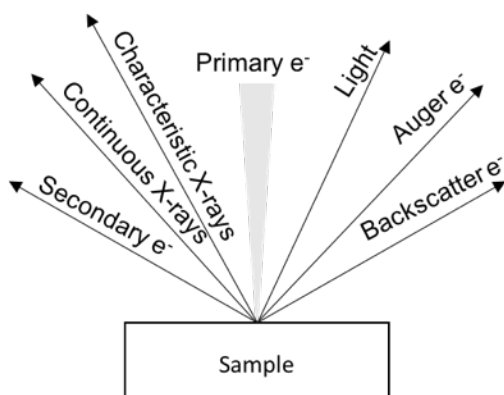


Figure 27: Signals detectable in a SEM (after Hjelen, 1986)

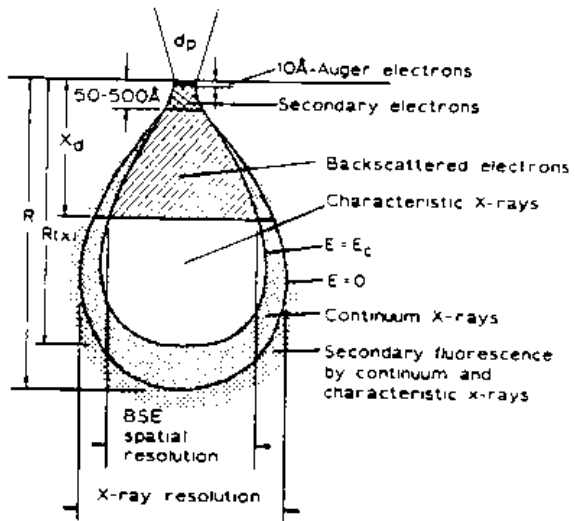


Figure 28: Signals' depth of investigation in SEM (Hjelen, 1986)

Further, a schematic diagram (figure 29) by Hjelen (1986) demonstrates how a SEM operates. A tungsten filament (F) is heated and electrons are produced. Electrons move through a potential difference and through a column with magnetic lenses (L_1 , L_2 , and L_3). These lenses focus the electron beam on the sample surface (S). Between two lenses, a scanning coil (SC) focuses the electron beam so as to scans the sample surface simultaneously with a screen. When the electron beam collides with the sample, secondary electrons are reflected and are collected by the collector (C). The electron current is enhanced by the amplifier and is used to adjust the light in the cathode ray tube (CRT). The SEM is maintained under high vacuum (Hjelen, 1986).

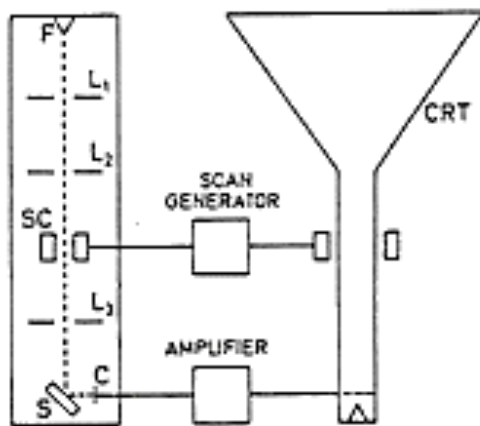


Figure 29: Schematic Diagram of a SEM by Hjelen (1986)

Secondary electrons are formed when electrons of high energy collide with electrons on the sample surface. Secondary electrons produce pictures with high depth of field and resolution in the SEM, and can therefore be a good tool for uneven surfaces. Furthermore, backscatter electrons can be used to visualize differences in atomic number, where a high atomic number

shows a lighter shade of gray, whereas a lower atomic number show a darker shade of gray. This is because heavy elements emit more backscatter electrons than lighter elements. Figure 30 illustrates the relationship between atomic number, voltage, and the distribution of backscatter electrons.

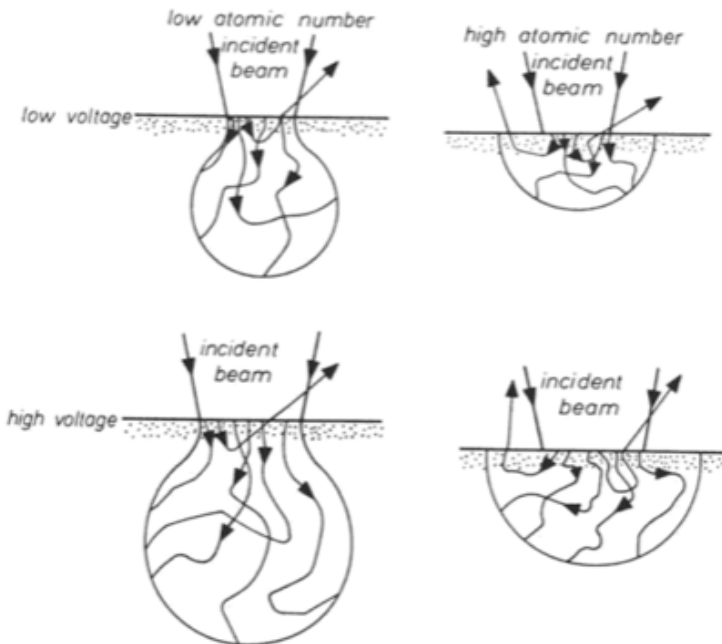


Figure 30: Distribution of backscatter electrons with atomic number and voltage (Duncumb & Shields, 1963; Theisen, 1965; Hjelen, 1986)

X-rays are created when the electron beam hits the sample surface and are created in two ways:

- 1) electrons are slowed down in the electrostatic field around the core and x-rays are created as continuous spectra of wavelengths, known as continuous x-rays; and
- 2) The electron beam ionizes the atoms in the sample and characteristic x-rays are formed, known as characteristic x-rays (figure 31).

For continuous x-ray emission, the intensity of photons increase with increasing atomic number, therefore it can be used to identify which atoms are present in the sample. Moreover, the photons emitted during ionization (also known as Auger electrons) are characteristic of an element. One can therefore achieve a quantitative percentage of elements present in the sample.

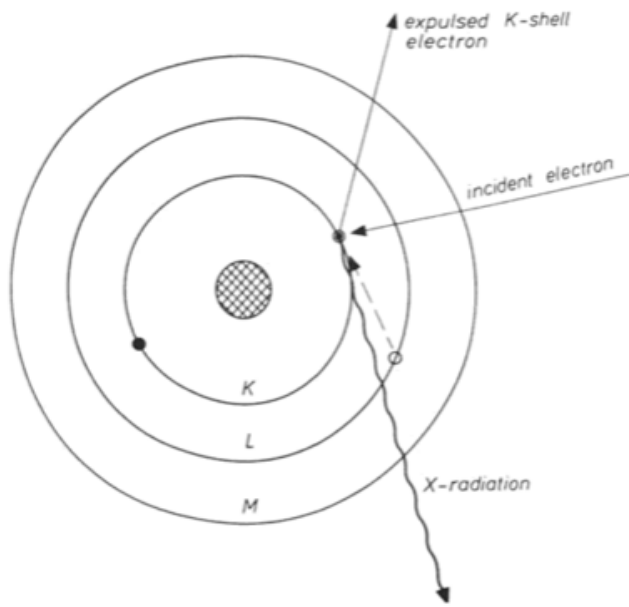


Figure 31: Schematic illustration of electron beam ionizing an atom, and characteristic x-ray (Theisen, 1965)

Cathodoluminescence images can reveal zones that are not visible in other microscopes. These zones can reveal the history recrystallization, e.g. growth of crystals. This is because the cathodoluminescence emission is partly a factor of composition. Cathodoluminescence images can often be used in combination with backscatter electron images, which these show similar features, although cathodoluminescence images often are of higher detail.

The use of a SEM is advantageous in that it allows for easy sample preparation. For single grains, these grains must be placed in an epoxy compound in a mould (or similar), and then be coated with gold, palladium, or copper (for the electric current). Similarly, for other purposes, such as thin sections, the sample surface must be coated.



Figure 32: Zeiss Supra 35-VP FE-SEM-EDS at UIS

For this project, a Zeiss Supra 35-VP FE-SEM-EDS (Field Emission Scanning Electron microscope and Energy Dispersive X-ray Spectroscopy) (figure 32) at the University of Stavanger was used to identify minerals and to perform a semi-quantitative chemical analysis of grains. The SEM was used at a high vacuum, an aperture size of 30 µm, an acceleration voltage of 15-25kV, and a working distance of 10-12mm. For all measurements, the brightness and contrast settings were adjusted for better visual appearance. All other settings were set at default. This was done using Zeiss software. For EDS measurements, EDAX Genesis software was used.

Optical Analysis

For an optical analysis, grains were placed on a carbon tape on slides and coated with palladium. Moreover, these slides were placed into the SEM chamber and surface area was analyzed using secondary electrons, and backscatter electrons were used to verify mineral composition

X-Ray Diffraction

An X-ray Diffractometer (XRD) was used for an X-Ray diffraction analysis. The XRD has three essential parts; an X-ray tube, a sample holder, and an x-ray detector. When using an XRD, X-rays are created when a filament is heated in order to produce electrons, which are further accelerated toward a targeted material so as to bombard the targeted material with. Some

electrons have sufficient energy to dislocate electrons in the inner shell of the targeted material. This will produce a characteristic C-ray spectrum, which is distinctive for a particular material. The X-rays are then recorded in a detector. The signals are further visible on a monitor, and are therefore ready for analysis.

The limitation of the XRD is that it is best suited for homogenous phases, when identifying a particular unknown material. Moreover, the possibility of signal peaks overlying each other may occur and give false interpretations. On the other hand, the strengths of the XRD is that it allows for minimal sample preparation (need powdered samples); it is a rapid technique for mineral identification, and it allows for relatively easy data interpretation (Nesse, 2011).

The XRD used for this project was a Bruker D8 Advance eco (figure 33) for high intensity operation at a voltage of 40kV and a current of 25mA, which is generally used for whole rock analysis. A few samples were powdered using an agate hand mill (Kuibis Formation, Numees Formation, and Holgat Formation), although the samples had too few grains for milling. Moreover, the following parameters were used: 2θ : 4-70°; slit opening: 0.6 mm; time: 0.2sec/step; and increments of 0.01. The Diffrac.Suite.eva software was used for analysis. The analyzing procedure was to first identify the large peaks first, and then to identify the smaller peaks.

Figure 33: Bruker D8 Advance eco, at University of Stavanger



Mineral Liberation Analyzer (MLA)

A Mineral Liberation Analyzer (MLA) is a SEM with an energy dispersive X-ray spectrometer (EDX). Moreover, the MLA is connected to a particular computer software for automatic operations and data acquisition. According to Sylvester (2012) the MLA machine can acquire quantitative data, such as mineralogy, porosity, shape and sizes of grains, textural maps, etc. The MLA uses backscatter electron images to determine location and boundaries of grains. The MLA also uses these images are used by the MLA for characteristic x-ray spectra, which are compared with a standard library spectra for identification. This new technique was first introduced in 1997 by Gu and Napier-Munn (Fandrich et al., 2007).

Advantages of mineralogical identification using the MLA include: automated analysis, reduction of operational bias and human error; analysis of more grains, thereby increasing the

reliability of the statistical model; and ability to distinguish micrometer scale minerals. On the other hand, the MLA may be limited in its ability to distinguish minerals with similar chemical composition, and polymorphs; and there is a lack of reference material (Sylvester, 2012).

The principle of a MLA is the same as for a SEM, although the output data is different; as a mineral library is created. Prior to data collection, a standard library must be created. This is usually done by collecting x-ray spectra of high quality for minerals in the samples. By creating the library from the sample, Fandrich et al. (2007) states that “(...) ensures that measurement conditions are reflected in the standards, such as beam energy (...), and it also provides for an elemental deportment that better reflects the chemistry of the sample”.

For this project, the MLA scans were performed at Technische Universität Bergakademie Freiberg in Germany, using a FEI Quanta 600 F SEM with two Bruker XFlash 6130 EDS (figure 34). Two parallel EDS machines were used to reduce time of measuring. Moreover, the software used for measurements was MLA Measurement 3.1; whereas the software used for x-ray spectra gathering and measurements was a Bruker Esprit, which was imported to MLA Mineral Editor 3.1. which was also set with a standard list Mineral Reference Editor 3.1. The acceleration voltage was 25kV, and the working distance was 12mm.

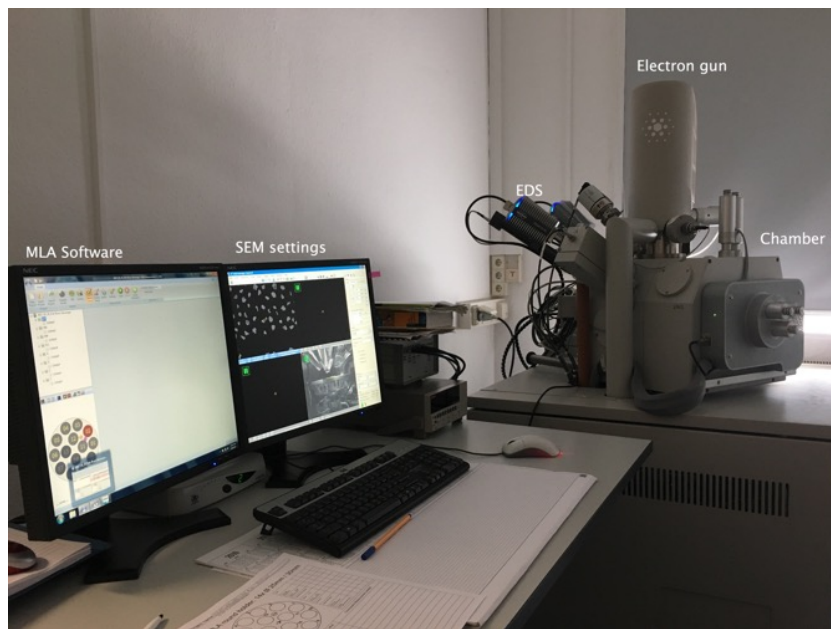


Figure 34: FEI Quanta 600 F SEM with Bruker XFlash 6130 EDS at Technische Universität Bergakademie Freiberg, Germany

The grain mounds were first cleaned and then were coated with carbon using a Leica EM MED020 (figure 35), after which the mounds were placed in a sample holder. Tape was used to prevent overcharging.

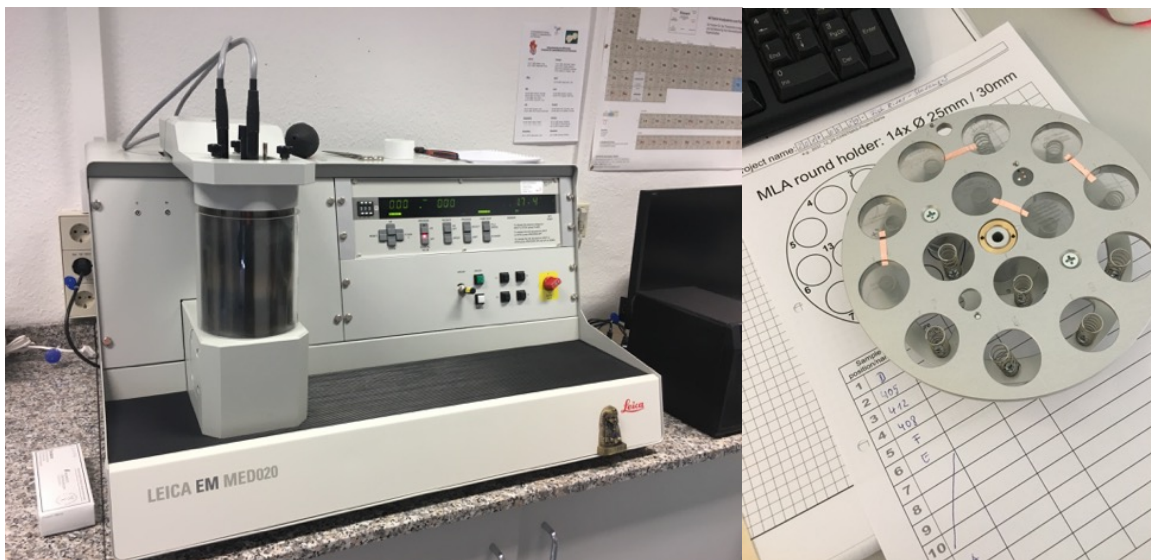


Figure 35: (left) Leica EM MED020 Carbon Coater (right) samples in sample holder with tape

The procedure of the MLA analysis was as follows; first BSE image was created to visualize chemical differences through atomic density. Further, the lower boundary was set to extract the background, in this case 25-30 for the epoxy. Then the machine was set to do an automatic quick scan with the standard list. Following this procedure, all unknown minerals were identified and classified. After the library was completed, the following settings were introduced; acquisition time: 9 ms; voltage: 25 kV; Emission Current: 212 nA; Spot Size: 5.91. The scan was set for high-resolution overnight. The settings also included standard block with quartz, copper, gold, and silver for calibration.

After the high-resolution scan was finished, the last unknown minerals were identified. However, small inclusions in grains could not be resolved and were in some cases scripted to change to host mineral. Another difficulty with the MLA scans was that it was not possible to distinguish between some minerals, for example garnets and epidote. This was further analyzed with a microprobe.

Electron Microprobe Analysis (EMPA)

In principle, an Electron Microprobe Analysis (EMPA) is the same as a SEM, although an EMPA can also perform a chemical analysis. Similar to the SEM, the EMPA includes four essential parts: an electron source; several electromagnetic lenses; a sample chamber; and detectors. The microprobe uses X-rays to identify an element and to measure the concentration of the element. However, as the microprobe in principle is the same as a SEM, other detector signals are also present, such as backscattered electrons, secondary electrons, and cathodoluminescence. These signals can be used to create images, such as those created in the

SEM. These images can be used to aim the electron beam at a targeted material, and also to carry out a chemical analysis of the targeted material/mineral.

The microprobe is limited in its inability to analyze hydrous minerals and to distinguish different oxidation states. Moreover, chemical formulas must often be recalculated as the microprobe reports the elements observed as oxides. Lastly, element overlap may occur and, therefore, one should always be cautious when analyzing the reports generated by the microprobe (Nesse, 2011). On the other side, the use of an electron microprobe is advantageous in that it allows for nondestructive, quantitative chemical analysis, including spot analysis, as well as high quality images.

For this project, all measurements and settings were set by Prof. Bernhard Schultz at TU Freiberg. A JEOL microprobe JXA 8900 was used (figure 36).

Figure
36: JEOL
microprobe JXA
8900 at
Technische
Universität
Bergakademie
Freiberg,
Germany

Geochemistry: U-Pb dating

All rocks have geochemical signatures, which these depend on multiple factors; e.g. tectonic setting, provenance, weathering, fluid movement. The main signatures can be categorized by rock type; igneous, metamorphic, and sedimentary rocks.

Geochemical signatures of igneous rocks are controlled by near-surface processes (e.g. melt outgassing, contact with groundwater); processes in the magma chamber (e.g. fractional crystallization, contamination, magma mixtures, liquids, processes due to open systems); source (e.g. partial melting, source mixture); the composition of the source; and lastly the tectonic setting (Rollinson, 1993). See figure 37 for main processes that control the signatures of igneous rocks.



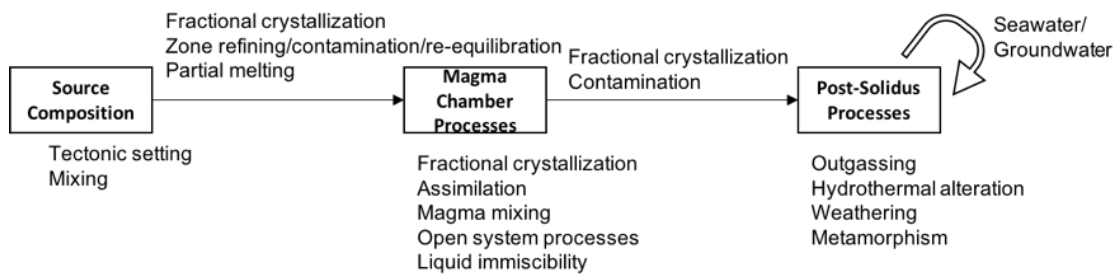


Figure 37: Processes affecting the geochemical signature for igneous rocks, modified after Rollinson (1993)

Moreover, the geochemical signatures of metamorphic rocks are controlled by the protolith, element mobility, fluid movement, and diffusion in solid state (Rollinson, 1993). See figure 38 for main processes that control the signatures of metamorphic rocks.

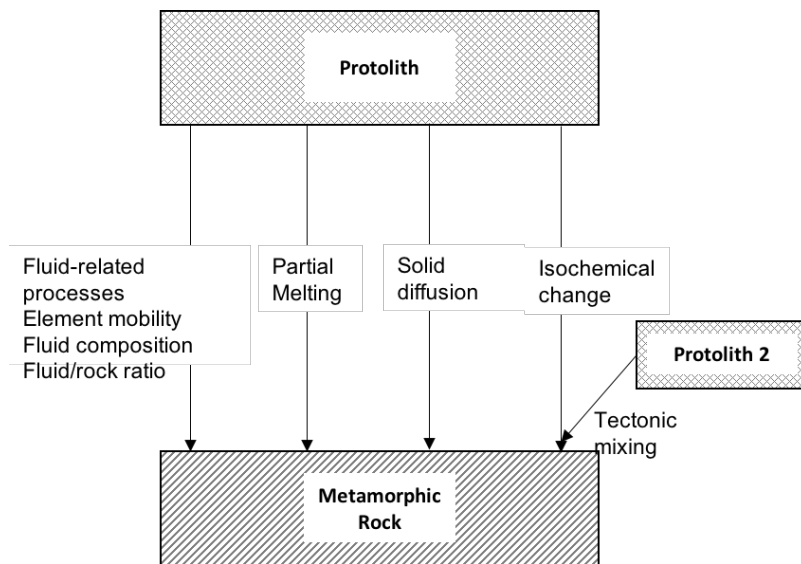


Figure 38: Processes affecting the geochemical signature for metamorphic rocks, modified after Rollinson (1993)

Lastly, the geochemical signatures of sedimentary rocks are controlled by provenance (tectonic setting, chemistry of source, and source mixture); weathering; transport and erosion (maturity, water chemistry); depositional processes; and diagenesis (e.g. pore water, temperatures) (Rollinson, 1993). See figure 39 for main processes that control the signatures of sedimentary rocks.

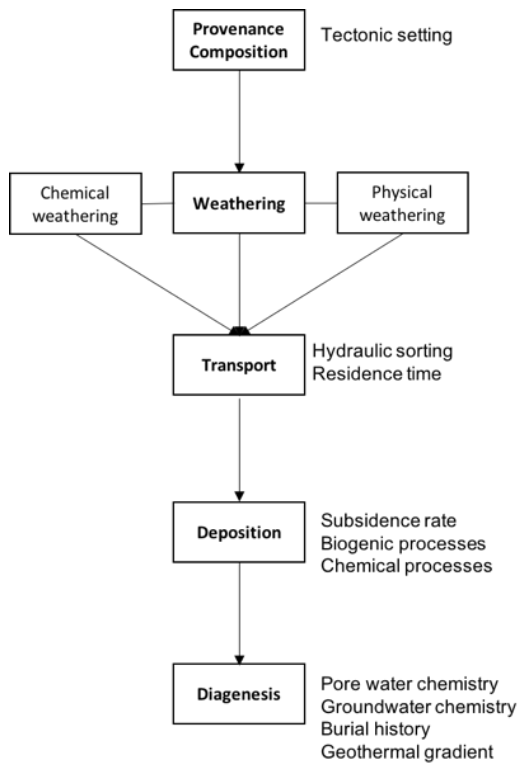


Figure 39: Processes affecting the geochemical signature for sedimentary rocks, modified after Rollinson (1993)

Many methods are used for analyzing geochemical signatures. The main methods include: Ion and electron microprobes, mass spectrometry, x-ray fluorescence, neutron activation analysis, atomic absorption spectrophotometry, and inductively coupled plasma emission spectrometry. When choosing a methodology, it is essential to know what elements to analyze and for what purpose. Isotope ratios, for example, can be analyzed using mass spectrometry (Rollinson, 1993).

Moreover, geochemical analyses may be affected by multiple sources of error, including contamination, calibration, and peak overlap. Contamination can occur during all stages of the analysis, from sample preparation to inserting the sample into the machine. This, for example, can be limited by for example careful cleaning. Similar to XRD, peak overlap can occur in context of various analyzing techniques. Lastly, using a standard reference for calibration can affect the results. This must therefore be considered when choosing standards and measuring these with great accuracy (Rollinson, 1993).

U-Pb dating of Zircon

U-Pb dating of zircons has become an important tool to interpret age of deposition within the field of provenance, and other fields (Nesse, 2012). Moreover, this technique is rather quick and easy to carry out and presents data that are easy to interpret.

The results from the U-Pb analysis are presented in a table. The data can be further plotted in a Concordia-discordia diagram showing $^{206}\text{Pb}/^{238}\text{U}$ vs $^{207}\text{Pb}/^{235}\text{U}$, such as the example shown in figure 40 of a single zircon analysis. The Concordia line represents zircons that have been in closed systems, whereas the Discordia line represents zircons where Pb is lost through time in an open system (Schoene, 2014).

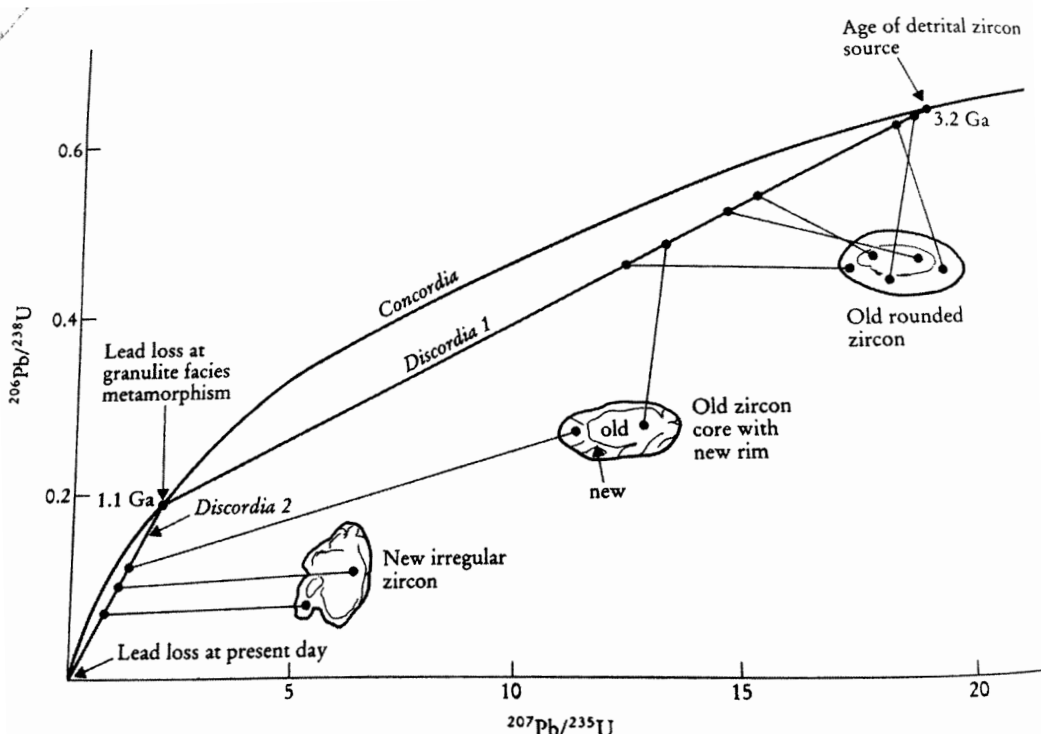


Figure 40: Example of Concordia-discordia diagram with $^{206}\text{Pb}/^{238}\text{U}$ vs $^{207}\text{Pb}/^{235}\text{U}$ (Rollinson (1993) after Kröner et al. (1987))

Lead consist of four stable isotopes, where ^{204}Pb represents the only non-radiogenic isotope, whereas the other isotopes are results of decay from uranium and thorium. Jaffey et al. (1971) presented the parent-daughter relationships, shown in table 4. From the isotopes, both $^{238}\text{U} \rightarrow ^{206}\text{Pb}$ and $^{235}\text{U} \rightarrow ^{207}\text{Pb}$ can be used for analyzing zircons. This is because the half-life of thorium is similar to the age of the universe.

Table 4: Parent-daughter relationship of uranium and thorium, after Jaffey et al. (1971). U: uranium, Pb: lead, Th: thorium, t: time, Byr: billion years, yr: years

Decay route	$t_{1/2}$ Byr	Decay constant λ , yr^{-1}
$^{238}\text{U} \rightarrow ^{206}\text{Pb}$	4.47	1.55125×10^{-10}
$^{235}\text{U} \rightarrow ^{207}\text{Pb}$	0.704	9.8485×10^{-10}
$^{232}\text{Th} \rightarrow ^{208}\text{Pb}$	14.01	0.49475×10^{-10}

When plotted, these parent-daughter relationships represent the backbone of the Concordia, when plotted. General equations (eq. 1-3) have been derived for an open system in which all decay reactions dependent on time (Dickin, 2005):

$$^{206}Pb_p = ^{206}Pb_i + ^{238}U(e^{\lambda_{238}t} - 1) \quad (\text{eq. 1})$$

$$^{207}Pb_p = ^{207}Pb_i + ^{235}U(e^{\lambda_{235}t} - 1) \quad (\text{eq. 2})$$

$$^{208}Pb_p = ^{208}Pb_i + ^{232}Th(e^{\lambda_{232}t} - 1) \quad (\text{eq. 3})$$

These equations can be further derived for minerals that containing uranium (and not lead) during deposition (eq. 4-5, derived from eq. 1) (Dickin, 2005):

$$^{206}Pb = ^{238}U(e^{\lambda_{238}t} - 1) \quad (\text{eq. 4})$$

$$\frac{^{206}Pb}{^{238}U} = (e^{\lambda_{238}t} - 1) \quad (\text{eq. 5})$$

Similar calculations can be done for eq. 2 (eq. 6) (Dickin, 2005);

$$\frac{^{207}Pb}{^{235}U} = (e^{\lambda_{235}t} - 1) \quad (\text{eq. 6})$$

For this project, Thomas Meldahl Olsen and Sofie Knudatter Arntzen (Bachelor students at University of Stavanger, 2017) carried out the U-Pb dating of zircons at the Institute for Mineralogy at the University of Münster, Germany during March-April 2017. A Laser Ablation-Inductively Coupled Plasma-Mass Spectrometry (LA-ICP-MS Element2, Photon Machines Analyze G2) was used for the dating. Olsen and Arntzen (at the University of Stavanger) then used the SEM for determining the correct placement of the laser, and for distinguishing between zoned zircons and non-zoned zircons. Lastly, cathodoluminescence images of zircons (in mounds) were obtained. Further, the laser spot had a diameter of 25 and 35µm. Firstly, the data was analyzed using a Microsoft Excel spreadsheet (Kooijman et al., 2012), after which the data were modified using a Common Pb Correction after Stacey & Kramers (1975). Lastly, the data were analyzed further and probability density plots and Concordia plots were created using a Isoplot 3.75 (Ludwig, 2012) plug in Microsoft Excel.

Heavy Mineral Studies – Single grain

All minerals have a specific chemical composition occurring in specific environments. Therefore, analyzing the minerals can indicate which environments are involved in the provenance. A summary of a selection of identified minerals with occurrence and other remarks can be seen in table 5.

Table 5: Overview of a selection of minerals with chemical formula, occurrence and other remarks. (1) Deer et al., 1992 (2) Nesse, 2012

Mineral Group	Mineral	Chemical Formula	Occurrence & other remarks
Apatite	Fluorapatite	$\text{Ca}_5(\text{PO}_4)_3\text{F}$	
	Chlorapatite	$\text{Ca}_5(\text{PO}_4)_3\text{Cl}$	Can occur in limestone, shale, ironbeds, and phosphate beds. ⁽²⁾
	Hydroxyapatite	$\text{Ca}_5(\text{PO}_4)_3\text{OH}$	
	Carbonate-apatite	$\text{Ca}_5(\text{PO}_4)_3(\text{CO}_3,\text{OH})_3(\text{F},\text{OH})$	Can occur in limestone, shale, ironbeds, and phosphate beds. Can derive from skeletal material or seawater precipitation. ⁽²⁾
Amphibole	Hornblendes	$(\text{Na}, \text{K})_{0-1}\text{Ca}_2(\text{Mg}, \text{Fe}^{2+}, \text{Fe}^{3+}, \text{Al})_5\text{Si}_{16-7.5}\text{Al}_{2-0.5}\text{O}_{22}(\text{OH})_2$	Hornblende marks a large range of different chemistries, and therefore hornblende can occur in a variety of environments, including both igneous and metamorphic. Hornblende is also stable under a large range of P-T, although increasing metamorphic grade can produce changes in the chemical composition. Many reactions can occur with hornblende, for example hornblende with quartz can transform to orthopyroxene, augite, and plagioclase with high metamorphic grade. ⁽¹⁾
Glaucophane		$\text{Na}_2\text{Mg}_2\text{Al}_2[\text{Si}_8\text{O}_{22}](\text{OH})_2$	Occurs as a result of metamorphosed basaltic rocks, by jadeite alteration, and metamorphosed eclogite. ⁽¹⁾
Gedrite		$(\text{Mg},\text{Fe}^2)_k\text{Al}_3[\text{Si}_6\text{Al}_2\text{O}_{22}](\text{OH},\text{F})_2$	Occurs in metamorphic and metasomatic rocks. However, high metamorphism will alter gedrite (and other orthoamphibole) to orthopyroxene. ⁽¹⁾
Kaersutite		$(\text{Na}, \text{K})\text{Ca}_2(\text{Mg}, \text{Fe}^{2+}, \text{Fe}^{3+}, \text{Al})_4(\text{Ti}, \text{Fe}^{3+})_2[\text{Si}_6\text{Al}_5\text{O}_{22}](\text{O},\text{OH},\text{F})_2$	Occurs in alkaline volcanic rocks; phenocrysts (trachybasalts, trachyandesites, trachytes, and alkali rhyolites), dykes, monzonites, and eclogite. ⁽¹⁾
Richterite		$(\text{Na})\text{CaNa}(\text{Mg},\text{Fe}^{3+}, (\text{OH},\text{F})_2$	Usually occurs in contact metamorphic limestones and skarns, and in alkaline-peralkaline basalts, lamprophyres and mica-peridotites, and hydrothermal settings. ⁽¹⁾
Baryte	BaSO ₄		Occurs in hydrothermal veins, or has a product of weathering of limestones. ⁽¹⁾
Carbonates	Calcite	CaCO_3	Occurs as primary precipitation, fossil shells, secondary cementation, hydrothermal deposits (veins), and alkaline igneous rocks. ⁽¹⁾

	Dolomite	$\text{CaMg}(\text{CO}_3)_2$	Usually occurs in sedimentary rocks, as secondary dolomite derived from magnesium fluids altering aragonite or calcite, or as primary evaporate deposits. However, dolomite can occur in metamorphic and metasomatic rocks. ⁽¹⁾
	Ankerite	$\text{Ca}(\text{Mg}, \text{Fe}^{2+}, \text{Mn})(\text{CO}_3)_2$	Occurs in hydrothermal and low-grade metasomatic. ⁽¹⁾
	Epidote	$\text{Ca}_2\text{Al}_2\text{O}(\text{Al}, \text{Fe}^{3+})\text{OH}[\text{Si}_2\text{O}_7][\text{SiO}_4]$	Occur in metamorphic deposits (greenschist and amphibole facies). It can also be produced as an alteration of plagioclase in hydrothermal environments. ⁽¹⁾
Garnet	Almandine	$\text{Fe}^{2+} \text{Al}_2\text{Si}_3\text{O}_12$	Occurs in metamorphosed argillaceous sediments, thermal metamorphism of pelitic rocks, igneous rocks (granitic aplites and pegmatites, xenocrysts, calc-alkali granites and rhyolites), can also occur with pyrope in granulite facies. ⁽¹⁾
Grossular		$\text{Ca}_3\text{Al}_2\text{Si}_5\text{O}_12$	Characteristic of thermal and regional metamorphism of impure calcareous rocks (such as skarn, for local metamorphism), metamorphosed basaltic rocks, or diopside. ⁽¹⁾
Spessartine		$\text{Mn}_3\text{Al}_2\text{Si}_3\text{O}_12$	Less common than the other garnets, occur in skarns, Mn-rich metasomatic rocks by regional metamorphism or intrusions, or in granite pegmatites and aplites. ⁽¹⁾
Pyrope		$\text{Mg}_3\text{Al}_2\text{Si}_3\text{O}_12$	Occurs in ultrabasic rocks (e.g. kimberlites, mica peridotite), or in sands and gravels sourced by ultrabasic rocks. Used as a tracer for kimberlites. ⁽¹⁾
Ilmenite		FeTiO_3	Usually an accessory mineral in igneous and metamorphic rocks, but can be detrital sediments in sedimentary rocks. Manganese ilmenite occurs in granitic rocks and carbonates. ⁽¹⁾
Mica	Biotite	$\text{K}_2(\text{Mg}, \text{Fe}^{2+})_{6-4}(\text{Fe}^{3+}, \text{Al}, \text{Ti})_{0-2}[\text{Si}_{6-5}\text{Al}_{2-3}\text{O}_{20}] (\text{OH}, \text{F})_4$	Occurs in a large range of environments; metamorphic rocks, intrusive and extrusive igneous rocks, and as sediment and cement. It can also occur by high grade metamorphism of muscovite and amphibole, or metamorphism of dolomite and muscovite. ⁽¹⁾
	Muscovite	$\text{K}_2\text{Al}_4[\text{Si}_6\text{Al}_2\text{O}_{20}](\text{OH}, \text{F})_4$	Similar to biotite, it occurs in a large range of environments; metamorphic rocks (greenschist to amphibolite facies), igneous rocks (most commonly in granites, and less commonly in rhyolites), and as sediment and cement in sedimentary rocks. ⁽¹⁾
	Monazite	$(\text{Ce}, \text{La}, \text{Th})\text{PO}_4$	Usually occurs in granitic rocks as rare accessory minerals. Can be found in streams and beach sands as detrital minerals. ⁽¹⁾
	Rutile	TiO_2	Occurs in a wide range of environments; igneous (mainly plutonic), and metamorphic rocks (more common in amphibolites and eclogites, and less common in metamorphosed limestones). Can occur intrusive in other minerals, such as quartz. Can occur as detrital sediments and high concentration can be found in beach sands. ⁽¹⁾

			Plots with Cr vs Nb can classify the origin of the rutile; low Nb and Cr basaltic eclogites, high Cr gabbroic eclogite, and high Nb metapelites (Zack et al., 2002)
Spinel Group	Chromite	$\text{Fe}^{2+}\text{Cr}_2\text{O}_4$	Occur in mafic and ultramafic rocks. ⁽²⁾ Can form bands in igneous rocks. Can also occur in basaltic rocks with olivine-rich inclusions. Can be found in sands and streams as detrital sediments. ⁽¹⁾
	Uvöspinel	$\text{Fe}^{2+}\text{TiO}_4$	Used to classify tectonic setting and origin (Zimmermann and Spallati, 2009)
Sphene	Titanite	$\text{CaTi}[\text{SiO}_4](\text{O}, \text{OH}, \text{F})$	Occur in metamorphic rocks (contact/regional metamorphic limestones) and Al-rich xenoliths. ⁽¹⁾
	Stilpnomelane	$(\text{K}, \text{Na}, \text{Ca})_{0.6}(\text{Mg}, \text{Fe}^{2+}, \text{Fe}^{3+})_6\text{Si}_8\text{Al}[(\text{O}, \text{OH})_{27} 2\cdot 4\text{H}_2\text{O}]$	Common accessory mineral in igneous (intermediate and acid plutonic rocks, particularly in nepheline syenites), metamorphic rocks (gneiss, schists, skarns, and metamorphosed impure calc-silicates), and detrital grains in sedimentary rocks. ⁽¹⁾
Tourmaline		$(\text{Na}, \text{Ca})(\text{Mg}, \text{Fe}, \text{Mn}, \text{Li}, \text{Al})_3(\text{AlMg}, \text{Fe}^{3+})_6[\text{Si}_6\text{O}_{18}](\text{BO}_3)_3(\text{O}, \text{OH})_3(\text{OH}, \text{F})$	Occur in low-grade metamorphism (greenschist: with chlorite, muscovite and albite, blueschists: with glaucophane and garnet), silicate-iron formations, and sulphide deposits. ⁽¹⁾
	Zircon	$\text{Zr}[\text{SiO}_4]$	Typical for granite pegmatites, hydrothermal veins, and metamorphism (boron metasomatic or recrystallization). Specific conditions, such as late-stage granitic veins or pegmatites, lithium tourmaline can form with specific colors and compositions. Further, Mg-tourmaline forms in metamorphic or metasomatic rocks. Lastly, authigenic tourmaline can be found in limestones and detrital in sandstones. ⁽¹⁾
			Classification scheme presented by Henry and Guidotti (1985) can classify tourmalines according to Al-Fe-Mg-Ca concentrations.
	Zircon	$\text{Zr}[\text{SiO}_4]$	Commonly found in igneous rocks (especially plutonic) and metamorphic rocks. Very weathered resistant, so zircon grains can survive multiple recycling events and sedimentation. ⁽¹⁾

Results

Semi-quantification

The following table (table 6) shows the semi-quantification of the magnetic fraction (Mf), the apatite fraction (Af), and the zircon fraction (Zf) for all formations.

Table 6. Mineral Distribution of magnetic, apatite, and zircon fractions for all formations from SEM

Kuibis Formation		Numeens Formation		Holgat Formation		Blaubeker Formation		Matchless		Aubures Formation		Klein Aub Formation	
Mf n=33	Af n=106	Mf n=162	Af n=84	Mf n=108	Af n=52	Mf n=180	Af n=106	Big Mf n=58	Af n=113	Zf n=64	Mf n=141	Af n=100	Zf n=52
Amphibole (gedrite)	0,3 %							2,8 %			0,6 %		0,7 %
Amphibole (glaucophane)	0,3 %							11,1 %			0,9 %		
Amphibole (hornblend)	1,2 %										70,2 %	11,8 %	1,6 %
Amphibole (kaersutite)	0,3 %							1,9 %					
Amphibole (richterite)	0,3 %							1,9 %					
Calcite	1,2 %							3,9 %	1,9 %		0,6 %	1,5 %	
Dolomite	2,1 %							16,7 %	3,8 %				
Ankerite	1,8 %							11,6 %	9 %				
Apatite w/AlMgSi													
F-apatite	33,1 %		10,5 %		12,0 %		25,0 %	1,1 %		3,4 %	1,7 %		3,8 %
Cl-apatite											36,3 %	1,4 %	13,0 %
Baryte												2,0 %	8,9 %
Chromite	4,4 %												
Spinel group (unknown)													
Uvospinel								1,1 %		1,4 %		0,8 %	
Biotite											1,5 %		32,6 %
Muscovite	3,6 %			1,9 %								1,4 %	
Illite	0,6 %							3,7 %	5,8 %			0,7 %	
Quartz	26,9 %		15,4 %		21,3 %		15,4 %	20,6 %		37,7 %	3,4 %	10,9 %	0,8 %
Feldspar (orthoclase)	0,9 %		0,9 %		3,7 %		2,4 %	0,9 %				22,0 %	74,1 %
												5,7 %	19,6 %
												12,0 %	0,8 %

Feldspar (albite)	1.8 %	2.8 %	3.7 %	1.2 %		1.9 %	10.6 %	45,3 %	1.7 %		5.3 %	5.7 %	11.0 %	1,9 %	3,0 %	10,7 %	1,8 %	
Feldspar (anorthite)															1,6 %			
Feldspar (labradorite)	1,2 %					0,8 %					1,7 %	0,6 %	11,8 %	23,0 %		1,0 %		
Nepheline			1,9 %	1,9 %							2,8 %	1,7 %				6,0 %		
Garnet (almandine)															1,5 %			
Garnet (grossular)	0,3 %														9,4 %		0,7 %	
Garnet (pyrope)	0,6 %																3,8 %	
Garnet (spessartine)	0,3 %														6,2 %	5,9 %	2,1 %	
Gehlenite						1,9 %												
Titanite	0,3 %		0,6 %	1,2 %		1,9 %		1,7 %	2,8 %		5,3 %	73,4 %	2,8 %	1,0 %	5,8 %	9,8 %	1,8 %	19,6 %
Ilmenite								8,9 %	0,9 %		5,1 %	4,4 %	1,6 %	0,7 %			1,5 %	
Ilmenite w/Mn						3,1 %					0,6 %							
Iron oxide	5,6 %					15,4 %		25,0 %							25,5 %	1,0 %	11,4 %	
Rutile	5,0 %	2,8 %				13,6 %	21,3 %	17,3 %	1,7 %	1,9 %	3,4 %				1,4 %		0,9 %	
Epidote												0,6 %						
Olivine	0,3 %																	
Tourmaline						0,8 %												
Zircon	5,6 %	0,9 %	1,2 %	2,8 %		25,0 %	7,2 %	2,8 %	77,6 %	1,1 %		1,6 %	86,5 %	0,8 %	0,9 %	46,4 %		
Stilpnomelane	1,8 %	0,9 %	9,3 %	1,9 %	0,8 %	3,8 %	7,2 %		1,7 %				1,9 %	13,6 %		2,7 %		
Monazite			0,9 %	8,0 %	1,9 %				3,9 %									
Unknown															1,5 %			

MLA

All the data received from the MLA measurements were processed and presented using MLA Dataview 3.1, see appendix B for a full overview.

Table 7: Mineral Distribution of magnetic fraction for all formations from MLA

Mineral	Kuibis Mf - Wt%	Holgat Mf - Wt%	Numees Mf - Wt%	Blaubeker Mf - Wt%	Aubures Mf - Wt%	Klein Aub Mf - Wt%	Matchless Mf-Wt%
Framework Silicates	25,08	13,07	14,99	26,80	8,96	11,67	16,08
Sheet silicates	5,64	9,64	21,92	24,00	7,44	13,51	1,05
Chain Silicates	1,03	0,46	0,74	0,91	0,73	0,58	51,68
Ring silicates	0,99	6,03	1,13	0,32	1,87	14,74	26,20
Orthosilicates	5,14	2,47	2,46	3,75	4,48	9,83	1,99
Carbonates	2,40	19,26	4,71	6,18	0,32	0,01	0,64
Sulfates, sulfide	0,09	0,05	0,00	0,00	0,00	0,00	0,00
Phosphates	32,72	9,33	13,88	2,11	0,60	0,26	0,38
Oxides, H-oxides	19,55	39,06	39,42	35,07	74,91	48,55	1,35
Native	6,37	0,03	0,00	0,00	0,01	0,01	0,00
Total	100,00	100,00	100,00	100,00	100,00	100,00	100,00

The framework silicates include quartz, plagioclase, and albite; sheet silicates include biotite, chamosite, and muscovite; chain silicates include kaersutite, hastingsite (with and without Mn), and enstatite; ring silicates include epidote, clinozoisite, and tourmaline; orthosilicates include titanite, almandine, and zircon; carbonates include calcite, ankerite, and dolomite; sulfates/sulfide include barite and galena; phosphates include apatite, monazite-Ce, and xenotime-Y; oxides/H-oxides include rutile, chromite, iron oxides, ulvöspinel, ilmenite, and hollandite; and, lastly, the native minerals include FeCr, Zn(OH)2, and MnPbO. Even though these fractions are Franz Separated, some grains below the density requirement still pass the separation. Therefore, a filter was applied to remove the grains below the density (>2.95 for the magnetic fraction). As a result of this, the percentage of the framework minerals is reduced, table 8. Moreover, the original mineral distribution for apatite and zircon is seen in table 9, and with filter in table 10. Full particle density distribution can be seen in appendix C.

Table 8: Mineral Distribution of magnetic fraction for all formations from MLA with a density filter of >2.95

Mineral	Kuibis Mf - Wt%	Holgat Mf - Wt%	Numees Mf - Wt%	Blaubeker Formation-Wt%	Aubures Mf - Wt%	Klein Aub Mf - Wt%	Matchless Mf - Wt%
Framework Silicates	4,96	7,91	10,58	19,72	5,82	5,96	12,91
Sheet silicates	3,75	6,83	18,53	22,81	5,96	8,97	1,02
Chain Silicates	1,21	0,43	0,51	0,91	0,67	0,59	53,24
Ring silicates	1,07	9,53	1,31	0,30	2,00	16,66	27,71
Orthosilicates	7,41	3,77	2,77	4,92	4,51	10,86	2,12
Carbonates	0,12	9,00	3,36	3,62	0,16	0,01	0,61
Sulfates, sulfide	0,13	0,06	0,00	0,00	0,00	0,00	0,00
Phosphates	47,63	14,59	18,74	2,33	0,62	0,27	0,39
Oxides, H-oxides	24,16	47,44	43,75	44,77	79,72	56,08	1,47
Native	9,23	0,05	0,00	0,00	0,01	0,02	0,00
Total	100,00	100,00	100,00	100,00	100,00	100,00	100,00

Table 9: Mineral Distribution of apatite and zircon fractions for all formations from MLA

Mineral	Kui Af - Wt%	Num Af - Wt%	Hol Af - Wt%	Hol Zf - Wt%	BBCL Af - Wt%	BBCL Zf - Wt%	Aub Af - Wt%	Aub Zf - Wt%	Sin Af - Wt%	Sin Zf - Wt%	Match Af - Wt%	Match Zf - Wt%
Framework Silicates	26,87	0,45	15,58	19,00	74,68	1,61	62,87	1,48	78,90	13,24	19,13	1,57
Sheet silicates	1,74	2,92	3,19	2,57	13,46	0,79	15,88	1,31	8,70	3,90	0,50	0,23
Chain Silicates	0,09	0,03	0,15	0,05	0,14	0,26	0,08	0,11	0,02	0,07	0,26	0,18
Ring silicates	0,03	0,00	0,10	0,04	0,28	0,05	0,01	0,03	0,05	0,04	19,63	5,48
Orthosilicates	0,84	0,04	0,17	30,81	2,22	94,20	2,26	92,66	2,64	67,76	29,65	84,82
Carbonates	0,06	0,02	12,41	4,91	6,97	0,33	0,24	0,08	0,01	0,01	0,28	0,21
Sulfates, sulfide	0,00	0,00	0,00	0,60	0,00	0,04	0,00	0,00	0,00	0,44	0,00	0,00
Phosphates	69,35	96,30	58,62	20,61	1,39	1,52	18,05	1,41	9,58	11,34	29,56	0,49
Oxides, H-oxides	1,03	0,23	9,71	21,40	0,88	1,20	0,61	2,80	0,10	3,21	1,00	7,02
Native	0,00	0,00	0,00	0,00	0,00	0,00	0,00	0,12	0,00	0,00	0,00	0,00
Total	100,00	100,00	100,00	100,00	100,00	100,00	100,00	100,00	100,00	100,00	100,00	100,00

Table 10: Mineral Distribution of apatite and zircon fractions for all formations from MLA with a density filter of 2.7-3.3 g/cm³ for apatite and >3.37 g/cm³

Mineral	Kui Af - Wt%	Num Af - Wt%	Hol Af - Wt%	Hol Zf - Wt%	BBCL Af - Wt%	BBCL Zf - Wt%	Aub Af - Wt%	Aub Zf - Wt%	Sin Af - Wt%	Sin Zf - Wt%	Match Af - Wt%	Match Zf - Wt%
Framework Silicates	1,5	0,24	1,66	11,84	10,53	5,36	3,93	2,17	8,02	5,05	13,17	1
Sheet silicates	1,07	0,54	1	1,87	3,18	1,83	1	2,97	3,48	5,18	0,46	0,21
Chain Silicates	0,11	0,03	0	0,15	1,56	0,68	0	0,31	0	0,17	0,27	0,18
Ring silicates	0,04	0	0,03	0,18	9,21	0	0,02	0,04	0	0,08	17,17	5,48
Orthosilicates	0	0,01	0,01	0,08	0	1,74	0	30,23	3,49	52,24	23,32	85,9
Carbonates	0,08	0,02	2,21	4,49	5,25	1,12	0,08	0,07	0,08	0,01	0,25	0,12
Sulfates, sulfide	0	0	0	2,6	0	0,15	0	0	0	1,21	0	0
Phosphates	97,05	99,1	94,3	1,81	64	4,66	92,63	1,51	84,39	1,62	45,21	0,07
Oxides, H-oxides	0,04	0,06	0,77	48,27	5,56	4,74	2,34	7	0,01	7,49	0,16	7,01
Native	0	0	0	0	0	0	0	0	0	0	0	0
Total	100	100	100	100	100	100	100	100	100	100	100	100

Following shows images captured by the SEM at TU Freiberg during the MLA analysis.

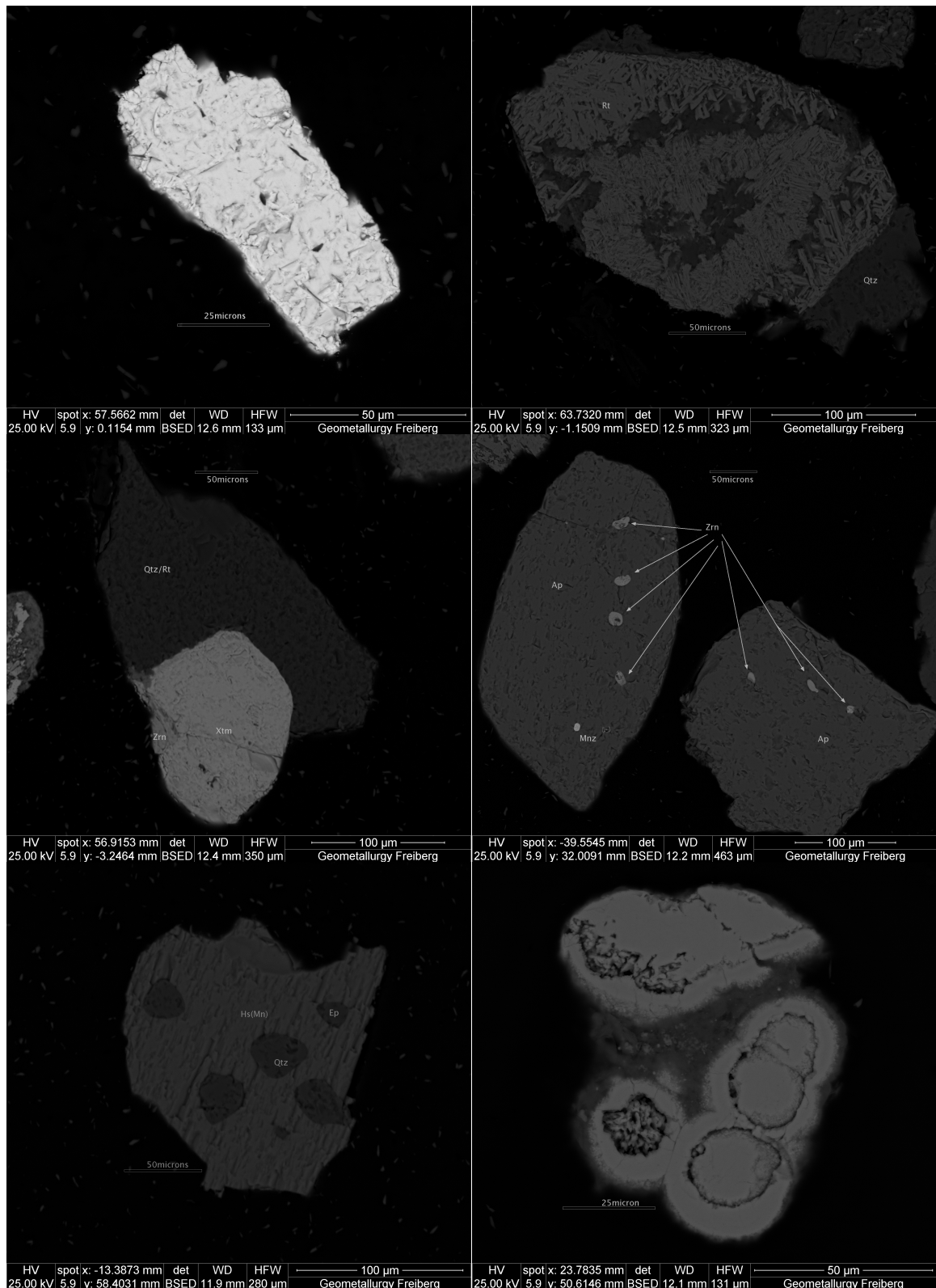
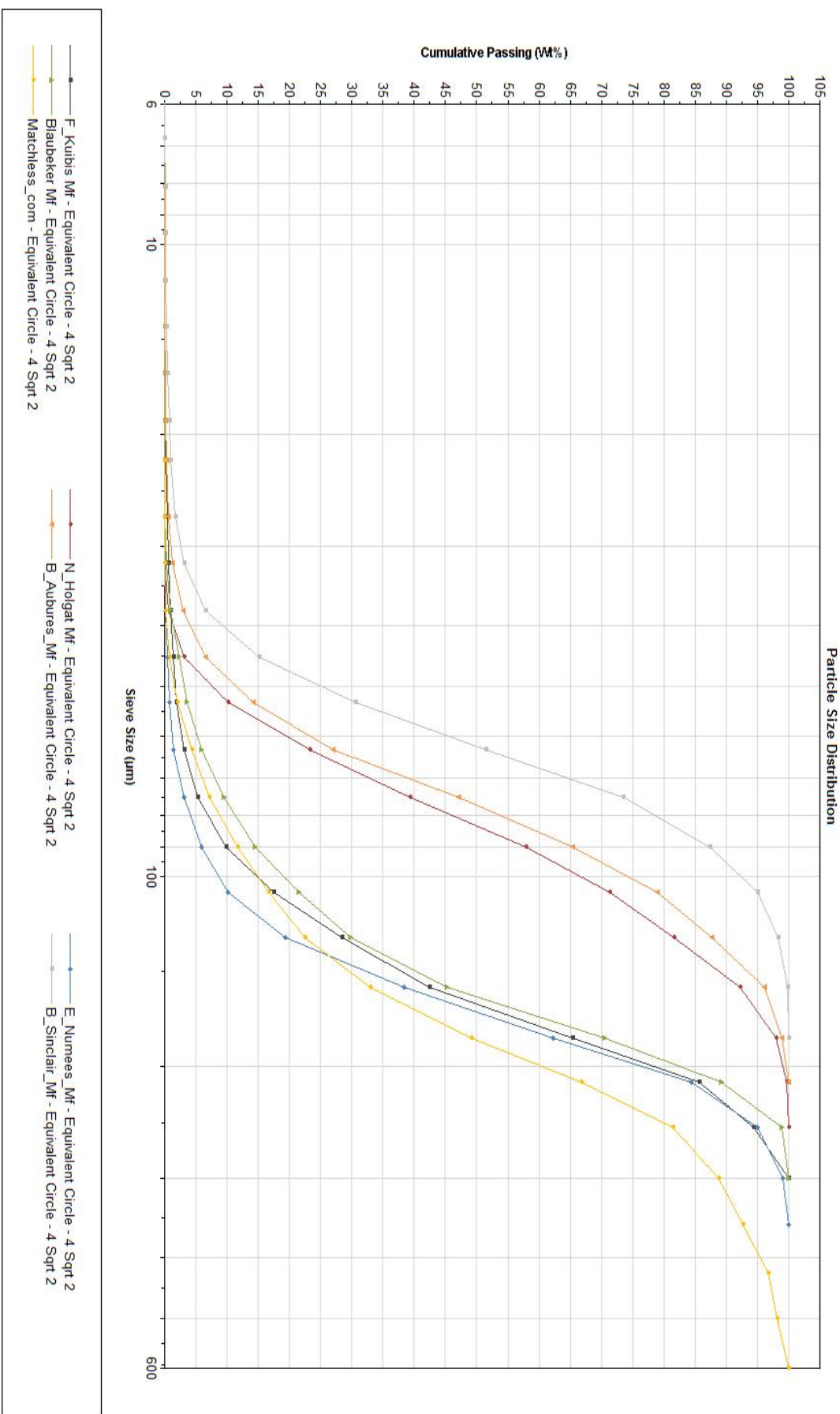
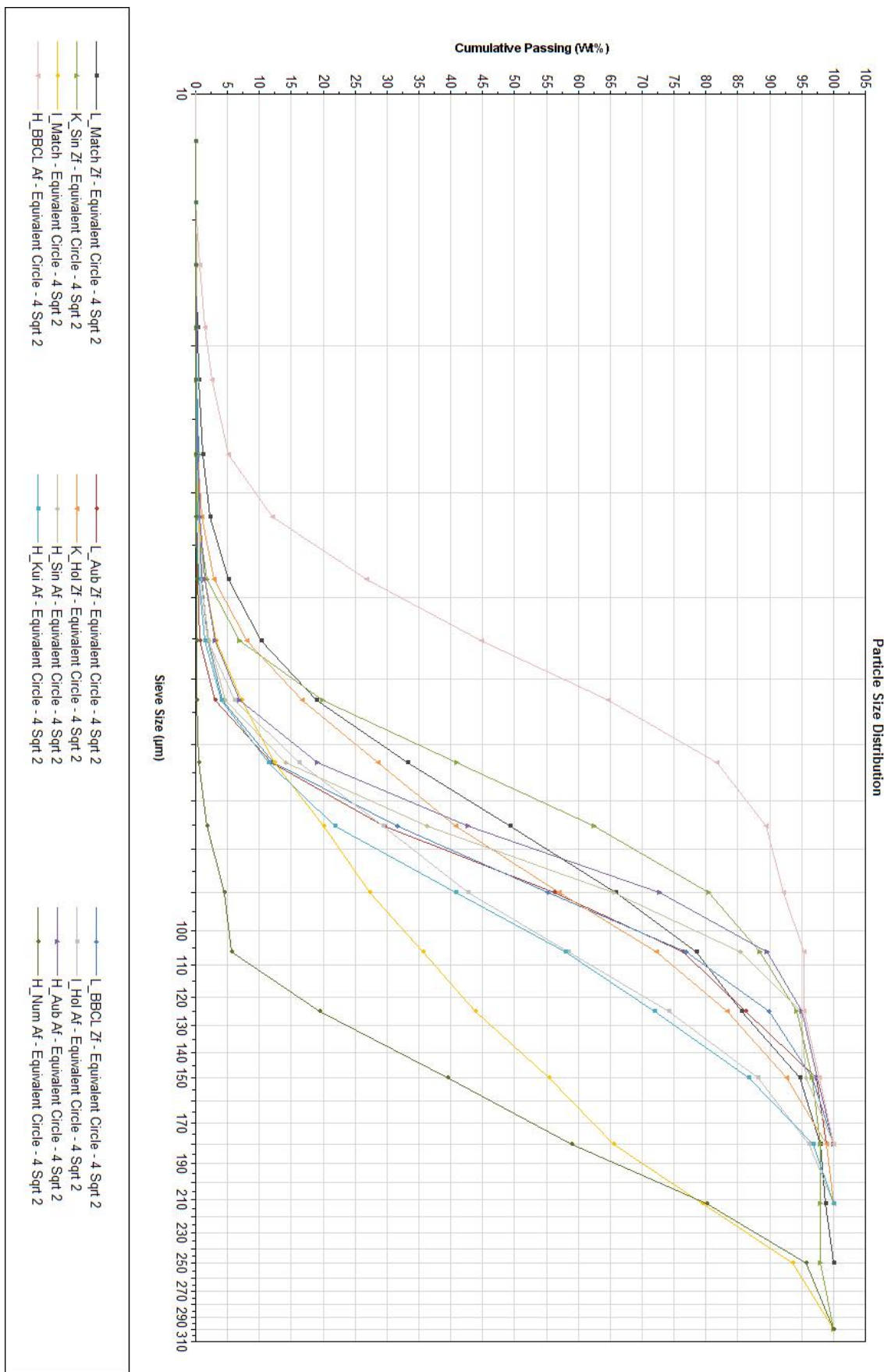


Figure 41: (top left) Galena found in the Kuibis Formation, (top right) Rutile needles in quartz in the Kuibis Formation, (mid left) Quartz with rutile, zircon and xenotime found in the Kuibis Formation, (mid right) Apatite grains with monazite and zircons in the Numees Formation, (bottom left) Hastingsite-Mn with quartz and epidote in the Matchless Amphibolite, and (bottom right) iron oxide, potentially mineralized fossil in the Blaubeker Formation

The following graph shows the particle size distribution for all formations, full distribution can be seen in appendix D.



Graph 1: Grain size distribution from MLA measurements for magnetic fraction of all formations



XRD

The following graphs show the result of the XRD analysis, with the identified minerals.

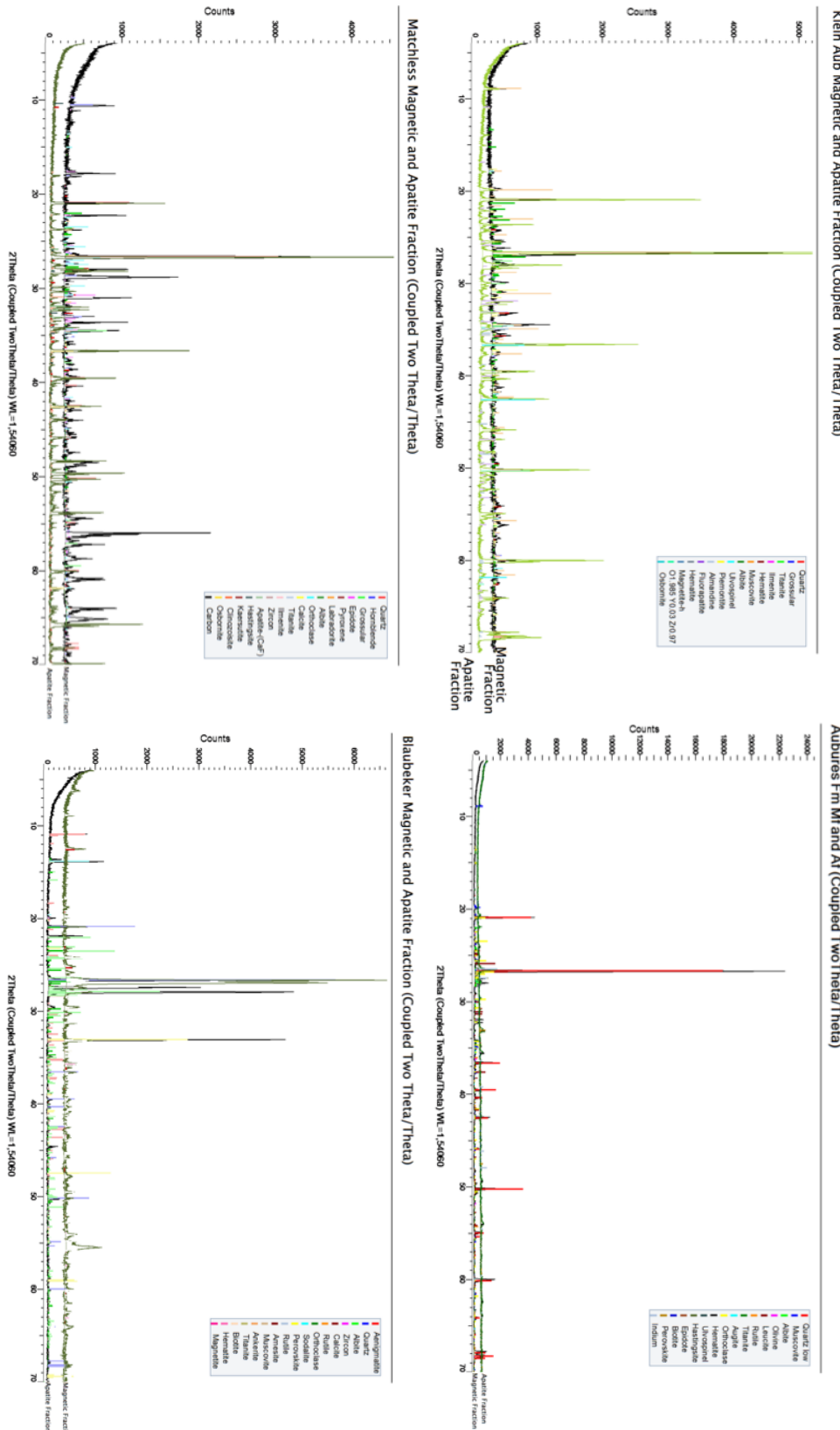


Figure 42: XRD results of (top left) Klein Aub Formation Magnetic and Apatite Fractions; (top right) Aubures Formation Magnetic and Apatite Fractions; (bottom left) Matchless Amphibolite Magnetic and Apatite Fractions; and (bottom right) Blaubeker Formation Magnetic and Apatite Fractions

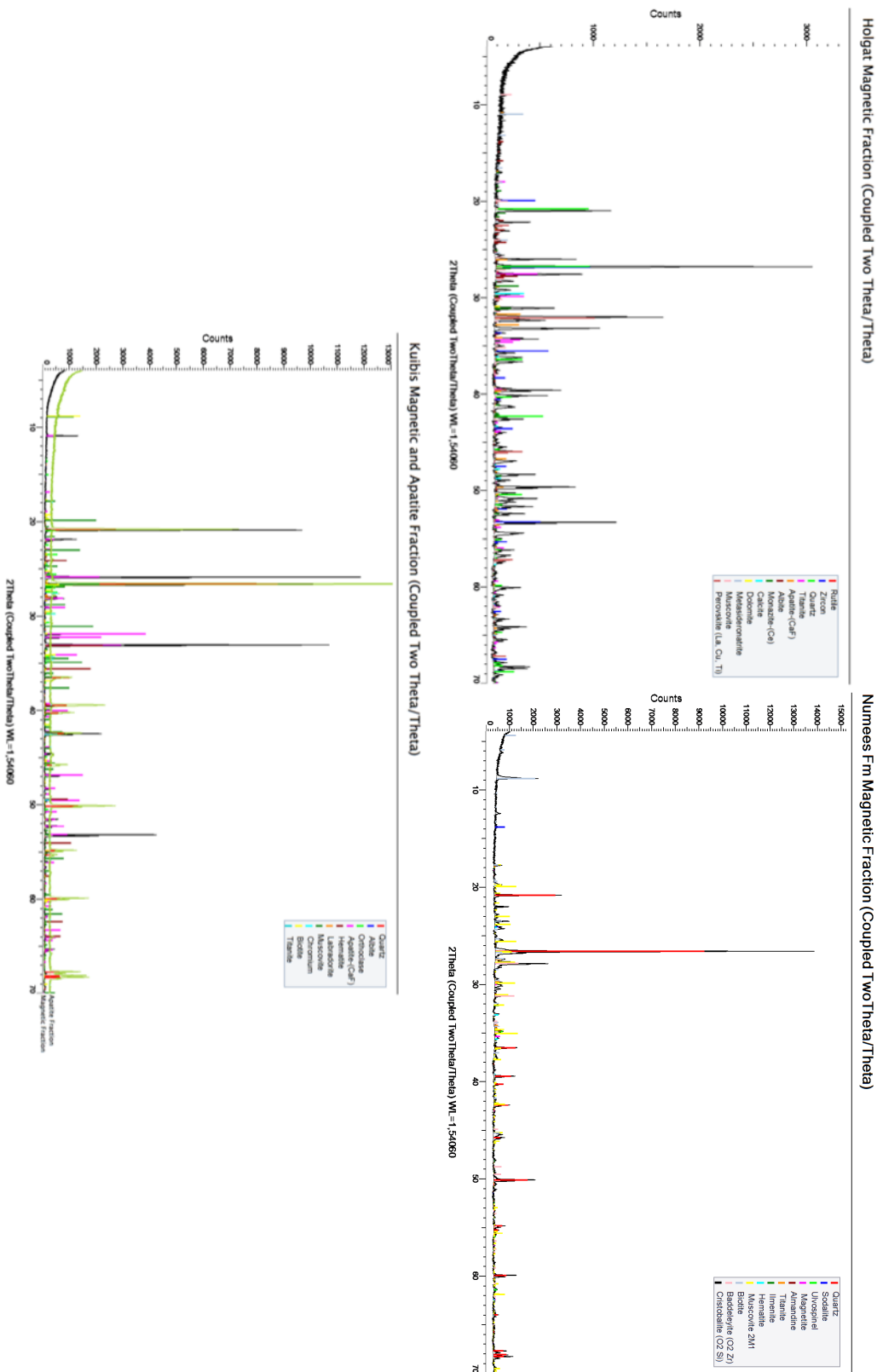
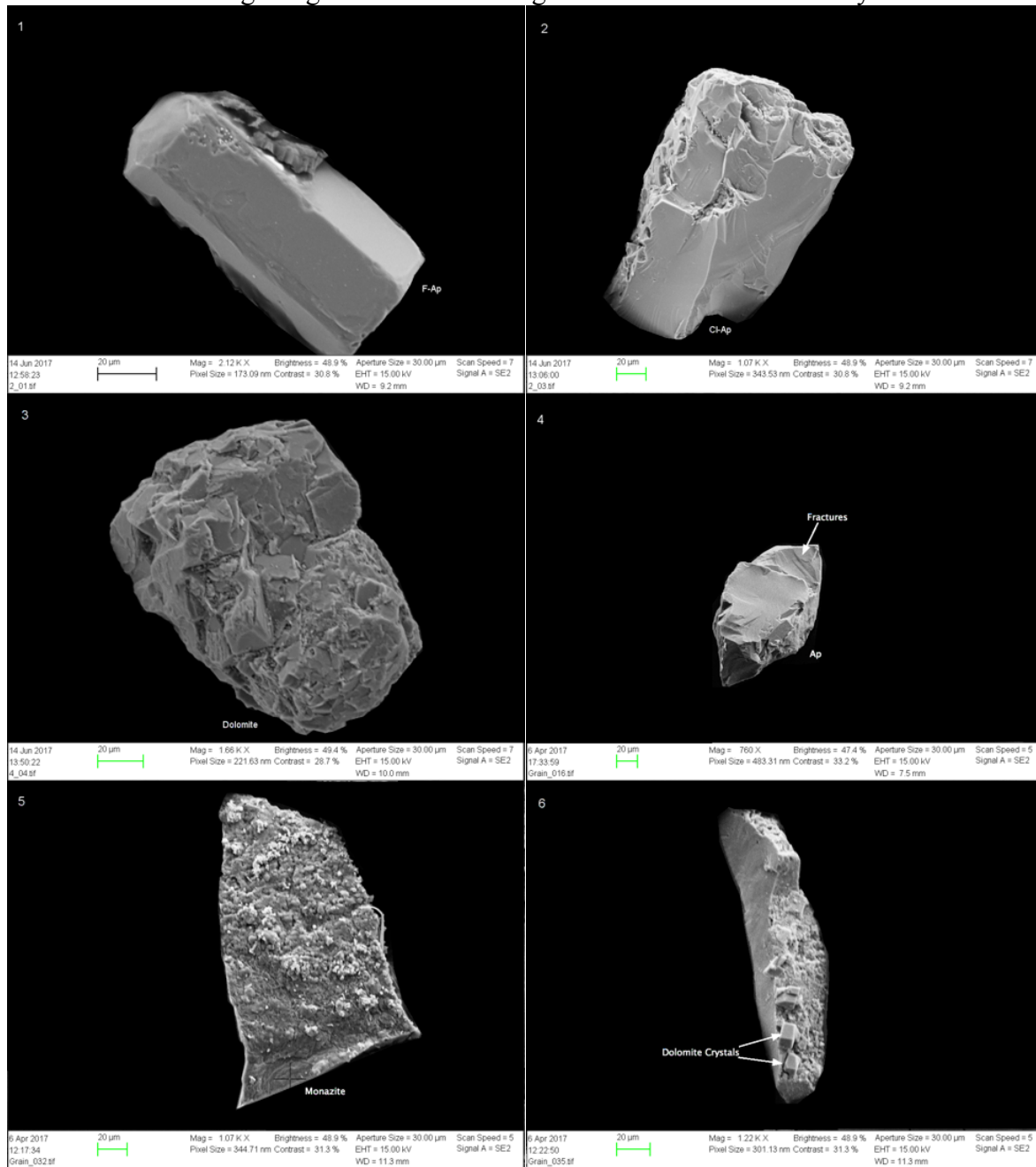


Figure 43: XRD results of (top left) Holgat Magnetic Fraction; (top right) Numees Formation Magnetic Fraction; (bottom) Kuibis Magnetic and Apatite Fractions

Optical Analysis

The following images were taken using the SEM and the secondary electron detector.



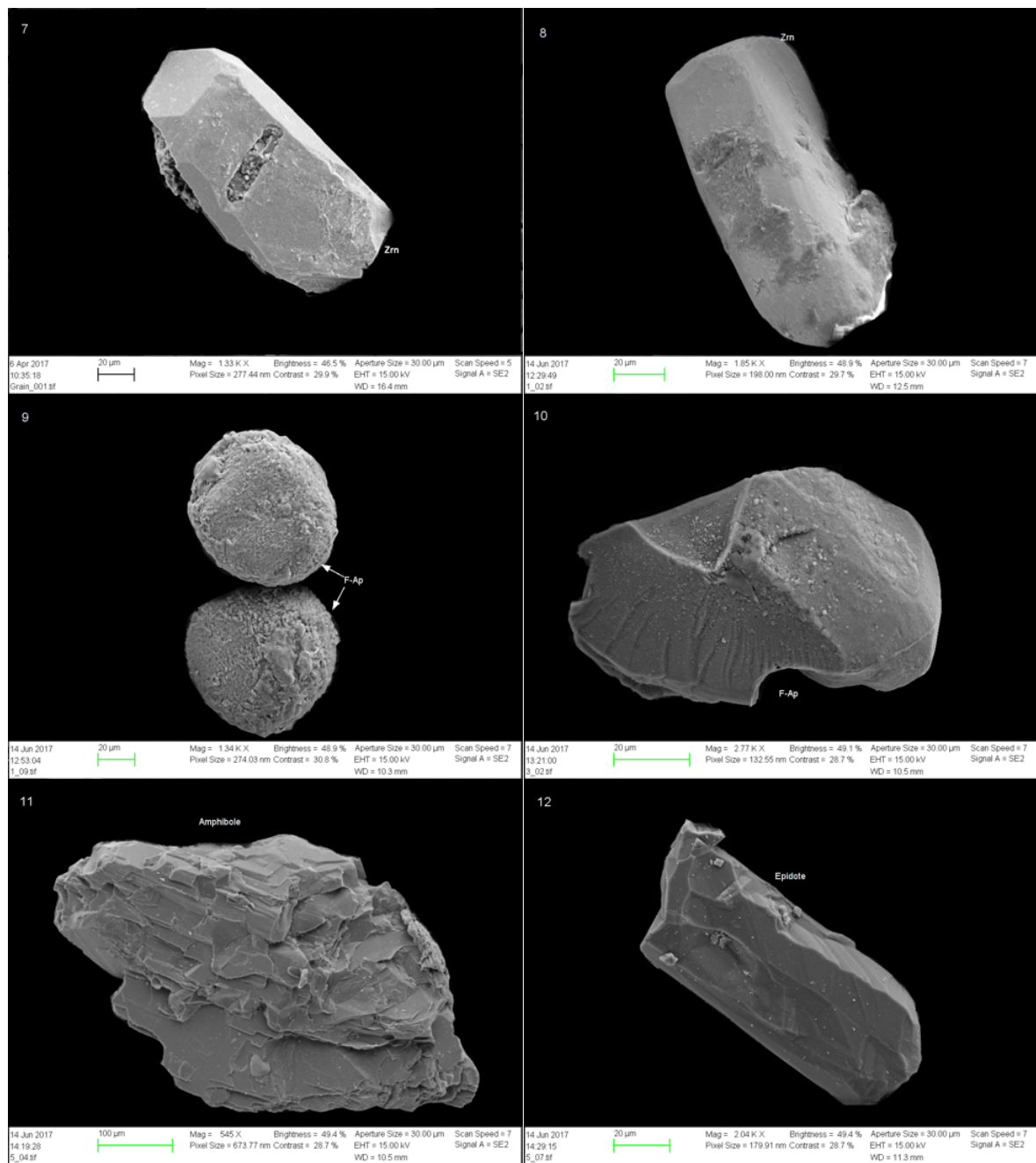


Figure 44: (1) F-Apatite, Kuibis Formation, (2) Cl-Apatite, Kuibis Formation, (3) Dolomite, Holgat Formation, (4) F-Apatite, Numees Formation, (5) Monazite, Blaubecker Formation, (6) Dolomite, Blaubecker Formation, (7) Zircon, Blaubecker Formation, (8) Zircon, Aubures Formation, (9) 2xF-Apatite, Aubures Formation, (10) F-Apatite, Klein Aub Formation, (11) Amphibole, Matchless, (12) Epidote, Matchless

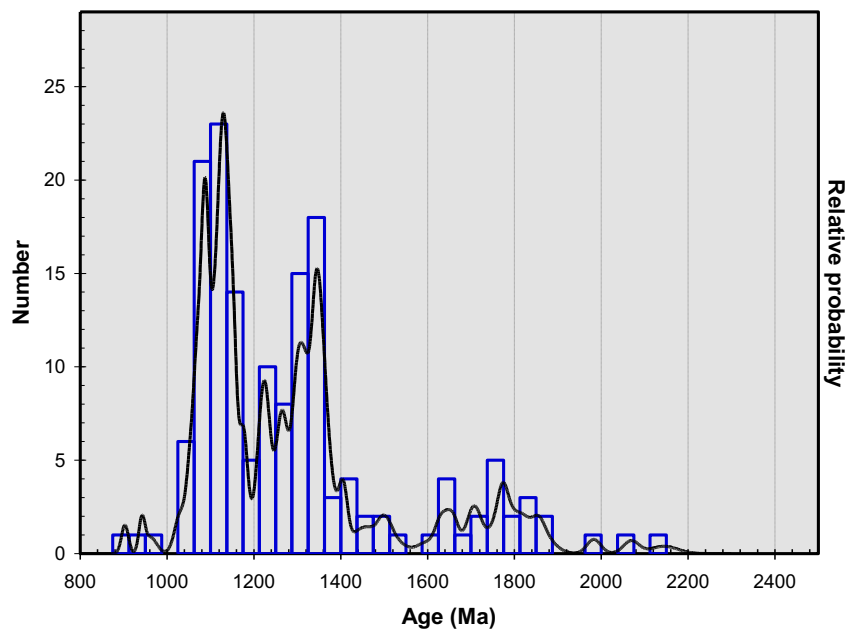
Most grains show fractures and transportation marks, although most zircons (figure 44-7 and 8), as well as some apatites (figure 44-1) and epidotes (figure 44-12), show crystal shape. Moreover, dolomite and calcite crystals are visible on the grain surfaces. Another interesting feature, are a few very round and spherical fapatite grains (figure 44-9).

Geochemistry - Isotope dating

All isotope data were analyzed using Isoplot (Ludwig, 2003) to create Probability Density Plots and Concordia Plots. All data is available in Appendix E. The U-Pb data for the Klein Aub Formation, Aubures Formation, and Blaubeker Formation were provided from previous studies by Dr. Udo Zimmermann, whereas the data for Kuibis Formation is new data for this project.

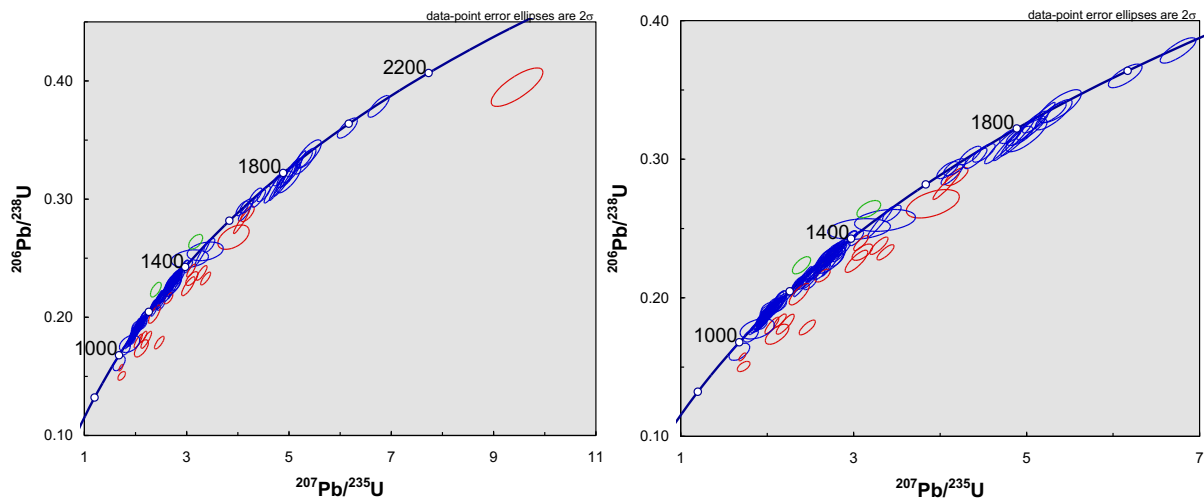
Klein Aub Formation - Sinclair Group

Disputes exist concerning the age of the Sinclair Group (see Geological Setting section) and, therefore, dating detrital zircons can be of importance for interpreting the age of the rock successions. The following graph shows the probability density of the zircons dated. The main peaks are between ca. 1000-1400 Ma, with the oldest zircon dates 2154 ± 31 Ma and the youngest dates being 942 ± 7 Ma.



Graph 3: Probability Density Plot showing the distribution of zircon ages of the Klein Aub Formation

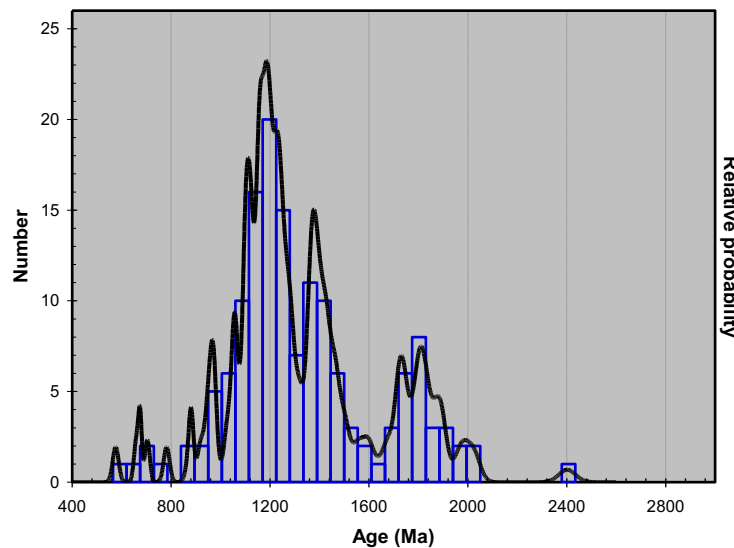
The Concordia plot is presented in graph 4. Most zircons plot on the Concordia (blue circles), whereas some zircons plot above the Concordia (green circles, U lost) and, lastly, some zircons plot below the Concordia (red circles, Pb lost).



Graph 4: Concordia Plots of Klein Aub Formation

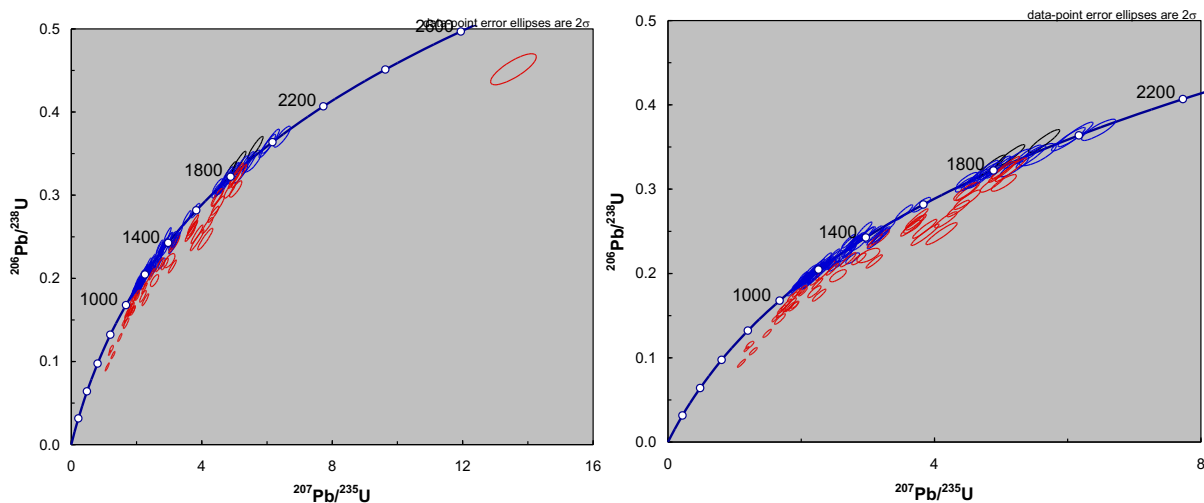
Aubures Formation

With respect to the geological history of Namibia, another question is whether the Aubures Formation is part of the Sinclair Group or not (see Geological Setting section). The probability density plot for the Aubures Formation can be seen in the following graph. It is worth noting is the main peaks between ca. 1000-1600 Ma, with the oldest zircon dates being 2405 ± 34 Ma and the youngest being 576 ± 12 Ma.



Graph 5: Probability Density plot showing the distribution of zircon ages of Aubures Formation

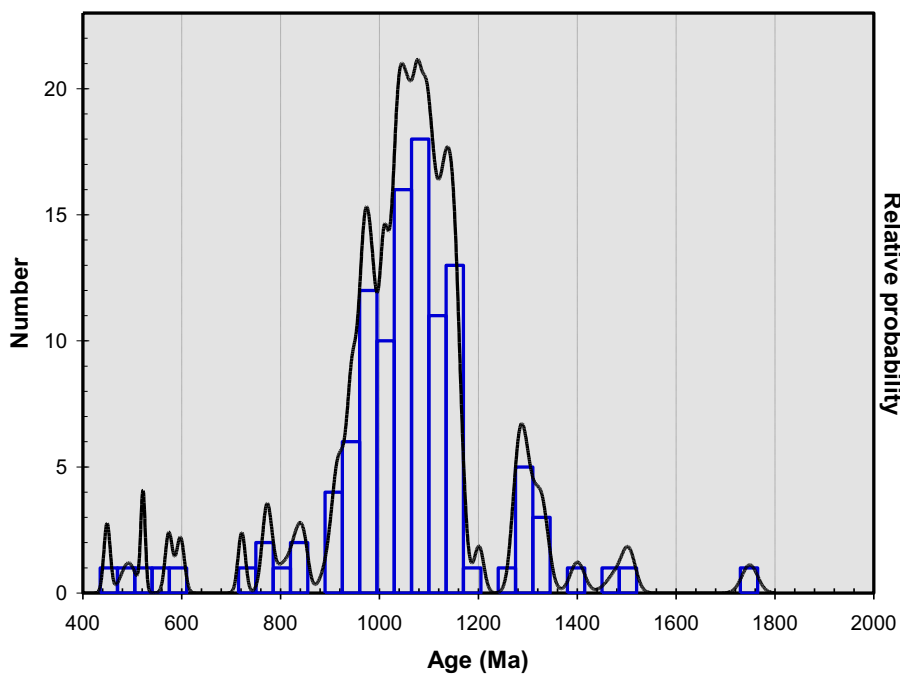
The Concordia plot is presented in graph 6. Most zircons plot on the Concordia (blue circles), whereas some zircons plot below (red circles) and above (black circles) the Concordia.



Graph 6: Concordia Plots of Aubures Formation

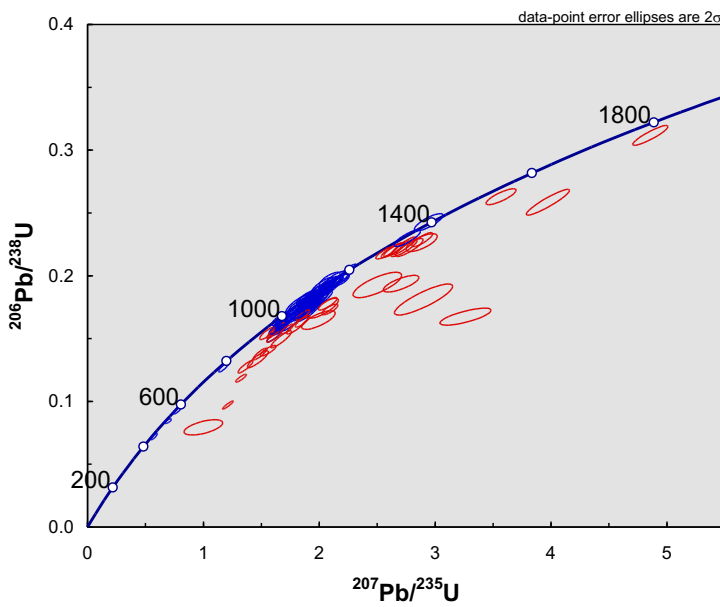
Blaubeker Formation

The probability density plot for the Blaubeker Formation (graph 7) shows that the main population of U-Pb ages falls in the range of ca. 900-1200 Ma, with the youngest zircon dating being 574 ± 8 Ma and the oldest zircon dating to 1749 ± 16 Ma.



Graph 7: Probability Density plot showing the distribution of zircon ages of Blaubeker Formation

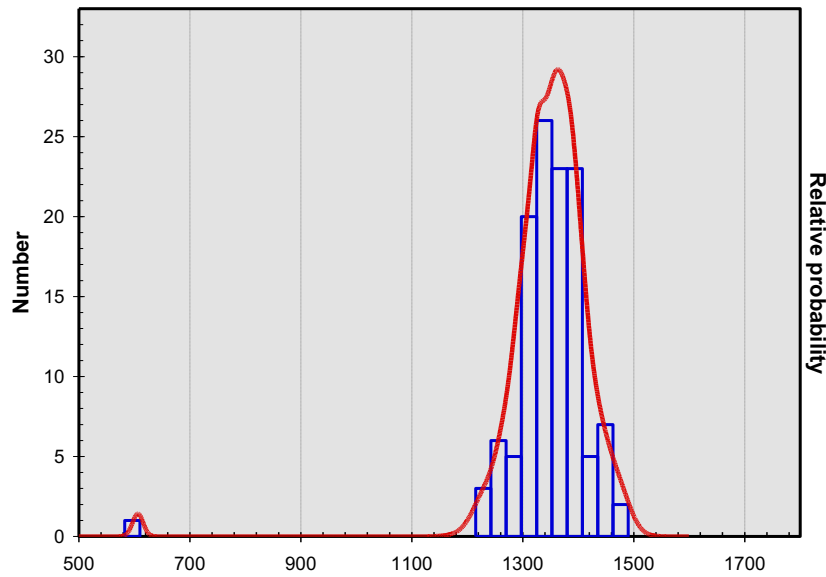
Concordia plots for the Blaubeker Formation can be seen in the following graph. The zircons dated within the main peak population plot along the Concordia, whereas the other zircons plot outside the Concordia (red circles).



Graph 8: Concordia Plot of Blaubeker Formation

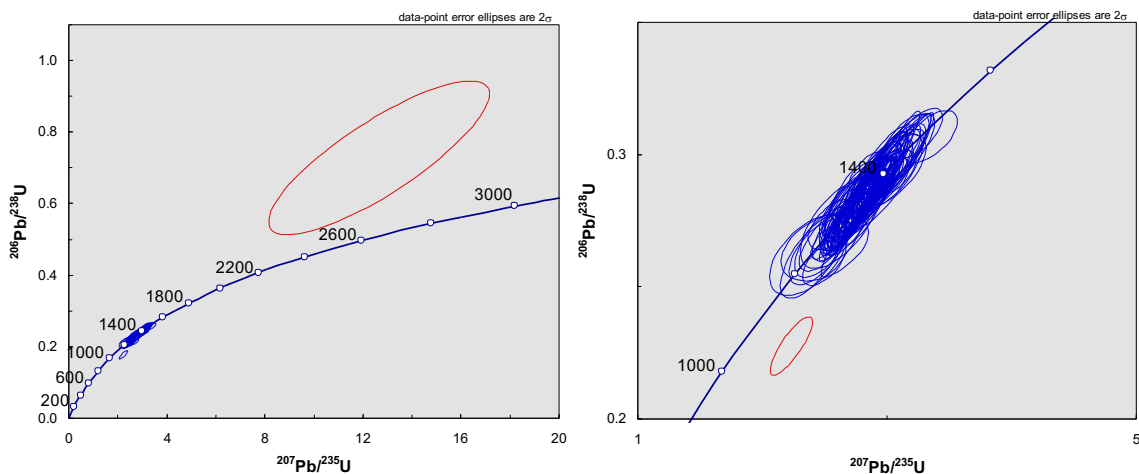
Blaubeker Clast

The probability density plot for a clast in the Blaubeker Formation (graph 9, photo of clast is shown in figure 15) shows that the main population of U-Pb ages falls in the range of ca. 1200-1500 Ma; with the oldest zircon being 1481 ± 19 Ma. Although the youngest zircon dates to 606 ± 10 Ma, this measurement only accounts for one zircon and therefore can be disregarded from the main population.



Graph 9: Probability Density plot showing the distribution of zircon ages of Blaubeker Clast

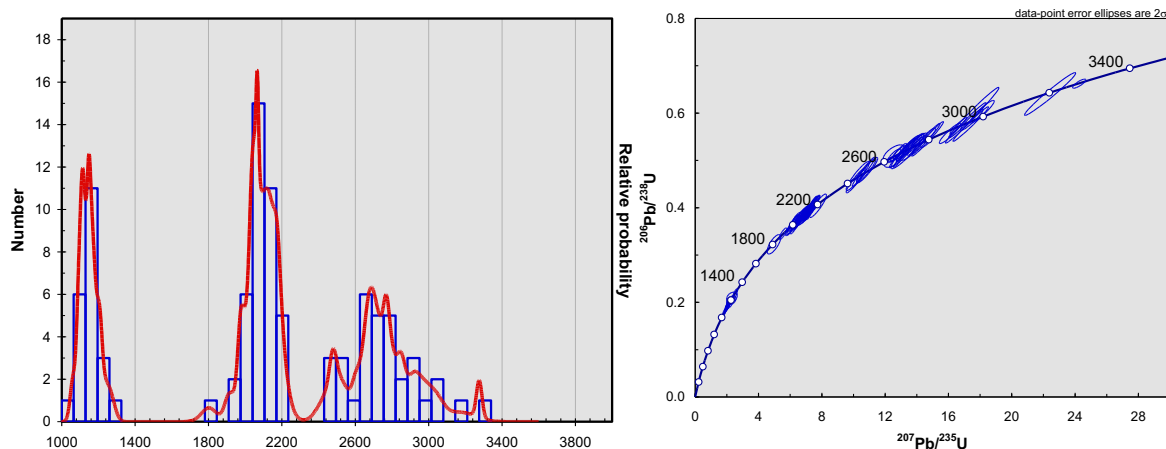
Moreover, all zircons plot on the Concordia, however with two exceptions (graph 10).



Graph 10: Concordia Plots of a clast sampled in the Blaubecker Formation

Kuibis Formation

The probability density plot for the Kuibis Formation (graph 11A) shows that there are possibly two main populations of U-Pb ages; i.e. ca. 1000-1300 Ma and ca. 1900-2200 Ma, with the youngest zircon dating to 1034 ± 47 Ma and the oldest dating to 3276 ± 30 Ma. All zircons plot along the Concordia (graph 11B).



Graph 11: (left) Probability Density plot showing the distribution of zircon ages of Kuibis Formation (right) Concordia Plot of Kuibis Formation

EMPA

The follow tables show the results from the microprobe analysis done at TU-Freiberg, full tables are found in appendix F.

Klein Aub Formation

*Table 11: EMPA data for Klein Aub Formation with mean value and standard deviation for each measured grain - Magnetic Fraction. *Boron cannot be measured by this technique, so a standard of 10.5 wt% must be added to the total, given by Prof. Bernhard Schulz at Institut für Mineralogie der TU Freiberg*

	Tourmaline	Tiamo-magnetic or titanohematite	Ilmenite	Titanite								Magnetite											
				1	2	3	1	1	2	3	4	5	6	7	1	2	3	4	5	6	7	8	9
Na ₂ O	Mean	2.0196	2.569	1.936	0.019	0.001	0	0.018	0.021	0.016	0.010	0.018	0.021	0	0.009	0.042	0.5	0.0355	0.062	0.0044	0.035	0.054	0.008
	SD	0.055	2.160	0.052	0.824	0.002	0.000	0.014	0.021	0.016	0.017	0.015	0.021	0.000	0.015	0.044	0.004	0.045	0.004	0.025	0.038	0.012	
K ₂ O	Mean	0.050	0.063	0.006	0.101	0.032	0.019	0.002	0.014	0.213	0.005	0.199	0.013	0.000	0.497	0.131	0.016	0.235	0.203	0.035	0.006	0.005	
	SD	0.007	0.045	0.005	0.123	0.038	0.019	0.003	0.009	0.056	0.005	0.100	0.013	0.000	0.247	0.115	0.002	0.222	0.143	0.032	0.004	0.003	
MnO	Mean	0.101	0.234	0.016	0.078	0.068	0.091	0.009	0.048	0.104	0.016	0.068	0.054	0.052	0.118	0.052	0.147	0.090	0.071	0.084	0.047	0.411	
	SD	0.002	1.351	0.016	0.050	0.039	0.020	0.005	0.026	0.092	0.018	0.068	0.028	0.002	0.130	0.019	0.073	0.020	0.023	0.038	0.043	0.124	
TiO ₂	Mean	0.998	0.334	0.298	6.667	53.264	37.66	40.93	41.8	33.57	72.368	31.806	35.399	0.212	9.188	14.070	32.936	1.023	2.963	6.781	0.865	11.637	
	SD	0.011	17.184	0.094	3.366	12.755	0.191	5.358	4.581	0.183	34.061	2.060	4.695	0.014	6.876	2.521	1.647	0.023	0.337	3.494	0.541	2.191	
MgO	Mean	2.797	0.334	8.689	0.360	0.065	0.000	0.035	0.075	0.000	1.076	0.377	0.000	0.196	0.044	0.000	0.106	0.106	0.322	0.000	0.087		
	SD	0.142	0.153	0.199	0.576	0.092	0.000	0.035	0.017	0.000	0.971	0.364	0.000	0.148	0.044	0.000	0.027	0.106	0.379	0.000	0.122		
CaO	Mean	0.221	0.042	1.334	0.068	0.093	28.08	21.79	21.58	27.48	11.964	26.398	27.162	0.019	2.251	0.071	0.060	0.108	0.052	0.081	0.036	0.043	
	SD	0.004	0.5589	0.069	0.027	0.039	0.016	1.647	6.207	0.814	7.999	1.683	4.639	0.004	2.948	0.002	0.004	0.026	0.002	0.020	0.010	0.007	
FeO	Mean	11.451	16.429	3.918	79.941	40.422	0.790	8.574	2.440	1.538	1.866	1.940	2.778	88.395	69.472	73.089	58.421	82.938	83.537	79.900	87.864	77.969	
	SD	0.084	8.141	0.108	40.511	13.379	0.091	2.922	0.880	0.329	2.161	0.947	1.317	0.127	34.644	3.296	1.189	1.010	1.992	3.677	0.220	2.292	
Cr ₂ O ₃	Mean	0.001	0.010	0.050	0.050	0.001	0.000	0.014	0.000	0.016	0.035	0.024	0.004	0.036	0.002	0.043	0.000	0.053	0.000	0.283	0.001	0.203	
	SD	0.001	1.925	0.019	0.127	0.002	0.000	0.020	0.000	0.016	0.038	0.020	0.004	0.008	0.003	0.030	0.000	0.045	0.000	0.149	0.001	0.005	
Al ₂ O ₃	Mean	32.755	30.603	31.565	1.025	0.188	1.262	3.189	1.192	2.910	0.257	4.731	4.011	0.067	1.998	0.770	0.049	0.938	0.834	1.079	0.000	0.075	
	SD	0.074	7.527	0.422	1.313	0.234	0.025	0.292	0.158	0.151	0.151	1.412	0.342	0.020	1.210	0.430	0.049	0.448	0.593	0.421	0.01	0.105	
V ₂ O ₃	Mean	0.047	0.017	0.014	0.415	1.023	0.648	0.773	0.857	0.663	1.416	0.887	0.650	0.200	0.217	1.262	0.639	0.055	0.433	0.542	0.044	0.340	
	SD	0.034	0.021	0.018	0.209	0.867	0.028	0.133	0.165	0.040	0.658	0.242	0.067	0.054	0.152	0.018	0.001	0.006	0.130	0.234	0.031	0.060	
SiO ₂	Mean	35.104	34.986	36.737	1.170	0.402	30.096	23.565	23.285	32.572	12.515	30.474	23.536	0.073	5.447	0.950	0.468	2.728	1.386	0.765	0.176	0.117	
	SD	0.043	17.461	0.085	1.261	0.407	0.087	1.763	6.624	1.694	8.758	0.724	2.508	0.025	3.851	0.600	0.309	0.734	0.742	0.651	0.047	0.166	
Total	Mean	85.54*	85.62*	84.56*	89.894	95.561	98.65	98.87	91.27	99.15	100.45	97.623	94.005	89.055	90.526	92.749	88.336	89.588	89.907	89.093	90.895		

	SD	0,101	0,228	0,286	0,636	0,076	0,079	0,649	7,008	0,158	50,271	1,113	4,677	0,095	45,692	0,398	2,664	0,441	0,084	0,486	0,292	0,831
--	----	-------	-------	-------	-------	-------	-------	-------	-------	-------	--------	-------	-------	-------	--------	-------	-------	-------	-------	-------	-------	-------

Aubures Formation

Table 12: EMPA data for Aubures Formation with mean value and standard deviation for each measured grain - Magnetic Fraction. *Boron cannot be measured by this technique, so a standard of 10.5 wt% must be added to the total, given by Prof. Bernhard Schulz at Institut für Mineralogie der TU Freiberg

	Tourmaline	Titanite				Magnetite								
	1	1	2	3	4	1	2	3	4	5	6	7	8	
Na2O	Mean	1,900	0,003	0,0192	0,016	0,022	0,006	0,000	0,005	0,018	0,020	0,000	0,003	0,018
	SD	0,388	0,003	0,030	0,018	0,015	0,011	0,000	0,009	0,022	0,021	0,000	0,005	0,015
K2O	Mean	0,0417	0,003	0,0389	0,000	0,025	0,009	0,006	0,010	0,062	0,001	0,050	0,002	0,005
	SD	0,028	0,003	0,075	0,000	0,017	0,009	0,008	0,013	0,065	0,002	0,050	0,003	0,004
MnO	Mean	0,0904	0,112	0,107	0,030	0,006	0,080	0,359	0,012	0,311	0,112	0,096	0,168	0,072
	SD	0,029	0,016	0,032	0,026	0,003	0,039	0,118	0,009	0,131	0,043	0,005	0,072	0,033
TiO2	Mean	0,310	37,775	36,322	36,977	36,079	0,174	3,331	0,070	5,520	0,140	0,743	0,195	0,127
	SD	0,113	0,057	0,714	0,164	6,176	0,034	2,300	0,016	1,067	0,083	0,375	0,174	0,049
MgO	Mean	7,058	0	0,026	0,001	0,561	0,000	0,025	0,066	0,127	0,000	0,000	0,000	0,000
	SD	0,492	0,000	0,052	0,001	0,362	0,000	0,046	0,115	0,129	0,000	0,000	0,000	0,000
CaO	Mean	0,622	28,151	28,072	28,724	23,194	0,016	0,090	0,023	0,063	0,013	0,051	0,030	0,033
	SD	0,222	0,024	0,395	0,126	2,561	0,006	0,033	0,010	0,009	0,007	0,009	0,011	0,022
FeO	Mean	6,2721	0,890	1,385	1,434	0,811	87,980	83,830	87,490	81,440	87,946	85,723	88,299	85,881
	SD	2,204	0,038	0,398	0,090	0,081	0,256	2,431	0,588	1,051	0,513	0,015	0,774	0,377
C2O3	Mean	0,041	0,024	0,014	0,086	0,021	0,049	0,045	0,039	0,112	0,021	0,009	0,047	2,604
	SD	0,001	0,017	0,014	0,058	0,013	0,026	0,004	0,024	0,028	0,021	0,009	0,031	0,066
Al2O3	Mean	31,383	1,388	1,593	1,274	3,850	0,296	0,285	0,073	1,058	0,110	0,232	0,041	0,000
	SD	1,340	0,035	0,244	0,027	1,058	0,055	0,068	0,102	0,285	0,031	0,107	0,043	0,000
V2O3	Mean	0,027	0,757	0,700	0,820	0,708	0,215	0,130	0,085	0,342	0,290	0,025	0,191	0,291
	SD	0,020	0,007	0,031	0,040	0,120	0,035	0,023	0,012	0,057	0,019	0,025	0,048	0,037
SiO2	Mean	35,927	30,221	30,108	30,445	30,572	0,054	0,338	0,391	0,698	0,061	0,484	0,213	0,067
	SD	0,718	0,188	0,258	0,302	2,630	0,047	0,092	0,343	0,489	0,046	0,224	0,148	0,049
Total	Mean	83,67*	99,324	98,381	99,806	95,849	88,878	88,440	88,264	89,751	88,714	87,412	89,188	89,099
	SD	0,451	0,075	0,627	0,291	2,206	0,183	0,391	0,209	0,453	0,028	0,436	0,314	

Table 13: EMPA data for Autubres Formation with mean value and standard deviation for each measured grain - Zircon Fraction

	Ilmenite (?)	Rutile	Titanite									
	1	1	2	3	4	1	2	3	4	5	6	7
Na2O	Mean	0	0	0.009	0.011	0.045	0.000	0.009	0.014	0.021	0.014	0.000
	SD	0	0	0.020	0.011	0.103	0.000	0.017	0.014	0.015	0.016	0.000
K2O	Mean	0.008	0.014	0.000	0.009	0.031	0.001	0.002	0.005	0.010	0.008	0.002
	SD	0.008	0.008	0.000	0.014	0.015	0.001	0.003	0.005	0.006	0.011	0.002
MnO	Mean	0.062	0.013	0.010	0.009	0.016	0.051	0.035	0.042	0.050	0.054	0.047
	SD	0.021	0.009	0.012	0.014	0.024	0.001	0.038	0.006	0.052	0.018	0.005
TiO2	Mean	66.553	99.589	100.993	100.281	98.012	39.135	25.586	37.273	38.220	34.886	35.961
	SD	4.245	0.069	0.566	0.465	5.852	0.304	28.949	0.005	18.967	0.649	0.495
MgO	Mean	0.098	0.000	0.000	0.000	0.041	0.000	0.000	0.000	0.000	0.000	0.000
	SD	0.085	0.000	0.000	0.000	0.094	0.000	0.000	0.000	0.000	0.000	0.000
CaO	Mean	3.958	0.037	0.026	0.024	0.101	28.597	19.311	28.883	28.125	27.447	28.752
	SD	0.061	0.004	0.003	0.013	0.125	0.317	21.642	0.038	14.054	1.269	0.227
FeO	Mean	26.626	0.143	0.138	0.081	0.291	0.458	0.414	0.892	0.597	1.304	0.943
	SD	3.151	0.038	0.051	0.041	0.523	0.150	0.453	0.023	0.269	0.466	0.051
Cr2O3	Mean	0.020	0.103	0.020	0.037	0.022	0.055	0.012	0.000	0.032	0.012	0.037
	SD	0.021	0.066	0.030	0.032	0.035	0.058	0.022	0.000	0.027	0.029	0.031
Al2O3	Mean	0.544	0.070	0.032	0.028	0.255	0.755	0.886	1.550	1.171	1.883	2.373
	SD	0.238	0.021	0.014	0.026	0.488	0.150	0.986	0.017	0.617	0.772	0.017
V2O3	Mean	1.121	1.683	1.606	1.719	1.582	0.753	0.471	0.782	0.702	0.725	0.674
	SD	0.106	0.048	0.083	0.829	0.104	0.085	0.417	0.035	0.352	0.033	0.034
SiO2	Mean	2.081	0.015	0.009	0.000	0.835	30.318	20.569	30.674	30.223	28.810	30.511
	SD	1.192	0.015	0.020	0.000	1.843	0.184	17.983	0.052	0.158	3.476	0.158
Total	Mean	97.482	101.666	102.843	102.192	101.230	100.122	67.296	100.113	99.149	95.143	99.300
	SD	1.419	0.064	0.671	0.514	2.804	0.578	59.575	0.021	0.414	5.769	0.221
												1.333

Matchless Amphibolite

Table 14: EMPA data for Matchless Amphibolite with mean value and standard deviation for each measured grain - Magnetic Fraction

	Amphibole												Titanite/Sphene				Pyroxene?		
	1	2	3	4	5	6	7	8	9	10	11	12	1	2	3	4	1	2	
Na2O	Mean	0,934	1,018	1,229	1,174	1,184	1,164	1,082	1,189	1,186	0,913	1,196	1,141	0,180	0,000	0,005	0,328	0,020	0,003
	SD	0,188	0,165	0,020	0,089	0,022	0,023	0,029	0,039	0,042	0,527	0,037	0,030	0,267	0,000	0,007	0,464	0,020	0,004
K2O	Mean	0,339	0,394	0,430	0,453	0,394	0,324	0,460	0,468	0,422	0,319	0,410	0,484	0,022	0,009	0,007	0,121	0,005	0,000
	SD	0,115	0,153	0,019	0,095	0,036	0,007	0,036	0,009	0,032	0,179	0,016	0,065	0,018	0,007	0,006	0,165	0,004	0,000
MnO	Mean	0,291	0,269	0,227	0,313	0,207	0,155	0,274	0,299	0,250	0,216	0,235	0,247	0,064	0,074	0,034	0,110	3,905	4,245
	SD	0,017	0,028	0,024	0,163	0,025	0,031	0,012	0,040	0,031	0,010	0,015	0,028	0,025	0,032	0,012	0,104	0,430	0,776
TiO2	Mean	0,320	0,330	0,488	3,154	0,430	0,493	0,502	0,468	0,428	0,391	0,483	0,561	27,859	37,367	37,484	25,252	0,068	0,067
	SD	0,079	0,049	0,024	4,526	0,025	0,036	0,046	0,051	0,015	0,128	0,044	0,109	16,109	0,306	0,313	17,565	0,032	0,056
MgO	Mean	10,611	10,073	9,278	9,073	9,734	10,715	9,936	9,095	9,599	7,089	9,682	9,106	0,000	0,000	0,000	3,395	2,094	2,212
	SD	1,659	1,301	0,117	0,479	0,072	0,062	0,347	0,054	0,206	4,060	0,093	0,203	0,000	0,000	0,000	4,801	0,034	0,063
CaO	Mean	11,909	11,808	11,611	10,927	11,813	11,667	11,843	11,626	14,577	11,740	11,668	26,159	28,784	28,620	23,198	8,865	7,219	
	SD	0,259	0,271	0,074	1,220	0,089	0,027	0,092	0,006	0,101	5,072	0,045	0,059	4,160	0,130	0,102	7,921	0,255	0,340
FeO	Mean	14,240	14,530	14,887	16,150	14,237	14,058	14,632	14,891	14,495	12,350	14,378	14,705	0,149	0,249	0,200	5,130	26,291	27,569
	SD	0,938	0,507	0,061	2,948	0,287	0,105	0,302	0,101	0,287	3,766	0,163	0,151	0,045	0,022	0,030	6,607	0,905	0,733
Cr2O3	Mean	0,013	0,018	0,039	0,023	0,002	0,063	0,047	0,139	0,114	0,045	0,091	0,049	0,009	0,014	0,038	0,033	0,026	0,040
	SD	0,014	0,018	0,032	0,017	0,003	0,023	0,016	0,016	0,050	0,035	0,026	0,032	0,009	0,021	0,032	0,047	0,019	0,037
Al2O3	Mean	12,377	13,268	14,951	14,389	14,809	13,408	13,921	15,264	14,696	18,156	14,816	15,496	9,992	2,400	2,122	5,819	20,266	20,376
	SD	2,791	2,146	0,282	1,492	0,237	0,162	0,731	0,044	0,354	5,042	0,154	0,401	13,216	0,042	0,118	5,189	0,142	0,157
V2O3	Mean	0,059	0,032	0,049	0,077	0,084	0,027	0,060	0,025	0,095	0,062	0,032	0,066	0,536	0,740	0,753	0,497	0,010	0,017
	SD	0,031	0,020	0,017	0,120	0,037	0,021	0,017	0,023	0,039	0,045	0,019	0,030	0,304	0,050	0,038	0,319	0,018	0,025
SiO2	Mean	45,862	45,191	43,816	41,078	44,336	45,106	44,374	43,533	43,663	42,722	43,650	43,037	34,420	31,094	31,080	36,270	38,358	38,157
	SD	2,445	2,054	0,236	4,212	0,207	0,115	0,647	0,240	0,308	2,217	0,111	0,548	6,029	0,103	0,083	6,974	0,378	0,144
Total	Mean	96,956	97,030	97,003	96,811	97,229	97,180	97,131	96,997	96,571	96,841	96,713	96,561	99,389	100,731	100,743	100,153	99,909	99,905
	SD	0,934	0,635	0,154	0,219	0,790	0,242	0,313	0,447	0,352	0,764	0,158	0,297	1,953	0,413	0,339	1,521	0,390	0,502

Table 15: EMPA data for Matchless Amphibolite with mean value and standard deviation for each measured grain - Zircon Fraction

	Titanite										Rutile		
	1	2	3	4	5	6	7	8	9	10	11	1	2
Na2O	Mean	0,0027	0,010	0,007	0,010	0,019	0,003	0,007	0,015	0,018	0,010	0,002	0,000
	SD	0,003	0,018	0,007	0,018	0,016	0,008	0,012	0,020	0,018	0,008	0,004	0,019
K2O	Mean	0,001	0,003	0,006	0,000	0,006	0,004	0,004	0,002	0,001	0,004	0,006	0,002
	SD	0,001	0,006	0,005	0,001	0,008	0,008	0,003	0,004	0,001	0,006	0,007	0,006
MnO	Mean	0,045	0,055	0,074	0,041	0,044	0,079	0,063	0,065	0,052	0,067	0,077	0,004
	SD	0,026	0,018	0,008	0,015	0,029	0,035	0,067	0,026	0,001	0,075	0,044	0,010
TiO2	Mean	37,114	37,973	36,586	37,273	37,147	37,043	36,984	36,346	36,976	36,705	36,941	99,924
	SD	0,268	0,615	0,321	0,378	18,565	0,221	18,479	1,095	0,200	18,312	0,738	49,783
MgO	Mean	0,000	0,000	0,000	0,000	0,000	0,000	0,000	0,000	0,000	0,000	0,000	0,000
	SD	0,000	0,000	0,000	0,000	0,000	0,000	0,000	0,000	0,001	0,000	0,000	0,000
CaO	Mean	28,920	28,736	28,928	28,945	28,614	28,247	28,635	28,332	29,089	28,545	28,686	0,025
	SD	0,134	0,135	0,102	0,095	14,174	0,817	14,267	0,901	0,200	14,322	0,556	0,012
FeO	Mean	0,229	0,443	0,196	0,227	0,242	0,197	0,200	0,218	0,230	0,225	0,240	0,485
	SD	0,014	0,079	0,007	0,023	0,128	0,055	0,122	0,052	0,031	0,134	0,069	0,319
C2O3	Mean	0,009	0,000	0,015	0,005	0,022	0,021	0,023	0,011	0,022	0,013	0,018	0,052
	SD	0,009	0,000	0,015	0,010	0,017	0,034	0,021	0,015	0,022	0,014	0,024	0,036
Al2O3	Mean	2,272	1,585	2,489	2,249	2,305	2,212	2,196	2,419	2,299	2,313	2,102	0,054
	SD	0,028	0,066	0,118	0,123	1,161	0,098	1,135	0,131	0,080	1,150	0,089	0,049
V2O3	Mean	0,624	0,765	0,589	0,595	0,637	0,664	0,739	0,566	0,600	0,561	0,646	1,750
	SD	0,023	0,031	0,014	0,044	0,319	0,025	0,353	0,041	0,031	0,274	0,055	0,828
SiO2	Mean	30,463	30,438	30,639	30,793	30,389	30,504	30,405	31,508	31,806	30,287	31,556	0,000
	SD	0,161	0,140	0,172	0,159	0,189	0,335	0,150	2,605	0,001	0,340	1,572	0,000
Total	Mean	99,679	100,007	99,528	100,139	99,423	98,974	99,254	99,484	101,093	98,730	100,275	102,240
	SD	0,459	0,323	0,315	0,206	0,150	1,212	0,559	0,642	0,473	0,422	0,275	0,366
													0,430

Blaubeker Formation

Table 16: EMPA data for Blaubeker Formation with mean value and standard deviation for each measured grain - Magnetic Fraction

	Magnetite				Ilmenite			Rutile
	1	2	3	4	1	2	3	1
Na2O	Mean	0.006	0.019	0.000	0.005	0.015	0.030	0.010
	SD	0.007	0.020	0.000	0.007	0.025	0.035	0.010
K2O	Mean	0.036	0.018	0.134	0.002	0.011	0.012	0.052
	SD	0.059	0.014	0.189	0.002	0.010	0.009	0.005
MnO	Mean	0.049	0.022	0.070	0.095	0.015	0.104	0.000
	SD	0.030	0.014	0.024	0.053	0.012	0.032	0.329
TiO2	Mean	0.442	4.578	0.000	0.651	54.353	0.014	60.542
	SD	0.133	2.180	0.000	0.191	12.998	0.017	1.044
MgO	Mean	0.000	0.037	1.162	0.000	0.002	0.984	0.000
	SD	0.000	0.037	0.314	0.000	0.003	0.038	0.000
CaO	Mean	0.017	0.024	0.317	0.037	0.075	0.417	0.023
	SD	0.009	0.013	0.056	0.018	0.078	0.017	0.008
FeO	Mean	88.164	83.457	74.209	87.691	38.271	74.838	35.501
	SD	0.569	1.709	1.861	0.298	14.260	0.095	0.560
C2O3	Mean	0.017	0.009	0.008	0.032	0.017	0.023	0.002
	SD	0.019	0.009	0.006	0.016	0.018	0.017	0.002
Al2O3	Mean	0.148	0.453	0.676	0.027	0.123	0.000	0.022
	SD	0.169	0.117	0.956	0.033	0.076	0.000	0.158
V2O3	Mean	0.087	0.113	0.013	0.041	1.042	0.015	1.195
	SD	0.011	0.044	0.009	0.034	0.185	0.013	0.003
SiO2	Mean	0.283	0.946	5.202	0.337	0.317	4.659	0.115
	SD	0.341	0.194	0.923	0.246	0.216	0.226	0.720
Total	Mean	89.251	89.677	81.791	88.917	94.240	81.095	97.462
	SD	0.081	0.783	0.494	0.612	94.226	0.349	0.584
								4.647

Numees Formation

Table 17: EMPA data for Numees Formation with mean value and standard deviation for each measured grain - Magnetic Fraction

	Garnet						Titanite						Rutile									
	1	2	3	4	5	6	7	8	9	10	1	2	3	4	1	2	3	4	5	6		
Na2O	Mean	0.008	0.007	0.024	0.016	0.004	0.009	0.071	0.011	0.029	0.002	0.008	0.013	0.001	0.030	0.012	0.002	0.000	0.007	0.011	0.000	
	SD	0.008	0.013	0.021	0.020	0.004	0.007	0.038	0.005	0.017	0.004	0.009	0.015	0.001	0.047	0.014	0.004	0.000	0.005	0.010	0.000	
K2O	Mean	0.002	0.005	0.003	0.006	0.006	0.003	0.005	0.006	0.006	0.005	0.002	0.011	0.005	0.000	0.006	0.003	0.002	0.009	0.006	0.005	
	SD	0.003	0.006	0.005	0.008	0.007	0.003	0.007	0.006	0.003	0.004	0.002	0.005	0.000	0.005	0.003	0.009	0.007	0.007	0.006		
MnO	Mean	1.624	0.118	0.358	0.655	0.527	3.265	3.545	0.417	0.363	0.192	0.037	0.050	0.062	0.029	0.019	0.015	0.004	0.016	0.012	0.026	
	SD	0.030	0.029	0.041	0.036	0.019	0.060	0.139	0.002	0.019	0.047	0.021	0.021	0.027	0.038	0.015	0.011	0.006	0.012	0.017	0.022	
TiO2	Mean	0.022	0.104	0.065	0.033	0.036	0.013	0.070	0.028	0.018	0.034	43.496	36.252	37.022	70.404	101.812	101.248	101.594	102.119	102.733	100.960	
	SD	0.038	0.024	0.034	0.030	0.037	0.019	0.009	0.003	0.014	0.047	3.497	0.680	0.279	27.216	0.397	0.206	0.308	0.267	0.326	0.824	
MgO	Mean	5.244	0.017	8.421	4.408	8.177	1.645	2.881	7.638	6.939	8.696	0.002	0.000	0.000	0.003	0.000	0.000	0.000	0.000	0.000	0.000	
	SD	0.062	0.012	0.056	0.024	0.050	0.042	0.201	0.177	0.065	0.061	0.003	0.000	0.006	0.000	0.000	0.000	0.000	0.000	0.000		
CaO	Mean	3.156	23.215	6.974	1.091	2.584	2.080	8.334	1.596	1.349	0.736	25.013	28.394	28.051	12.670	0.013	0.015	0.021	0.020	0.022	0.032	
	SD	0.024	0.201	0.045	0.038	0.024	0.217	0.082	0.000	0.017	0.034	3.678	0.336	0.173	11.860	0.005	0.011	0.011	0.004	0.001	0.013	
FeO	Mean	30.34	5	9.448	22.851	34.856	27.924	34.884	26.023	29.671	31.196	30.220	4.147	0.750	1.077	1.952	0.142	0.470	0.261	0.159	0.467	0.169
	SD	0.312	0.135	0.192	0.179	0.087	0.061	0.367	0.012	0.143	0.122	4.269	0.012	0.077	2.581	0.049	0.023	0.051	0.024	0.118	0.026	
Cr2O3	Mean	0.032	0.007	0.064	0.041	0.062	0.029	0.002	0.003	0.062	0.014	0.023	0.026	0.015	0.031	0.086	0.041	0.052	0.183	0.052	0.082	
	SD	0.038	0.012	0.023	0.025	0.045	0.030	0.003	0.027	0.018	0.019	0.031	0.012	0.046	0.029	0.031	0.014	0.029	0.021	0.047		
Al2O3	Mean	21.03	24.466	21.385	20.936	21.590	20.560	20.416	21.350	21.292	21.615	0.852	2.978	1.586	0.896	0.045	0.026	0.014	0.033	0.015	0.081	
	SD	0.125	24.414	0.080	0.071	0.093	0.132	0.087	0.007	0.069	0.137	0.058	0.094	0.023	0.965	0.027	0.013	0.013	0.010	0.010		
V2O3	Mean	0.015	38.105	0.006	0.021	0.036	0.020	0.077	0.000	0.028	0.030	0.932	0.775	0.788	1.478	2.310	2.210	2.170	2.230	2.066	2.457	
	SD	0.016	0.167	0.006	0.021	0.040	0.020	0.027	0.000	0.025	0.022	0.138	0.014	0.025	0.537	0.022	0.015	0.038	0.019	0.054	0.015	
SiO2	Mean	38.26	95.534	39.372	37.909	39.065	37.145	37.952	38.532	38.317	39.195	26.720	30.652	30.216	13.607	0.009	0.013	0.000	0.000	0.000	0.007	
	SD	0.077	0.427	0.270	0.229	0.157	0.183	0.066	0.047	0.178	0.246	3.626	0.363	0.214	13.016	0.015	0.014	0.000	0.000	0.000	0.009	
Total	Mean	99.75	0.007	99.723	99.971	100.011	99.654	99.376	99.261	99.600	100.738	101.231	99.902	98.832	101.100	104.455	104.044	104.118	104.777	105.383	103.818	
	SD	0.482	0.013	0.284	0.480	0.308	0.310	0.372	0.250	0.393	0.440	0.548	0.389	0.488	2.729	0.256	0.255	0.295	0.237	0.422	0.760	
Magnetite																						
Amphibole																						
1 2 3 4 5 1																						

Na ₂ O	Mean	0.017	0.025	0.011	0.056	0.020
	SD	0.023	0.025	0.012	0.078	0.022
K ₂ O	Mean	0.007	0.342	0.003	0.009	0.086
	SD	0.007	0.921	0.006	0.010	0.117
MnO	Mean	0.178	0.010	0.159	0.066	0.427
	SD	0.112	0.013	0.151	0.049	0.346
TiO ₂	Mean	30.96	24.044	11.578	13.990	7.609
	SD	15.75	0	6.044	6.610	4.438
MgO	Mean	0.027	0.077	0.000	0.000	3.727
	SD	0.024	0.133	0.000	0.000	5.110
CaO	Mean	0.030	0.052	0.009	0.016	0.090
	SD	0.020	0.014	0.004	0.016	0.117
FeO	Mean	60.39	65.098	79.373	77.263	59.572
	SD	3	3.570	0.802	4.673	27.934
Cr ₂ O ₃	Mean	0.045	0.028	0.059	0.037	0.065
	SD	0.030	0.026	0.023	0.040	0.027
Al ₂ O ₃	Mean	0.048	0.906	0.008	0.033	6.095
	SD	0.027	1.177	0.008	0.037	8.400
V ₂ O ₃	Mean	0.864	0.487	0.523	0.468	0.381
	SD	0.223	0.116	0.062	0.141	0.354
SiO ₂	Mean	0.245	1.625	0.013	0.006	9.248
	SD	0.407	2.212	0.022	0.012	12.990
Total	Mean	92.82	92.895	91.735	91.944	87.318
	SD	0.551	0.560	0.128	0.315	6.081

Holgat Formation

Table 18: EMPA data for Holgat Formation with mean value and standard deviation for each measured grain - Magnetic Fraction. *Boron cannot be measured by this technique, so a standard of 10.5 wt% must be added to the total, given by Prof. Bernhard Schulz at Institut für Mineralogie der TU Freiberg

	Tourmaline															Rutile									
	1	2	3	4	5	6	7	8	9	10	11	12	13	14	15	16	17	1	2	3	4	5	6	7	
Na2O	Mean	2,05	1,85	1,78	1,94	2,01	1,71	1,66	1,52	1,83	1,89	1,63	1,79	1,90	1,99	1,87	1,74	1,90	0,01	0,00	0,01	0,00	0,02	0,01	0,02
	SD	0,21	0,01	0,05	0,09	0,04	0,06	0,01	0,09	0,08	0,05	0,01	0,02	0,05	0,05	0,05	0,06	0,16	0,01	0,02	0,03	0,00	0,04	0,01	0,02
K2O	Mean	0,04	0,04	0,02	0,31	0,03	0,03	0,01	0,03	0,02	0,04	0,01	0,04	0,64	0,05	0,03	0,02	0,03	0,47	0,00	0,12	0,19	0,16	0,25	0,10
	SD	0,01	0,01	0,00	0,18	0,01	0,01	0,01	0,01	0,01	0,01	0,01	0,01	0,62	0,03	0,01	0,00	0,02	0,40	0,61	0,16	0,39	0,09	0,23	0,02
MnO	Mean	0,04	0,04	0,01	0,04	0,10	0,03	0,01	0,02	0,03	0,05	0,02	0,01	0,01	0,03	0,04	0,02	0,06	0,00	0,01	0,02	0,00	0,01	0,389	0,02
	SD	0,02	0,02	0,01	0,03	0,02	0,02	0,01	0,02	0,02	0,01	0,02	0,00	0,01	0,01	0,02	0,02	0,03	0,07	0,01	0,02	0,00	0,00	0,593	0,02
TiO2	Mean	0,69	0,84	0,48	0,75	0,46	0,93	1,20	0,70	0,68	0,62	0,68	0,75	0,95	0,51	0,98	0,74	0,62	88,21	98,46	96,95	93,61	85,64	94,01	95,28
	SD	0,01	0,11	0,16	0,04	0,13	0,03	0,12	0,21	0,05	0,02	0,17	0,05	0,07	0,06	0,14	0,04	0,36	10,87	14,94	8,84	3,74	19,78	1,88	2,73
MgO	Mean	6,48	4,51	6,47	6,11	4,26	4,56	4,99	5,00	4,60	5,73	5,58	6,03	6,30	6,96	5,30	5,20	5,07	0,23	0,00	0,01	0,78	0,01	0,45	0,13
	SD	1,25	0,43	0,17	0,29	0,10	0,10	0,06	0,15	0,06	0,50	0,15	0,01	0,07	0,26	0,03	0,06	0,05	0,23	0,01	0,40	0,02	0,16	0,19	
CaO	Mean	0,54	0,36	0,50	0,34	0,09	0,55	0,70	0,94	0,60	0,57	0,64	1,01	0,82	0,99	0,57	0,65	0,55	0,05	0,06	0,01	0,09	0,05	0,12	0,04
	SD	0,15	0,09	0,02	0,02	0,00	0,03	0,01	0,21	0,04	0,01	0,13	0,03	0,05	0,11	0,08	0,01	0,40	0,01	0,01	0,00	0,04	0,01	0,10	0,01
FeO	Mean	7,17	8,02	4,78	6,05	8,47	7,82	7,94	7,88	9,17	7,71	6,70	7,78	6,15	7,48	7,54	7,50	7,29	0,72	0,55	0,66	1,16	0,57	0,94	0,65
	SD	0,13	0,52	0,18	0,11	0,12	0,14	0,09	0,12	0,21	0,12	0,05	0,08	0,07	0,40	0,26	0,20	0,33	0,17	0,24	0,18	0,64	0,26	0,18	0,19
Cr2O3	Mean	0,02	0,00	0,03	0,03	0,00	0,02	0,04	0,12	0,01	0,07	0,03	0,05	0,16	0,01	0,03	0,02	0,01	0,00	0,11	0,07	0,02	0,11	0,08	
	SD	0,03	0,04	0,03	0,03	0,00	0,02	0,01	0,05	0,02	0,03	0,02	0,02	0,01	0,01	0,03	0,01	0,01	0,00	0,11	0,05	0,02	0,02	0,04	
Al2O3	Mean	30,51	32,86	33,31	32,29	32,29	32,29	32,1	32,6	31,89	32,1	32,8	31,5	32,1	30,9	32,67	33,1	33,0	1,17	0,03	0,11	1,10	0,40	1,06	0,36
	SD	1,89	0,28	0,21	0,34	0,07	0,26	0,30	0,37	0,36	0,33	0,32	0,05	0,16	0,14	0,11	0,05	0,36	1,17	1,63	0,17	0,66	0,29	0,49	0,18
V2O3	Mean	0,06	0,00	0,02	0,00	0,03	0,08	0,00	0,03	0,04	0,01	0,00	0,03	0,01	0,00	0,06	0,07	0,02	0,00	0,00	0,07	0,03	0,00	0,03	
	SD	0,05	0,09	0,04	0,00	0,05	0,02	0,00	0,04	0,05	0,02	0,00	0,04	0,02	0,00	0,04	0,05	0,02	0,00	0,00	0,09	0,05	0,00	0,07	
SiO2	Mean	35,20	35,11	35,93	36,14	35,7	34,7	35,3	34,6	35,27	35,3	35,3	34,6	34,9	35,3	35,34	35,4	35,1	9,38	0,00	0,72	1,78	11,99	1,70	2,28
	SD	0,14	0,06	0,11	0,22	0,05	0,36	0,08	0,35	0,21	0,21	0,03	0,02	0,13	0,23	0,26	0,15	0,45	9,25	13,17	0,87	1,70	20,63	0,89	2,81
Total	Mean	82,8*	83,63*	83,33*	84,0*	83,9*	83,4*	83,5*	84,1*	84,1*	83,4*	*	*	*	*	84,4*	*	*	100,3	99,21	98,66	98,81	98,89	98,67	98,99
	SD	0,39	0,33	81,56	0,22	0,15	0,37	0,14	0,22	0,08	0,25	0,07	0,08	0,11	0,40	0,34	0,46	0,24	0,41	1,17	0,13	1,23	0,83	0,29	0,22

Kuibis Formation

Table 19: EMPA data for Kuibis Formation with mean value and standard deviation for each measured grain - Magnetic Fraction

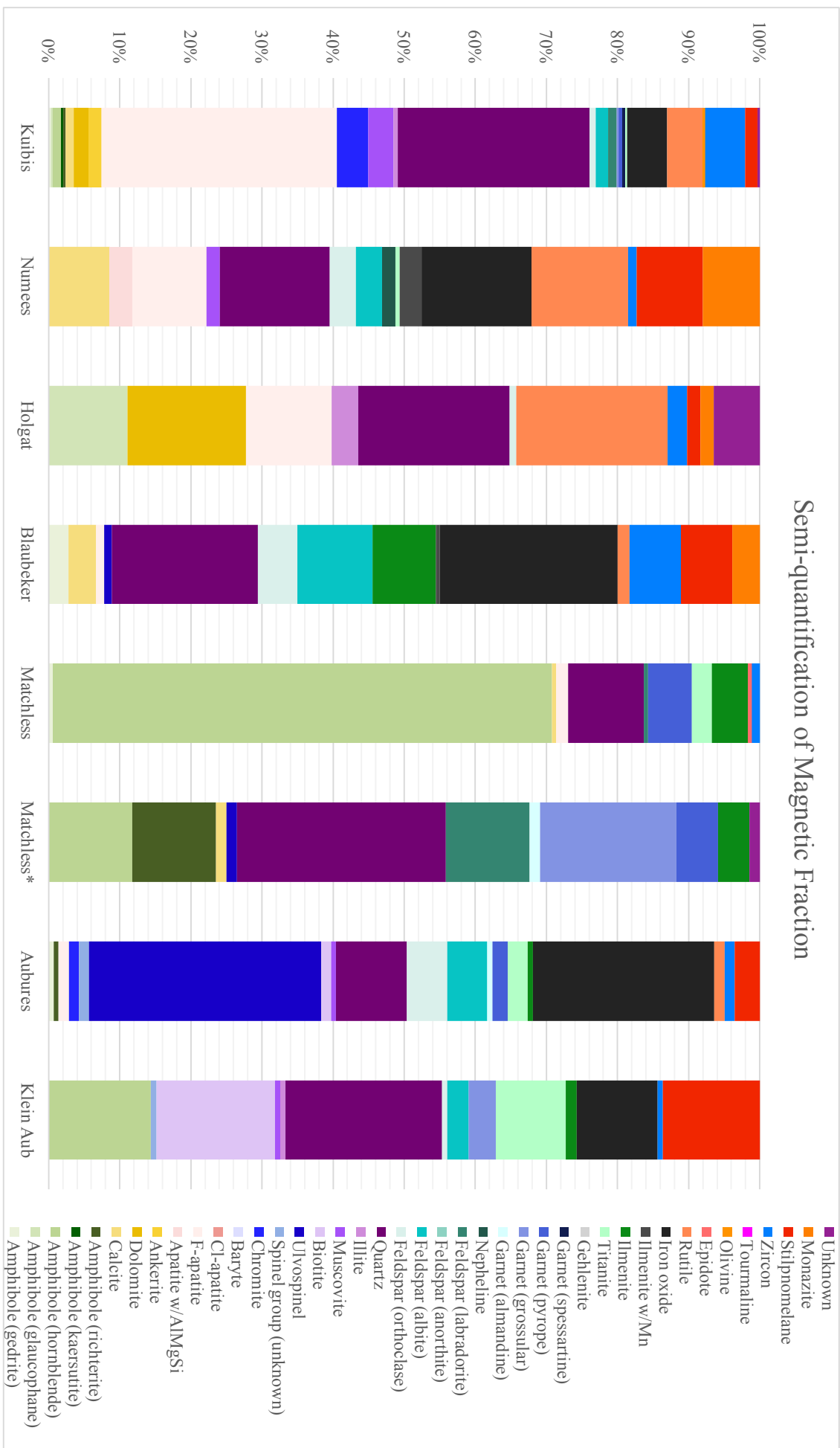
	Magnetite			Rutile			Tourmaline											
	1	2	3	1	2	3	4	5	6	1	2	3	4	5	6	7	1	
Na2O	Mean	0,030	0,025	0,050	0,034	0,020	0,018	0,000	0,000	0,011	2,253	2,118	2,074	2,301	1,744	0,007	1,702	2,253
	SD	0,033	0,018	0,038	0,025	0,029	0,018	0,000	0,000	0,008	0,015	0,045	0,057	0,225	0,052	0,007	0,021	0,015
K2O	Mean	0,004	0,098	0,003	0,013	0,010	0,005	0,006	0,005	0,009	0,063	0,033	0,017	0,033	0,041	0,006	0,037	0,063
	SD	0,007	0,111	0,001	0,012	0,006	0,006	0,005	0,006	0,007	0,006	0,009	0,010	0,020	0,009	0,006	0,002	0,006
MnO	Mean	0,012	0,055	0,004	0,016	0,007	0,009	0,012	0,007	0,022	0,145	0,115	0,060	0,052	0,115	14,317	0,103	0,145
	SD	0,012	0,056	0,006	0,014	0,008	0,013	0,009	0,011	0,022	0,028	0,017	0,022	0,032	0,023	0,155	0,013	0,028
TiO2	Mean	0,000	0,012	0,007	77,874	100,215	99,225	100,861	101,371	99,748	0,553	0,686	0,897	1,022	0,121	0,027	0,101	0,553
	SD	0,000	0,011	0,011	20,765	1,069	0,142	0,308	0,865	2,272	0,090	0,125	0,037	0,057	0,042	0,028	0,019	0,090
MgO	Mean	0,658	0,627	0,686	6,637	0,000	0,309	0,003	0,010	0,017	4,717	3,944	4,897	6,104	0,879	0,200	0,903	4,717
	SD	0,101	0,070	0,104	5,515	0,000	0,187	0,005	0,017	0,029	0,071	0,323	0,133	2,562	0,036	0,014	0,035	0,071
CaO	Mean	0,573	0,742	0,541	0,067	0,053	0,041	0,033	0,030	0,053	0,774	0,538	0,344	0,214	0,072	0,316	0,079	0,774
	SD	0,038	0,055	0,065	0,018	0,039	0,019	0,011	0,007	0,038	0,027	0,012	0,107	0,186	0,007	0,020	0,016	0,027
FeO	Mean	73,425	73,273	72,998	1,957	0,347	0,332	0,131	0,094	0,195	12,217	11,307	8,669	7,624	13,718	28,085	13,661	12,217
	SD	0,370	1,644	1,562	1,739	0,109	0,064	0,040	0,052	0,021	0,075	0,499	0,273	2,397	0,110	0,168	0,167	0,075
Cr2O3	Mean	0,004	0,016	0,023	0,082	0,013	0,042	0,066	0,026	0,025	0,012	0,018	0,039	0,024	0,004	0,032	0,033	0,012
	SD	0,004	0,027	0,023	0,045	0,018	0,033	0,049	0,021	0,021	0,018	0,023	0,026	0,022	0,005	0,023	0,006	0,018
Al2O3	Mean	0,012	0,532	0,000	4,020	0,083	0,282	0,050	0,045	0,056	28,175	29,978	31,263	30,419	31,819	19,818	31,656	28,175
	SD	0,014	0,174	0,000	3,481	0,060	0,112	0,010	0,042	0,025	0,178	0,088	0,196	1,138	0,122	0,043	0,096	0,178
V2O3	Mean	0,205	0,176	0,328	1,524	2,062	2,012	2,74	2,280	1,920	0,017	0,020	0,069	0,068	0,007	0,003	0,027	0,017
	SD	0,027	0,068	0,066	0,404	0,031	0,052	0,044	0,055	0,023	0,016	0,027	0,019	0,029	0,013	0,005	0,019	0,016
SiO2	Mean	3,678	4,221	3,301	6,179	0,226	0,731	0,049	0,059	0,100	35,535	35,445	36,041	36,459	35,562	36,979	35,373	35,535
	SD	0,309	0,670	0,152	5,311	0,321	0,492	0,057	0,055	0,146	0,245	0,106	0,153	0,707	0,184	0,037	0,059	0,245
Total	Mean	78,601	79,776	77,940	98,404	103,036	103,006	103,384	103,928	102,156	84,463	84,201	84,370	84,085	99,789	83,674	84,463	
	SD	0,571	1,477	1,562	5,214	0,595	0,337	0,289	0,797	1,995	0,361	0,376	0,089	0,167	0,188	0,118	0,319	0,361

Interpretation

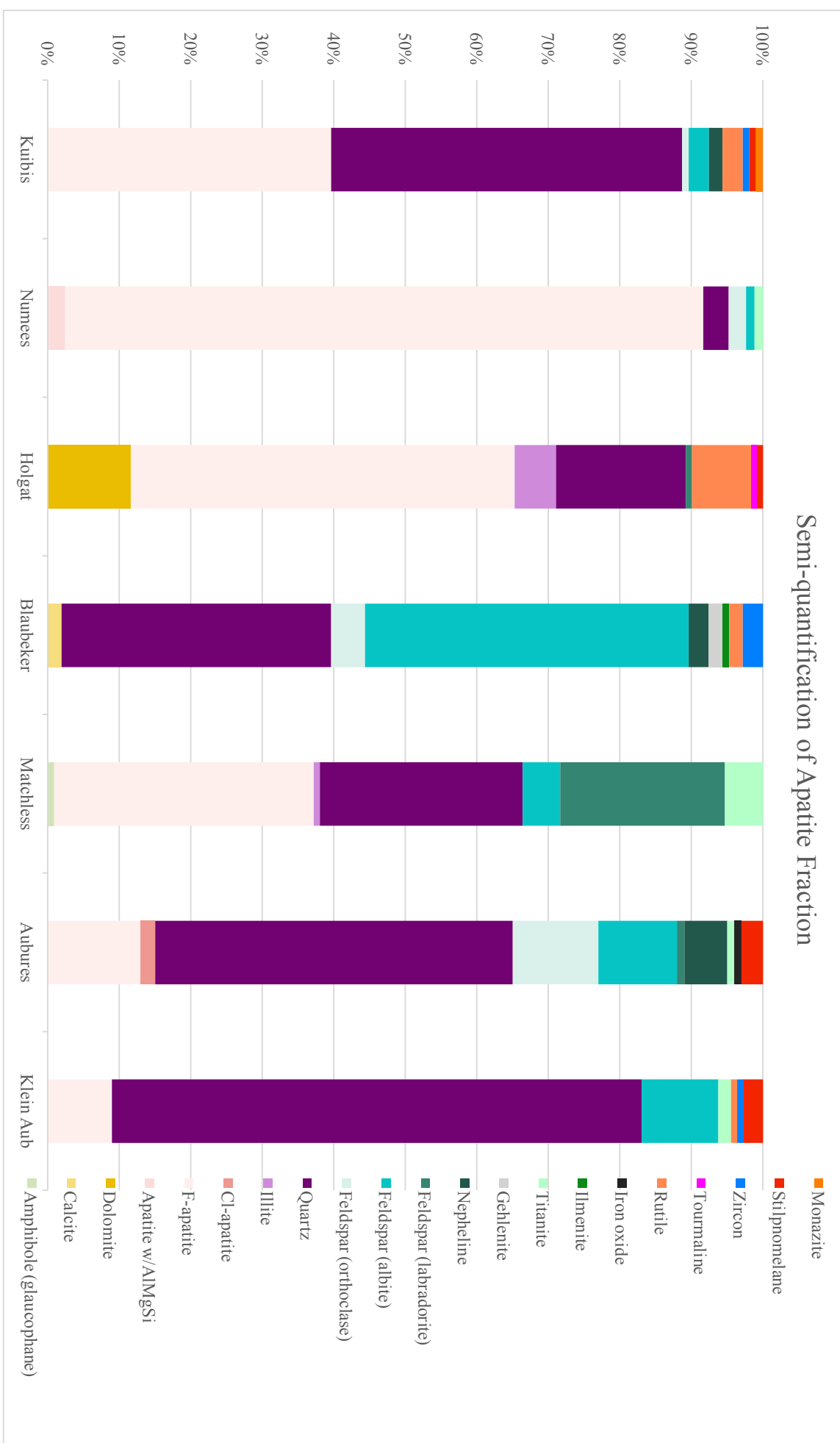
SEM & MLA

The following graphs (12-17) illustrate the different minerals identified using the SEM (graph 12-14) and the MLA (graph 15-17). The quantitative analysis carried out using the MLA scan compares somewhat to the semi-quantitative analysis carried out using FE-SEM-EDS. A general problem with the MLA scan was that it could not distinguish between F-apatite, Cl-apatite, and OH-apatite. These minerals have therefore been as one group for the MLA scans. It was also difficult to distinguish amphiboles from garnets. For this problem, the general geological setting was used to determine amphibole vs. garnets, although a microprobe analysis will be carried out to distinguish these minerals. Lastly, differentiation of hematite vs. magnetite was also impossible using the MLA scans. It was therefore decided to group all these minerals into one group; i.e. magnetite, as these minerals were found in the magnetic fraction. It is, however, important to remember that some of these grains may be hematite grains.

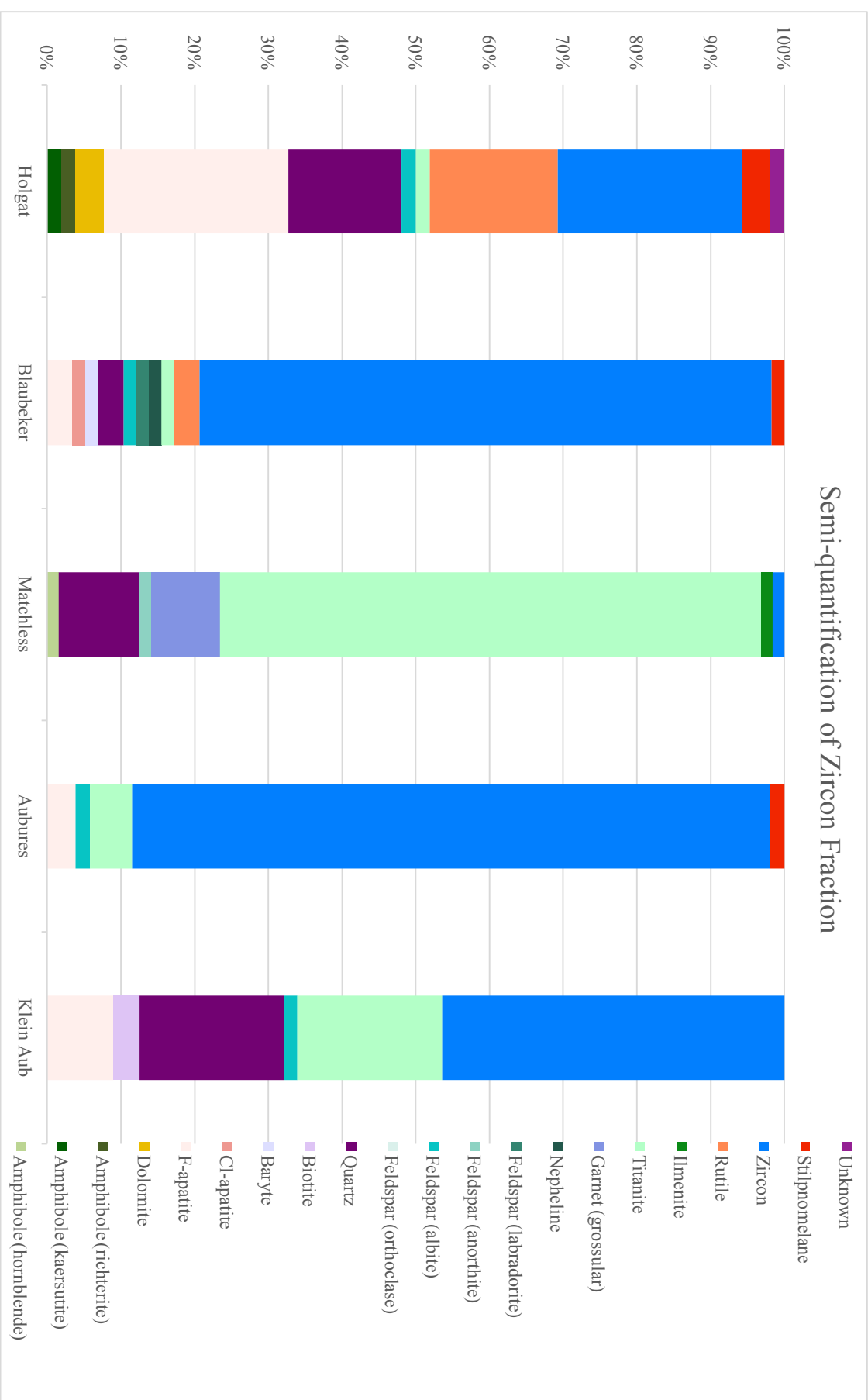
From the SEM analysis, five different amphiboles were identified (gedrite, glaucophane, hornblende, kaersutite, and richterite), whereas the MLA scan suggest only two amphiboles; kaersutite and hastingsite. Moreover, the MLA scan could not distinguish between ilmenite and ilmenite with Mn. These minerals, however, were visible in the SEM.



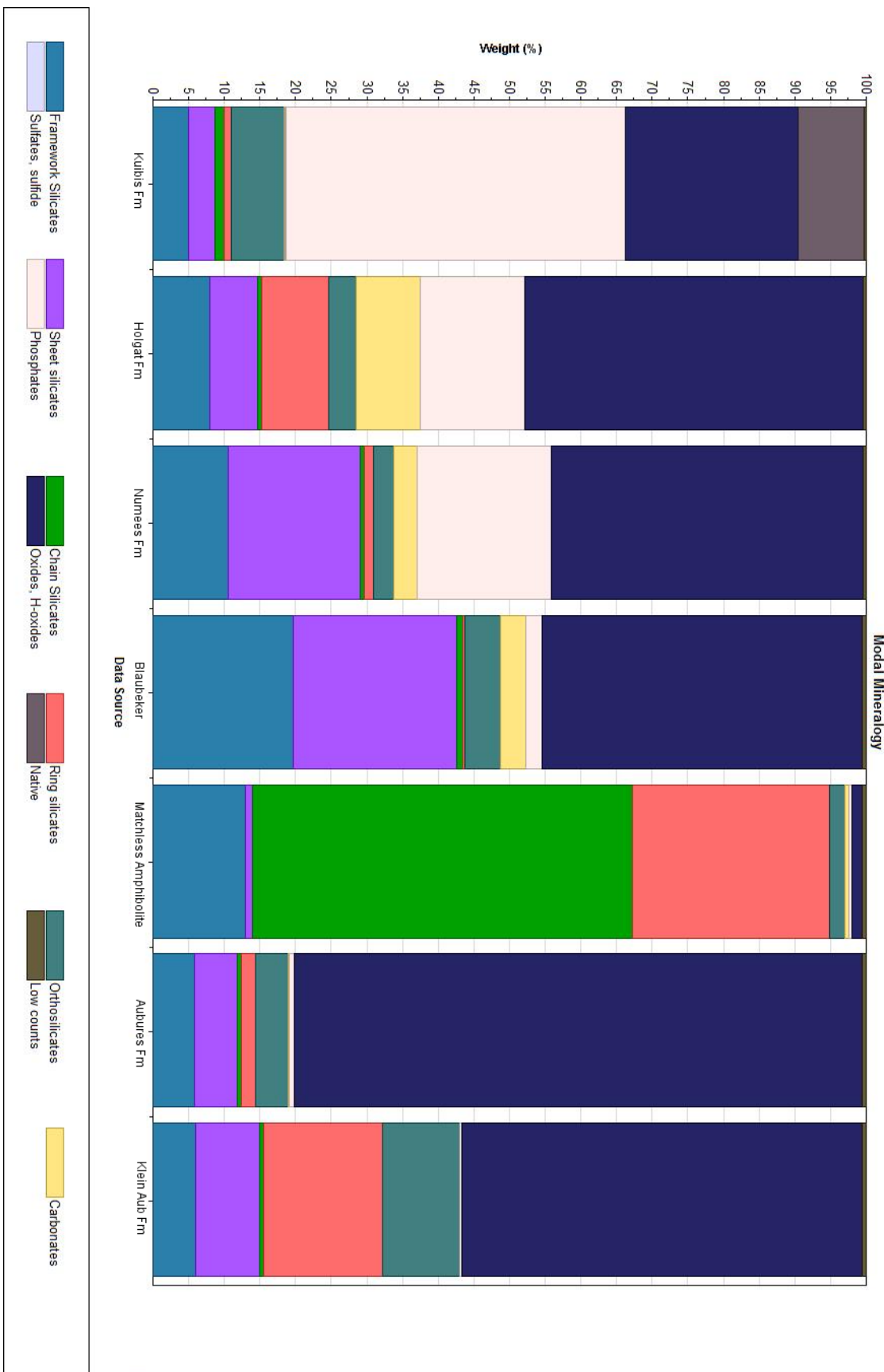
Graph 12: Semi-quantification of Magnetic Fraction



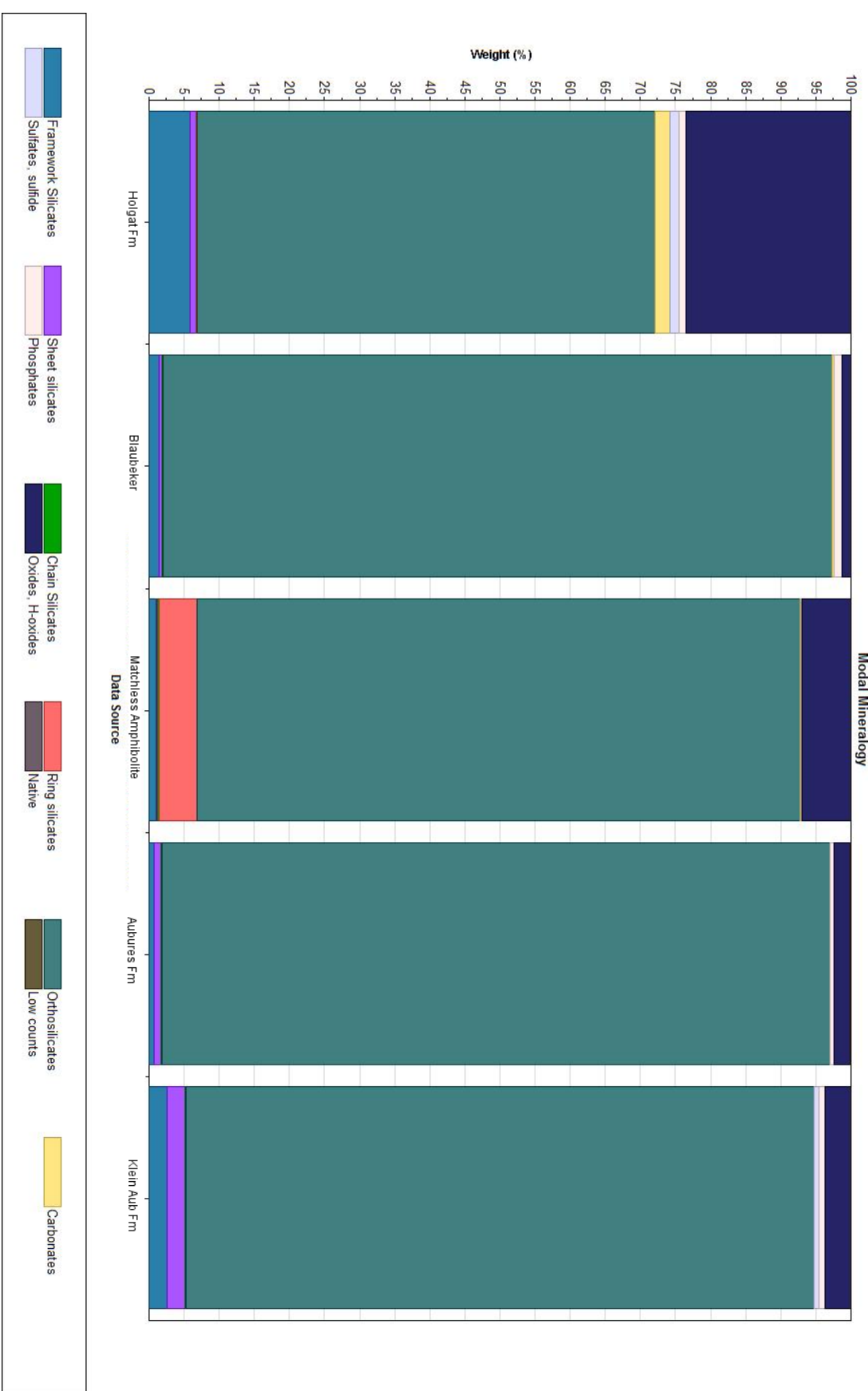
Graph 13: Semi-quantification of Apatite Fraction



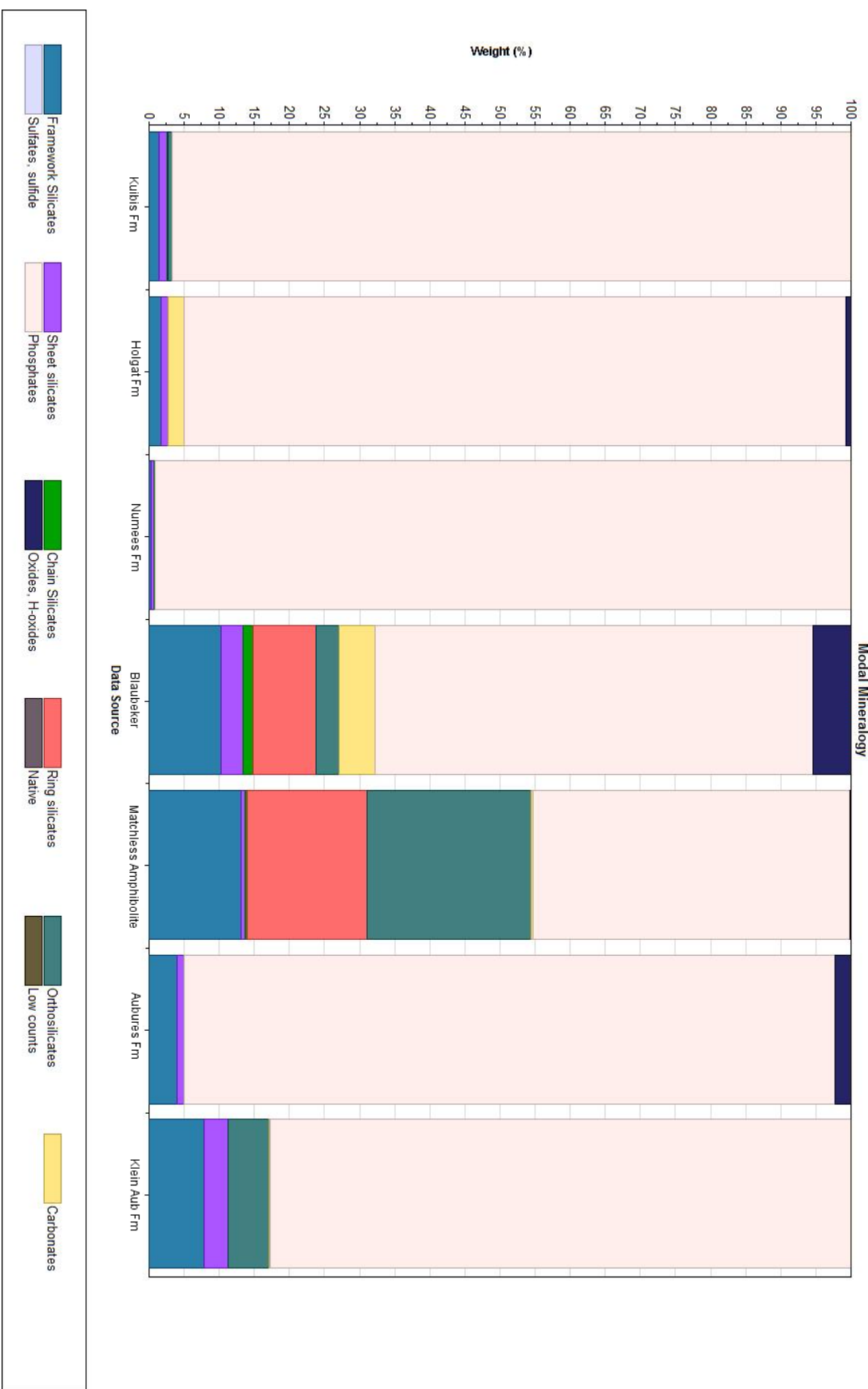
Graph 14: Semi-quantification of Zircon Fraction



Graph 15: Mineral distribution from MLA measurements for magnetic fraction of all formations, filtered with density requirement > 2.95



Graph 16: Mineral distribution from MLA measurements for zircon fraction of all formations, filtered with density requirement > 3.3

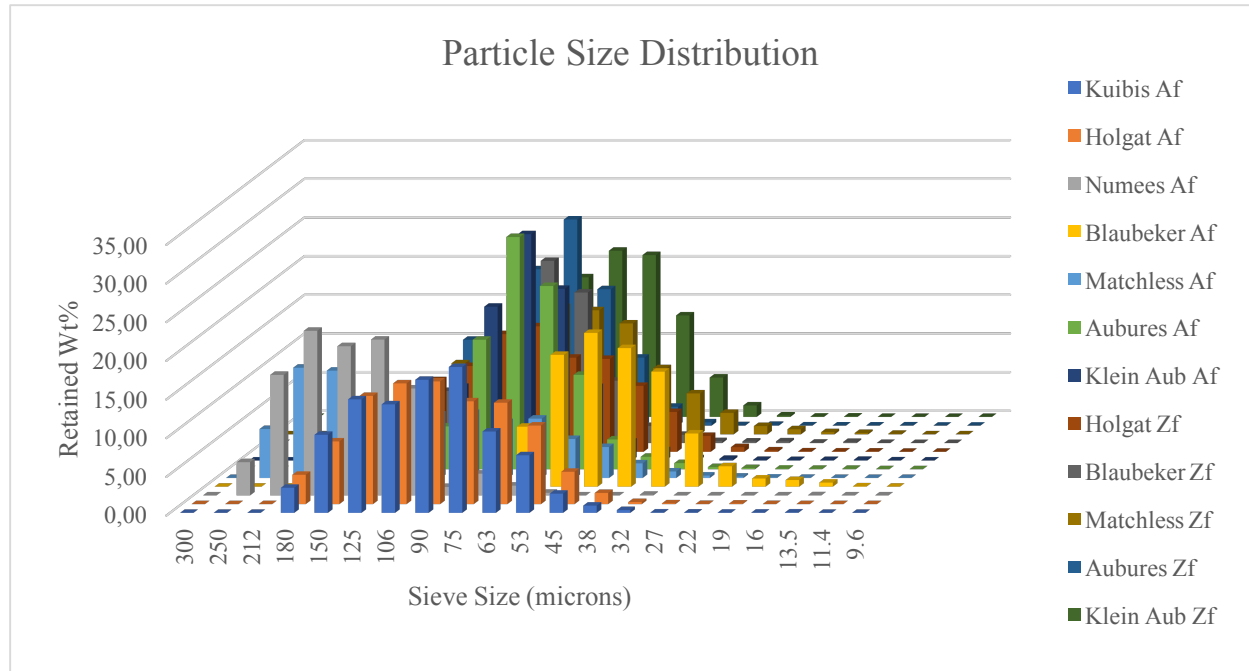


Graph 17: Mineral distribution from MLA measurements for apatite fraction of all formations, filtered with density requirement > 2.95 and < 3.3 .

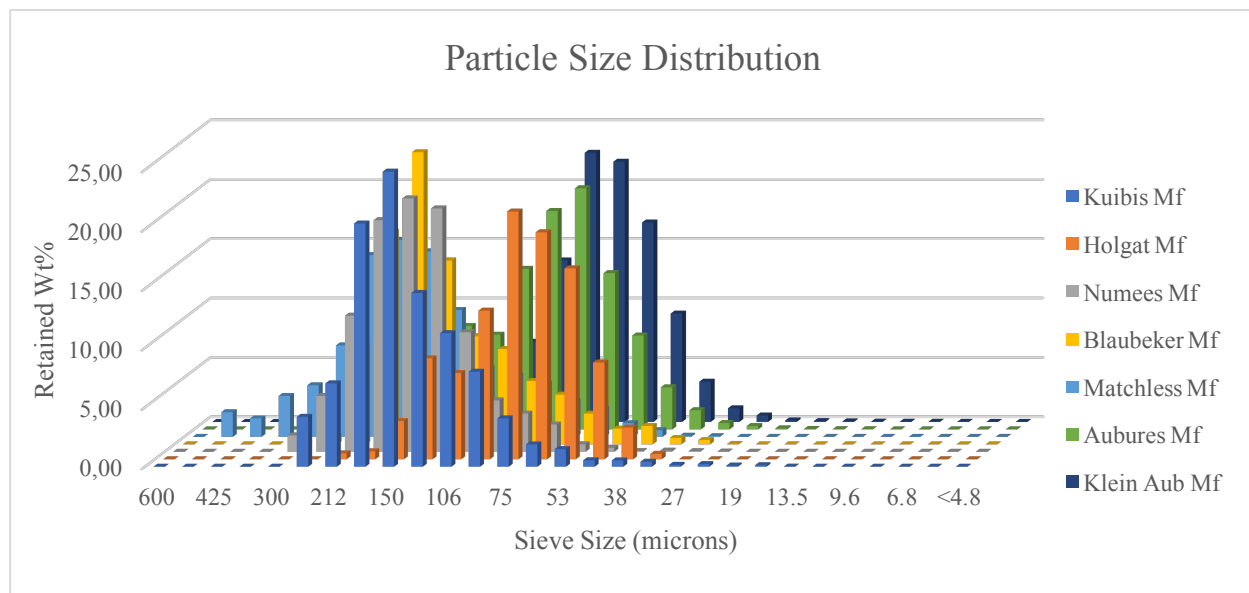
At sample site, the Holgat Formation stratigraphically overlays the Numees Formation and, therefore, the mineralogy should be similar unless the source dramatically changed through time. For example, graph 17 shows a decrease in apatite from Numees Formation to Holgat Formation. Moreover, Holgat Formation shows evidence of a larger percentage of rutile than that of the Numees Formation(graph 15). A higher percentage of micas, amphiboles and iron oxides are also found in the Numees Formation as compared to the Holgat Formation(graph 15). Further, the Numees Formation contains larger heavy minerals than those of the Holgat Formation(graph 1, 2, 18 and 19), which suggests a closer source area and flow systems of higher energy.

As the zircon dating shows ages no younger than 1000 Ma, this project has attempted to find different methods of dating these rock formations. Therefore, as all zircons probably originate from the metamorphic basement, non-metamorphosed minerals, such as monazite, apatite, chromite, etc., should be identified and analyzed.

Another important aspect is the particle size of the grains (graph 18 and 19). With respect to the siliciclastic rocks, the Numees Formation generally contains the largest grains, whereas the Klein Aub Formation contains the smallest grains. On the other hand, the Kuibis and Holgat apatite fractions contain similar sized grains, whereas the Holgat Formation contains smaller magnetic fraction grains as compared to those of the Kuibis Formation. Another interesting result is the similarity between the grain size distribution of the Klein Aub Formation and that of the Aubures Formation, where both formations generally have smaller grain sizes. The amphibolite, on the other hand, shows generally larger crystals than those of the siliciclastic rocks.



Graph 18: Particle Size Distribution of apatite and zircon fractions for all formations, full spreadsheet can be found in Appendix D



Graph 19: Particle Size Distribution of magnetic fractions for all formations, full spreadsheet can be found in Appendix D

Sediments can be transported in four main ways; i.e. with the assistance of fluids, wind, ice, and gravity; or a mixture of these transport modes. The transport mode(s) involved will affect the size of the grains at deposition. When transported in fluids, the sediments are moved through rolling, saltation, or suspension, which also affect the size of the sediment grains. Moreover, a minimum velocity is required to allow the grains to be entrained in the fluid flow, generally known as the critical velocity (Nichols, 2012). The Hjulstrom diagram presents the relationship between water flow velocity and grain size, figure 45.

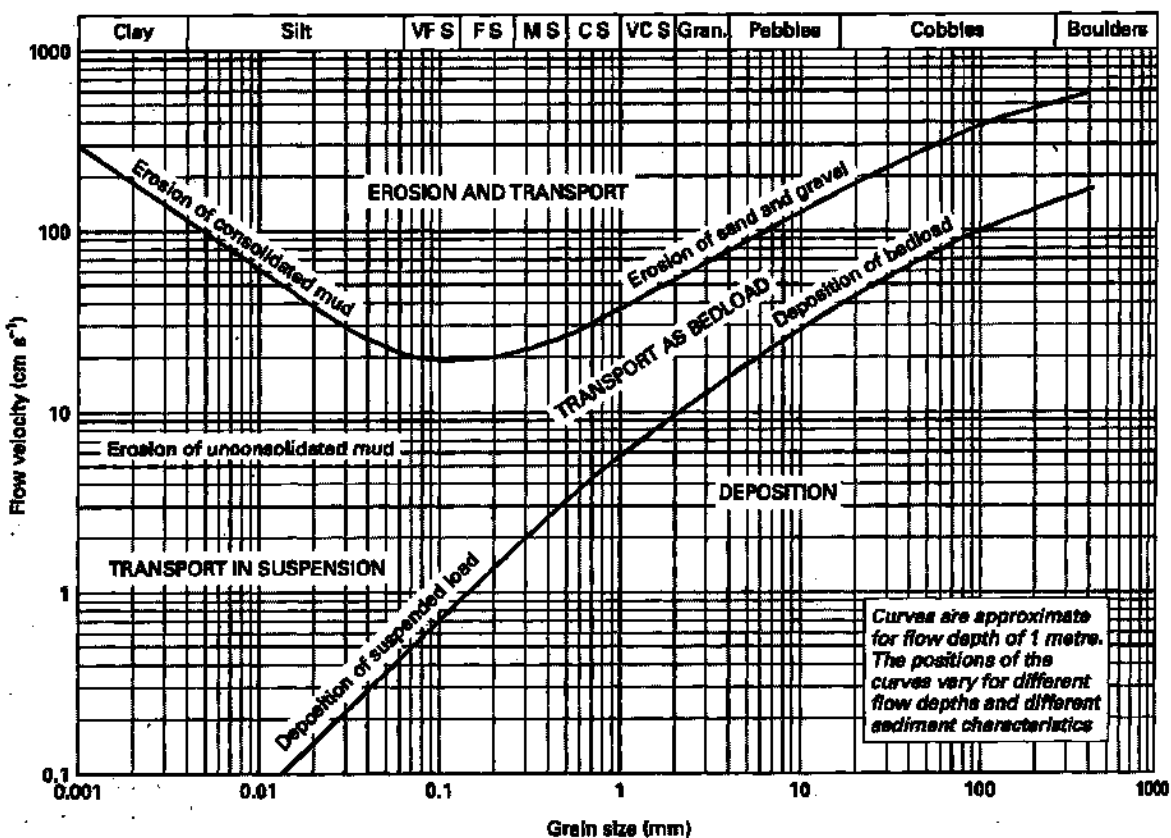


Figure 45: The Hjulstrom Diagram (Nichols, 2012)

As this research only uses mineral fractions, the Hjulstrom diagram cannot be used for evaluating the relationship between water flow velocity and grain size for this project. However, Stokes Law can be used to determine the settling velocity of particles, using particle size and density, fluid type, and fluid viscosity to determine the settling velocity V , as follows:

$$V = g \times D^2 \times (\rho_s - \rho_f) \div 18\mu \quad (\text{eq. 7})$$

Where V : terminal settling velocity, g : gravity, D : grain diameter, $\rho_s - \rho_f$: density difference between particle and fluid, μ : fluid viscosity.

However, this equation can only be used for fine sand or smaller grain sizes and therefore is not applicable for the clasts in diamictites. Nonetheless, the following table shows the terminal settling velocity for the siliciclastic rocks calculated from Stokes Law.

Table 20: Terminal settling velocity

	Density (g/cm³)	Grain diameter (cm)	Velocity min density (cm/s)	Velocity for max density (cm/s)		
Kuibis	2,62	2,65	0,002	0,03	0,04	8,09
Holgat	2,87	3,28	0,0025	0,025	0,06	7,77
Numees	2,82	3,17	0,0025	0,045	0,06	23,95
Blaubeker	2,62	2,65	0,0015	0,025	0,02	5,62

Aubures	2,62	4,65	0,0025	0,0375	0,06	27,97
Klein Aub	2,65	4,65	0,002	0,0375	0,04	27,97

Generally, the Blaubeker Formation shows the lowest terminal velocity, whereas the Aubures Formation and Klein Aub Formation have the highest terminal velocities. Moreover, the Klein Aub Formation and the Aubures Formation have similar mineralogies and mineral sizes. Therefore, Klein Aub Formation and the Aubures Formation seem to have been deposited in similar settings. Similarly, the Numees Formation have a high terminal velocity, suggesting a higher energy environment compared to the other formations (Kuibis Formation, Holgat Formation, and Blaubeker Formation) that are distinct with lower energy environments.

U-Pb Dating

The results from the U-Pb dating can be interpreted in multiple ways. The dating of the youngest zircon density population can be interpreted as the oldest possible age. However, this age is not compatible with the biological evidence from fossils found in the few fossil-carrying formations. In the case of the Klein Aub Formation and the Aubures Formation, for example, the U-Pb ages showed similar density populations, which makes the age determination of both formations difficult and highly uncertain. Except for being able to determine that the source consists of old metamorphic and igneous rocks, possibly from the metamorphic basement, few conclusions can therefore be made from the U-Pb dating.

XRD

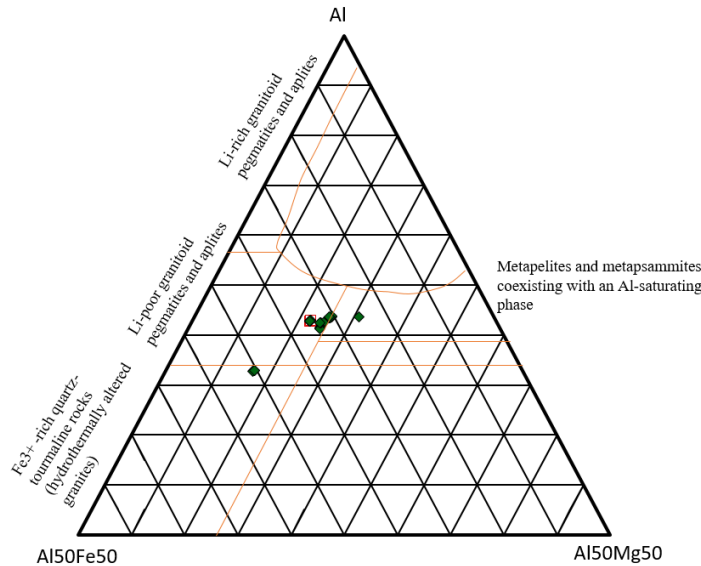
The XRD results showed similar mineral identifications as those of the MLA/SEM work. However, the XRD results identified various amphiboles and distinguished amphiboles from epidotes, tourmalines, and possibly pyroxenes. The results from the XRD showed evidence of the minerals hornblende, hastingsite, kaersutite, grossular, epidote, and ideal-pyroxene for the Matchless Amphibolite, which suggests that the minerals found through the SEM/MLA work should not all be identified as amphiboles. Moreover, the Klein Aub Formation showed evidence of the minerals grossular, almandine, and piemontite. Piemontite is associated with low-grade regional metamorphism, with exposures reported in the Paleoproterozoic Transvaal Group in Northern Kalahari Kalahari Manganese Field, South Africa (Gutzmer & Beukes, 1996). The Aubures Formation, however, showed evidence of the minerals epidote, hastingsite, augite, perovskite, and possibly leucite. The minerals perovskite, sodalite, amesite, and possibly aenigmatite were identified in the Blaubeker Formation. The

XRD results for the Holgat Formation showed evidence of the minerals perovskite and metasideronatrite, which is a rare mineral that deposits in arid environments, possibly by dehydration of sideronatrite (Moreton, 1995). The Numees Formation, however, showed indications of the minerals sodalite, almandine, baddeleyite, and cristobalite. Cristobalite has very typical crystallization requirements of 1471°C (Licker, 2003). Moreover, baddeleyite is known from the Limpopo Province in South Africa (e.g. Wingate, 2001; Olsson et al., 2010). Baddeleyite can also be used for U-Pb dating for mafic rocks (Olsson et al., 2010). Lastly, the XRD results for the Kuibis Formation suggested higher values of chromium as compared to that of the other formations.

EMPA

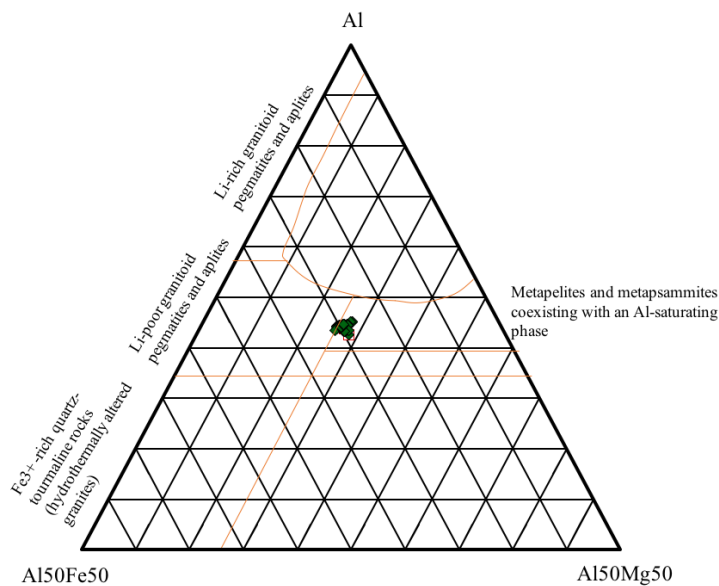
Tourmaline

Ternary diagrams were created for the tourmalines found in the Kuibis Formation(graph 20), Holgat Formation(graph 21), Numees (graph 22), Aubures Formation(graph 23) and Klein Aub Formation(graph 24).



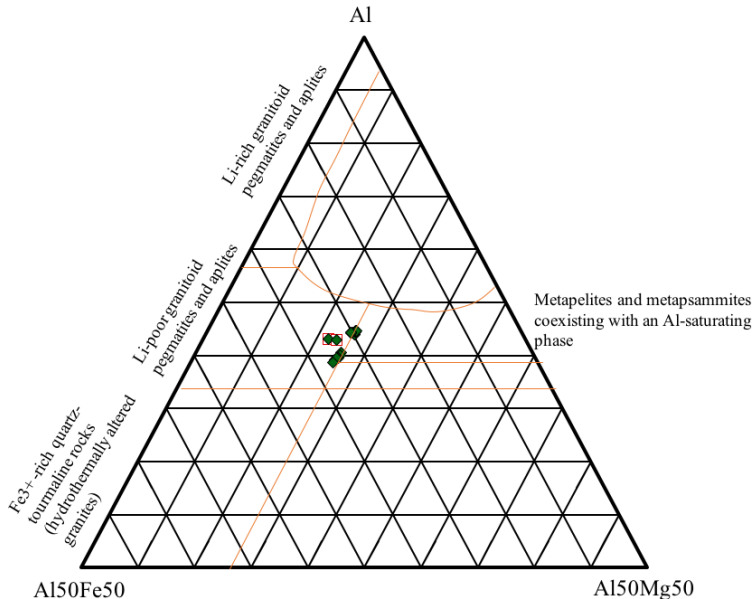
Graph 20: Ternary diagram of tourmalines for Kuibis Formation after Henry & Guidotti (1985)

From this diagram, the tourmalines can be interpreted to originate from mainly Li-poor granitoid pegmatites/aplites, as well as Fe³⁺-rich quartz-tourmaline rocks (hydrothermally altered granites), and metapelites and metapsammites coexisting with an Al-saturating phase, after Henry & Guidotti's (1985) model, for the Kuibis Formation.



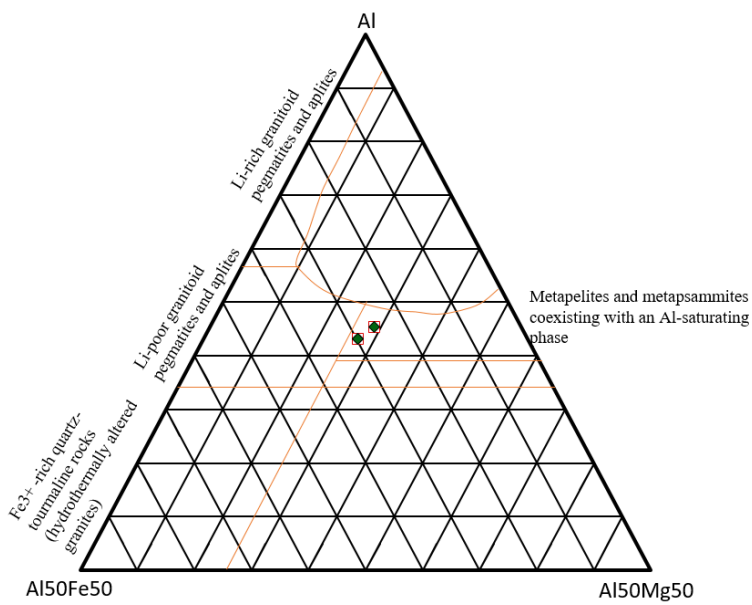
Graph 21: Ternary diagram of tourmalines for Holgat Formation, after Henry & Guidotti (1985)

The Holgat Formation tourmalines plot only within the metapelites and metapsammites coexisting with an Al-saturating phase according to Henry & Guidotti's (1985) model. In contrast, the tourmalines found in the Numees Formation only plot within the Li-poor granitoids pegmatites and aplites (graph 22).



Graph 22: Ternary diagram of tourmalines for Numees Formation after Henry & Guidotti (1985)

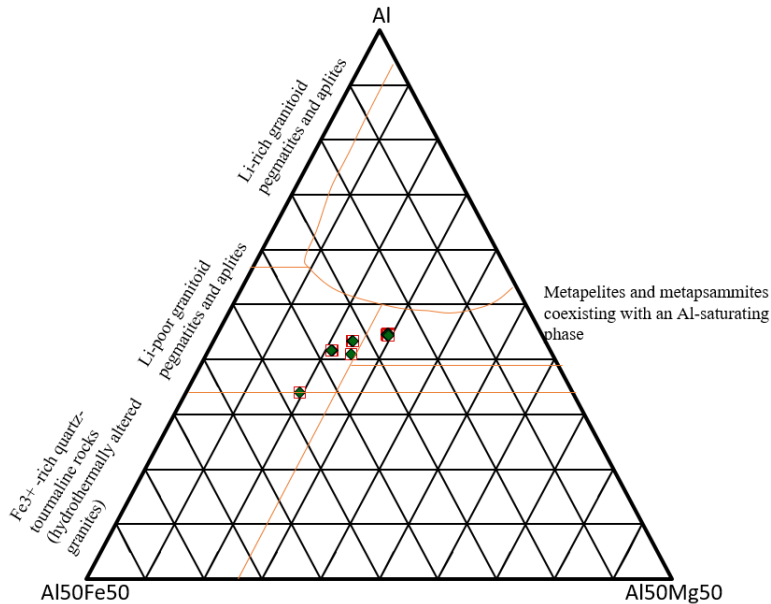
The tourmalines found in the Aubures Formation shows a source of metapelites and metapsammites coexisting with an Al-saturating phase origin, graph 23.



Graph 23: Ternary diagram of tourmalines for Aubures Formation after Henry & Guidotti (1985)

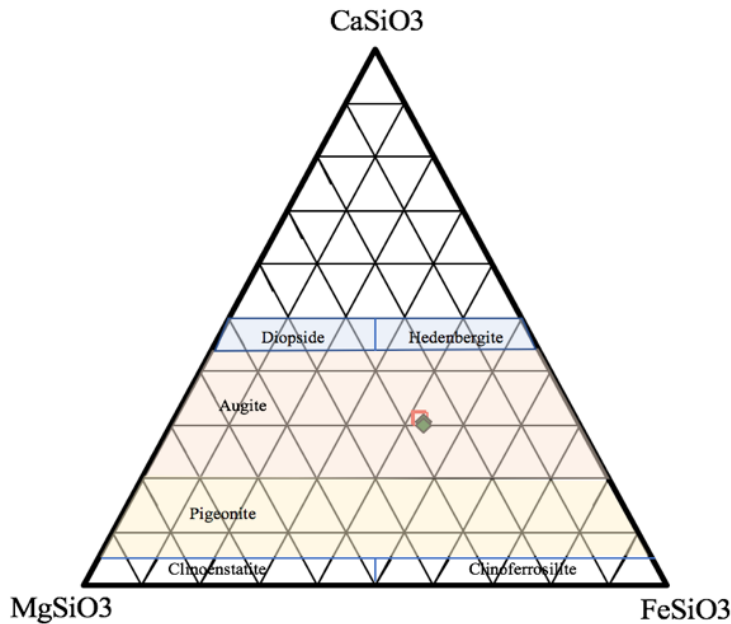
Lastly, the following diagram shows the results for the tourmalines analyzed in the Klein Aub Formation. This shows that the tourmalines generally plot within the Li-poor granitoids

pegmatites and aplites and metapelites and metapsammites coexisting with an Al-saturating phase, according to Henry & Guidotti's (1985) model.



Graph 24: Ternary diagram of tourmalines for Klein Aub Formation after Henry & Guidotti (1985)

Pyroxene

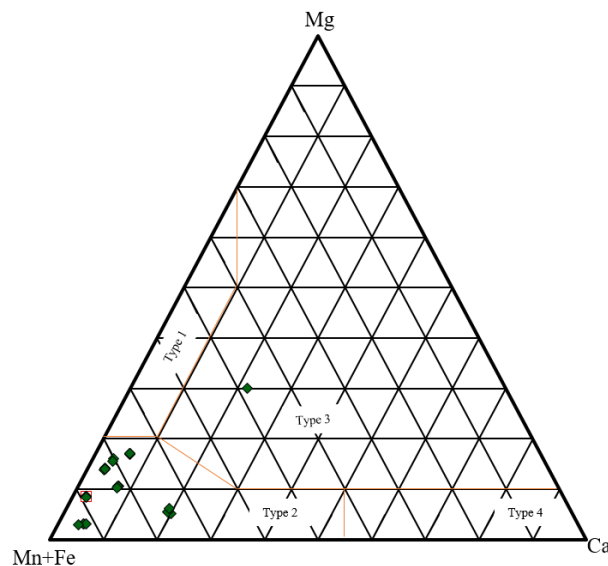


Graph 25: Ternary diagram of pyroxenes from Matchless Amphibolite, plotting after Marshall (1996) and composition names according to Morimoto (1989)

The ternary diagram of pyroxene suggest augite origin for the Matchless Amphibolite.

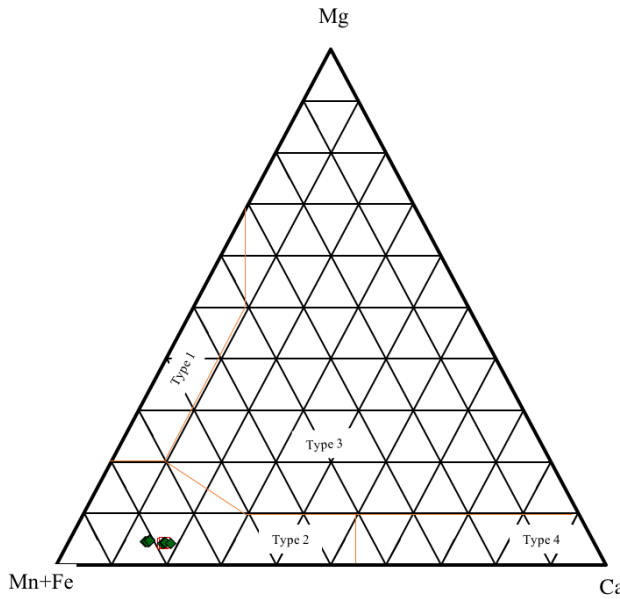
Garnet

Garnets were only identified in the Numees Formation for the siliciclastic rocks, as well as the Matchless Amphibolite.



Graph 26: Ternary diagram of garnet from the Numees Formation, plotting after plotting after Marshall (1996) and endmembers after Morton et al. (2004)

All garnets plot within the type 2 (Mn+Fe rich) garnets, with one exception. These type 2 garnets include larger garnet groups such as almandine and spessartine (Morton et al., 2004), although Stalder and Rozendaal (2002) also reported calderite in the mid-Proterozoic Gamsberg Zn-Pb deposits in the Namaqua Province in South Africa.



Graph 27: Ternary diagram of garnet from the Matchless Amphibolite, plotting after plotting after Marshall (1996) and endmembers after Morton et al. (2004)

Garnets found in the Matchless Amphibolite plot all within the Mn+Fe rich garnets (almandine/spessartine), very low in Mg. The low Mg concentration is evident in the pyroxenes as well.

Amphibole

Most of the amphibole compositions identified using the microprobe, suggest mostly high concentration of Fe, Ca, and Al. These amphiboles should be further analyzed for determining the pro lith.

Hydrocarbon industry

The methodology used for this project can be relevant to all stages of the hydrocarbon (HC) industry; from exploration to production, and for analyzing reservoir characteristics; and also for understanding and predicting reservoir distribution and quality. Moreover, this methodology can be used for correlation where biostratigraphy is not available (Morton, 2007).. In some cases, it has also been used to correlate during geosteering to evaluate drilling evolution (e.g. sidetrack, termination, and maintain angle) (Morton, 2007). Lastly, these methods have been used to predict and understand tight gas reservoir sandstones, as well as developing better imaging of rock porosity (Desbois et al., 2011).

Conclusions

The seven samples of Neoproterozoic, and partly possible Mesoproterozoic, age have been processed for high resolution heavy mineralogy and partly for detrital zircon dating with U-Pb isotopes. The samples have been collected in Namibia and are from the following formations: Klein Aub Formation, Aubures Formation, Blaubeker Formation, Numees Formation, Holgat Formation, Kuibis Formation, and Matchless Amphibolite.

Generally, the U-Pb data measured for the Klein Aub Formation suggest a zircon population of 1000-1400 Ma, with the youngest zircon dating to 942 ± 7 Ma. This data does not give an accurate prediction of the age of the rock, and therefore other applications have been used in this project. The MLA scans show a large percentage of oxides/hydroxides and more ring silicates. Moreover, the analysis show small grains; 4.8-150 microns, although with high density, that require a larger terminal velocity than the other siliciclastic rocks. Further, the EMPA analysis of the tourmalines suggest Li-poor granitoids pegmatites and aplites, and metapelites and metapsammites coexisting with an Al-saturated phase sources. Lastly, the XRD confirms the SEM, MLA, and EMPA analyze, although piemontite, associated with low-grade regional metamorphism (found in the Northern Kalahari Manganese Field, South Africa), is also reported in the XRD analysis.

The Aubures Formation, however, shows a larger zircon population from the U-Pb dating: 1000-1600 Ma. This could suggest a different source, in combination with the source(s) for the Klein Aub Formation. Moreover, the EMPA analysis of the tourmalines suggest only metapelites and metapsammites coexisting with an Al-saturated phase source, in contrast with the Klein Aub Formation. This could indicate a stop in supply from one of the source rocks found in the Klein Aub Formation. Moreover, the MLA scans show larger grains: 9.6-250 microns, although also with a high density; suggesting a higher terminal velocity. Also, from the optical analysis, the Aubures Formation have very round, spherical apatite grains, which has not been identified in the Klein Aub Formation. The MLA results also show a higher percentage of oxides/hydroxides. The XRD analysis show evidence of epidote, hastingsite, augite, perovskite and leucite, leucite has been reported in the 1.34-1.33 Ga plutonic rocks of the Irumide belt in Zambia (De Waele et al., 2006) and in the Mesoproterozoic Pilanesberg Complex in NW South Africa (Elburg & Cawthorn, 2017), in comparison to the Klein Aub Formation that suggest garnets and epidote.

Moreover, the conglomeratic Blaubeker Formation generally shows lower amounts of phosphates, but higher amounts of sheet silicates, ring silicates, and oxides/hydroxides. Also, the Blaubeker Formation shows larger amounts of carbonates compared to the other formations

(except for the Holgat Formation which directly overlays carbonates). Generally, the grains are between 11.4-250 microns, although the smaller grains are dominated in the apatite fraction. The grains are also less dense than the other formations, resulting in the lowest terminal velocity. The XRD identified possible minerals such as perovskite, sodalite (reported in the 1.34-1.33 Ga plutonic rocks of the Irumide belt in Zambia, De Waele et al., 2006 and in the Mesoproterozoic Pilanesberg Complex in NW South Africa, Elburg & Cawthorn, 2017), and amesite (reported in as an alteration produced in the Limpopo Belt, Southern Africa, Schreyer & Abraham, 1976), which have not been identified in the MLA/EMPA analysis. The EMPA analysis shows evidence of magnetite, ilmenite, and rutile. The U-Pb analysis show that the clast analyzed have an older zircon population of 1200-1500 Ma compared to the matrix that has 900-1200 Ma, suggesting separate sources.

The EMPA analysis of the Numees Formation shows evidence of garnets; almandine/spessartine or calderite, where the latter could originate from the Proterozoic Namaqua Province. A few tourmaline grains were also identified by the EMPA, with Li-poor granitoids pegmatites and aplites origin. Moreover, the XRD analysis suggest sodalite, almandine, baddeleyite, and cristobalite. The cristobalite crystallizes under specific conditions, and could therefore become an important mineral to research to determine the provenance. The grain size is within the range of 13.5-300 microns, and are also rather dense, resulting in a high terminal velocity, especially compared to the overlaying Holgat Formation. Moreover, the Numees Formation show larger amounts of phosphates and sheet silicates compared to the Holgat Formation, and lower amounts of carbonates, also suggesting possible change in source/energy.

In contrast to the Numees Formation, no garnets were identified in the Holgat Formation stratigraphically close and younger than the Numees Formation, although tourmalines were. These tourmalines plot within the metapelites and metapsammites coexisting with an Al-saturating phase, and therefore they have been delivered from a different source. Further, the XRD suggest perovskite, where the latter crystallizes in arid environments. The grains sizes are between 13.5-212 microns, also with a lower density resulting in a terminal velocity comparable to the Blaubeker Formation. As stated above, the Holgat Formation has the largest amount of carbonates, affected by the underlying carbonates of the Bloeddrif Member. As well as, larger amounts of ring silicates and oxide/hydroxides compared to the Numees Formation.

Furthermore, the basal rocks of the Ediacaran to Lower Paleozoic Nama Group, the Kuibis Formation, show higher values for chromium, according to the XRD analysis, as well as the MLA suggest higher amounts of native minerals, and phosphates. The grains are between

13.5-250 microns, and have a similar terminal velocity as the Holgat Formation. No age conclusion can be made from the U-Pb analysis as there are 2 main zircon populations of 1000-1300 Ma and 1900-2200 Ma, with a third potential population of Archean age. The EMPA analysis of tourmalines suggest a different origin than the other tourmalines, where these are dominated by Li-poor granitoid pegmatites/aplites and Fe³⁺-rich quartz-tourmaline rocks (hydrothermally altered granites), in combination with the metapelites and metapsammites coexisting with and Al-saturating phase, which is the same tourmaline origin found in the other formations.

The results for the Matchless Amphibolite shows how the importance different methodologies, where for example the MLA classified some pyroxenes and garnets as amphiboles, which the XRD and the EMPA could distinguish. Additionally, the protolith of the Matchless Amphibolite is a Mg poor, Fe-Mn-Ca-Al rich igneous rock based on pyroxenes, amphiboles, and garnets, where more analysis is required for a more precise estimate.

In conclusion, from this work, it seems that all Formations could be of Neoproterozoic age, although further analyses must be done to confirm this. This work also shows the importance of microprobe analysis in combination with MLA scans. Moreover, when U-Pb analysis do not provide sufficient results, other matters are important to evaluate. Therefore, more work should be done to analyze different minerals, such as monazites and titanites, to better evaluate the provenance of these different formations to further evaluate the origin of the Precambrian Earth.

Further Work

As this project has explored different ways of carrying out a provenance study, it is apparent that more work needs to be done. For example, thin sections can be made from whole rocks, and analysis of porosity and diagenesis may be carried out. Further, an improved MLA/EMPA procedure should be developed for future work, using for example slides instead of mounds to access the core, and not just the surface, of the minerals. As the U-Pb dating does not provide adequate results, dating of monazites, titanites, and possibly baddeleyite, is also recommended. As it is disputed whether or not the Numees Formation and the Blaubeker Formation of the study have a glacial origin, it is also suggested to use SEM imaging for carrying out a more detailed study of the grain surfaces of particles of these formations. As heavy mineral fractions were the only available samples for this project, terminal velocities for all fractions should also be considered to gain more information about the depositional environment. And lastly, analyze the potential fossil found in the Blaubeker Formation for provenance.

References

- Augustsson, C., Rüsing, T., Niemeyer, H., Kooijman, E., Berndt, J., Bahlburg, H., Zimmermann, U., 2015. 0.3 byr of drainage stability along the Palaeozoic palaeo-Pacific Gondwana margin; a detrital zircon study. *Journal of the Geological Society*, vol. 172: 186-200.
- Barton, E.S., 1983. Reconnaissance isotopic investigations in the Namaqua Mobile Belt and implications for Proterozoic crustal evolution – Namaqualand Geotraverse. *Special Publication of the Geological Society of South Africa*, vol. 10: 45-66.
- Becker, T., Schreiber, U., Kampunzu, A.B., Armstrong, R., 2006. Mesoproterozoic rocks of Namibia and their plate tectonic setting. *Journal of African Earth Sciences*, vol. 46: 112-140.
- Becker, T., Schalk, K.E.L., 2008. The Sinclair Supergroup of the Rehoboth volcanic arc from the Sossusvlei-Gamsberg area to the Gobabis region. In Miller, R. McG., (ed.) *The Geology of Namibia*: 8-68 – 8-104.
- Bertrand-Sarfati, J., Moussine-Poichkine, A., Amard, B., Aït Kaci Ahmed, A., 1995. First Ediacaran fauna found in western Africa and evidence for an Early Cambrian glaciation. *Geology*, vol. 23: no. 2: 133-136.
- Blanco, G., Rajesh, H.M., Germs, G.J.B., Zimmermann, U., 2009. Chemical composition and tectonic setting of Chromian Spinels from the Ediacaran-Early Paleozoic Nama Group, Namibia. *The Journal of Geology*, vol. 117: 325-341.
- Blignault, H.J., van Aswegen, G., van der Merwe, S.W., Colliston, W.P., 1983. The Namaqualand geotraverse and environs: part of the Proterozoic Namaqua Mobile Belt. *Special Publication of the Geological Society of South Africa*, vol. 10: 1-29.
- Borg, G., 1988. The Koras-Sinclair-Ghanzi rift in southern Africa. Volcanism, sedimentation, age relationships and geophysical signature of a late middle Proterozoic rift system. *Precambrian Research*, vol. 38: 75-90.
- Borg, G., 1995. Metallogenesis of Neoproterozoic basins in Namibia and Botswana. *Communications of the Geological Society of Namibia*, vol. 10: 109-119.
- Borg, G., Maiden, K.J., 1987. Alteration of Late Middle Proterozoic volcanics and its relation to statabound copper- silver-gold mineralization along the margin of the Kalahari Craton in SWA/Namibia and Botswana. *Geological Society, London, Special Publications*, vol. 33: 347-354.
- Brain, C.K., 2001. Some observations on *Cloudina*, a terminal Proterozoic index fossil from Namibia. *Journal of African Earth Sciences*, vol. 33: 475-480.
- Brasier, M.D., Lindsay, J.F., 2001. Did Supercontinental Amalgamation Trigger the "Cambrian Explosion"? In Zhuravlev, A., Riding, R., (eds.) *The Ecology of the Cambrian Radiation*: 69-89.
- Breitkopf, J.H., 1989. Geochemical evidence for magma source heterogeneity and activity of a mantle plume during advanced rifting in the southern Damara Orogen, Namibia. *Lithos*, vol. 23: 115-122.
- Chatterjee, N., 2012. Electron Microprobe Analysis. MIT Electron Microprobe Facility, Cambridge, MA, USA.
- Condon, D.J., Prave, A.R., Benn, D.I., 2002. Neoproterozoic glacial-rainout intervals: Observations and implications. *Geology*, vol. 30: no. 1: 35-38.
- Conway-Morris, S., Mattes, B.W., Chen Menge, 1990. The early skeletal organism *Cloudina*: New occurrences from Oman and possibly China. *American Journal of Science*, vol. 290-A: 245-260.
- Deer, W.A., Howie, R.A., Zussman, J., 1992. 2nd ed. *An Introduction to the Rock-Forming Minerals*. Pearson Education Limited, Essex, UK.

- Derry, L.A., Brasier, M.D., Corfield, R.M., Rozanov, A. Yu., Zhuravlev, A. Yu., 1994, Sr and C isotopes in Lower Cambrian carbonates from the Siberian craton: A paleoenvironmental record during the “Cambrian explosion”. *Earth and Planetary Science Letters*, vol. 128: 671-681.
- Desbois, G., Urai, J.L., Kukla, P.A., Konstanty, J., Baerle, C., 2011. High-resolution 3D fabric and porosity model in a tight gas sandstone reservoir: A new approach to investigate microstructures from mm- to nm- scale combining argon beam cross-sectioning and SEM imaging. *Journal of Petroleum Science and Engineering*, vol. 78: no. 2: 243-257.
- Dickin, A.P., 2005. 2nd ed. *Radiogenic Isotope Geology*. Cambridge University Press, UK.
- Doolittle, W.F., 1999. Phylogenetic Classification and the Universal Tree. *Science*, vol. 284: 33-37.
- Duncumb, P., Shields, P.K., 1963. The present state of quantitative X-ray microanalysis Part 1: Physical basis. *British Journal of Applied Physics*, vol. 14: no. 10: 617.
- Dzik, J., 1999. Organic membranous skeleton of the Precambrian metazoans from Namibia. *Geology*, vol. 27: no. 6: 519-522.
- Eerola, T., 2001. Chapter 5: Climate change at the Neoproterozoic-Cambrian Transition. In Zhuravlev, A., Riding, R., (eds.) *The Ecology of the Cambrian Radiation*: 90-106.
- Elburg, M.A., Cawthorn, R.G., 2017. Source and evolution of the alkaline Pilansberg Complex, South Africa. *Chemical Geology*, vol. 455: 148-165.
- Eyles, N., Januszczak, N., 2004. ‘Zipper-rift’: a tectonic model for Neoproterozoic glaciations during the breakup of Rodinia after 750 Ma. *Earth-Science Reviews*, vol. 65: 1-73.
- Fandrich, R., Gu, Y., Burrows, D., Moeller, K., 2007. Modern SEM-based mineral liberation analysis. *International Journal of Mineral Processing*, vol. 83: 310-320.
- Frimmel, H.E., Hartnady, C.J.H., Koller, F., 1996. Geochemistry and tectonic setting of magmatic units in the Pan-African Gariep Belt, Namibia. *Chemical Geology*, vol. 130: 101-121.
- Frimmel, H.E., 2008. Neoproterozoic Gariep Orogen. In Miller, R. McG., (ed.) *The Geology of Namibia*: 14-1 – 14-37.
- Garzanti, E., Vermeesch, P., Padoan, M., Resentini, A., Vezzoli, G., Andò, S., 2014. Provenance of Passive-Margin Sand (Southern Africa). *The Journal of Geology*, vol. 122: 17-42.
- Gaucher, C., Frimmel, H.E., Germs, G.J.B., 2005. Organic-walled microfossils and biostratigraphy of the upper Port Nolloth Group (Namibia): implications for latest Neoproterozoic glaciations. *Geological Magazine*, vol. 142: 539-559.
- Germs, G.J.B., 1973. Possible Sprigginid Worm and a New Trace Fossil from the Nama Group, South West Africa. *Geology*, vol. 1: no. 2: 69-70.
- Germs, G.J.B., 1974. The Nama Group in South West Africa and it’s relationship to the Pan African geosyncline. *Journal of Geology*, vol. 82: 301-317.
- Germs, G.J.B., 1983. Implications of sedimentary facies and depositional environmental analysis of the Nama Group in South West Africa/Namibia. *Geological Society of South Africa Special Publication*, vol. 11; 89-114.
- Germs, G.J.B., 1995. The Neoproterozoic of southwestern Africa, with emphasis on platform stratigraphy and palaeontology. *Precambrian Research*, vol. 73: 137-151.

- Geyer, G., 2005. The Fish River Subgroup in Namibia: stratigraphy, depositional environments and the Proterozoic-Cambrian boundary problem revisited. *Geological Magazine*, vol. 142: 465-498.
- Gorjan, P., Walter, M.R., Swart, R., 2003. Global Neoproterozoic (Sturtian) post-glacial sulphide-sulfur isotope anomaly recognised in Namibia. *Journal of African Earth Sciences*, vol. 36: 89-98.
- Gresse, P.G., von Veh, M.W., Frimmel, H.E., 2006. Namibian (Neoproterozoic) to Early Cambrian Successions. In Johnson, M.R., Anhaeusser, C.R., Thomas, R.J. (eds.), *The Geology of South Africa*: 395-420.
- Grötzinger, J.P., 2000. Facies and paleoenvironmental setting of Thrombolite-Stromatolite Reefs, Terminal Proterozoic Nama Group (ca. 550-543 Ma), central and southern Namibia. *Communications of the Geological Society of Namibia*, vol. 12: 251-264.
- Grötzinger, J.P., Bowring, S.A., Saylor, B.Z., Kaufman, A.J., 1995. Biostratigraphy and geochronology constraints on early animal evolution. *Science*, vol. 270: 598-604.
- Grötzinger, J.P., Miller, R.McG., 2008. Nama Group. In Miller, R.McG. (ed.), *The Geology of Namibia*: 13-229 – 13-272.
- Gu, Y., Napier-Munn, T., 1997. JK/Philips mineral liberation analyzer – an introduction. *Minerals Processing '97 Conf.*, Cape Town, South Africa: 2.
- Gutzmer, J., Beukes, N.J., 1996. Mineral paragenesis of the Kalahari manganese field, South Africa. *Ore Geology Reviews*, vol. 11: 405-428.
- Hawkesworth, C.J., Kramers, J.D., Miller, R. McG., 1981. Old model Nd ages in Namibian Pan-African rocks. *Nature*, vol. 289: 278-282.
- Handley, J.R.F., 1965. General geological succession on the Farm Flein Aub 350, and Environs, Rehoboth District, South West Africa. *Transactions of the geological society of South Africa*, vol. 68: 211-224.
- Hegenberger, W., 1993. Stratigraphy and sedimentology of the late Precambrian Witvlei and Nama Groups, east of Windhoek. *Geological Survey of Namibia, Memoir* 17.
- Henry, D.J., Guidotti, C.V., 1985. Tourmaline as a petrogenetic indicator mineral: an example from the staurolite-grade metapelites of NW Maine. *American Mineralogist*, vol. 70: 1-15.
- Henry, D.J., Guidotti, C.V., 1985. Tourmaline as a petrogenetic indicator mineral: an example from the staurolite-grade metapelites of NW Maine. *American Mineralogist*, vol. 70: 1-15.
- Hjelen, J., 1986. Scanning elektron-mikroskop. Trondheim, SINTEF, Avdeling for metallurgi, NTH.
- Hoal, B.G., 1989. The geological history of the Awasi Mountain terrain and its relationship to the Sinclair Sequence and Namaqualand Metamorphic Complex. *Communications of the Geological Society of Namibia*, vol. 5: 43-53.
- Hoffmann, K.H., 1989. New aspects of lithostratigraphic subdivision and correlation of late Proterozoic to early Cambrian rocks of the southern Damara Belt and their correlation with the central and northern Damara Belt and the Gariep Belt. *Communications of the Geological Society of Namibia*, vol. 5: 59-67.
- Hoffman, P.F., Kaufman, A.J., Halverson, G.P., 1998a. Comings and goings of global glaciations on a Neoproterozoic tropical platform in Namibia. *GSA Today*, vol. 8: 1-9.
- Hoffman, P.F., Kaufman, A.J., Halverson, G.P., Schrag, D.P., 1998b. A Neoproterozoic Snowball Earth. *Science*, vol. 281: 1342-1346.
- Hoffman, P.F., Schrag, D.P., 1999. The Snowball Earth. *Scientific American*, vol. 9: 38.

- Jacobs, J., Pisarevsky, S., Thomas, R.J., Becker, T., 2008. The Kalahari Craton during the assembly and dispersal of Rodinia. *Precambrian Research*, vol. 160: 142-158.
- Jaffey, A.H., Flynn, K.F., Glendenin, L.E., Bentley, W.C., Essling, A.M., 1971. Precision measurement of the half-lives and specific activites of U235 and U238. *Physical Review C*, vol. 4: 1889-1907.
- Johnson, M.R., Anhaeusser, C.R., Thomas, R.J., 2006. The Geology of South Africa. Geological Society of South Africa, Johannesburg & the Council of Geoscience, Pretoria.
- Kaufman, A.J., Hayes, J.M., Knoll, A.H., Germs, G.J.B., 1991. Isotopic compositions of carbonates and organic carbon from upper Proterozoic successions in Namibia: stratigraphic variation and the effects of diagenesis and metamorphism. *Precambrian research*, vol. 49: 301-327.
- Kaufman, A.J., Jacobsen, S.J., Knoll, A.H., 1993. The Vendian record of Sr and C isotopic variations in seawater: Implications for tectonic and paleoclimate. *Earth and Planetary Science Letters*, vol. 120: 409-430.
- Kennedy, M.J., Christie-Blick, N., Sohl, L.E., 2001a. Are Proterozoic cap carbonates and isotopic excursions a record of gas hydrate destabilization following Earth's coldest intervals? *Geology*, vol. 29: 443-446.
- Kennedy, M.J., Christie-Blick, N., Prave, A.R., 2001n. Carbon isotopic composition of Neoproterozoic glacial carbonates as a test of paleoceanographic models for snowball Earth phenomena. *Geology*, vol. 29: no. 12: 1135-1138.
- Kennedy, M.J., Christie-Blick, N., Sohl, L.E., 2001. Are Proterozoic cap carbonates and isotopic excursions a record of gas hydrate destabilization following Earth's coldest intervals? *Geology*, vol. 29, no. 5: 443-446.
- Kooijman, E., Berndt, J., Mezger, K., 2012. U-Pb dating of zircon by laser ablation ICP-MS: Recent improvements and new insights. *European Journal of Mineralogy*, vol. 24: 5-21.
- Kröner, A., 1974. The Gariep Group, Part 1: Late Precambrian formations in the western Richtersveld, northern Cape Province. *Bulletin of Precambrian Research Unit*, vol. 13: 1-115.
- Kröner, A., Williams, I.S., Compston, W., Baur, N., Vitanage, P.W., Perera, L.R.K., 1987. Zircon ion microprobe dating of high-grade rocks in Sri Lanka. *Jounral of Geology*, vol. 95: 775-791.
- Lazcano, A., 1994. The transition from nonliving to living. In Bengtson, S. (ed.) *Early Life on Earth*. Nobel Symposium No. 84. Columbia U.P., New York: 60-69.
- Licker, M.D., 2003 (publisher)., 2nd ed. *Dictionary of Geology and Mineralogy*. McGraw-Hill Companies, Inc., US.
- Lowe, D.R., 1994. Early environments: Constraints and opportunities for early evolution. In Bengtson, S. (ed.) *Early Life on Earth*. Nobel Symposium No. 84. Columbia U.P., New York: 24-35.
- Ludwig, K., 2003. User's Manual for Isoplot 3.75 A Geochronological toolkit for Microsoft Excel. Berkeley Geochronology Center Special Publication 5.
- Mapani, B., Cornell, D., van Schijndel, V., 2014. Geochronology and tectonic evolution of the Hohewarte Complex, central Namibia: New insights in Paleoproterozoic to Early Neoproterozoic crustal accretion processes. *Journal of African Earth Sciences*, vol. 99: 228-244. Jones and Bartlett Publishers, Inc., Sudbury, MA. 168p.
- Margulis, L., Dolan, M.F., 2002. *Early Life, Evolution on the Precambrian Earth*. 2nd edition.
- Martin, H., 1965. The Precambrian geology of South West Africa and Namaqualand. *Precambrian Research Unit*, University of Cape Town, South Africa.

- Marshall, D., 1996. Ternplot: An Excel spreadsheet for Ternary diagrams. Computers and Geosciences, vo. 22: no. 6: 697-699.
- Martin, H., Porada, H., Walliser, O.H., 1985. Mixtite deposits of the Damara sequence, Namibia, problems of interpretation. *Palaeogeography, Palaeoclimatology, Palaeoecology*, vol. 51: 159-196.
- McCourt, S., Hanson, R., Key, R., 2006. Preface: Mesoproterozoic orogenic belts in southern and central Africa. *Journal of African Earth Sciences*, vol. 46: v-xi.
- McMillian, M.D., 1968. Geology of the Witpus-Sendelingsdrif area. *Bulletin Precambrian Research Unit, University of Cape Town*, vol. 4: 177.
- Miller, R. McG., 1979. The Okahandja Lineament, a fundamental tectonic boundary in the Damara Orogen of South West Africa/Namibia. *Transactions of the Geological Society of South Africa*, vol. 82: 349-361.
- Miller, R. McG., 1983. Tectonic implications of the contrasting geochemistry of Damaran mafic volcanic rocks, South West Africa/Namibia. *Special Publications, Geological Society of South Africa*, vol. 11: 115-138.
- Miller, R. McG., 2008. The geology of Namibia in three volumes. Windhoek, Ministry of Mines and Energy.
- Moreton, S., Ryback, G., Aspen, P., 1995. Basaluminite, Hydronium Jarosite, Metasideronatrite and Sideronatrite. Four Sulphate Minerals New to Ireland: From Ballybunnion, County Kerry. *Irish Journal of Earth Sciences*, vol. 14: 1-5.
- Morimoto, N., 1989. Nomenclature of Pyroxenes. *Canadian Mineralogist*, vol. 27: 143-156.
- Morton, A., Hallsworth, C., Chalton, B., 2004. Garnet compositions in Scottish and Norwegian basement terrains: a framework for interpretation of North Sea sandstone provenance. *Marine and Petroleum Geology*, vol. 21: 393-410.
- Morton, A., 2007. The role of heavy mineral analysis as a geosteering tool during drilling of high-angle wells. *Developments in Sedimentology*, vol. 58: 1123-1142.
- Nesse, W., 2011. 2nd ed. *Introduction to Mineralogy*. Oxford University Press, New York.
- Nichols, G., 2012. 2nd ed. *Sedimentology and Stratigraphy*. Wiley-Blackwell, West Sussex, UK.
- Olsson, J.R., Söderlund, U., Klausen, M.B., Ernst, R.E., 2010. U-Pb baddeleyite ages linking major Archean dyke swarms to volcanic-rift forming events in the Kaapvaal craton (South Africa), and a precise age for the Bushveld Complex. *Precambrian Research*, vol. 183: 490-500.
- Praekely, H.E., Germs, G.J.B., Kennedy, J.H., 2008. A distinct unconformity in the Cango Caves Group of the Neoproterozoic to early Paleozoic Saldania Belt in South Africa: its regional significance. *South African Journal of Geology*, vol. 111: 357-268.
- Reed, S.J.B., 1993. 2nd ed. *Electron Microprobe Analysis*. Cambridge University Press, UK.
- Reed, S.J.B., 2005. 2nd ed. *Electron Microprobe Analysis and Scanning Electron Microscopy in Geology*. Cambridge University Press, UK.
- Retallack, G.J., 2013. Ediacaran life on land. *Nature*, vol. 493: 89-92.
- Rollinson, H., 1993. 2nd ed. *Using geochemical data: evaluation, presentation, interpretation*. Routledge, NY.
- Rooney, A.D., Macdonald, F.A., Strauss, J.V., Dudás, F.Ö., Hallmann, C., Selby, D., 2014. Re-Os geochronology and coupled Os-Sr isotope constraints on the Sturtian snowball Earth. *PNAS*, vol. 111: no. 1: 51-56.
- Rosenblum, S., 1958. Magnetic Susceptibilities of minerals in the Frantz Isodynamic Magnetic Separator. *The American Mineralogist*, vol. 43: 170-173.

- Runnegar, B., 1993. Proterozoic eukaryotes: Evidence from biology and geology. In Bengtson, S. (ed.) Early Life on Earth. Nobel Symposium No. 84. Columbia U.P., New York: 287-297.
- Saylor, B.Z., Grotzinger, J.P., 1996. Reconstruction of Proterozoic-Cambrian boundary exposures through the recognition of thrust deformation in the Nama Group of southern Namibia. Communications of the Geological Society of Namibia, vol. 11: 1-12.
- Sawyer, E.W., 1981. Damaran structural and metamorphic geology of an area southeast of Walvis Bay, South West Africa/Namibia. Memoir, Geological Survey of South West Africa/Namibia, Department of Economic Affairs.
- Schermerhorn, L.J.G., 1974. Late Precambrian Mixtites: Glacial and/or nonglacial? American Journal of Science, vol. 274: 673-824.
- Schoene, B., 2014. 4.10 U-Th-Pb Geochronology. Reference Module in Earth Systems and Environmental Sciences, vol. 4: 341-378.
- Schreyer, W., Abraham, K., 1976. Natural Boron-Free Kornerupine and Its Breakdown Products in a Sapphirine Rock of the Limpopo Belt, Southern Africa. Contributions to Mineralogy and Petrology, vol. 54: 109-126.
- Schwellnus, C.M., 1941. The Nama tillite in the Klein-Karas Mountains, South West Africa. Transactions of the Geological Society of South Africa, vol. 44: 19-33.
- Seilacher, A., 1989. Vendozoa: Organismic construction in the Proterozoic biosphere. Lethaia, vol. 22: 229-239.
- Seilacher, A., 1992. Vendobionta and Psammocorallia: lost constructions of Precambrian evolution. Journal of the Geological Society, London, vol. 147: 607-613.
- Seilacher, A., 1993. Early multicellular life: Late Proterozoic fossils and the Cambrian explosion. In Bengtson, S. (ed.) Early Life on Earth. Nobel Symposium No. 84. Columbia U.P., New York: 389-400.
- Seslavinsky, K.B., Maidanskaya, I.D., 2001. Chapter 3: Global Facies Distributions from late Vendian to Mid-Ordovician. In Zhuravlev, A., Riding, R., (eds.) The Ecology of the Cambrian Radiation: 47-68.
- Smith, A. G., 2001. Chapter 2: Paleomagnetically and Tectonically Based Global Maps for Vendian to Mid-Ordovician Time. In Zhuravlev, A., Riding, R., (eds.) The Ecology of the Cambrian Radiation: 11-46.
- Sprigg, R.C., 1947. Early Cambrian (?) jellyfishes from the Flinders Ranges, South Australia. Transactions of the Royal Society of South Australia, vol. 71: 212-224.
- Stacey, J.S., Kramers, J.D., 1975. Approximation of terrestrial lead isotope evolution by a two-stage model. Earth and Planetary Science Letters, vol. 26: no. 2: 207-221.
- Stalder, M., Rozendaal, A., 2002. Graftonite in phosphatic iron formations associated with the mid-Proterozoic Gamsberg Zn-Pb deposit, Namaqua Province, South Africa. Mineralogical Magazine, vol. 66: no. 6: 915-927.
- Stanistreet, I.G., Kukla, P.A., Henry, G., 1991. Sedimentary basinal responses to a Late Precambrian Wilson cycle: the Damara Orogen and Nama Foreland, Namibia. Journal of African Earth Sciences, vol. 13: 141-156.
- Sylvester, P. J., 2012. Chapter 1: Use of the mineral liberation analyzer (MLA) for mineralogical studies of sediments and sedimentary rocks. Mineralogical Association of Canada Short Course 42: 1-16.
- Theisen, R., 1965. Quantitative Electron Microprobe Analysis. Springer-Verlag, Berlin.
- Watters, B.R., 1978. Petrogenesis of the felsic rock units of the late-Precambrian Sinclair Group, South West Africa. Geologische Rundschau, vol. 67: no. 2: 743-773.

- Weiguo, S., 1993. Early multicellular fossils. In Bengtson, S. (ed.) *Early Life on Earth*. Nobel Symposium No. 84. Columbia U.P., New York: 358-369.
- Wilde, S.A., Valley, J.W., Peck, W.H., Graham, C.M., 2001. Evidence from detrital zircons for the existence of continental crust and oceans on the Earth 4.4 Gyr ago. *Nature*, vol. 409: 175-178.
- Wingate, M.T.D., 2001. SHRIMP baddeleyite and zircon ages for an Umkondo dolerite sill, Nyanga Mountains, Eastern Zimbabwe. *South African Journal of Geology*, vol. 104: 13-22.
- Zack, T., Kronz, A., Foley, S.F., Rivers, T., 2002. Trace element abundances in rutiles from eclogites and associated garnet mica schists. *Chemical Geology*, vol. 184: 97-122.
- Zimmermann, U., Spalletti, L.A., 2009. Provenance of the Lower Paleozoic Balcarce Formation (Tandilia System, Buenos Aires Province, Argentina): Implications for paleogeographic reconstructions of SW Gondwana. *Sedimentary Geology*, vol. 219: 7-23.
- Zimmermann, U., 2010. Correlation of Neoproterozoic successions by any means? – Comments on interpretations made by Praekelt et al. (2008). *South African Journal of Geology*, vol. 113: 130-134.
- Zimmermann, U., Tait., J., Crowley, Q.G., Pashley, V., Straathof, G., 2011. The Witputs diamictite in southern Namibia and associated rocks: constraints for a global glaciation? *International Journal of Earth Sciences*, vol. 100: 511-526.

Appendix A – Full Semi-Quantification of Heavy Minerals using SEM

Kuibis Fm		Numees Fm		Holgat Fm		Blaubeker Fm		Matchless			Aubures Fm			Klein Aub Fm						
Mf	Af	Mf	Af	Mf	Af	Zf	Mf	Af	Zf	Mf	Af	Zf	Mf	Af	Zf					
n=338	n=106	n=162	n=84	n=108	n=52	n=180	n=106	n=58	n=178	n=68	n=113	n=64	n=141	n=100	n=52	n=132	n=112	n=56		
Amphibole (gedrite)	0,3 %						2,8 %			0,6 %			0,7 %							
Amphibole (glaucomphane)	0,3 %									11,1 %			0,9 %							
Amphibole (hornblende)	1,2 %												70,2 %	11,8 %	1,6 %			14,4 %		
Amphibole (kaesutite)	0,3 %									1,9 %										
Amphibole (richterite)	0,3 %									1,9 %			11,8 %							
Calcite	1,2 %									3,9 %	1,9 %		0,6 %	1,5 %						
Dolomite	2,1 %									16,7 %	11,6 %	3,8 %								
Ankerite	1,8 %																			
Apatite w/AlMgSi																				
F-apatite	33,1 %	39,6 %	10,5 %	89,3 %	12,0 %	53,7 %	25,0 %	1,1 %	3,4 %	1,7 %	36,3 %		1,4 %	13,0 %	3,8 %			8,9 %		
Cl-apatite													1,7 %					2,0 %		
Baryte													1,7 %							
Chromite	4,4 %													1,4 %						
Spinel group (unknown)														1,4 %				0,8 %		
Uvospinel										1,1 %			1,5 %							
Biotite													32,6 %							
Muscovite	3,6 %			1,9 %									1,4 %					3,6 %		
Illite	0,6 %												0,7 %					0,8 %		
Quartz	26,9 %	49,1 %	15,4 %	3,6 %	21,3 %	18,2 %	15,4 %	20,6 %	37,7 %	3,4 %	10,7 %	29,4 %	28,3 %	%	9,9 %	50,0 %	22,0 %	74,1 %	19,6 %	
Feldspar (orthoclase)	0,9 %	0,9 %	3,7 %	2,4 %	0,9 %						5,6 %	4,7 %						0,8 %		
Feldspar (albite)	1,8 %	2,8 %	3,7 %	1,2 %							1,9 %		10,6 %	45,3 %	1,7 %			5,7 %	11,0 %	1,9 %
Feldspar (anorthite)																		3,0 %	10,7 %	1,8 %
																		1,6 %		

Feldspar (labradorite)	1,2 %	0,8 %	1,7 %	0,6 %	11,8 %	23,0 %	1,0 %
Nepheline	1,9 %	1,9 %	2,8 %	1,7 %			6,0 %
Garnet (almandine)				1,5 %			0,7 %
Garnet (grossular)	0,3 %			19,1 %	9,4 %		3,8 %
Garnet (pyrope)	0,6 %			6,2 %	5,9 %		2,1 %
Garnet (spessartine)	0,3 %			1,9 %			
Gehlenite							
Titanite	0,3 %	0,6 %	1,2 %	1,9 %	1,7 %	2,8 %	73,4
Ilmenite				8,9 %	0,9 %	5,1 %	4,4 %
Ilmenite w/Mn		3,1 %		0,6 %			
Iron oxide	5,6 %	15,4 %		25,0 %		25,5 %	1,0 %
Rutile	5,0 %	2,8 %	13,6 %	21,3 %	8,3 %	17,3 %	1,7 %
Epidote				1,7 %	1,9 %	3,4 %	0,6 %
Olivine	0,3 %						
Tourmaline			0,8 %				
Zircon	5,6 %	0,9 %	1,2 %	2,8 %	25,0 %	7,2 %	2,8 %
Stilpnomelane	1,8 %	0,9 %	9,3 %	1,9 %	0,8 %	3,8 %	7,2 %
Monazite		0,9 %	8,0 %		1,9 %	3,9 %	
Unknown	0,3 %		6,5 %	1,9 %		1,5 %	

Appendix B – Full MLA distribution

Magnetic Fraction

Klein Aub Fm				Aubures Fm				Matchless Amphibolite				Blaubeker Fm				Holgat Fm				Numees Fm				Kuibis Fm			
Mineral	Wt%	Particle Count	Grain Count	Wt%	Particle Count	Grain Count	Wt%	Particle Count	Grain Count	Wt%	Particle Count	Grain Count	Wt%	Particle Count	Grain Count	Wt%	Particle Count	Grain Count	Wt%	Particle Count	Grain Count	Wt%	Particle Count	Grain Count			
Quartz	9,26	1543	2317	6,49	468	775	15,24	679	2193	17,02	711	1860	11,30	1860	4079	9,33	361	1687	22,57	446	1090						
Plagioclase	0,24	252	352	0,11	62	82	0,70	406	1269	0,26	175	391	0,14	154	222	0,12	97	175	0,39	49	101						
Albite	2,17	851	1298	2,36	340	621	0,14	108	194	9,52	511	1059	1,63	701	1050	5,53	330	1242	2,12	157	342						
Kaetsutie	0,36	284	421	0,21	63	113	40,43	632	1164	0,26	196	328	0,36	341	428	0,37	109	267	0,12	51	113						
Hastingsite	0,00	10	11	0,00	3	3	0,01	10	12	0,01	21	22	0,02	43	44	0,01	16	21	0,00	4	4						
Hastingsite_Mn	0,14	180	200	0,34	213	304	11,19	269	474	0,34	320	544	0,06	53	73	0,13	78	154	0,10	59	119						
Calcite	0,00	4	4	0,31	34	39	0,59	169	250	2,11	293	1262	2,07	561	896	4,47	171	971	0,50	48	105						
Ankerite	0,01	9	9	0,02	14	16	0,06	86	119	4,05	300	1391	2,60	966	2171	0,24	96	264	0,86	45	302						
Dolomite	0,00	0	0	0,00	0	0	0,00	0	0	0,02	17	29	14,59	1427	2556	0,00	0	0	1,03	42	223						
Biotite	0,80	703	940	1,27	492	868	0,00	12	12	4,44	532	2724	0,64	393	606	3,22	353	1780	1,98	194	506						
Chamosite	0,13	97	115	0,57	187	311	0,56	85	199	10,10	571	1736	0,11	50	74	2,40	264	918	0,75	127	353						
Muscovite	12,58	2462	4315	5,61	708	1579	0,48	230	516	9,46	724	2861	8,90	2060	5174	16,30	516	2500	2,91	305	947						
Rutile	0,24	23	30	1,05	80	152	0,01	3	3	3,12	209	648	38,62	1904	4731	11,13	251	1853	11,32	97	661						
Chromite	0,00	0	0	0,00	1	2	0,00	0	0	0,00	0	0	0,00	0	0	0	0	0	0,52	66	246						
FeCr (Chromiferide)	0,01	6	9	0,01	4	4	0,00	0	0	0,00	0	0	0,00	0	0	0	1	1	6,17	92	156						
Magnetite	38,74	1817	2461	60,54	1164	1841	0,15	27	46	21,10	800	3321	0,12	26	48	19,36	248	740	6,77	154	311						
Magnetite_Mn	0,42	291	329	0,95	344	505	0,01	7	9	0,62	267	571	0,00	0	0	0,50	125	362	0,71	57	119						
Uvospinel	8,63	779	1302	10,73	542	1275	0,01	4	5	3,34	542	1829	0,00	1	1	2,79	207	1251	0,03	14	25						
Titanite	8,24	692	983	2,88	144	225	1,86	158	271	0,45	59	70	0,17	200	243	1,28	141	685	0,23	9	45						
Ilmenite	0,49	91	132	1,63	118	268	1,18	97	143	6,88	285	895	0,07	55	67	5,65	174	971	0,16	30	70						
Hollandite	0,02	1	1	0,00	0	0	0,00	0	0	0,02	7	11	0,26	10	20	0,00	0	0	0,03	5	10						
Zn(OH)2	0,00	0	0	0,00	0	0	0,00	0	0	0,00	0	0	0,00	0	0	0	0	0	0,13	4	4						
MnPbO	0,00	0	0	0,00	0	0	0,00	0	0	0,00	0	0	0,03	1	18	0,00	0	0	0,07	3	3						

Barite	0,00	1	2	0,00	1	1	0,00	0	0	0,00	4	4	0,05	28	35	0,00	1	1	0,00	1	1
Almandine	0,02	23	24	0,03	28	30	0,01	7	13	0,06	66	92	0,00	3	3	0,01	15	17	0,16	26	27
Enstatite	0,07	75	85	0,17	82	118	0,06	100	146	0,31	206	496	0,03	29	39	0,23	108	251	0,81	115	314
Epidote	7,44	574	1374	1,31	49	108	1,52	728	2418	0,20	161	274	0,06	76	80	0,08	54	83	0,03	17	44
Clinzoisite	7,06	603	1609	0,44	38	186	24,63	850	2014	0,05	35	51	0,04	59	64	0,06	25	32	0,06	15	37
Tourmaline	0,24	14	17	0,12	26	32	0,05	38	53	0,08	44	66	5,94	125	138	1,00	20	28	0,89	20	32
Apatite	0,25	82	89	0,60	55	61	0,38	82	97	1,35	271	510	7,33	303	309	12,66	157	206	31,79	225	233
Monzonite-(Ce)	0,01	2	2	0,00	0	0	0,00	0	0	0,70	38	225	1,81	78	86	1,21	42	177	0,71	14	18
Xenotime-(Y)	0,00	0	0	0,00	0	0	0,00	0	0	0,05	36	61	0,20	17	19	0,00	6	7	0,22	15	26
Galenia	0,00	0	0	0,00	0	0	0,00	0	0	0,00	1	1	0,00	0	0	0,00	0	0	0,09	1	1
Zircon	1,57	59	62	1,57	45	47	0,12	38	40	3,24	158	217	2,29	98	101	1,17	44	59	4,76	38	42
Unknown	0,00	8	8	0,00	26	27	0,00	0	0	0,00	135	154	0,00	628	637	0,00	120	141	0,00	44	56
Total	100,00	3957	21277	100,00	1510	11220	100,00	1149	14235	100,00	1299	26751	100,00	3002	26470	100,00	630	18754	100,00	864	8752

Apatite Fraction

Mineral	Holgat Fm				Matchless Amphibolite				Klein Aub Fm				Aubures Fm				Blaubeker Fm				Kuibis Fm			
	Wt %	Particle Count	Grain Count	Wt%	Particle Count	Grain Count	Wt%	Particle Count	Grain Count	Wt%	Particle Count	Grain Count	Wt%	Particle Count	Grain Count	Wt%	Particle Count	Grain Count	Wt%	Particle Count	Grain Count			
Quartz	14,16	185	366	17,62	198	289	68,48	345	364	47,87	359	399	34,30	520	531	25,35	255	271	0,29	13	22			
Plagioclase	0,05	10	11	1,41	90	220	0,19	12	16	0,15	17	19	0,42	34	35	0,06	7	7	0,02	2	2			
Abrite	1,37	55	68	0,10	12	18	10,23	131	163	14,85	192	251	39,96	691	725	1,46	39	45	0,14	6	6			
Kaersutite	0,14	18	19	0,22	10	13	0,01	1	1	0,01	3	3	0,07	6	6	0,04	9	10	0,03	2	2			
Hastingsite	0,00	0	0	0,01	2	2	0,00	0	0	0,00	0	0	0,01	1	1	0,00	0	0	0,00	0	0			
Hastingsite_Mn	0,00	1	1	0,02	4	5	0,01	1	1	0,02	3	3	0,05	6	6	0,00	1	1	0,00	0	0			
Calcite	2,07	71	117	0,28	15	17	0,01	1	1	0,23	7	7	5,75	95	108	0,01	2	2	0,02	1	1			
Ankerite	0,70	67	87	0,00	0	0	0,00	0	0	0,01	1	1	1,15	52	63	0,02	2	3	0,00	0	0			
Dolomite	9,64	153	230	0,00	0	0	0,00	0	0	0,00	0	0	0,07	3	4	0,03	2	3	0,00	0	0			

	0,10	14	14	0,02	2	3	0,03	5	6	0,13	16	16	0,03	4	4	0,15	19	22	0,04	2	2
Biotite	0,02	2	2	0,00	1	1	0,00	1	1	0,01	3	3	0,09	9	10	0,21	11	12	0,02	2	2
Chamosite	3,07	172	338	0,47	34	60	8,66	283	521	15,75	287	433	13,34	313	358	1,37	70	94	2,86	20	40
Muscovite	9,71	129	327	0,98	5	12	0,10	5	5	0,01	3	3	0,73	7	13	0,94	7	16	0,18	1	6
Rutile	0,00	0	0	0,00	0	0	0,00	0	0	0,00	0	0	0,00	0	0	0,00	0	0	0,00	0	0
Chromite	0,00	0	0	0,00	0	0	0,00	0	0	0,00	0	0	0,00	0	0	0,00	0	0	0,00	0	0
FeCr	(Chromiferide)	0,00	0	0,00	0	0	0,00	0	0	0,00	0	0	0,00	0	0	0,00	0	0	0,00	0	0
Magnetite	0,00	1	1	0,01	1	1	0,00	1	1	0,60	6	6	0,09	5	6	0,09	3	3	0,03	1	2
Magnetite_Mn	0,00	0	0	0,00	0	0	0,00	0	0	0,00	0	0	0,00	0	0	0,00	0	0	0,00	0	0
Uvospinel	0,00	0	0	0,00	0	0	0,00	0	0	0,00	0	0	0,05	2	2	0,00	0	0	0,00	0	0
Titanite	0,08	12	12	29,62	121	161	2,30	31	54	0,63	6	7	0,04	2	2	0,00	0	0	0,03	2	3
Ilmenite	0,00	0	0	0,01	5	5	0,00	0	0	0,00	0	0	0,01	1	1	0,00	0	0	0,03	1	1
Hollandite	0,00	0	0	0,00	0	0	0,00	0	0	0,00	0	0	0,00	0	0	0,00	0	0	0,00	0	0
Zn(OH)2	0,00	0	0	0,00	0	0	0,00	0	0	0,00	0	0	0,00	0	0	0,00	0	0	0,00	0	0
MnPbO	0,00	0	0	0,00	0	0	0,00	0	0	0,00	0	0	0,00	0	0	0,00	0	0	0,00	0	0
Banite	0,00	2	2	0,00	0	0	0,00	0	0	0,00	0	0	0,00	0	0	0,00	0	0	0,00	0	0
Almandine	0,00	0	0	0,00	0	0	0,00	0	0	0,00	0	0	0,04	2	2	0,00	0	0	0,00	0	0
Enstatite	0,01	1	1	0,00	0	0	0,00	0	0	0,05	6	6	0,01	2	3	0,05	5	7	0,00	0	0
Epidote	0,01	1	1	0,10	15	21	0,03	3	3	0,01	2	2	0,06	6	7	0,00	0	0	0,00	0	0
Clinozoisite	0,10	6	6	19,52	206	404	0,02	3	3	0,00	0	0	0,02	1	1	0,02	2	3	0,00	0	0
Tourmaline	0,00	0	0	0,01	1	1	0,00	0	0	0,00	0	0	0,20	2	2	0,02	2	2	0,00	0	0
Apatite	58,60	315	320	29,56	155	157	9,58	42	42	18,05	99	100	1,39	13	13	69,33	251	255	96,29	76	78
Monazite-(Ce)	0,02	6	6	0,00	0	0,00	0	0	0,00	0	0	0,00	0	0	0,02	1	1	0,00	0	0	
Xenotime-(Y)	0,00	0	0	0,00	0	0	0,00	0	0	0,00	0	0	0,00	0	0	0,00	4	4	0,00	1	1
Galena	0,00	0	0	0,00	0	0	0,00	0	0	0,00	0	0	0,00	0	0	0,00	0	0	0,00	1	1
Baddeleyite	0,00	0	0	0,00	0	0	0,00	0	0	0,00	0	0	0,00	0	0	0,00	0	0	0,00	0	0
Zircon	0,09	6	6	0,03	4	6	0,35	2	2	1,63	8	8	2,14	14	16	0,84	9	9	0,01	3	4
Unknown	0,00	132	146	0,00	1	1	0,00	4	5	0,00	4	5	0,00	9	10	0,00	4	5	0,00	2	2
Low_Counts	0,00	0	0	0,00	0	0	0,00	0	0	0,00	0	0	0,00	0	0	0,00	0	0	0,00	0	0
No_XRay	0,00	0	0	0,00	0	0	0,00	0	0	0,00	0	0	0,00	0	0	0,00	0	0	0,00	0	0
Total	100,00	520	2082	100,00	445	1397	100,00	436	1189	100,00	621	1272	100,00	1423	1929	100,00	503	775	100,00	80	175

Zircon Fraction

Mineral	Klein Aub Fm			Aubures Fm			Matchless Amphibolite			Blaubeker Fm			Holgat Fm		
	Wt%	Particle Count	Grain Count	Wt%	Particle Count	Grain Count	Wt%	Particle Count	Grain Count	Wt%	Particle Count	Grain Count	Wt%	Particle Count	Grain Count
Quartz	10,76	282	387	0,90	56	69	1,10	80	88	0,33	10	12	18,57	198	321
Plagioclase	0,04	14	15	0,02	7	8	0,44	85	99	0,27	4	8	0,01	2	2
Albite	2,43	104	126	0,56	41	50	0,03	6	6	1,02	6	13	0,42	39	44
Kersutite	0,02	5	5	0,01	2	2	0,12	20	22	0,10	2	6	0,03	4	4
Hastingsite	0,01	2	2	0,05	17	17	0,00	1	1	0,05	3	3	0,00	0	0
Hastingsite_Mn	0,00	0	0	0,02	5	5	0,05	9	9	0,08	4	4	0,01	1	1
Calcite	0,01	2	2	0,08	7	7	0,20	22	26	0,11	5	6	1,03	49	82
Ankerite	0,00	0	0	0,00	0	0	0,01	5	5	0,23	7	10	0,26	29	36
Dolomite	0,00	0	0	0,00	0	0	0,00	0	0	0,00	0	0	3,62	127	181
Biotite	0,05	8	9	0,14	19	19	0,07	5	5	0,00	0	0	0,09	13	13
Chamosite	0,01	2	2	0,04	8	10	0,03	7	8	0,18	7	11	0,01	2	2
Muscovite	3,84	380	603	1,14	135	194	0,14	27	29	0,61	13	17	2,47	140	209
Rutile	3,04	53	60	2,16	14	17	6,32	45	52	0,88	3	5	21,39	226	513
Chromite	0,00	0	0	0,00	0	0	0,00	0	0	0,00	0	0	0,00	0	0
FeCr(Chromiferide)	0,00	0	0	0,00	0	0	0,00	0	0	0,00	0	0	0,00	0	0
Magnetite	0,05	8	9	0,19	10	13	0,16	7	20	0,22	7	7	0,01	2	2
Magnetite_Mn	0,00	0	0	0,01	1	1	0,52	2	2	0,00	0	0	0,00	0	0
Uvospinel	0,10	2	2	0,02	1	1	0,00	1	1	0,00	0	0	0,00	0	0
Titanite	21,79	272	363	10,05	58	61	84,70	1179	1224	0,44	3	5	0,05	8	8
Ilmenite	0,02	6	6	0,43	1	3	0,03	10	12	0,09	2	2	0,00	0	0
Hollandite	0,00	0	0	0,00	0	0	0,00	0	0	0,00	0	0	0,00	0	0
Zn(OH)2	0,00	0	0	0,00	0	0	0,00	0	0	0,00	0	0	0,00	0	0
MnPbO	0,00	0	0	0,00	0	0	0,00	0	0	0,00	0	0	0,00	0	0
Barite	0,44	5	5	0,00	0	0	0,00	0	0	0,04	1	1	0,60	6	7

A.E. Myhra

Almandine	0,02	3	3	0,01	2	2	0,00	0	0	0,02	2	2	0,00	0	0
Enstatite	0,04	6	7	0,03	8	8	0,00	0	0	0,03	1	1	0,01	1	1
Epidote	0,01	3	3	0,00	0	0	0,20	39	41	0,02	1	1	0,03	2	3
Clinzoisite	0,03	6	6	0,01	2	2	5,27	339	464	0,00	0	0	0,01	1	1
Tourmaline	0,00	0	0	0,02	4	4	0,00	3	3	0,03	1	2	0,00	1	1
Apatite	11,34	141	145	1,40	46	55	0,49	13	13	1,27	26	35	20,58	179	179
Monazite-(Ce)	0,00	0	0	0,00	0	0	0,00	0	0	0,00	0	0	0,02	2	2
Xenotime-(Y)	0,00	0	0	0,01	2	2	0,00	0	0	0,25	12	14	0,01	5	6
Galena	0,00	0	0	0,00	0	0	0,00	0	0	0,00	0	0	0,00	0	0
Baideleyite	0,00	0	0	0,12	1	1	0,00	0	0	0,00	0	0	0,00	0	0
Zircon	45,95	459	465	82,60	478	493	0,12	3	3	93,74	123	130	30,76	239	242
Unknown	0,00	14	14	0,00	7	9	0,00	1	1	0,00	2	2	0,00	135	139
Low_Counts	0,00	0	0	0,00	0	0	0,00	0	0	0,00	0	0	0,00	0	0
No_XRay	0,00	0	0	0,00	0	0	0,00	0	0	0,00	0	0	0,00	0	0
Total	100,00	966	2239	100,00	569	1053	100,00	1250	2164	100,00	132	297	100,00	676	1999

Appendix C – Particle Density Distribution

Weight of Particles (%)

Density Distribution	Kuibis				Holgat				Numees				Blauteker				Authures				Klein Aub				Matchless			
	Mf	Af	Mf	Af	Zf	Mf	Af	Mf	Af	Zf	Mf	Af	Zf	Mf	Af	Zf	Mf	Af	Zf	Mf	Af	Zf	Mf	Af	Zf			
0.0 < D \leq 0.1	0,00	0,00	0,00	0,00	0,01	0,00	0,00	0,00	0,00	0,00	0,00	0,00	0,00	0,00	0,00	0,00	0,00	0,00	0,00	0,00	0,00	0,00	0,00	0,00	0,00	0,00		
0.1 < D \leq 0.2	0,00	0,00	0,00	0,00	0,00	0,00	0,00	0,00	0,00	0,00	0,00	0,00	0,00	0,00	0,00	0,00	0,00	0,00	0,00	0,00	0,00	0,00	0,00	0,00	0,00	0,00		
0.2 < D \leq 0.3	0,00	0,00	0,00	0,00	0,06	0,00	0,00	0,00	0,00	0,00	0,00	0,00	0,00	0,00	0,00	0,00	0,00	0,00	0,00	0,00	0,00	0,00	0,00	0,00	0,00	0,00		
0.3 < D \leq 0.4	0,03	0,00	0,01	0,04	0,04	0,00	0,00	0,00	0,00	0,00	0,00	0,00	0,00	0,00	0,00	0,00	0,00	0,00	0,00	0,00	0,00	0,00	0,00	0,00	0,00	0,00		
0.4 < D \leq 0.5	0,00	0,00	0,11	0,02	0,22	0,01	0,00	0,00	0,00	0,00	0,00	0,00	0,00	0,00	0,00	0,00	0,00	0,00	0,00	0,00	0,00	0,00	0,00	0,00	0,00	0,00		
0.5 < D \leq 0.6	0,00	0,00	0,11	0,08	0,17	0,00	0,00	0,00	0,00	0,00	0,00	0,00	0,00	0,01	0,00	0,00	0,00	0,00	0,00	0,00	0,00	0,00	0,00	0,00	0,00	0,00		
0.6 < D \leq 0.7	0,00	0,00	0,12	0,33	0,15	0,00	0,00	0,04	0,00	0,00	0,00	0,00	0,00	0,00	0,00	0,00	0,00	0,00	0,00	0,00	0,00	0,00	0,00	0,00	0,00	0,00		
0.7 < D \leq 0.8	0,00	0,39	0,00	0,34	0,00	0,33	0,00	0,02	0,00	0,00	0,00	0,00	0,00	0,00	0,00	0,00	0,00	0,00	0,00	0,00	0,00	0,00	0,00	0,00	0,00	0,00		
0.8 < D \leq 0.9	0,13	0,00	0,41	0,43	0,11	0,02	0,00	0,01	0,00	0,00	0,01	0,00	0,00	0,00	0,00	0,00	0,00	0,00	0,00	0,00	0,00	0,00	0,00	0,00	0,00	0,00		
0.9 < D \leq 1.0	0,08	0,00	0,52	0,70	0,25	0,00	0,00	0,00	0,00	0,00	0,02	0,00	0,00	0,00	0,00	0,00	0,00	0,00	0,00	0,00	0,00	0,00	0,00	0,00	0,00	0,00		
1.0 < D \leq 1.1	0,20	0,00	0,55	0,91	0,29	0,30	0,00	0,07	0,00	0,00	0,05	0,00	0,00	0,01	0,00	0,00	0,00	0,00	0,00	0,00	0,00	0,00	0,00	0,00	0,00	0,00		
1.1 < D \leq 1.2	0,01	0,00	0,66	0,61	0,43	0,05	0,00	0,07	0,00	0,00	0,05	0,00	0,02	0,00	0,00	0,00	0,00	0,00	0,00	0,00	0,00	0,00	0,00	0,00	0,00	0,00		
1.2 < D \leq 1.3	0,00	0,00	0,69	1,06	0,21	0,27	0,00	0,14	0,08	0,00	0,03	0,00	0,00	0,02	0,00	0,00	0,00	0,00	0,00	0,00	0,00	0,00	0,00	0,00	0,00	0,00		
1.3 < D \leq 1.4	0,18	0,00	0,70	0,85	0,44	0,32	0,00	0,01	0,04	0,00	0,04	0,00	0,00	0,00	0,00	0,00	0,00	0,02	0,00	0,00	0,00	0,00	0,00	0,00	0,00	0,00		
1.4 < D \leq 1.5	0,37	0,10	1,28	1,55	0,23	0,77	0,00	0,02	0,00	0,00	0,04	0,07	0,00	0,02	0,00	0,00	0,00	0,00	0,00	0,00	0,00	0,00	0,00	0,00	0,00	0,00		
1.5 < D \leq 1.6	0,17	0,00	1,65	0,25	0,43	0,60	0,00	0,42	0,14	0,00	0,08	0,00	0,00	0,01	0,00	0,00	0,00	0,00	0,00	0,00	0,00	0,00	0,00	0,00	0,00	0,00		
1.6 < D \leq 1.7	0,25	0,00	1,66	1,57	0,54	0,00	0,21	0,00	0,00	0,04	0,00	0,00	0,00	0,03	0,00	0,00	0,00	0,00	0,00	0,00	0,00	0,00	0,00	0,00	0,00	0,00		
1.7 < D \leq 1.8	0,54	0,00	1,46	2,11	0,19	0,93	0,00	0,55	0,00	0,00	0,17	0,12	0,00	0,00	0,00	0,00	0,00	0,00	0,00	0,00	0,00	0,00	0,00	0,00	0,00	0,00		
1.8 < D \leq 1.9	0,00	1,79	1,23	0,25	1,22	0,00	1,07	0,20	0,00	0,09	0,00	0,00	0,08	0,00	0,00	0,00	0,00	0,00	0,00	0,00	0,00	0,00	0,00	0,00	0,00	0,00		
1.9 < D \leq 2.0	0,53	0,00	1,61	3,56	0,15	0,62	0,00	0,43	0,12	0,00	0,00	0,00	0,00	0,00	0,00	0,00	0,00	0,00	0,00	0,00	0,00	0,00	0,00	0,00	0,00	0,00		
2.0 < D \leq 2.1	0,42	0,00	1,23	2,37	0,14	0,52	0,00	0,41	0,00	0,00	0,01	0,16	0,00	0,03	0,00	0,00	0,00	0,00	0,00	0,00	0,00	0,00	0,00	0,00	0,00	0,00		
2.1 < D \leq 2.2	0,47	0,00	1,31	1,82	0,38	0,71	0,00	0,84	0,00	0,00	0,09	0,00	0,00	0,05	0,14	0,00	0,00	0,12	0,00	0,00	0,00	0,00	0,00	0,00	0,00	0,00		
2.2 < D \leq 2.3	0,39	0,00	1,26	1,65	0,21	2,11	0,00	0,79	0,00	0,00	0,07	0,00	0,07	0,00	0,07	0,00	0,00	0,15	0,00	0,00	0,00	0,00	0,00	0,00	0,00	0,00		
2.3 < D \leq 2.4	0,18	0,00	0,95	1,78	0,34	1,62	0,00	1,43	0,00	0,00	0,04	0,00	0,00	0,24	0,00	0,09	0,00	0,00	0,00	0,00	0,00	0,00	0,00	0,00	0,00	0,00		
2.4 < D \leq 2.5	0,94	0,00	0,68	1,48	0,17	1,50	0,00	1,69	0,00	0,00	0,30	0,00	0,16	0,43	0,61	0,07	0,00	0,00	0,00	0,00	0,00	0,00	0,00	0,00	0,00	0,00		
2.5 < D \leq 2.6	2,78	0,00	0,99	0,91	0,09	1,00	0,00	2,64	1,01	0,00	1,13	0,00	0,00	1,47	0,00	0,13	0,07	0,00	0,00	0,00	0,00	0,00	0,00	0,00	0,00	0,00		
2.6 < D \leq 2.7	17,06	2,95	2,86	5,80	1,27	4,16	0,16	6,29	7,79	0,02	1,95	62,61	0,45	4,93	83,46	11,03	0,55	5,61	0,09	0,00	0,00	0,00	0,00	0,00	0,00	0,00	0,00	
2.7 < D \leq 2.8	2,09	0,11	2,74	2,33	3,33	0,00	5,12	8,64	0,29	0,82	6,01	0,22	2,73	2,00	0,62	0,61	1,72	0,01	0,00	0,00	0,00	0,00	0,00	0,00	0,00	0,00		
2.8 < D \leq 2.9	2,19	0,87	9,82	2,85	8,51	6,52	2,34	5,48	10,68	0,71	1,48	8,79	0,60	3,00	1,13	0,31	2,77	2,51	0,00	0,00	0,00	0,00	0,00	0,00	0,00	0,00		
2.9 < D \leq 3.0	4,04	0,37	3,57	2,53	5,33	2,96	0,00	5,91	1,41	0,00	1,83	0,34	0,42	1,65	0,83	0,29	7,82	2,41	0,06	0,00	0,00	0,00	0,00	0,00	0,00	0,00		
3.0 < D \leq 3.1	2,85	1,09	4,75	4,03	3,42	4,89	1,42	7,92	0,09	0,00	0,73	0,22	0,12	2,58	0,78	1,33	17,55	4,93	0,24	0,00	0,00	0,00	0,00	0,00	0,00	0,00		
3.1 < D \leq 3.2	32,37	68,35	14,98	54,58	23,39	16,50	94,67	8,63	1,84	0,00	1,84	17,81	0,92	3,38	9,30	10,83	30,94	36,70	0,62	0,00	0,00	0,00	0,00	0,00	0,00	0,00	0,00	
3.2 < D \leq 3.3	0,88	1,71	3,41	0,72	1,55	5,24	1,09	9,21	0,24	0,37	1,59	1,20	0,38	5,86	0,20	2,67	25,63	22,12	1,84	0,00	0,00	0,00	0,00	0,00	0,00	0,00	0,00	
3.3 < D \leq 3.4	1,17	0,28	2,37	3,45	8,13	0,00	4,76	0,28	0,70	2,77	0,18	0,38	9,41	1,20	4,58	12,59	14,27	4,37	0,00	0,00	0,00	0,00	0,00	0,00	0,00	0,00		
3.4 < D \leq 3.5	1,61	0,25	3,49	0,00	1,56	4,14	0,00	3,96	0,04	0,42	3,74	0,47	9,12	7,06	0,00	14,74	0,61	9,62	84,36	0,00	0,00	0,00	0,00	0,00	0,00	0,00	0,00	
3.5 < D \leq 3.6	1,25	0,00	3,86	0,00	2,20	1,45	0,00	3,42	0,13	0,00	2,53	0,00	0,00	0,15	0,16	0,09	0,95	0,00	0,00	0,00	0,00	0,00	0,00	0,00	0,00	0,00		

3.6 < D <= 3.7	1,53	0,08	3,40	0,17	1,67	3,23	0,00	3,89	0,00	1,26	1,66	0,71	0,10	1,78	0,00	1,32	0,00	0,00	0,16
3.7 < D <= 3.8	1,23	0,39	3,52	0,44	1,10	2,21	0,00	2,70	0,00	0,90	1,45	0,00	0,96	1,60	0,00	1,67	0,03	0,00	0,00
3.8 < D <= 3.9	0,51	0,30	3,67	0,41	1,27	1,26	0,00	1,11	0,21	0,65	1,74	0,00	0,56	2,29	0,00	1,43	0,00	0,00	0,51
3.9 < D <= 4.0	1,16	0,00	3,99	0,00	1,54	3,19	0,00	2,36	0,25	0,00	2,13	0,00	0,75	2,89	0,11	2,21	0,00	0,03	1,06
4.0 < D <= 4.1	0,58	0,00	3,63	0,17	0,83	2,44	0,00	1,82	0,00	1,53	2,79	0,00	0,75	2,55	0,00	1,64	0,00	0,00	1,62
4.1 < D <= 4.2	1,93	0,00	4,01	0,00	2,29	2,44	0,00	1,93	0,00	0,00	1,71	0,00	1,07	2,91	0,00	2,41	0,06	0,00	1,04
4.2 < D <= 4.3	1,02	0,00	2,35	0,00	1,45	2,68	0,00	1,44	0,61	0,63	2,57	0,00	1,71	2,16	0,10	2,73	0,47	0,00	2,26
4.3 < D <= 4.4	0,34	0,00	0,16	0,00	0,33	1,74	0,00	1,22	0,00	0,90	2,97	0,00	2,28	2,68	0,00	2,54	0,00	0,00	0,00
4.4 < D <= 4.5	1,52	0,00	0,42	0,00	1,43	0,90	0,00	1,16	0,14	8,12	2,15	0,00	5,94	3,42	0,00	4,99	0,00	0,00	0,01
4.5 < D <= 4.6	1,23	0,00	0,44	0,00	0,46	0,84	0,00	2,26	0,00	24,72	3,66	0,07	14,69	3,54	0,00	5,62	0,09	0,00	0,00
4.6 < D <= 4.7	2,25	0,07	1,05	0,00	26,97	2,31	0,00	2,20	0,95	58,79	4,65	1,15	58,07	5,33	0,00	26,33	0,02	0,00	0,12
4.7 < D <= 4.8	0,78	0,00	0,14	0,00	0,00	2,44	0,00	0,60	0,05	0,00	6,58	0,00	0,07	5,35	0,00	0,00	0,04	0,00	0,00
4.8 < D <= 4.9	0,38	0,00	0,02	0,00	0,00	1,61	0,00	0,48	0,00	0,00	7,72	0,08	0,00	4,95	0,00	0,12	0,00	0,00	0,00
4.9 < D <= 5.0	0,23	0,00	0,05	0,00	0,00	0,86	0,00	0,78	0,00	0,00	14,14	0,00	0,00	4,93	0,00	0,00	0,00	0,00	0,66
5.0 < D <= 5.1	3,32	0,00	0,29	0,00	0,95	0,00	0,00	3,46	0,00	0,00	12,27	0,00	0,06	4,94	0,00	0,00	0,00	0,00	0,00
5.1 < D <= 5.2	1,09	0,07	0,86	0,00	0,00	0,23	0,00	1,08	0,02	0,00	10,27	0,00	0,00	3,34	0,00	0,00	0,01	0,00	0,03
5.2 < D <= 5.3	0,28	0,00	0,00	0,00	0,00	0,00	0,00	0,00	0,00	0,00	0,00	0,00	0,19	0,02	0,00	0,00	0,00	0,00	0,00
5.3 < D <= 5.4	0,49	0,00	0,00	0,00	0,00	0,00	0,00	0,00	0,00	0,00	0,00	0,00	0,00	0,00	0,00	0,00	0,00	0,00	0,00
5.4 < D <= 5.5	0,33	0,00	0,00	0,00	0,00	0,00	0,00	0,00	0,00	0,00	0,00	0,00	0,00	0,00	0,00	0,00	0,00	0,00	0,00
5.5 < D <= 5.6	0,28	0,00	0,00	0,00	0,00	0,00	0,00	0,00	0,00	0,00	0,00	0,00	0,00	0,00	0,00	0,00	0,00	0,00	0,00
5.6 < D <= 5.7	0,69	0,00	0,00	0,00	0,00	0,00	0,00	0,00	0,00	0,00	0,00	0,00	0,00	0,00	0,00	0,00	0,00	0,00	0,00
5.7 < D <= 5.8	0,77	0,00	0,00	0,00	0,00	0,00	0,00	0,00	0,00	0,00	0,00	0,00	0,00	0,00	0,00	0,00	0,00	0,00	0,00
5.8 < D <= 5.9	1,05	0,00	0,00	0,00	0,00	0,00	0,00	0,00	0,00	0,00	0,00	0,00	0,00	0,00	0,00	0,00	0,00	0,00	0,00
5.9 < D <= 6.0	0,51	0,00	0,00	0,00	0,00	0,00	0,00	0,00	0,00	0,00	0,00	0,00	0,00	0,00	0,00	0,00	0,00	0,00	0,00
6.0 < D <= 6.1	0,24	0,00	0,00	0,00	0,00	0,00	0,00	0,00	0,00	0,00	0,00	0,00	0,00	0,00	0,00	0,00	0,00	0,00	0,00
6.1 < D <= 6.2	0,19	0,00	0,00	0,00	0,00	0,00	0,00	0,00	0,00	0,00	0,00	0,00	0,00	0,00	0,00	0,00	0,00	0,00	0,00
6.2 < D <= 6.3	0,16	0,00	0,00	0,00	0,00	0,00	0,00	0,00	0,00	0,00	0,00	0,00	0,00	0,00	0,00	0,00	0,00	0,00	0,00
6.3 < D <= 6.4	0,70	0,00	0,00	0,00	0,00	0,00	0,00	0,00	0,00	0,00	0,00	0,00	0,00	0,00	0,00	0,00	0,00	0,00	0,00
6.4 < D <= 6.5	0,69	0,00	0,00	0,00	0,00	0,00	0,00	0,00	0,00	0,00	0,00	0,00	0,00	0,00	0,00	0,00	0,00	0,00	0,00
6.5 < D <= 6.6	0,88	0,00	0,00	0,00	0,00	0,00	0,00	0,00	0,00	0,00	0,00	0,00	0,00	0,00	0,00	0,00	0,00	0,00	0,00
6.6 < D <= 6.7	0,41	0,00	0,00	0,00	0,00	0,00	0,00	0,00	0,00	0,00	0,00	0,00	0,00	0,00	0,00	0,00	0,00	0,00	0,00
6.7 < D <= 6.8	0,00	0,00	0,00	0,00	0,00	0,00	0,00	0,00	0,00	0,00	0,00	0,00	0,00	0,00	0,00	0,00	0,00	0,00	0,00
6.8 < D <= 6.9	0,00	0,10	0,00	0,00	0,00	0,00	0,00	0,00	0,00	0,00	0,00	0,00	0,00	0,00	0,00	0,00	0,00	0,00	0,00
6.9 < D <= 7.0	0,00	0,00	0,00	0,00	0,00	0,00	0,00	0,00	0,00	0,00	0,00	0,00	0,00	0,00	0,00	0,00	0,00	0,00	0,00
7.0 < D <= 7.1	0,00	0,00	0,00	0,00	0,00	0,00	0,00	0,00	0,00	0,00	0,00	0,00	0,00	0,00	0,00	0,00	0,00	0,00	0,00
7.1 < D <= 7.2	0,00	0,00	0,00	0,00	0,00	0,00	0,00	0,00	0,00	0,00	0,00	0,00	0,00	0,00	0,00	0,00	0,00	0,00	0,00
7.2 < D <= 7.3	0,00	0,00	0,00	0,00	0,00	0,00	0,00	0,00	0,00	0,00	0,00	0,00	0,00	0,00	0,00	0,00	0,00	0,00	0,00
7.3 < D <= 7.4	0,09	0,00	0,00	0,00	0,00	0,00	0,00	0,00	0,00	0,00	0,00	0,00	0,00	0,00	0,00	0,00	0,00	0,00	0,00
7.4 < D <= 7.5	0,00	0,00	0,00	0,00	0,00	0,00	0,00	0,00	0,00	0,00	0,00	0,00	0,00	0,00	0,00	0,00	0,00	0,00	0,00

Appendix D – Particle Size Distribution

Weight %

Sieve Size (microns)	Klein Aub Fm			Aubures Fm			Matchless Amphibolite			Blaubecker Fm			Holgat Fm			Numees Fm			Kuibis Fm		
	Mf	Af	Zf	Mf	Af	Zf	Mf	Af	Zf	Mf	Af	Zf	Mf	Af	Zf	Mf	Af	Mf	Af		
600	0,00	0,00	0,00	0,00	0,00	0,00	0,00	0,00	0,00	0,00	0,00	0,00	0,00	0,00	0,00	0,00	0,00	0,00	0,00	0,00	
500	0,00	0,00	0,00	0,00	0,00	0,00	1,87	0,00	0,00	0,00	0,00	0,00	0,00	0,00	0,00	0,00	0,00	0,00	0,00	0,00	
425	0,00	0,00	0,00	0,00	0,00	0,00	1,40	0,00	0,00	0,00	0,00	0,00	0,00	0,00	0,00	0,00	0,00	0,00	0,00	0,00	
355	0,00	0,00	0,00	0,00	0,00	0,00	3,99	0,00	0,00	0,00	0,00	0,00	0,00	0,00	0,00	0,00	0,00	0,00	0,00	0,00	
300	0,00	0,00	0,00	0,00	0,00	0,00	3,92	0,00	0,00	0,00	0,00	0,00	0,00	0,00	0,00	0,00	0,97	0,00	0,00	0,00	
250	0,00	0,00	0,00	0,00	0,00	0,00	2,13	7,45	6,33	0,00	1,14	0,00	0,00	0,00	0,00	0,00	4,08	4,30	5,63	0,00	
212	0,00	0,00	0,00	0,00	0,00	0,00	14,64	14,25	1,20	9,57	0,00	0,31	0,00	0,00	10,52	15,58	8,68	0,00			
180	0,00	0,00	1,05	1,02	0,00	0,00	17,64	13,88	0,81	18,83	0,00	0,00	1,75	3,79	1,06	22,14	21,27	20,26	3,24		
150	0,17	4,36	1,66	2,93	2,59	1,18	16,16	10,21	3,19	25,24	2,19	3,30	5,70	8,11	6,35	23,90	19,29	22,92	10,09		
125	1,46	0,67	11,10	8,40	2,32	2,51	10,53	11,47	9,18	15,45	2,43	6,74	10,71	13,99	9,25	19,09	20,14	14,17	14,68		
106	3,39	9,53	9,79	8,66	5,54	5,72	5,76	8,19	7,07	8,17	0,00	13,09	10,24	15,61	11,10	9,18	13,83	10,90	14,03		
90	7,59	19,88	20,21	13,66	16,75	8,02	4,96	8,42	12,78	7,01	3,27	21,63	13,35	15,87	15,21	4,21	1,09	7,53	17,20		
75	13,87	29,26	26,65	18,29	30,03	18,05	4,45	7,23	16,47	5,11	2,63	23,56	18,64	13,29	16,23	2,71	2,81	4,64	18,86		
63	22,99	22,19	17,64	20,05	23,69	21,48	2,90	7,67	16,05	3,50	7,76	19,46	16,04	13,11	12,17	1,73	1,26	2,08	10,52		
53	20,79	9,51	8,79	12,79	12,20	20,93	2,29	5,05	14,34	2,33	17,04	8,06	13,13	10,16	12,01	0,69	0,34	1,32	7,45		
45	15,47	2,44	2,44	7,57	3,85	13,12	1,26	4,00	8,55	1,28	19,88	2,21	6,93	4,18	8,52	0,37	0,00	0,53	2,48		
38	8,62	1,33	0,43	3,60	1,61	5,09	0,59	1,89	5,30	1,37	17,92	1,07	2,64	1,44	5,15	0,20	0,00	0,44	0,94		
32	3,49	0,30	0,06	1,76	0,79	1,48	0,12	0,84	2,78	0,62	14,87	0,25	0,55	0,27	2,05	0,09	0,08	0,34	0,36		
27	1,31	0,22	0,10	0,63	0,28	0,19	0,06	0,31	1,08	0,34	6,88	0,20	0,00	0,09	0,60	0,10	0,00	0,15	0,04		
22	0,75	0,08	0,37	0,15	0,04	0,00	0,17	0,66	0,03	2,64	0,22	0,00	0,02	0,18	0,01	0,00	0,18	0,03			
19	0,28	0,06	0,02	0,12	0,08	0,05	0,00	0,05	0,28	0,00	1,06	0,05	0,00	0,07	0,05	0,00	0,00	0,11	0,02		
16	0,23	0,07	0,02	0,07	0,05	0,01	0,00	0,02	0,18	0,00	0,86	0,15	0,00	0,01	0,04	0,00	0,00	0,11	0,02		
13,5	0,17	0,09	0,03	0,04	0,05	0,00	0,00	0,08	0,00	0,53	0,02	0,00	0,00	0,03	0,00	0,01	0,01	0,05			
11,4	0,11	0,01	0,00	0,04	0,01	0,00	0,00	0,00	0,04	0,00	0,00	0,00	0,00	0,00	0,00	0,00	0,00	0,00	0,00		
9,6	0,07	0,00	0,00	0,01	0,00	0,00	0,00	0,00	0,00	0,00	0,00	0,00	0,00	0,00	0,00	0,00	0,00	0,00	0,00		
8,1	0,07	0,00	0,00	0,00	0,00	0,00	0,00	0,00	0,00	0,00	0,00	0,00	0,00	0,00	0,00	0,00	0,00	0,00	0,00		
6,8	0,04	0,00	0,00	0,00	0,00	0,00	0,00	0,00	0,00	0,00	0,00	0,00	0,00	0,00	0,00	0,00	0,00	0,00	0,00		
5,7	0,03	0,00	0,00	0,00	0,00	0,00	0,00	0,00	0,00	0,00	0,00	0,00	0,00	0,00	0,00	0,00	0,00	0,00	0,00		
4,8	0,02	0,00	0,00	0,00	0,00	0,00	0,00	0,00	0,00	0,00	0,00	0,00	0,00	0,00	0,00	0,00	0,00	0,00	0,00		
4,1	0,00	0,00	0,00	0,00	0,00	0,00	0,00	0,00	0,00	0,00	0,00	0,00	0,00	0,00	0,00	0,00	0,00	0,00	0,00		

Appendix E – U-Pb dating

Klein Aub Formation

Name	U	^{206}Pb	$^{206}\text{Pb}_{\text{U}} (\%)$	206/204	Ratios						Discordance	Ages	
					$^{207}\text{Pb}/^{206}\text{Pb}^*$	1SE	$^{207}\text{Pb}/^{235}\text{U}^*$	1SE	$^{206}\text{Pb}/^{238}\text{U}^*$	1SE	Rho		
PL-01	638	42,3	0,00E+00	13854	0,05322	0,00023	0,40468	0,00536	0,055144	0,00072	0,951	-2,3	-
PL-02	681	45,1	0,00E+00	19625	0,05314	0,00022	0,40341	0,00558	0,055061	0,000728	0,956	3,3	-
SIN-002	113	32,4	0,00E+00	10548	0,08628	0,00038	2,75044	0,04672	0,231206	0,003793	0,966	-0,3	-
SIN-001	79	32,6	0,00E+00	50313	0,11319	0,00058	5,08413	0,10029	0,325763	0,006206	0,966	-2,1	-0,2
SIN-003	223	51,8	0,00E+00	16429	0,07941	0,00033	2,07699	0,034	0,189702	0,00306	0,968	-5,8	-3,7
SIN-004	98	28,5	0,00E+00	22854	0,0876	0,00039	2,83829	0,04787	0,23499	0,003822	0,964	-1,1	-
SIN-003-CORR	223	51,8	2,80E-01	16429	0,07708	0,00031	2,01018	0,03288	0,189141	0,002996	0,968	-0,6	-
SIN-005	62	14	0,00E+00	4074	0,07674	0,00039	1,93334	0,0288	0,182712	0,002556	0,939	-3,2	-0,5
SIN-006	268	70	0,00E+00	80421	0,08127	0,00032	2,34849	0,03528	0,209281	0,003041	0,966	-0,1	-
SIN-007	31	8,6	0,00E+00	2551	0,08491	0,00058	2,59028	0,04195	0,221263	0,003246	0,906	-2,1	-
SIN-008	372	118,7	0,00E+00	3607	0,09755	0,00046	3,4	0,06292	0,255671	0,00452	0,966	-7,8	-6
SIN-008-CORR	372	118,7	4,10E-01	3607	0,09417	0,00044	3,30617	0,06043	0,254618	0,004498	0,967	-3,7	-1,7
SIN-009	192	42,8	0,00E+00	9734	0,0774	0,00035	1,94421	0,03017	0,182188	0,002707	0,958	-5	-2,7
SIN-010	181	45,8	0,00E+00	11119	0,08093	0,00037	2,30582	0,03765	0,206652	0,003241	0,96	-0,8	-
SIN-011-CORR	534	149,6	5,60E-01	2334	0,08395	0,00036	2,59151	0,04962	0,223876	0,004179	0,975	0,9	-
SIN-012	81	23	0,00E+00	7862	0,08537	0,00042	2,71303	0,04609	0,230486	0,003752	0,958	1,1	-
SIN-013	129	34,2	0,00E+00	2235	0,09194	0,00089	2,4768	0,05104	0,216745	0,003439	0,854	-15,1	-11,7
SIN-013-CORR	129	34,2	1,00E+00	2235	0,08331	0,00087	2,5	0,04666	0,214438	0,003393	0,835	-2,1	-
SIN-014	96	22,5	0,00E+00	96	0,2119	0,00237	5,6545	0,10974	0,193333	0,00307	0,817	-66,2	-65,2
SIN-014-CORR	96	22,5	1,60E+01	96	0,0756	0,00185	1,67844	0,0488	0,161022	0,00253	0,540	-12,1	-1,6
SIN-015	247	96,6	0,00E+00	6956	0,11519	0,00056	4,99622	0,09831	0,314586	0,005995	0,969	-7,3	-5,6
SIN-015-CORR	247	96,6	3,70E-01	6956	0,11217	0,00054	4,84831	0,09533	0,313471	0,005967	0,969	-4,8	-3
SIN-016	111	31,5	0,00E+00	9752	0,0873	0,0004	2,78984	0,04695	0,231778	0,003752	0,962	-1,9	-
SIN-011	549	153,9	0,00E+00	2506	0,08874	0,00032	2,75398	0,04833	0,225074	0,003863	0,978	-7,1	-5,6
PL-03	747	48,7	0,00E+00	46479	0,05327	0,00019	0,40384	0,00547	0,054984	0,000718	0,964	1,4	-
PL-04	622	40,4	0,00E+00	16148	0,05337	0,00021	0,40307	0,00527	0,054771	0,00681	0,952	-0,3	-
SIN-017	127	29,1	0,00E+00	8070	0,07728	0,00058	2,08156	0,02449	0,195354	0,001767	0,769	2,1	-
SIN-018	117	50,8	0,00E+00	47952	0,12366	0,00107	6,14042	0,07963	0,360127	0,003481	0,745	-1,6	-
SIN-019	169	48,9	0,00E+00	15479	0,09099	0,00068	3,03853	0,03475	0,242202	0,002102	0,759	-3,7	-1
SIN-019-CORR	175	50,3	7,10E-02	17318	0,09042	0,00067	3,02852	0,03532	0,24292	0,002177	0,769	-2,5	-

SIN-020	266	97,5	0,00E+00	9635	0,10916	0,00087	4,59428	0,05491	,305258	0,00273	0,748	4,3	-1,9		1785	14	1748	10	1717	13
SIN-020-CORR	266	97,5	2,30E-01	9635	0,10729	0,00084	4,50523	0,05362	,304562	0,002722	0,751	-2,6	-0,1		1754	14	1732	10	1714	13
SIN-021	94	20,5	0,00E+00	667	0,1057	0,00104	2,69635	0,05057	,185012	0,002954	0,851	-39,8	-37,5		1727	17	1327	14	1094	16
SIN-021-CORR	94	20,5	2,10E+00	667	0,08858	0,0009	2,20951	0,04238	,180906	0,002943	0,848	-25,1	-21,8		1395	19	1184	13	1072	16
SIN-022	215	78,3	0,00E+00	14193	0,10415	0,00081	4,34642	0,05195	,30266	0,002743	0,758	0,3	.		1699	14	1702	10	1704	14
SIN-023	310	82	0,00E+00	2172	0,09333	0,00087	2,8468	0,04228	,221226	0,002549	0,776	-15,2	-12,2		1495	17	1368	11	1288	13
SIN-023-CORR	310	82	7,70E-01	2172	0,08693	0,00083	2,6	0,03938	,21945	0,002541	0,773	-6,5	-2,9		1359	17	1309	11	1279	13
SIN-024	234	52,1	0,00E+00	3498	0,08048	0,00068	2,08945	0,02406	,188308	0,001465	0,675	-8,7	-5,5		1209	16	1145	8	1112	8
SIN-024-CORR	234	52,1	5,30E-01	3498	0,07606	0,00065	1,96362	0,02274	,187253	0,001458	0,672	1	.		1097	17	1103	8	1106	8
SIN-025	283	66,7	0,00E+00	720	0,1006	0,00112	2,76749	0,03887	,199529	0,001707	0,609	-30,9	-28,5		1635	20	1347	10	1173	9
SIN-025-CORR	283	66,7	2,50E+00	720	0,08005	0,00099	2,1441	0,03238	,194265	0,001675	0,571	-4,9	-0,1		1198	24	1163	10	1144	9
SIN-026	229	72,8	0,00E+00	434	0,13062	0,00427	4,74821	0,16506	,26365	0,00314	0,343	-31,8	-26,2		2106	55	1776	29	1508	16
SIN-026-CORR	229	72,8	5,30E+00	434	0,0889	0,00417	3,06319	0,1485	,249614	0,003063	0,253	2,6	.		1404	86	1424	37	1436	16
SIN-027	456	100,1	0,00E+00	240	0,13878	0,00225	3,50909	0,07783	,183389	0,002775	0,682	-55,2	-53,3		2212	27	1529	18	1085	15
SIN-027-CORR	457	100	5,80E+00	253	0,08839	0,00178	2,1	0,05579	,173688	0,00296	0,646	-27,7	-22,3		1389	36	1153	18	1032	16
SIN-028	110	25,3	0,00E+00	6949	0,07894	0,00061	2,1402	0,02511	,196637	0,001742	0,755	-1,2	.		1171	14	1162	8	1157	9
SIN-029	45	11,2	0,00E+00	4145	0,08603	0,00078	2,49634	0,03164	,210451	0,001875	0,703	-8,8	-5,7		1339	17	1271	9	1231	10
SIN-030	375	130,2	0,00E+00	294	0,15564	0,00321	6,13334	0,15645	,285814	0,004285	0,588	-36,9	-33,9		2409	34	1995	22	1621	21
SIN-030-CORR	375	130,2	6,30E+00	294	0,10603	0,00295	3,91564	0,1232	,267828	0,004206	0,491	-13,1	-6,2		1732	50	1617	26	1530	21
SIN-031	190	53,1	0,00E+00	18611	0,08791	0,00066	2,84061	0,03292	,234344	0,002078	0,765	-1,9	.		1381	14	1366	9	1357	11
SIN-032	86	23,7	0,00E+00	7137	0,08841	0,00079	2,81466	0,03539	,230911	0,002033	0,700	-4,1	-0,9		1391	17	1359	9	1339	11
SIN-033	44	11,7	0,00E+00	4127	0,08534	0,00071	2,67661	0,0365	,227484	0,002455	0,791	-0,2	.		1323	16	1322	10	1321	13
SIN-034	533	112,9	0,00E+00	452	0,10465	0,00132	2,61968	0,04594	,181562	0,0020205	0,692	-40,2	-37,7		1708	23	1306	13	1076	12
SIN-034-CORR	517	110,1	3,60E+00	432	0,07602	0,00122	1,81138	0,03569	,172819	0,001966	0,577	-6,7	.		1096	32	1050	13	1028	11
SIN-035	132	30,9	0,00E+00	7432	0,0802	0,00068	2,15693	0,03021	,195058	0,002169	0,794	-4,8	-1,2		1202	17	1167	10	1149	12
SIN-036	51	17,6	0,00E+00	2515	0,11253	0,00103	4,49891	0,05885	,289969	0,002717	0,716	-12,3	-9,8		1841	16	1731	11	1641	14
SIN-036-CORR	51	17,6	8,50E-01	2515	0,10567	0,00095	4,18965	0,05428	,287545	0,002691	0,722	-6,3	-3,6		1726	16	1672	11	1629	13
SIN-037	55	15,1	0,00E+00	3017	0,09034	0,00087	2,87802	0,04172	,231049	0,002506	0,748	-7,2	-3,8		1433	18	1376	11	1340	13
SIN-037-CORR	55	15,1	6,80E-01	3017	0,08474	0,00082	2,68078	0,03908	,22944	0,002496	0,746	1,9	.		1310	18	1323	11	1332	13
SIN-038	557	124,4	0,00E+00	698	0,10558	0,00091	2,68502	0,03682	,188009	0,001977	0,767	-37,2	-35,3		1689	16	1324	10	1111	11
SIN-038-CORR	557	124,4	2,30E+00	698	0,08495	0,00072	2,14942	0,02926	,183509	0,001951	0,781	-18,9	-16		1314	16	1165	9	1086	11
SIN-039	142	46,1	0,00E+00	353	0,13723	0,00406	5,10518	0,16357	,269819	0,003324	0,385	-33,4	-28,8		2192	49	1837	27	1540	17
SIN-039-CORR	142	46,1	5,20E+00	353	0,09533	0,00392	3,36254	0,14447	,255813	0,003228	0,294	-4,8	.		1535	74	1496	34	1468	17
SIN-040	243	62,9	0,00E+00	192096	0,08418	0,00067	2,51521	0,03127	,216704	0,000208	0,772	-2,7	.		1297	15	1276	9	1264	11

SIN-041	145	31,9	0,00E+00	6391	0,0776	0,00063	1,98837	0,02505	0,185458	0,001793	0,768	-4,2	-0,6		1141	16	1112	9	1097	10
SIN-042	217	48	0,00E+00	5678	0,07821	0,00063	2,0197	0,02316	0,187294	0,001534	0,714	-4,3	-0,9		1152	15	1122	8	1107	8
SIN-043	271	76,2	0,00E+00	15739	0,08698	0,00069	2,84398	0,03355	0,23715	0,002054	0,738	1	.		1360	14	1367	9	1372	11
PL-101	597	37,6	0,00E+00	12701	0,05348	0,00042	0,40124	0,00465	0,05441	0,000464	0,735	-2,3	.		349	16	343	3	342	3
PL-102	572	36,2	0,00E+00	10350	0,05343	0,00039	0,40336	0,00443	0,054754	0,00045	0,748	-1	.		347	16	344	3	344	3
SIN-044	268	59,8	0,00E+00	4650	0,08858	0,00063	2,85437	0,03441	0,233696	0,002279	0,809	-3,3	-0,5		1395	13	1370	9	1354	12
SIN-044-CORR	268	59,8	3,50E-01	4650	0,08571	0,00066	2,75209	0,03301	0,232871	0,002268	0,812	1,5	.		1332	13	1343	9	1350	12
SIN-045	503	105,1	0,00E+00	1605	0,08892	0,00063	2,5936	0,03309	0,211555	0,002241	0,830	-12,9	-10,3		1402	13	1299	9	1237	12
SIN-045-CORR	503	105,1	9,10E-01	1605	0,0814	0,00057	2,35215	0,02977	0,209573	0,002218	0,836	-0,4	.		1231	13	1228	9	1227	12
SIN-046	292	52,2	0,00E+00	1453	0,08483	0,00067	2,13882	0,02755	0,182859	0,001835	0,785	-19	-16,3		1312	15	1161	9	1083	10
SIN-046-CORR	290	51,5	1,00E+00	1497	0,07615	0,00061	1,90901	0,02549	0,181824	0,001949	0,803	-2,2	.		1099	16	1084	9	1077	11
SIN-047	408	75,9	0,00E+00	596	0,10372	0,00084	2,64547	0,04127	0,184985	0,002463	0,854	-38,4	-36,5		1692	15	1313	11	1094	13
SIN-047-CORR	408	75,9	2,50E+00	596	0,08275	0,00071	2,05364	0,03294	0,179996	0,002435	0,844	-16,9	-13,6		1263	16	1134	11	1067	13
SIN-048	323	70,5	0,00E+00	728	0,10078	0,00088	3,06194	0,04352	0,2220354	0,00247	0,788	-23,9	-21,4		1639	16	1423	11	1284	13
SIN-048-CORR	323	70,5	2,10E+00	728	0,08342	0,00075	2,47957	0,03577	0,215566	0,002422	0,779	-1,8	.		1279	17	1266	10	1258	13
SIN-049	185	41,4	0,00E+00	9776	0,089	0,00061	2,8	0,0318	0,225514	0,002079	0,802	-7,3	-4,7		1404	13	1347	9	1311	11
SIN-049-CORR	185	41,4	3,60E-01	9776	0,08601	0,00059	2,66441	0,03052	0,224672	0,00207	0,804	-2,6	.		1338	13	1319	8	1307	11
PL-01	889	47,3	0,00E+00	32956	0,05267	0,0003	0,40466	0,00368	0,055722	0,0004	0,788	11,4	3,8		315	12	345	3	350	2
SIN-050	291	84,5	0,00E+00	42763	0,10493	0,00073	4,18517	0,05245	0,289274	0,003024	0,834	-5	-2,5		1713	12	1671	10	1638	15
SIN-050-CORR	291	84,5	1,30E-01	42763	0,10386	0,00071	4,13737	0,05176	0,288908	0,003019	0,835	-3,9	-1,4		1694	12	1662	10	1636	15
SIN-051	177	39,6	0,00E+00	14028	0,08484	0,00054	2,653308	0,02935	0,225082	0,002053	0,818	-0,3	.		1312	12	1310	8	1309	11
SIN-052	334	63	0,00E+00	36998	0,07655	0,00048	2,02339	0,02177	0,191697	0,001675	0,812	2,1	.		1110	12	1123	7	1131	9
SIN-053	311	56	0,00E+00	9740	0,07858	0,00066	2,10376	0,03211	0,194168	0,002478	0,836	-1,7	.		1162	16	1150	11	1144	13
SIN-053-CORR	311	56	2,20E-01	9740	0,07677	0,00064	2,1	0,03123	0,193737	0,002472	0,838	2,6	.		1115	16	1133	10	1142	13
SIN-054	413	85,2	0,00E+00	2382	0,08634	0,00056	2,4903	0,0278	0,209187	0,001901	0,814	-9,9	-7,4		1346	12	1269	8	1224	10
SIN-054-CORR	413	85,2	6,10E-01	2382	0,08132	0,00052	2,33097	0,02584	0,20789	0,001887	0,819	-1	.		1229	12	1222	8	1218	10
SIN-055	386	69,9	0,00E+00	772	0,09214	0,00071	2,31823	0,02834	0,182484	0,001736	0,778	-28,8	-26,7		1470	14	1218	9	1081	9
SIN-055-CORR	386	69,9	2,00E+00	772	0,07583	0,0006	1,86882	0,0232	0,178752	0,001706	0,769	-3	.		1090	15	1070	8	1060	9
SIN-056	293	56,1	0,00E+00	3117	0,08199	0,00058	2,18346	0,02424	0,193137	0,001653	0,771	-9,4	-6,6		1245	13	1176	8	1138	9
SIN-056-CORR	293	56,1	5,00E-01	3117	0,07779	0,00055	2,06086	0,02289	0,19213	0,001643	0,770	-0,8	.		1142	13	1136	8	1133	9
SIN-057	91	28	0,00E+00	12556	0,10641	0,00074	4,41005	0,05409	0,300583	0,003028	0,821	-2,9	-0,5		1739	13	1714	10	1694	15
SIN-058	66	11,6	0,00E+00	6260	0,07522	0,00049	1,83927	0,02064	0,177348	0,001621	0,814	-2,2	.		1074	13	1060	7	1052	9
SIN-059	210	52,2	0,00E+00	1273	0,11417	0,00083	3,70844	0,0447	0,23559	0,002272	0,8	-29,9	-28,1		1867	13	1573	10	1364	12
SIN-059-CORR	210	52,2	1,10E+00	1273	0,10495	0,00074	3,36894	0,04037	0,232824	0,002254	0,808	-23,5	-21,6		1713	13	1497	9	1349	12
PL-02	516	26,7	0,00E+00	16061	0,05291	0,00032	0,39711	0,00396	0,054432	0,000435	0,801	5,2	.		325	13	340	3	342	3

SIN-060	137	30	0,00E+00	14675	0,08467	0,00055	2,60035	0,02922	0,222738	0,00204	0,815	-1	.		1308	12	1301	8	1296	11
SIN-061	129	24,9	0,00E+00	51721	0,0808	0,00061	2,18957	0,02722	0,196542	0,00194	0,794	-5,4	-2,2		1217	15	1178	9	1157	10
SIN-061-CORR	129	24,9	2,00E-01	51721	0,07916	0,0006	2,14066	0,02664	0,196141	0,001936	0,793	-2	.		1176	14	1162	9	1155	10
SIN-062	90	29,4	0,00E+00	9224	0,11359	0,00083	5,05034	0,06683	0,322472	0,003556	0,833	-3,4	-1		1858	12	1828	11	1802	17
SIN-063	252	48,7	0,00E+00	11019	0,07966	0,00049	2,15222	0,02401	0,195946	0,001817	0,831	-3,2	-0,4		1189	11	1166	8	1154	10
SIN-063-CORR	252	48,7	2,10E-01	11019	0,07794	0,00048	2,10123	0,0234	0,195529	0,001813	0,833	0,6	.		1145	11	1149	8	1151	10
PL-03	499	25,9	0,00E+00	13662	0,05291	0,00031	0,39709	0,003396	0,054435	0,000441	0,811	5,4	.		325	12	340	3	342	3
SIN-064	130	30,9	0,00E+00	1139	0,11146	0,00085	3,70028	0,04883	0,240786	0,002586	0,814	-26,3	-24,4		1823	13	1571	11	1391	13
SIN-064-CORR	130	30,9	1,30E+00	1139	0,10052	0,00075	3,29227	0,04308	0,237541	0,002556	0,822	-17,6	-15,3		1634	13	1479	10	1374	13
SIN-065	204	49	0,00E+00	2250	0,09345	0,00061	3,08614	0,03521	0,239522	0,002248	0,823	-8,4	-6		1497	12	1429	9	1384	12
SIN-066	159	32,2	0,00E+00	756	0,09469	0,001	2,55617	0,03411	0,195793	0,001589	0,608	-26,5	-23,9		1522	19	1288	10	1153	9
SIN-066-CORR	159	32,2	2,00E+00	756	0,07803	0,00094	2,0622	0,03003	0,191667	0,001566	0,561	-1,6	.		1148	23	1136	10	1130	8
SIN-068	298	53,3	0,00E+00	11779	0,0769	0,00049	1,94761	0,02116	0,183687	0,001614	0,809	-3,1	-0,1		1119	12	1098	7	1087	9
SIN-068-CORR	298	53,3	1,20E-01	11779	0,07589	0,00048	1,91963	0,02083	0,183455	0,001612	0,810	-0,6	.		1092	12	1088	7	1086	9
SIN-069	263	57,9	0,00E+00	6033	0,08861	0,00059	2,73815	0,03317	0,224112	0,002268	0,835	-7,3	-4,7		1396	12	1339	9	1304	12
SIN-069-CORR	263	57,9	3,10E-01	6033	0,08601	0,00057	2,64939	0,032	0,2234	0,002261	0,838	-3,2	-0,4		1338	12	1314	9	1300	12
PL-04	572	29,7	0,00E+00	18813	0,05314	0,00032	0,40144	0,00409	0,054786	0,00045	0,805	2,7	.		335	14	343	3	344	3
PL-05	544	28,2	0,00E+00	11024	0,05311	0,00032	0,40201	0,00398	0,054902	0,000429	0,788	3,4	.		333	14	343	3	345	3
PL-101	573	21,4	0,00E+00	12358	0,05287	0,00029	0,4088	0,00429	0,056074	0,000502	0,854	9	1,3		323	12	348	3	352	3
PL-102	365	13,5	0,00E+00	7862	0,05425	0,00033	0,41336	0,00447	0,055266	0,000494	0,826	-9,3	-1,8		381	14	351	3	347	3
SIN-170	126	16,7	0,00E+00	9049	0,07918	0,00047	2,11132	0,02428	0,193395	0,00119	0,854	-3,4	-0,6		1177	12	1153	8	1140	10
SIN-171	243	34	0,00E+00	289	0,14229	0,00132	3,6729	0,05554	0,187211	0,002334	0,789	-55,3	-54,1		2255	15	1565	12	1106	12
SIN-171-CORR	241	33,3	5,20E+00	290	0,10007	0,00098	2,46392	0,0387	0,178571	0,002186	0,779	-37,7	-35,5		1625	18	1262	11	1059	12
SIN-172	141	22,4	0,00E+00	1222	0,0985	0,00097	2,9705	0,03918	0,218715	0,001917	0,665	-22,1	-19,6		1596	18	1400	10	1275	10
SIN-172-CORR	141	22,4	1,20E+00	1222	0,08866	0,00092	2,64106	0,03585	0,216046	0,001901	0,648	-10,7	-7,4		1397	19	1312	10	1261	10
SIN-173	155	23,6	0,00E+00	2055	0,08837	0,00063	2,57539	0,02846	0,210893	0,001779	0,763	-12,7	-10,3		1395	13	1294	8	1234	9
SIN-173-CORR	155	23,6	8,00E-01	2055	0,08186	0,00059	2,36029	0,02614	0,20913	0,001768	0,763	-1,6	.		1242	14	1231	8	1224	9
SIN-174	92	26,4	0,00E+00	1717	0,12316	0,00116	5,68849	0,0934	0,334994	0,00451	0,82	-8	-5,2		2002	16	1930	14	1863	22
SIN-174-CORR	92	26,4	8,90E-01	1717	0,11603	0,00109	5,3	0,08721	0,332108	0,004474	0,821	-2,9	.		1896	16	1871	14	1849	22
SIN-175	341	46,6	0,00E+00	1673	0,08466	0,00085	2,12898	0,03222	0,182281	0,002068	0,749	-18,9	-15,6		1308	19	1158	10	1080	11
SIN-175-CORR	341	46,6	9,60E-01	1673	0,07653	0,00081	1,90498	0,02969	0,180527	0,002062	0,733	-3,8	.		1109	21	1083	10	1070	11
SIN-176	338	50,7	0,00E+00	5330	0,07963	0,00049	2,20123	0,0226	0,200496	0,001653	0,803	-0,9	.		1188	12	1181	7	1178	9
SIN-176-CORR	338	50,7	2,60E-01	5330	0,07743	0,00047	2,13472	0,02188	0,199947	0,00165	0,805	4,1	1,2		1132	12	1160	7	1175	9
SIN-177	175	26,4	0,00E+00	1128	0,09274	0,00066	2,68776	0,0301	0,210189	0,001815	0,771	-18,7	-16,5		1483	13	1325	8	1230	10

A.E. Myhre

SIN-177-CORR	175	26.4	1.30E+00	1128	0,0848	0,00058	2,32389	0,02616	0,207244	0,001796	0,771	-1,7	.		1233	14	1221	8	1214	10
PI-103	702	26.8	0,00E+00	19573	0,05317	0,00029	0,40382	0,00336	0,055083	0,000348	0,76	2,9	.		336	12	344	2	346	2
SIN-078	179	29.6	0,00E+00	65627	0,08787	0,00054	2,8	0,02702	0,23122	0,001723	0,773	-3,1	-0,7		1380	11	1356	7	1341	9
SIN-079	140	15,7	0,00E+00	2595	0,08521	0,00055	1,86356	0,01835	0,158613	0,001179	0,755	-3,02	-28,4		1320	12	1068	7	949	7
SIN-079-CORR	140	15,7	7,50E-01	2595	0,07897	0,0005	1,71331	0,01681	0,157343	0,001171	0,750	-21	-18,8		1172	12	1014	6	942	7
SIN-080	207	32,3	0,00E+00	32554	0,08531	0,00053	2,64278	0,02941	0,224675	0,002082	0,833	-1,3	.		1323	11	1313	8	1307	11
SIN-081	193	32,2	0,00E+00	14632	0,08765	0,00055	2,81415	0,02762	0,23286	0,001746	0,764	-2	.		1375	12	1359	7	1349	9
SIN-081-CORR	193	32,2	9,50E-02	14632	0,08686	0,00055	2,7862	0,02731	0,232635	0,001744	0,765	-0,7	.		1357	12	1352	7	1348	9
SIN-082	397	63	0,00E+00	27616	0,07884	0,00049	2,03438	0,02145	0,192007	0,001617	0,799	1,5	.		1117	13	1127	7	1132	9
SIN-083	198	27,4	0,00E+00	26652	0,07736	0,00048	2,05273	0,01947	0,192459	0,001371	0,751	0,4	.		1130	13	1133	6	1135	7
SIN-084	126	20,5	0,00E+00	14691	0,08653	0,00053	2,75874	0,02714	0,231221	0,001786	0,785	-0,8	.		1350	12	1344	7	1341	9
SIN-085	138	26,3	0,00E+00	1358	0,09881	0,00125	3,6397	0,05585	0,2667154	0,002304	0,562	-5,3	-1,6		1602	24	1558	12	1526	12
SIN-085-CORR	140	26,6	1,40E+00	1368	0,08725	0,0013	3,17516	0,05629	0,263947	0,002536	0,542	11,8	7,4		1366	27	1451	14	1510	13
SIN-086	114	14,7	0,00E+00	342	0,11967	0,00141	2,60561	0,03983	0,157911	0,001537	0,637	-55,3	-53,9		1951	21	1302	11	945	9
SIN-086-CORR	114	14,7	4,40E+00	342	0,08332	0,0012	1,72786	0,03027	0,150401	0,001508	0,572	-31,3	-27,6		1277	27	1019	11	903	8
SIN-087	178	25,2	0,00E+00	8367	0,08258	0,00065	2,06231	0,02093	0,181132	0,001173	0,638	-16	-13,5		1259	14	1136	7	1073	6
SIN-087-CORR	178	25,2	5,00E-01	8567	0,07842	0,00062	1,9482	0,01986	0,180174	0,001168	0,636	-8,4	-5,4		1158	14	1098	7	1068	6
SIN-088	191	28,4	0,00E+00	54890	0,08221	0,00062	2,14277	0,0217	0,189034	0,00129	0,674	-11,7	-9,1		1251	14	1163	7	1116	7
SIN-088-CORR	191	28,4	6,40E-01	54890	0,07687	0,00058	1,99012	0,02023	0,187757	0,001284	0,673	-0,8	.		1118	15	1112	7	1109	7
PI-104	738	31,5	0,00E+00	17221	0,05324	0,0003	0,40621	0,00338	0,055334	0,00034	0,737	2,4	.		339	12	346	2	347	2
SIN-089	312	51,4	0,00E+00	1086	0,10161	0,00077	3,23305	0,03712	0,230773	0,001996	0,754	-21,1	-19		1654	14	1465	9	1339	10
SIN-089-CORR	312	51,4	1,50E+00	1086	0,08959	0,00068	2,80823	0,03226	0,2277339	0,001971	0,755	-7,5	-4,8		1417	14	1358	9	1321	10
SIN-090	294	71,4	0,00E+00	45309	0,11606	0,00081	5,343353	0,06063	0,333929	0,002999	0,780	-2,4	-0,1		1896	12	1876	10	1857	14
SIN-090-CORR	294	71,4	7,80E-02	45309	0,11543	0,0008	5,31063	0,06018	0,3336881	0,002987	0,790	-1,9	.		1887	12	1871	10	1856	14
SIN-091	67	8,7	0,00E+00	11192	0,07645	0,00049	1,93678	0,01937	0,183727	0,00141	0,767	-1,9	.		1107	12	1094	7	1087	8
SIN-092	77	10	0,00E+00	6304	0,07597	0,00047	1,92773	0,01851	0,184045	0,001348	0,762	-0,5	.		1094	12	1091	6	1089	7
SIN-093	116	32,2	0,00E+00	21703	0,12937	0,00098	6,75143	0,08435	0,378495	0,003752	0,793	-1,1	.		2089	13	2079	11	2069	18
SIN-094	157	23,4	0,00E+00	25373	0,0809	0,0005	2,34925	0,02512	0,210601	0,001835	0,815	1,2	.		1219	12	1227	8	1232	10
SIN-095	187	46,9	0,00E+00	10493	0,11233	0,00087	4,91696	0,05121	0,317478	0,002204	0,667	-3,7	-1,6		1837	14	1805	9	1777	11
SIN-095-CORR	187	46,9	2,60E-01	10493	0,1102	0,00085	4,81134	0,04985	0,316661	0,002197	0,670	-1,9	.		1803	14	1787	9	1773	11
SIN-096	266	53,8	0,00E+00	12015	0,09004	0,00065	3,03191	0,03168	0,244226	0,00184	0,721	-1,4	.		1426	13	1416	8	1409	10
SIN-096-CORR	266	53,8	2,10E-01	12015	0,08829	0,00064	2,96645	0,03092	0,243695	0,001835	0,723	1,4	.		1389	13	1399	8	1406	10
SIN-097	199	31,3	0,00E+00	6335	0,08159	0,00059	2,25537	0,02159	0,200478	0,001267	0,660	-5,1	-2,4		1236	13	1198	7	1178	7
SIN-097-CORR	199	31,3	3,10E-01	6335	0,07899	0,00057	2,17633	0,02081	0,199821	0,001263	0,661	0,2	.		1172	14	1174	7	1174	7
SIN-098	279	48,8	0,00E+00	5637	0,09107	0,00061	3,07399	0,03174	0,244806	0,001913	0,757	-2,8	-0,3		1448	12	1426	8	1412	10

SIN-098-CORR	279	48,8	3,80E-01	5637	0,08793	0,00059	2,95657	0,03042	0,243866	0,001904	0,759	2,1	.		1381	13	1397	8	1407	10
SIN-099	176	28,9	0,00E+00	8936	0,07832	0,00056	2,08154	0,02672	0,192762	0,002062	0,833	-1,8	.		1155	14	1143	9	1136	11
SIN-100	112	26,1	0,00E+00	18817	0,11321	0,00077	5,10075	0,06099	0,326766	0,003209	0,821	-1,8	.		1852	12	1836	10	1823	16
SIN-101	257	36,8	0,00E+00	970	0,09067	0,00065	2,42018	0,03021	0,19359	0,001985	0,821	-22,6	-20,4		1440	13	1249	9	1141	11
SIN-101-CORR	257	36,8	1,50E+00	970	0,07774	0,00055	2,04139	0,02564	0,190441	0,00197	0,824	-1,6	.		1140	14	1129	9	1124	11
PL-105	614	24,3	0,00E+00	19490	0,05277	0,00031	0,40012	0,00372	0,054995	0,000392	0,767	8,5	0,9		319	13	342	3	345	2
SIN-102	259	34,2	0,00E+00	8121	0,07849	0,0005	2,06775	0,02202	0,19107	0,001635	0,804	-3	-0,1		1159	12	1138	7	1127	9
SIN-102-CORR	259	34,2	2,60E-01	8121	0,07627	0,00048	2,00363	0,02132	0,190541	0,001631	0,804	2,2	.		1102	13	1117	7	1124	9
SIN-103	134	20,6	0,00E+00	138	0,17927	0,00248	6,32603	0,14807	0,255925	0,004827	0,806	-49,6	-47,6		2646	23	2022	21	1469	25
SIN-103-CORR	134	20,6	1,10E+01	138	0,08682	0,00171	2,72684	0,07317	0,222779	0,004143	0,678	-2,7	.		1357	37	1336	20	1323	22
SIN-104	339	43,9	0,00E+00	653	0,09677	0,00087	2,49349	0,03163	0,186886	0,001682	0,709	-31,9	-29,8		1563	16	1270	9	1104	9
SIN-104-CORR	331	45,6	2,20E+00	671	0,07713	0,00079	1,94346	0,02672	0,182746	0,001686	0,671	-4,1	.		1125	20	1096	9	1082	9
SIN-105	163	26,3	0,00E+00	19943	0,08601	0,00053	2,74245	0,02968	0,231253	0,00205	0,819	0,2	.		1338	12	1340	8	1341	11
PL-106	604	22,7	0,00E+00	16568	0,05314	0,00029	0,40972	0,00393	0,055916	0,000439	0,818	4,9	.		335	12	349	3	351	3
SIN-106	178	22,8	0,00E+00	18743	0,07908	0,00051	1,99919	0,02125	0,183349	0,001551	0,796	-8,2	-5,5		1174	13	1115	7	1085	8
SIN-106-CORR	178	22,8	1,70E-01	18743	0,07768	0,0005	1,96023	0,02082	0,183025	0,001548	0,796	-5,3	-2,4		1139	12	1102	7	1083	8
SIN-107	172	22	0,00E+00	3869	0,08097	0,00052	2,0426	0,02111	0,182964	0,00148	0,783	-12,2	-9,7		1221	12	1130	7	1083	8
SIN-107-CORR	172	22	4,40E-01	3869	0,07726	0,00049	1,94005	0,01999	0,182111	0,001472	0,785	-4,8	-1,9		1128	12	1095	7	1078	8
SIN-108	257	37,6	0,00E+00	1631	0,08581	0,00074	2,39154	0,03112	0,202133	0,001964	0,747	-12,1	-9		1334	17	1240	9	1187	11
SIN-108-CORR	257	37,6	9,40E-01	1631	0,07795	0,00007	2,15103	0,02849	0,200151	0,001953	0,737	2,9	.		1145	18	1165	9	1176	10
SIN-109	147	19,3	0,00E+00	1763	0,0886	0,00064	2,38975	0,02999	0,195625	0,002012	0,819	-19,1	-16,6		1396	14	1240	9	1152	11
SIN-109-CORR	147	19,3	1,20E+00	1763	0,07892	0,00056	2,10307	0,02628	0,193265	0,001984	0,821	-2,9	.		1170	14	1150	9	1139	11
SIN-110	191	28	0,00E+00	12366	0,08338	0,00056	2,51033	0,0315	0,218347	0,002319	0,846	-0,4	.		1278	13	1275	9	1273	12
PL-107	824	30,2	0,00E+00	18557	0,0532	0,00031	0,41434	0,00464	0,056491	0,000537	0,835	5,2	.		337	14	352	3	354	3
PL-201	685	49,1	0,00E+00	10635	0,05558	0,00021	0,40622	0,0049	0,054985	0,000625	0,943	-2,5	.		354	9	346	4	345	4
SIN-111	273	86,1	0,00E+00	28211	0,08713	0,00036	2,80963	0,0388	0,233874	0,003085	0,955	-0,7	.		1363	8	1358	10	1355	16
SIN-111-CORR	273	86,1	8,10E-02	28211	0,08646	0,00035	2,78575	0,03845	0,233681	0,003082	0,956	0,4	.		1348	8	1352	10	1354	16
SIN-112	142	35,1	0,00E+00	2723	0,0832	0,0005	2,12372	0,02922	0,18512	0,002289	0,899	-15,3	-12,8		1274	11	1157	9	1095	12
SIN-112-CORR	142	35,1	6,30E-01	2723	0,07795	0,00048	1,97626	0,02734	0,183884	0,002272	0,893	-5,4	-2,4		1146	12	1107	9	1088	12
SIN-113	154	38,6	0,00E+00	12719	0,07749	0,00044	2,03422	0,03189	0,190393	0,002784	0,933	-1	.		1134	11	1127	11	1124	15
SIN-114	54	22,7	0,00E+00	8906	0,11069	0,00073	4,7296	0,08822	0,309904	0,005403	0,935	-4,4	-2		1811	12	1772	16	1740	27
SIN-115	100	27,7	0,00E+00	11612	0,08131	0,00037	2,32819	0,03257	0,207665	0,00745	0,945	-1,1	.		1229	9	1221	10	1216	15
SIN-116	238	68,7	0,00E+00	33418	0,08182	0,00033	2,43036	0,03465	0,215443	0,002947	0,959	1,5	.		1241	8	1252	10	1258	16
SIN-117	186	48,6	0,00E+00	15429	0,0775	0,00035	2,0914	0,02862	0,195722	0,002529	0,944	1,8	.		1134	9	1146	9	1152	14

SIN-118	175	48,8	0,00E+00	3634	0,08707	0,00047	2,5	0,03541	0,208349	0,00273	0,926	-11,4	-9,2		1362	10	1272	10	1220	15
SIN-118-CORR	175	48,8	4,30E-01	3634	0,08351	0,00045	2,38822	0,03383	0,207415	0,002716	0,924	-5,7	-3,2		1281	10	1239	10	1215	14
SIN-119	101	38,5	0,00E+00	14143	0,10553	0,00051	4,09112	0,06338	0,281162	0,004135	0,949	-8,3	-6,5		1724	9	1653	13	1597	21
SIN-119-CORR	101	38,5	5,70E-02	14143	0,10507	0,00051	4,07097	0,06305	0,281003	0,004131	0,949	-7,8	-6		1716	9	1649	13	1596	21
SIN-120	96	41,1	0,00E+00	10452	0,11379	0,00067	4,97393	0,09561	0,317021	0,005803	0,952	-5,3	-3,2		1861	10	1815	16	1775	28
SIN-120-CORR	96	41,1	1,00E-01	10452	0,11297	0,00066	4,93329	0,09478	0,316708	0,005795	0,952	-4,6	-2,5		1848	10	1808	16	1774	28
SIN-121	46	8,5	0,00E+00	26903	0,08535	0,00078	2,6214	0,0316	0,222748	0,001751	0,652	-2,3	.		1324	17	1307	9	1296	9
SIN-122	528	85,6	0,00E+00	1508	0,08449	0,00101	2,27154	0,03278	0,194984	0,001587	0,564	-13	-9,2		1304	23	1203	10	1148	9
SIN-122-CORR	528	85,6	1,10E+00	1508	0,07539	0,00095	2,0029	0,02997	0,192684	0,001574	0,546	-5,8	1,7		1079	24	1116	10	1136	9
SIN-123	450	69,1	0,00E+00	4310	0,07892	0,00067	2,03022	0,02437	0,186575	0,001575	0,703	-6,3	-2,8		1170	16	1126	8	1103	9
SIN-123-CORR	432	68,8	3,40E-01	4525	0,07593	0,00072	1,9376	0,02629	0,185077	0,001807	0,720	0,1	.		1093	18	1094	9	1095	10
SIN-125	125	23,8	0,00E+00	4244	0,08905	0,00079	2,84729	0,03476	0,2331906	0,001932	0,683	-4,8	-1,7		1405	16	1368	9	1344	10
SIN-125-CORR	124	23,8	3,50E-01	4131	0,08636	0,00078	2,74856	0,03382	0,230825	0,001924	0,677	-0,6	.		1346	16	1342	9	1339	10
SIN-126	153	36,9	0,00E+00	43528	0,1014	0,00088	4,08466	0,04989	0,292155	0,00252	0,706	0,2	.		1650	15	1651	10	1652	13
SIN-127	494	108,6	0,00E+00	1649	0,10305	0,00094	3,74266	0,0485	0,26334	0,002418	0,709	-11,5	-8,9		1680	16	1581	10	1507	12
SIN-127-CORR	494	108,6	9,40E-01	1649	0,09568	0,00085	3,4	0,04391	0,260907	0,002399	0,721	-3,4	-0,4		1541	16	1514	10	1494	12
SIN-128	148	29,3	0,00E+00	567	0,11773	0,00139	3,89305	0,05772	0,239826	0,002147	0,604	-31	-28,8		1922	20	1612	12	1386	11
SIN-128-CORR	149	30,5	2,60E+00	588	0,09659	0,00114	3,10075	0,04875	0,2332817	0,002407	0,658	-14,9	-11,6		1559	21	1433	12	1349	13
SIN-129	213	40,8	0,00E+00	42053	0,08564	0,00071	2,76775	0,03178	0,234389	0,001859	0,691	2,3	.		1330	15	1347	9	1357	10
SIN-129-CORR	213	40,8	6,30E-03	42053	0,08559	0,00071	2,76596	0,03176	0,2334374	0,001859	0,691	2,4	.		1329	15	1346	9	1357	10
SIN-130	206	31,6	0,00E+00	16742	0,07552	0,00058	1,96688	0,0211	0,188903	0,001403	0,693	3,3	0,1		1082	14	1104	7	1115	8
SIN-131	105	37	0,00E+00	3014	0,17751	0,00252	9,7103	0,21378	0,396741	0,006681	0,765	-21,2	-18,2		2630	23	2408	20	2154	31
SIN-131-CORR	105	37	5,40E-01	3014	0,17378	0,00242	9,452912	0,20696	0,394773	0,006658	0,771	-20,3	-17,3		2594	23	2384	20	2145	31
PL-01	639	29,8	0,00E+00	11112	0,05213	0,00041	4	0,00457	0,056286	0,000452	0,711	21,8	10,8		291	17	345	3	353	3
PL-02	599	26	0,00E+00	10428	0,05243	0,00037	0,40609	0,00396	0,056173	0,000378	0,69	16,2	7,4		304	15	346	3	352	2
SIN-132	74	21,4	0,00E+00	3387	0,11766	0,00141	5,1696	0,10117	0,318669	0,004924	0,780	-8,2	-4,6		1921	21	1848	17	1783	24
SIN-132-CORR	74	21,4	4,40E-01	3387	0,11426	0,00136	4,99886	0,09732	0,317318	0,004897	0,793	-5,6	-1,8		1868	21	1819	16	1777	24
SIN-133	306	57	0,00E+00	646	0,10364	0,00013	2,9673	0,05934	0,207647	0,003237	0,78	-30,7	-27,7		1690	22	1399	15	1216	17
SIN-133-CORR	306	57	2,30E+00	646	0,08487	0,00106	2,37077	0,04756	0,202603	0,003171	0,78	-10,3	-5,5		1313	23	1234	14	1189	17
SIN-134	195	29,8	0,00E+00	8364	0,07774	0,00067	2,04307	0,02301	0,196062	0,001391	0,648	-1,5	.		1140	16	1130	8	1125	8
SIN-134-CORR	195	29,8	1,80E-01	8364	0,0763	0,00065	2,00144	0,02251	0,190252	0,001388	0,649	2	.		1103	16	1116	8	1123	8
SIN-135	288	43,8	0,00E+00	27455	0,076	0,00059	1,98998	0,02169	0,189899	0,001449	0,700	2,6	.		1095	15	1112	7	1121	8
SIN-136	131	20,7	0,00E+00	3406	0,08171	0,00099	2,14977	0,03122	0,190811	0,001512	0,546	-9,9	-5,7		1239	23	1165	10	1126	8
SIN-136-CORR	131	20,7	6,10E-01	3406	0,07674	0,00096	2,00598	0,02967	0,189593	0,001503	0,536	0,5	.		1114	24	1118	10	1119	8
SIN-137	248	36,8	0,00E+00	12045	0,07711	0,0006	1,96848	0,02188	0,185151	0,001458	0,709	-2,8	.		1124	15	1105	7	1095	8

SIN-137-CORR	248	36,8	1,50E-01	12045	0,0759	0,00059	1,9345	0,02145	0,184864	0,001456	0,710	0,1	.			1092	15	1093	7	1093	8
SIN-138	111	29	0,00E+00	15004	0,11258	0,00106	4,91801	0,06362	0,316821	0,002809	0,685	-4,2	-1,5			1842	17	1805	11	1774	14
SIN-139	141	22,5	0,00E+00	6008	0,07856	0,00068	2,12254	0,026	0,195057	0,001697	0,707	-0,7	.			1161	17	1156	8	1154	9
SIN-139-CORR	141	22,5	2,60E-01	6008	0,07643	0,00066	2,05938	0,02519	0,195428	0,001694	0,709	4,4	0,7			1106	17	1135	8	1151	9
SIN-140	279	41,1	0,00E+00	13811	0,07728	0,00061	1,96634	0,02148	0,184533	0,001436	0,702	-3,5	-0,2			1129	15	1104	7	1092	8
SIN-140-CORR	279	41,1	9,70E-02	13811	0,07649	0,0006	1,94416	0,02152	0,184346	0,001434	0,703	-1,7	.			1108	15	1096	7	1091	8
SIN-141	134	32,6	0,00E+00	12017	0,10272	0,00094	4,16686	0,05179	0,294201	0,002485	0,679	-0,8	.			1674	16	1668	10	1662	12
SIN-142	261	51,3	0,00E+00	1498	0,10458	0,0011	3,29458	0,05867	0,228484	0,003277	0,806	-24,6	-21,8			1707	19	1480	14	1327	17
SIN-142-CORR	261	51,3	9,30E-01	1498	0,09716	0,00099	3,03163	0,05361	0,226302	0,003263	0,815	-18	-14,7			1570	19	1416	14	1315	17
SIN-143	158	25,2	0,00E+00	12336	0,07783	0,00063	2,1607	0,02428	0,201336	0,001575	0,696	3,8	0,6			1143	16	1168	8	1182	8
SIN-144	152	25,3	0,00E+00	1017	0,09161	0,00153	2,45439	0,04837	0,194322	0,002019	0,527	-23,5	-19,2			1459	31	1259	14	1145	11
SIN-144-CORR	152	25,3	1,80E+00	1017	0,07699	0,00143	2,024	0,04318	0,190672	0,001979	0,487	0,4	.			1121	36	1124	14	1125	11
PL-03	579	26,8	0,00E+00	16278	0,05289	0,00045	4,04055	0,00504	0,05548	0,000504	0,720	7,7	.			324	19	345	4	348	3
SIN-145	214	32	0,00E+00	11369	0,07616	0,00059	1,97598	0,02257	0,188161	0,001571	0,731	1,2	.			1099	15	1107	8	1111	9
SIN-145-CORR	214	32	3,60E-02	11369	0,07587	0,00059	1,96762	0,02246	0,188091	0,00157	0,731	1,9	.			1092	15	1104	8	1111	9
SIN-146	119	18,6	0,00E+00	1701	0,08939	0,0012	2,42364	0,03808	0,196639	0,001614	0,522	-19,7	-16,1			1413	24	1250	11	1157	9
SIN-146-CORR	119	18,6	1,40E+00	1701	0,07817	0,00113	2,08926	0,03482	0,193838	0,001595	0,494	-0,9	.			1151	27	1145	11	1142	9
PL-04	705	30,6	0,00E+00	16352	0,05338	0,00037	4,41741	0,00422	0,056717	0,000416	0,725	3,2	.			345	15	354	3	356	3
SIN-147	157	29,3	0,00E+00	15367	0,08638	0,00071	2,7901	0,03359	0,234262	0,002065	0,732	0,8	.			1347	15	1353	9	1357	11
SIN-148	377	65,2	0,00E+00	980	0,09717	0,00085	2,90659	0,04555	0,216951	0,00282	0,830	-21,4	-18,7			1570	15	1384	12	1266	15
SIN-148-CORR	377	65,2	1,50E+00	980	0,08477	0,00071	2,4965	0,03887	0,213583	0,002805	0,844	-5,2	-1,7			1310	16	1271	11	1248	15
SIN-149	199	36,1	0,00E+00	1110	0,09018	0,00116	2,82109	0,04821	0,226893	0,002559	0,660	-8,6	-4,4			1429	24	1361	13	1318	13
SIN-149-CORR	199	36,1	1,50E+00	1110	0,0778	0,00107	2,39687	0,04287	0,223435	0,002541	0,636	15,3	9,7			1142	27	1242	13	1300	13
SIN-150	204	31,7	0,00E+00	13866	0,0777	0,00064	2,09607	0,0239	0,19566	0,001544	0,692	1,2	.			1139	16	1148	8	1152	8
SIN-151	38	6,2	0,00E+00	241	0,13395	0,00361	3,53901	0,10813	0,191624	0,002756	0,471	-51,6	-48,6			2150	47	1536	24	1130	15
SIN-151-CORR	38	6,4	6,60E+00	251	0,07694	0,00304	1,8839	0,08094	0,177595	0,002994	0,392	-6,4	.			1120	78	1075	28	1054	16
SIN-151r	42	6,1	0,00E+00	3736	0,07634	0,00065	1,93379	0,0235	0,183724	0,001591	0,713	-1,6	.			1104	17	1093	8	1087	9
SIN-152	57	9,9	0,00E+00	2171	0,09063	0,001	2,73988	0,03991	0,219258	0,002078	0,651	-12,3	-8,9			1439	21	1339	11	1278	11
SIN-152-CORR	57	9,9	7,50E-01	2171	0,08449	0,00095	2,53451	0,03734	0,217574	0,002066	0,644	-2,9	.			1304	21	1282	11	1269	11
SIN-153	74	13,8	0,00E+00	4266	0,0885	0,00076	2,87005	0,03699	0,235215	0,00226	0,746	-2,5	.			1393	16	1374	10	1362	12
SIN-154	175	26,4	0,00E+00	2385	0,08283	0,00092	2,1936	0,02997	0,192075	0,001543	0,588	-11,4	-7,7			1265	21	1179	10	1133	8
SIN-154-CORR	175	26,4	7,20E-01	2385	0,07683	0,00087	2,01936	0,02806	0,190627	0,001531	0,578	0,8	.			1117	22	1122	9	1125	8
SIN-155	236	36,3	0,00E+00	7845	0,07937	0,00071	2,10281	0,02563	0,192163	0,00158	0,675	-4,4	-0,8			1181	18	1150	8	1133	9
SIN-155-CORR	236	36,3	2,90E-01	7845	0,07696	0,00069	2,03303	0,02474	0,191581	0,001576	0,676	0,9	.			1120	18	1127	8	1130	9

A.E. Myhre

SIN-156	141	21,4	0,00E+00	8882	0,07732	0,00066	2,02309	0,02327	0,189776	0,001464	0,671	-0,9	.		1129	16	1123	8	1120	8
SIN-157	123	22,5	0,00E+00	12427	0,08531	0,00074	2,67033	0,03248	0,22703	0,001943	0,703	-0,3	.		1323	16	1320	9	1319	10
SIN-158	112	33,7	0,00E+00	9933	0,1168	0,00141	5,45673	0,1026	0,338822	0,004875	0,765	-1,6	.		1908	21	1894	16	1881	23
SIN-158-CORR	112	33,7	1,70E-01	9933	0,11548	0,00139	5,38639	0,10107	0,33828	0,004864	0,766	-0,6	.		1887	21	1883	16	1878	23
SIN-160	76	11,1	0,00E+00	17721	0,07674	0,00067	1,96204	0,02362	0,185435	0,001542	0,691	-1,7	.		1114	17	1103	8	1097	8
PL-05	438	19	0,00E+00	8341	0,05563	0,00043	0,41943	0,00446	0,056726	0,000396	0,657	0,1	.		355	18	356	3	356	2
PL-06	524	22,8	0,00E+00	10878	0,05355	0,00041	0,4202	0,00446	0,056912	0,000419	0,694	1,4	.		352	17	356	3	357	3

Aubures Formation

Name	U	^{206}Pb	$^{206}\text{Pb}_{\text{Q}}(\%)$	206/204	$^{207}\text{Pb}^{206}\text{Pb}^*$	1SE	$^{207}\text{Pb}^{235}\text{U}^*$	1SE	$^{206}\text{Pb}^{238}\text{U}^*$	1SE	Central (%)	Rho	Minimum (%)	rim	Discordance					Ages				
															207/206	1s	207/235	1s	206/238	1s				
A382-02-CPb	115	50,6	0,00E+00	6902	0,11813	0,0015	5,55321	0,11249	0,340948	0,005378	0,779	-2,2	.		1928	22	1909	17	1891	26				
PL-01	714	49,6	0,00E+00	9912	0,05412	0,00029	0,40293	0,00421	0,053994	0,000483	0,857	-10,1	-3,5		376	12	344	3	339	3				
AUB-001	208	51,7	0,00E+00	1299	0,09254	0,00058	2,46664	0,0302	0,193326	0,002037	0,861	-25	-23,1		1478	11	1262	9	1139	11				
AUB-001-Corr	208	51,7	1,10E+00	1299	0,08361	0,00052	2,20204	0,02698	0,191008	0,002015	0,861	-13,3	-10,8		1284	12	1182	9	1127	11				
AUB-002	370	55	0,00E+00	384	0,11022	0,00072	1,76107	0,02236	0,11588	0,001259	0,856	-64,1	-63,2		1803	11	1031	8	707	7				
AUB-002-Corr	364	54,3	4,00E+00	387	0,07746	0,00053	1,7855	0,01579	0,110344	0,00127	0,859	-42,6	-40,6		1133	13	791	7	675	7				
AUB-003	125	41,7	8,30E-01	2222	0,10988	0,0007	3,97489	0,06021	0,262374	0,003607	0,908	-18,4	-16,4		1797	11	1629	12	1502	18				
AUB-003-Corr	125	41,7	8,30E-01	2222	0,10338	0,00065	3,70788	0,05607	0,260122	0,003581	0,910	-13	-10,8		1686	11	1573	12	1490	18				
AUB-004	244	96,6	0,00E+00	4625	0,10979	0,00066	4,67346	0,06531	0,308737	0,003895	0,903	-3,9	-1,7		1796	10	1763	12	1734	19				
AUB-004-Corr	244	96,6	3,10E-01	4625	0,10735	0,00064	4,55561	0,06351	0,307771	0,00388	0,904	-1,6	.		1755	11	1741	12	1730	19				
PL-02	751	51,5	0,00E+00	16244	0,05272	0,00027	0,4	0,00414	0,054001	0,000497	0,873	7,3	.		317	11	336	3	339	3				
AUB-005	206	89,1	0,00E+00	23843	0,11499	0,00072	5,41536	0,07736	0,341565	0,00439	0,900	0,9	.		1880	11	1887	12	1894	21				
AUB-006	456	65,1	0,00E+00	421	0,11466	0,00094	1,77615	0,03228	0,112347	0,001823	0,893	-66,7	-65,7		1875	14	1037	12	686	11				
AUB-006-Corr	456	65,1	3,60E+00	421	0,08614	0,00075	1,28048	0,02413	0,107809	0,001802	0,887	-53,4	-51,5		1341	16	837	11	660	10				
AUB-007	158	29,4	0,00E+00	2341	0,0855	0,00049	1,74142	0,02117	0,147713	0,00158	0,88	-35,4	-33,7		1327	11	1024	8	888	9				
AUB-007-Corr	158	29,4	7,30E-01	2341	0,07958	0,00046	1,6076	0,01957	0,14651	0,00157	0,88	-27,5	-25,4		1187	11	973	8	881	9				
AUB-008	230	62,9	0,00E+00	1242	0,09765	0,00057	2,91967	0,04014	0,216857	0,002702	0,906	-21,9	-20		1580	10	1387	10	1265	14				
AUB-008-Corr	230	62,9	1,20E+00	1242	0,08823	0,0005	2,605	0,03579	0,21413	0,002676	0,91	-10,8	-8,5		1388	10	1302	10	1251	14				
AUB-009	30	7	0,00E+00	1839	0,07521	0,00056	1,9	0,0258	0,185692	0,002069	0,832	2,4	.		1074	14	1090	9	1098	11				
AUB-010	17	4,2	0,00E+00	1216	0,0759	0,00068	2,0035	0,031	0,191456	0,002654	0,839	3,7	.		1092	18	1117	11	1129	14				
AUB-011	175	53,4	0,00E+00	21650	0,08578	0,00048	2,86123	0,036	0,241924	0,002727	0,896	5,3	2,3		1333	11	1372	9	1397	14				
PL-03	673	45,2	0,00E+00	6555	0,05438	0,00028	0,40094	0,00495	0,053472	0,000601	0,91	-13,6	-7,6		387	11	342	4	336	4				

PL-04	669	45.2	0.00E+00	20623	0.05308	0.00028	0.39435	0.00465	0.053879	0.000566	0.892	1,8	.			332	12	338	3	338	3	
AUB-012	145	40.3	0.00E+00	718	0.10874	0.00095	3.34158	0.04999	0.222881	0.002709	0.812	-29,8	-	-27,7		1778	15	1491	12	1297	14	
AUB-012-Corr	145	40.3	2.10E+00	718	0.09225	0.00086	2.77242	0.04263	0.217978	0.002661	0.794	-15,1	-	-11,9		1472	18	1348	11	1271	14	
AUB-013	174	46.2	0.00E+00	1333	0.09309	0.00061	2.73401	0.0366	0.213004	0.002481	0.870	-18,1	-	-15,8		1490	12	1338	10	1245	13	
AUB-013-Corr	174	46.2	1.10E+00	1333	0.08429	0.00056	2.44673	0.03286	0.210515	0.002456	0.869	-5,7	-	-2,8		1299	13	1256	10	1232	13	
AUB-014	166	51.4	0.00E+00	4979	0.0907	0.00057	3.12052	0.04016	0.249536	0.002801	0.872	-	-0,3	.		1440	11	1438	10	1436	14	
AUB-014-Corr	166	51.4	3.30E-01	4979	0.08307	0.00055	3.01961	0.03885	0.248678	0.002791	0.872	3,8	-	0,8		1384	11	1413	10	1432	14	
AUB-015	229	51.2	0.00E+00	1868	0.08886	0.00054	2.2043	0.02937	0.179912	0.002135	0.891	-25,9	-	-23,9		1401	11	1182	9	1066	12	
AUB-015-Corr	229	51.2	8.00E-01	1868	0.08237	0.0005	2.02552	0.02701	0.178337	0.002122	0.892	-	-17	-	-14,6		1254	12	1124	9	1058	12
PL-05	628	42	0.00E+00	13554	0.05313	0.00028	0.39574	0.00424	0.054021	0.000505	0.873	-	1,5	.		334	12	339	3	339	3	
PL-101	782	43.5	0.00E+00	15789	0.05314	0.00027	0.3939	0.00473	0.053764	0.000585	0.906	0,9	.			335	11	337	3	338	4	
PL-102	565	30.9	0.00E+00	7380	0.05305	0.00029	0.38728	0.00483	0.05295	0.000593	0.897	0,6	.			331	12	332	4	333	4	
AUB-016	162	46.3	0.00E+00	2955	0.10325	0.00067	3.84998	0.07359	0.257938	0.004664	0.946	-	-18,4	-	-16,4		1770	11	1603	15	1479	24
AUB-016-Corr	159	46.4	5.50E-01	2997	0.10396	0.00065	3.68521	0.07895	0.257094	0.005268	0.956	-	-14,6	-	-12,4		1696	11	1568	17	1475	27
AUB-017	148	31.7	0.00E+00	14419	0.07855	0.00044	2.20934	0.02985	0.203987	0.002507	0.910	3,4	.	0,1		1161	11	1184	9	1197	13	
AUB-018	232	55.7	0.00E+00	11172	0.08713	0.00048	2.73821	0.03836	0.227922	0.002935	0.919	-3,2	-	-0,8		1363	10	1339	10	1324	15	
AUB-019	205	55.3	0.00E+00	6425	0.09601	0.00055	3.37558	0.0492	0.254984	0.003413	0.918	-6,1	-	-3,8		1548	10	1499	11	1464	18	
AUB-019-Corr	205	55.3	2.70E-01	6425	0.09288	0.00054	3.29125	0.04788	0.254271	0.003402	0.920	-	-3,4	-	-1		1506	10	1479	11	1460	17
AUB-020	78	29.7	0.00E+00	10531	0.12135	0.0008	6.00985	0.10384	0.359197	0.005738	0.925	0,1	.			1976	11	1977	15	1978	27	
AUB-021	24	4.6	0.00E+00	1197	0.07637	0.00068	1.96063	0.03172	0.1862	0.00251	0.833	-	-0,4	.		1105	17	1102	11	1101	14	
AUB-022	59	22.9	0.00E+00	10318	0.12157	0.0008	6,1	0.10745	0.364963	0.005942	0.927	1,5	.			1979	11	1993	15	2006	28	
PL-103	549	30	0.00E+00	9638	0.05294	0.00031	0.37924	0.00534	0.051953	0.000665	0.909	.	.	.		326	13	326	4	326	4	
AUB-23	96	20.1	0.00E+00	4234	0.07926	0.00047	2.1836	0.03039	0.199814	0.002516	0,905	-	-0,4	.		1179	12	1176	10	1174	14	
AUB-24	135	27.3	0.00E+00	1882	0.08699	0.00062	2.27886	0.03603	0.189991	0.002679	0.892	-19,1	-	-16,5		1360	14	1206	11	1121	15	
AUB-24-Corr	135	27.3	9.90E-01	1882	0.079	0.00058	2.04742	0.03257	0.18797	0.002652	0.887	-	-5,7	-	-2,2		1172	14	1131	11	1110	14
AUB-25	111	18.5	0.00E+00	2195	0.08449	0.00056	1.84774	0.0278	0.158606	0.002146	0.899	-	-29,3	-	-27,1		1304	12	1063	10	949	12
AUB-25-Corr	111	18.5	7.30E-01	2195	0.07862	0.00052	1.70568	0.02576	0.157344	0.002132	0.897	-	-20,4	-	-17,7		1163	12	1011	10	942	12
AUB-26	125	25.4	0.00E+00	7740	0.0811	0.00048	2.1662	0.03069	0.193726	0.002499	0.911	-	-7,3	-	-4,6		1224	11	1170	10	1142	13
AUB-27	45	10.5	0.00E+00	1516	0.09891	0.00127	3,1	0.05606	0.2245	0.002921	0.711	-	-20,5	-	-17		1604	23	1423	14	1306	15
AUB-27-Corr	45	10.5	1.50E+00	1516	0.08648	0.00124	2.6333	0.05085	0.220844	0.002868	0.672	-	-5,1	-	-		1349	26	1310	14	1286	15
AUB-28	142	26.2	0.00E+00	11282	0.08119	0.00048	1.98724	0.02657	0.177517	0.002123	0.895	-	-15,3	-	-12,8		1226	11	1111	9	1053	12
AUB-28-Corr	142	26.2	2.50E-01	11282	0.07913	0.00047	1.93147	0.02581	0.177029	0.002117	0.895	-	-11,5	-	-8,8		1175	11	1092	9	1051	12
AUB-029	264	45.5	0.00E+00	1455	0.08735	0.00056	1.98602	0.03607	0.164898	0.002805	0.936	-	-30,3	-	-28,2		1368	12	1111	12	984	16
AUB-029-Corr	264	45.5	1.00E+00	1455	0.07907	0.00051	1.77779	0.03248	0.163063	0.00279	0.937	-	-18,4	-	-15,6		1174	12	1037	12	974	15

PL-104	616	34	0.00E+00	7847	0.0542	0.00028	0.39906	0.00527	0.053398	0.000651	0.923	-11,9	-5,7		379	11	341	4	335	4
AUB-030	47	9,5	0.00E+00	3498	0,07739	0.00055	2,08572	0,02971	0,195469	0,002417	0,868	1,9	.		1131	14	1144	10	1151	13
AUB-031	206	40,3	0.00E+00	4163	0,0847	0.0005	2,1969	0,031	0,188108	0,002407	0,907	-16,4	-14,1		1309	11	1180	10	1111	13
AUB-031-Corr	206	5,50E-01	4163	0,08024	0,00048	2,0687	0,02918	0,186992	0,002393	0,907	-8,8	-6,1		1203	11	1139	10	1105	13	
AUB-032	111	38,4	0.00E+00	17519	0,10753	0.00067	4,87463	0,07736	0,328778	0,004793	0,919	4,9	1,4		1758	11	1798	13	1832	23
AUB-033	60	11,8	0.00E+00	6139	0,0762	0.00046	1,98777	0,02687	0,189192	0,002291	0,896	1,6	.		1100	12	1111	9	1117	12
AUB-034	87	21,4	0.00E+00	56974	0,08501	0,0005	2,77559	0,04121	0,236814	0,003225	0,917	4,6	1,1		1316	11	1349	11	1370	17
AUB-035	140	28,4	0.00E+00	26202	0,07605	0,00042	2,04971	0,02754	0,195465	0,002389	0,91	5,4	2		1096	11	1132	9	1151	13
AUB-036	175	40,4	0.00E+00	9549	0,08152	0,00047	2,49871	0,03481	0,222293	0,002819	0,91	5,4	2		1234	11	1272	10	1294	15
AUB-037	91	22,2	0.00E+00	6758	0,08611	0,00051	2,78767	0,04024	0,234788	0,003086	0,91	1,6	.		1341	12	1352	11	1360	16
AUB-038	195	41,6	0.00E+00	12759	0,08123	0,00045	2,30087	0,03232	0,205428	0,002656	0,92	-2	.		1227	10	1213	10	1204	14
AUB-039	82	17,4	0.00E+00	9397	0,07815	0,00047	2,19869	0,03045	0,204041	0,002551	0,903	4,4	0,9		1151	11	1181	10	1197	14
AUB-040	93	28,9	0.00E+00	12391	0,11525	0,00087	4,86602	0,07118	0,305842	0,003846	0,859	-9,9	-7,5		1884	13	1795	12	1720	19
AUB-041	65	13,5	0.00E+00	4600	0,07903	0,00048	2,18581	0,03108	0,200588	0,002576	0,903	0,5	.		1173	12	1177	10	1178	14
AUB-042	207	67,6	0.00E+00	1056	0,11634	0,00072	3,49196	0,051	0,217681	0,002876	0,905	-36,5	-35,1		1901	11	1525	12	1270	15
AUB-042-Corr	289	67,5	1.50E+00	1070	0,10483	0,00061	3,09767	0,05018	0,214323	0,003242	0,934	-29,5	-27,9		1711	10	1432	12	1252	17
AUB-043	85	19,1	0.00E+00	6750	0,08037	0,00045	2,36312	0,03372	0,213251	0,002801	0,921	3,7	0,3		1206	10	1232	10	1246	15
PL-105	561	30,3	0.00E+00	6725	0,05562	0,00033	0,39332	0,00599	0,051291	0,000718	0,919	-26,9	-21,5		437	13	337	4	322	4
PL-106	670	37,2	0.00E+00	8533	0,05313	0,00028	0,39278	0,00492	0,053613	0,000609	0,906	0,7	.		335	12	336	4	337	4
AUB-044	109	24,1	0.00E+00	12695	0,08554	0,00052	2,49005	0,03788	0,211465	0,002952	0,918	-7,3	-4,7		1325	11	1269	11	1237	16
AUB-045	89	30,2	0.00E+00	9517	0,10731	0,00067	4,757735	0,08268	0,321547	0,005211	0,932	2,8	.		1754	11	1777	15	1797	25
AUB-046	69	13,2	0.00E+00	3349	0,07577	0,00046	1,91289	0,022797	0,183107	0,002433	0,909	-0,5	.		1089	12	1086	10	1084	13
AUB-047	56	19,2	0.00E+00	4405	0,10269	0,00071	4,93925	0,08486	0,326578	0,005194	0,926	1,8	.		1794	11	1809	15	1822	25
AUB-048	202	52	0.00E+00	14359	0,08762	0,00049	2,97444	0,04648	0,246203	0,003594	0,934	3,6	0,1		1374	10	1401	12	1419	19
AUB-049	60	13,8	0.00E+00	3039	0,08415	0,00081	2,36001	0,05912	0,203411	0,004708	0,924	-8,6	-4,4		1296	19	1231	18	1194	25
AUB-050	35	8,8	0.00E+00	2917	0,09439	0,00069	3,19558	0,05743	0,245541	0,004034	0,914	-7,4	-4,5		1516	14	1456	14	1415	21
AUB-051	103	33,4	0.00E+00	8093	0,10878	0,00069	4,68214	0,07394	0,312187	0,004512	0,915	-1,8	.		1779	11	1764	13	1751	22
PL-107	638	35,7	0.00E+00	394187139	0,05348	0,00028	0,40143	0,00586	0,054441	0,000741	0,933	-2,2	.		349	11	343	4	342	5
PL-108	651	35,9	0.00E+00	15041	0,05357	0,00028	0,39846	0,00512	0,053947	0,000632	0,912	-4,2	.		353	11	341	4	339	4
AUB-52	188	51,1	0.00E+00	10028	0,1139	0,00074	3,39054	0,07725	0,254094	0,00463	0,941	-24,2	-22,3		1863	12	1632	16	1460	24
AUB-52-Corr	188	51,1	4.30E-01	10028	0,11054	0,00071	3,83507	0,0745	0,222939	0,004607	0,942	-21,9	-19,9		1808	11	1604	16	1454	24
AUB-53	25	4,8	0.00E+00	2057	0,07732	0,0006	2,02393	0,03216	0,189841	0,002628	0,871	-0,9	.		1130	15	1124	11	1121	14
AUB-54	143	40,4	0.00E+00	8609	0,11586	0,00075	4,436673	0,06691	0,277722	0,003591	0,912	-18,7	-16,7		1893	11	1719	13	1580	20
AUB-54-Corr	143	40,4	2.30E-01	8609	0,11407	0,00073	4,33755	0,06857	0,277062	0,0033981	0,913	-17,4	-15,4		1865	11	1704	13	1577	20
AUB-055	105	32,3	0.00E+00	11857	0,10981	0,00071	4,4992	0,07308	0,297171	0,004431	0,918	-7,5	-5,2		1796	11	1731	13	1677	22

AUB-056	90	19.6	0.00E+00	6912	0.08194	0.00051	2.36958	0.03539	0.209746	0.002853	0.911	-1.5	.			1244	12	1233	11	1227	15
AUB-057	26	5.5	0.00E+00	1512	0.07835	0.00068	2.19068	0.03727	0.202775	0.002974	0.862	3.3	.			1156	16	1178	12	1190	16
AUB-058	73	17.1	0.00E+00	8320	0.08629	0.00053	2.70372	0.04044	0.227255	0.003099	0.912	-2	.			1345	12	1329	11	1320	16
AUB-059	102	23.8	0.00E+00	8796	0.08732	0.00055	2.71762	0.04134	0.225726	0.003123	0.910	-4.5	-1.7			1368	12	1333	11	1312	16
AUB-060	125	26.6	0.00E+00	597	0.11469	0.00133	3.21153	0.0607	0.203088	0.003026	0.788	-39.8	-37.5			1875	19	1460	15	1192	16
AUB-060-Corr	125	26.6	2.60E+00	597	0.09381	0.00125	2.55248	0.05103	0.197345	0.002935	0.744	-24.9	-21.2			1504	24	1287	15	1161	16
AUB-062	78	16	0.00E+00	5096	0.08179	0.0005	2.2132	0.04488	0.196254	0.003795	0.954	-7.5	-4.7			1240	11	1185	14	1155	20
AUB-061Irr	56	12	0.00E+00	2856	0.07923	0.0005	2.23226	0.03976	0.204352	0.00334	0.934	1.9	.			1178	12	1191	12	1199	18
AUB-063	130	26.1	0.00E+00	6440	0.07508	0.00044	2.03182	0.02817	0.196267	0.002468	0.907	8.6	4.9			1071	11	1126	9	1155	13
AUB-064	356	36.2	0.00E+00	394	0.1153	0.00089	1.55228	0.03428	0.097646	0.002021	0.937	-71.2	-70.4			1885	14	951	14	601	12
AUB-064-Corr	356	36.2	3.70E+00	394	0.08548	0.00071	1.10215	0.02514	0.093515	0.001988	0.932	-59.1	-57.4			1326	15	754	12	576	12
PL-109	556	30.5	0.00E+00	7054	0.05283	0.00029	0.4003	0.00515	0.054957	0.000639	0.905	7.5	.			321	12	342	4	345	4
PL-110	729	39.9	0.00E+00	11718	0.05297	0.00028	0.40023	0.00484	0.054802	0.000598	0.902	5.2	.			327	11	342	4	344	4
AUB-065	118	32.4	0.00E+00	11078	0.09439	0.00059	3.54664	0.05234	0.272515	0.003649	0.907	2.8	.			1516	12	1538	12	1554	18
AUB-066	130	28.4	0.00E+00	15760	0.07911	0.00047	2.37435	0.03376	0.217682	0.002808	0.907	8.9	5.2			1175	12	1235	10	1270	15
AUB-067	52	18.6	0.00E+00	5876	0.11467	0.00077	5.64565	0.09638	0.357074	0.005599	0.918	5.8	2.1			1875	12	1923	15	1968	27
AUB-068	70	24	0.00E+00	9886	0.10977	0.00072	5.15009	0.08498	0.340281	0.005154	0.918	5.9	2.4			1796	11	1844	14	1888	25
AUB-069	121	32.3	0.00E+00	7078	0.11479	0.00082	4.1717	0.0688	0.263584	0.003919	0.901	-22	-19.9			1877	12	1668	14	1508	20
PL-111	655	35.5	0.00E+00	7959	0.05333	0.00032	0.39914	0.00565	0.054281	0.000695	0.904	-0.6	.			343	13	341	4	341	4
AUB-070	196	30.9	0.00E+00	469	0.10764	0.00092	2.24053	0.04395	0.150962	0.002662	0.899	-51.9	-50.3			1760	15	1194	14	906	15
AUB-070-Corr	196	30.9	3.00E+00	469	0.08352	0.00078	1.68093	0.03363	0.45967	0.002583	0.885	-33.6	-30.7			1281	17	1001	13	878	15
AUB-071	77	16.4	0.00E+00	25100	0.09072	0.00067	2.70596	0.04799	0.216323	0.00349	0.91	-13.6	-10.8			1441	13	1330	13	1262	18
AUB-072	190	36.1	0.00E+00	9739	0.08573	0.00057	2.24482	0.03351	0.18992	0.002543	0.897	-17.3	-14.7			1332	12	1195	10	1121	14
AUB-072-Corr	190	36.1	5.90E-01	9739	0.0809	0.00053	2.10485	0.03138	0.188707	0.002526	0.898	-9.3	-6.4			1219	12	1150	10	1114	14
AUB-073	21	4.3	0.00E+00	1405	0.07684	0.00074	2.13709	0.04158	0.201725	0.003409	0.869	6.6	1.3			1117	19	1161	13	1185	18
AUB-074	70	16.5	0.00E+00	11964	0.08341	0.0006	2.7069	0.04465	0.225375	0.003495	0.9	7.3	3.2			1279	14	1330	12	1363	18
AUB-075	143	25	0.00E+00	3710	0.09444	0.00069	2.26921	0.04199	0.174277	0.002965	0.919	-34.3	-32.2			1517	13	1203	13	1036	16
AUB-076	133	31	0.00E+00	14453	0.08258	0.00053	2.71187	0.04178	0.23818	0.003332	0.908	10.4	6.5			1259	12	1332	11	1377	17
AUB-077	98	24.5	0.00E+00	11322	0.08485	0.00052	2.95128	0.04596	0.25226	0.00361	0.919	11.7	7.9			1312	12	1395	12	1450	19
AUB-078	88	18.2	0.00E+00	6596	0.08155	0.00053	2.36042	0.03675	0.209926	0.002974	0.91	-0.6	.			1235	13	1231	11	1228	16
PL-112	756	40.8	0.00E+00	12936	0.05355	0.00032	0.40766	0.00546	0.055216	0.000663	0.898	-1.6	.			352	13	347	4	346	4
AUB-79	131	32.6	0.00E+00	2005	0.12071	0.00086	4.13108	0.09204	0.248205	0.005241	0.948	-30.4	-28.6			1667	12	1660	18	1429	27
AUB-79-Corr	131	32.6	8.80E-01	2005	0.11383	0.0008	3.83938	0.0862	0.245908	0.005215	0.95	-26.5	-24.6			1861	12	1605	18	1417	27
AUB-080	210	34.5	0.00E+00	1379	0.09065	0.00073	2.05871	0.04614	0.164713	0.003448	0.934	-34.2	-31.8			1439	15	1135	15	983	19

A.E. Myhre

AUB-080-Corr	210	34.5	1.10E+00	1379	0.08149	0.00068	1.82783	0.04143	0.162681	0.003431	0.93	-22.8	-19.6		1233	16	1055	15	972	19
AUB-081	155	30.6	0.00E+00	21268	0.07854	0.00053	2.14692	0.03308	0.198265	0.002752	0.901	0.5	.		1160	13	1164	11	1166	15
AUB-082	37	7.6	0.00E+00	2238	0.07812	0.00054	2.22766	0.03636	0.206813	0.003058	0.906	5.9	1.8		1150	13	1190	11	1212	16
PL-113	566	29.9	0.00E+00	8172	0.05329	0.00032	0.39101	0.00578	0.053212	0.000718	0.914	-2.1	.		341	13	335	4	334	4
AUB-083	215	34.4	0.00E+00	6213	0.07707	0.00052	1.89691	0.02503	0.178512	0.002025	0.859	-6.2	-3		1123	13	1080	9	1059	11
AUB-083-Corr	218	35.8	2.10E-01	6815	0.0753	0.00054	1.84969	0.02437	0.178158	0.001965	0.837	-2	.		1077	14	1063	9	1057	11
AUB-085	206	45.7	0.00E+00	31001	0.08632	0.00063	2.82082	0.04014	0.239526	0.002879	0.854	3.2	.		1345	14	1369	11	1384	15
AUB-086	182	27.3	0.00E+00	3539	0.08921	0.00066	2.01547	0.02627	0.163858	0.001758	0.823	-32.9	-30.8		1409	14	1121	9	978	10
AUB-086-Corr	182	27.3	5.50E-01	3539	0.08479	0.00062	1.90415	0.02469	0.162878	0.001748	0.827	-27.8	-25.4		1311	14	1083	9	973	10
AUB-087	394	69.1	0.00E+00	3769	0.08051	0.0006	2.11878	0.02966	0.190861	0.002257	0.845	-7.5	4.2	.	1210	14	1155	10	1126	12
AUB-087-Corr	394	69.1	4.30E-01	3769	0.07699	0.00057	2.01674	0.0282	0.189977	0.002248	0.846	.	.		1121	14	1121	9	1121	12
AUB-088	166	29.7	0.00E+00	73430	0.07674	0.0005	2.08479	0.0246	0.197026	0.001934	0.832	4.4	1.1		1115	12	1144	8	1159	10
AUB-089	67	18.9	0.00E+00	55108	0.10613	0.00081	4.46708	0.06238	0.305267	0.003574	0.838	-1.1	.		1734	13	1725	12	1717	18
PL-01	696	33.1	0.00E+00	20427	0.05264	0.00032	0.38698	0.00437	0.053318	0.000509	0.845	7.1	.		313	13	332	3	335	3
AUB-090	106	32.5	0.00E+00	19174	0.11294	0.00086	5.2	0.08173	0.336166	0.004576	0.872	1.3	.		1847	14	1858	13	1868	22
AUB-091	143	41.9	0.00E+00	17381	0.10891	0.00084	4.83091	0.07261	0.321693	0.004148	0.838	1.1	.		1781	14	1790	13	1798	20
AUB-092	141	30.3	0.00E+00	163405	0.08559	0.0006	2.82083	0.03754	0.238181	0.002694	0.85	3.4	0.2		1336	13	1361	10	1377	14
AUB-093	84	23.6	0.00E+00	84091	0.10489	0.00082	4.49117	0.06521	0.310541	0.003797	0.842	2.1	.		1712	14	1729	12	1743	19
AUB-094	316	36.7	0.00E+00	975	0.096	0.00074	1.73543	0.03004	0.131107	0.00203	0.834	-51.7	-50.1		1548	14	1022	11	794	12
AUB-094-Corr	316	36.7	1.50E+00	975	0.08377	0.00063	1.4889	0.02589	0.128902	0.002019	0.901	-41.7	-39.6		1287	14	926	11	782	12
AUB-095	208	54.6	0.00E+00	13763	0.11403	0.00091	4.52394	0.08234	0.287744	0.004713	0.9	-14.2	-11.7		1865	14	1735	15	1630	24
AUB-095-Corr	208	54.6	9.40E-02	13763	0.11329	0.0009	4.49061	0.08171	0.287473	0.00471	0.901	-13.7	-11.1		1853	14	1729	15	1629	24
AUB-096	113	21.7	0.00E+00	2954	0.09098	0.0007	2.6	0.03834	0.21008	0.002588	0.847	-16.5	-13.8		1446	15	1311	11	1229	14
AUB-096-Corr	113	21.7	5.20E-01	2954	0.08676	0.00066	2.49925	0.03627	0.208921	0.002577	0.85	-10.7	-7.7		1355	15	1272	11	1223	14
AUB-097	193	35	0.00E+00	29169	0.07774	0.00052	2.17409	0.02788	0.202818	0.002216	0.852	4.8	1.3		1140	13	1173	9	1190	12
AUB-098	193	51.6	0.00E+00	16592	0.10931	0.00084	4.48452	0.07457	0.297559	0.004387	0.887	-6.9	-4.2		1788	14	1728	14	1679	22
AUB-098-Corr	193	51.6	3.70E-02	16592	0.10902	0.00084	4.47102	0.07433	0.29745	0.004385	0.887	-6.6	-3.9		1783	13	1726	14	1679	22
AUB-099	50	7.8	0.00E+00	2478	0.08434	0.00076	2.01629	0.03315	0.173381	0.002384	0.836	-22.4	-19.3		1300	17	1121	11	1031	13
AUB-099-Corr	50	7.8	6.80E-01	2478	0.07884	0.00072	1.87113	0.03093	0.172121	0.002373	0.834	-13.4	-9.5		1168	18	1071	11	1024	13
AUB-100	266	28	0.00E+00	505	0.10184	0.00114	1.67569	0.03107	0.119335	0.001762	0.796	-59.3	-57.6		1658	20	999	12	727	10
AUB-100-Corr	266	28	3.00E+00	505	0.07729	0.001	1.22886	0.02435	0.11532	0.001737	0.760	-39.7	-36.1		1129	26	814	11	704	10
AUB-101	74	18.8	0.00E+00	9658	0.09803	0.00075	3.80505	0.05634	0.281515	0.003569	0.856	0.9	.		1587	14	1594	12	1599	18
AUB-102	56	15.5	0.00E+00	6240	0.1077	0.00085	4.6345	0.07887	0.312086	0.004702	0.885	-0.6	.		1761	14	1756	14	1751	23
AUB-103	135	25.8	0.00E+00	17808	0.08469	0.00064	2.48957	0.0388	0.21321	0.002904	0.874	-5.3	-1.9		1308	14	1269	11	1246	15
AUB-104	168	38.8	0.00E+00	2152	0.10915	0.00091	3.86917	0.05745	0.257089	0.003164	0.829	-19.4	-17		1785	15	1607	12	1475	16

AUB-104-Corr	168	38.8	6.30E-01	2152	0,10419	0,00085	3,6694	0,05419	0,255439	0,003142	0,833	-15,3	-12,8		1700	15	1565	12	1466	16
PL-02	291	13.4	0,000E+00	10539	0,05277	0,00036	0,3871	0,00457	0,053205	0,000513	0,816	4,9	.		319	16	332	3	334	3
AUB-105	30	4.8	0,000E+00	2925	0,07572	0,00059	1,93869	0,07625	0,185692	0,002048	0,814	1	.		1088	16	1095	9	1098	11
AUB-106	164	67.4	0,000E+00	11533	0,21889	0,00028	13,64521	0,28902	0,452109	0,007632	0,797	-22,8	-20,2		2973	20	2725	20	2405	34
AUB-106-Corr	164	67.4	1,60E-01	11533	0,21779	0,00278	13,55636	0,28674	0,451432	0,007619	0,798	-22,7	-20,1		2964	20	2719	20	2402	34
AUB-107	106	23.7	0,000E+00	11684	0,09521	0,00078	3,190084	0,05525	0,243053	0,003707	0,881	-9,4	-6,3		1532	15	1455	13	1403	19
AUB-108	59	9,7	0,000E+00	3173	0,08338	0,00085	2,19814	0,04139	0,178368	0,002895	0,862	-27,2	-24,2		1412	18	1180	13	1058	16
AUB-109	299	60	0,000E+00	33265	0,09795	0,0008	2,94403	0,0454	0,217993	0,00285	0,848	-21,8	-19,3		1585	15	1393	12	1271	15
AUB-109-Corr	299	60	2,90E-01	33265	0,09562	0,00078	2,86535	0,0441	0,21733	0,002843	0,850	-19,5	-16,9		1540	15	1373	12	1268	15
AUB-110	197	32.3	0,000E+00	12450	0,07669	0,00059	1,98168	0,02879	0,187415	0,002314	0,830	-0,6	.		1113	14	1109	10	1107	13
AUB-111	143	25.3	0,000E+00	11513	0,07825	0,00056	2,16097	0,02947	0,200283	0,002318	0,849	2,2	.		1153	14	1169	9	1177	12
PL-03	322	14.9	0,000E+00	5721	0,05295	0,00037	0,39028	0,00503	0,053462	0,00058	0,842	2,9	.		326	15	335	4	336	4
AUB-112	159	33.8	0,000E+00	2066	0,1258	0,00109	4,31856	0,10026	0,248984	0,005366	0,928	-33,1	-31		2040	15	1697	19	1433	28
AUB-112-Corr	159	33.8	6,90E-01	2066	0,12047	0,00102	4,10679	0,09542	0,247236	0,00535	0,931	-30,6	-28,4		1963	15	1656	19	1424	28
AUB-113	30	6,4	0,000E+00	3692	0,09088	0,00068	3,08972	0,05553	0,246584	0,004035	0,910	-1,8	.		1444	14	1430	14	1421	21
AUB-114	146	27.8	0,000E+00	12285	0,08248	0,00055	2,50599	0,03609	0,220356	0,002816	0,887	2,4	.		1257	12	1274	10	1284	15
AUB-115	213	37.8	0,000E+00	28326	0,07886	0,00057	2,18693	0,03462	0,201136	0,002839	0,892	1,2	.		1169	13	1177	11	1181	15
AUB-116	145	20,4	0,000E+00	1634	0,09233	0,00075	2,09022	0,03258	0,162605	0,002173	0,857	-37,6	-35,5		1493	14	1146	11	971	12
AUB-116-Corr	145	20,4	1,00E+00	1634	0,0849	0,00067	1,88241	0,02938	0,160804	0,00216	0,861	-28,8	-26,3		1313	14	1075	10	961	12
AUB-117	99	26,5	0,000E+00	7309	0,11892	0,00096	5,04093	0,0777	0,307424	0,004041	0,853	-12,5	-10		1940	14	1826	13	1728	20
AUB-118	89	29	0,000E+00	87693	0,12658	0,00105	6,46402	0,10455	0,370356	0,005136	0,857	-1,1	.		2051	14	2041	14	2031	24
AUB-119	208	32,3	0,000E+00	12266	0,08173	0,00058	2,03302	0,02992	0,180399	0,002328	0,877	-14,9	-12		1239	13	1127	10	1069	13
AUB-119-Corr	208	32,3	9,20E-02	12266	0,08098	0,00057	2,01219	0,0296	0,180221	0,002326	0,877	-13,6	-10,6		1221	13	1120	10	1068	13
AUB-120	140	23,6	0,000E+00	8346	0,08027	0,00056	2,16429	0,03473	0,195545	0,002831	0,902	-4,7	-1,4		1204	13	1170	11	1151	15
AUB-121	136	38,8	0,000E+00	29407	0,11551	0,00094	5,20049	0,08858	0,326552	0,004888	0,879	-4	-1,2		1888	14	1853	15	1822	24
PL-04	209	13.7	0,000E+00	6724	0,05333	0,00039	0,3978	0,00592	0,054101	0,000704	0,874	-0,9	.		343	17	340	4	340	4
PL-05	332	15,2	0,000E+00	7321	0,05359	0,00037	0,40207	0,00526	0,054413	0,000604	0,849	-3,6	.		354	16	343	4	342	4
PL-101	719	45,4	0,000E+00	1894	0,06004	0,00031	0,443325	0,00557	0,053545	0,000614	0,911	-45,6	-43,1		605	11	373	4	336	4
PL-102	542	33,7	0,000E+00	9857	0,05322	0,00026	0,38795	0,00473	0,052867	0,00059	0,916	-1,9	.		338	11	333	3	332	4
AUB-122	277	69,3	0,000E+00	15737	0,08104	0,00036	2,30744	0,0356	0,206493	0,00305	0,957	-1,1	.		1223	9	1215	11	1210	16
AUB-123	76	31,4	0,000E+00	7322	0,11687	0,00062	5,451	0,0921	0,338289	0,005425	0,949	-1,8	.		1909	9	1893	14	1878	26
AUB-124	245	61,4	0,000E+00	13700	0,08308	0,0004	2,39449	0,03572	0,209093	0,002949	0,946	-4,1	-1,8		1271	9	1241	11	1224	16
AUB-125	118	34,3	0,000E+00	16069	0,09282	0,00046	3,10172	0,04845	0,242347	0,003593	0,949	-6,4	-4,4		1484	9	1433	12	1399	19
AUB-126	83	19,7	0,000E+00	4771	0,07899	0,00039	2,14537	0,03073	0,19699	0,002647	0,938	-1,2	.		1172	9	1164	10	1159	14

A.E. Myhre

AUB-127	265	75,5	0,00E+00	4718	0,09761	0,00048	3,20114	0,0518	0,237849	0,003664	0,952	-14,3	-12,5		1579	9	1457	13	1376	19
AUB-127-																				
CORR	266	75,6	3,10E-01	5320	0,09485	0,00055	3,10775	0,04827	0,237628	0,003421	0,927	-11	-8,7		1525	11	1435	12	1374	18
AUB-128	175	69,1	0,00E+00	31984	0,11087	0,00054	4,98238	0,08429	0,325939	0,005278	0,957	0,3	.		1814	9	1816	14	1819	26
AUB-129	150	41	0,00E+00	561	0,12322	0,00176	3,9	0,0824	0,228683	0,003591	0,74	-37,3	-34,5		2003	25	1611	17	1328	19
AUB-129-																				
CORR	150	41	3,10E+00	561	0,09856	0,00171	3,00749	0,07034	0,221313	0,003481	0,673	-21,3	-16,7		1597	31	1410	18	1289	18
AUB-130	230	66,1	0,00E+00	9357	0,09485	0,00045	3,12667	0,04708	0,239071	0,00342	0,95	-10,4	-8,6		1525	9	1439	12	1382	18
AUB-130-																				
CORR	230	66,1	7,60E-02	9357	0,09424	0,00044	3,1041	0,04672	0,238883	0,003416	0,95	-9,7	-7,9		1513	8	1434	12	1381	18
AUB-131	178	43,9	0,00E+00	15745	0,07987	0,00035	2,26647	0,03389	0,205805	0,002939	0,955	1,2	.		1194	8	1202	11	1206	16
AUB-132	75	18,2	0,00E+00	5688	0,08265	0,00043	2,30262	0,03401	0,20206	0,002795	0,936	-6,5	-4,1		1261	10	1213	10	1186	15
AUB-133	207	59,5	0,00E+00	1233	0,10025	0,00085	3,30256	0,05443	0,238926	0,003382	0,859	-16,9	-14,1		1629	16	1482	13	1381	18
AUB-133-Corr	207	59,5	1,50E+00	1233	0,08309	0,00081	2,85715	0,04809	0,235227	0,003316	0,838	-1,8	.		1385	18	1371	13	1362	17
AUB-134	135	33,9	0,00E+00	7157	0,07828	0,00036	2,3	0,03594	0,209629	0,003185	0,956	6,9	3,1		1154	9	1201	11	1227	17
AUB-135	193	46,4	0,00E+00	14485	0,07825	0,00036	2,16695	0,0306	0,200843	0,002679	0,945	2,5	.		1153	9	1171	10	1180	14
PI-103	503	31,9	0,00E+00	57575	0,05322	0,00025	0,39469	0,00487	0,053792	0,000613	0,923	-0,1	.		338	10	338	4	338	4
AUB-136	240	67	0,00E+00	26631	0,08552	0,00037	2,74557	0,04019	0,232834	0,003255	0,955	1,8	.		1327	8	1341	11	1349	17
AUB-137	293	54,9	0,00E+00	667	0,09788	0,00007	2,11725	0,03426	0,156885	0,002276	0,897	-43,7	-42		1584	13	1154	11	939	13
AUB-137-Corr	293	54,9	2,20E+00	667	0,08024	0,00064	1,69468	0,02819	0,153185	0,002233	0,876	-25,3	-22,4		1203	15	1007	11	919	12
AUB-138	87	34,1	0,00E+00	8976	0,11288	0,00056	5,06764	0,08754	0,325604	0,005385	0,957	-1,8	.		1846	9	1831	15	1817	26
AUB-139	151	38,4	0,00E+00	10442	0,08185	0,00041	2,39742	0,03726	0,212424	0,003127	0,947	.	.		1242	9	1242	11	1242	17
AUB-140	128	30,1	0,00E+00	8627	0,07829	0,00036	2,12966	0,0304	0,197288	0,002669	0,948	0,6	.		1154	9	1158	10	1161	14
AUB-141	187	52,8	0,00E+00	9914	0,08615	0,00039	2,79859	0,0415	0,235613	0,003325	0,952	1,9	.		1341	8	1355	11	1364	17
AUB-142	129	50,3	0,00E+00	18221	0,11552	0,00059	5,14668	0,09551	0,333081	0,005768	0,962	-5,1	-3,2		1888	9	1844	16	1805	28
AUB-143	86	33,4	0,00E+00	7894	0,11352	0,00058	5,01668	0,08384	0,320506	0,0051	0,952	-4	-2,1		1857	9	1822	14	1792	25
AUB-144	313	92,4	0,00E+00	8246	0,09672	0,00045	3,28307	0,04761	0,246181	0,003382	0,947	-10,2	-8,4		1562	8	1477	11	1419	17
AUB-144-Corr	313	92,4	2,80E-01	8246	0,09449	0,00044	3,19827	0,04632	0,245474	0,003369	0,948	-7,5	-5,7		1518	8	1457	11	1415	17
AUB-146	137	34,7	0,00E+00	8936	0,08246	0,00039	2,40673	0,03448	0,211674	0,002864	0,944	-1,6	.		1257	8	1245	10	1238	15
AUB-147	106	34	0,00E+00	14576	0,10318	0,00054	3,77854	0,06946	0,265605	0,004683	0,959	-10,9	-9		1682	9	1588	15	1518	24
AUB-147-Corr	106	34	1,30E-01	14576	0,10214	0,00053	3,73538	0,06868	0,265249	0,004677	0,959	-9,9	-8		1663	9	1579	15	1517	24
AUB-148	198	48,7	0,00E+00	3758	0,09106	0,00048	2,58531	0,03922	0,205915	0,002927	0,937	-18,2	-16,3		1448	10	1296	11	1207	16
AUB-148-Corr	198	48,7	4,60E-01	3758	0,08734	0,00047	2,46751	0,03745	0,20491	0,002912	0,936	-13,3	-11,2		1368	10	1263	11	1202	16
AUB-150	75	14,3	0,00E+00	2599	0,08748	0,00048	1,94422	0,02982	0,161197	0,00231	0,934	-32	-30,3		1371	10	1096	10	963	13
AUB-150-Corr	75	14,3	5,90E-01	2599	0,0827	0,00046	1,82636	0,0281	0,160165	0,002299	0,933	-25,9	-23,9		1262	11	1055	10	958	13
AUB-151	149	33,4	0,00E+00	3481	0,09089	0,00043	2,36904	0,03616	0,189042	0,002742	0,950	-24,7	-23,1		1444	9	1233	11	1116	15

AUB-151-Corr	149	33.4	5.40E-01	3481	0.08653	0.00041	2.24227	0.03424	0,18795	0,002729	0.951	-19,3	-17,5
												1350	9
												1194	11
												1110	15

Blaubeker Formation

Sample name	207/235	1 sigma	206/238	1 sigma	207/206	1 sigma	207/235	1 sigma	206/238	1 sigma	207/206	1 sigma	%	10% discord filter	207/235	1 sigma	206/238	1 sign	
	intercept	abs err	intercept	abs err	average	abs err	age	abs err	age	abs err	age	abs err	discordant	Age	1 s abs err	intercept	abs err	intercept	abs err
BB10_111a	1,779210	0,040778	0,164124	0,003238	0,078621	0,000662	1037,9	14,8	979,7	17,9	1162,6	16,6	15,7%	1162,6	16,6	1,779210	0,040778	0,164124	0,0032
BB10_110a	1,661217	0,028497	0,157335	0,001879	0,076575	0,000707	993,8	10,8	941,9	10,5	1110,1	18,3	15,2%	1110,1	18,3	1,661217	0,028497	0,157335	0,0018
BB10_109a	2,033379	0,054272	0,174128	0,003241	0,084691	0,001375	1126,7	18,0	1034,8	17,8	1308,5	31,2	20,9%	1308,5	31,2	2,033379	0,054272	0,174128	0,0032
BB10_108a	1,664674	0,026283	0,162130	0,001793	0,074465	0,000599	995,2	10,0	968,6	9,9	1054,1	16,1	8,1%	1054,1	16,1	1,664674	0,026283	0,162130	0,0017
BB10_107a	1,684283	0,030290	0,163399	0,001959	0,074757	0,000779	1002,6	11,4	975,6	10,8	1062,0	20,8	8,1%	1062,0	20,8	1,684283	0,030290	0,163399	0,0019
BB10_106a	1,909633	0,033960	0,180297	0,002356	0,076815	0,000687	1084,5	11,8	1068,6	12,9	1116,4	17,7	4,3%	1116,4	17,7	1,909633	0,033960	0,180297	0,0023
BB10_105a	1,999303	0,040567	0,187725	0,002586	0,077240	0,000926	1115,3	13,6	1109,0	14,0	1127,4	23,7	1,6%	1127,4	23,7	1,999303	0,040567	0,187725	0,0025
BB10_104a	1,662930	0,030858	0,165904	0,002206	0,072695	0,000721	994,5	11,7	989,5	12,2	1005,5	20,0	1,6%	1005,5	20,0	1,662930	0,030858	0,165904	0,0022
BB10_103a	1,847774	0,033591	0,170179	0,002064	0,078746	0,000833	1062,6	11,9	1013,1	11,4	1165,8	20,8	13,1%	1165,8	20,8	1,847774	0,033591	0,170179	0,0020
BB10_102a	1,558449	0,028101	0,140387	0,001730	0,080510	0,000818	953,9	11,1	846,9	9,8	1209,5	19,9	30,0%	1209,5	19,9	1,558449	0,028101	0,140387	0,0017
BB10_101a	2,777314	0,048491	0,222513	0,002921	0,090388	0,000835	1349,5	13,0	1295,1	15,4	1433,7	17,5	9,7%	1433,7	17,5	2,777314	0,048491	0,222513	0,0029
BB10_100a	1,909855	0,041099	0,171301	0,003082	0,080738	0,000771	1084,5	14,2	1019,3	16,9	1215,1	18,7	16,1%	1215,1	18,7	1,909855	0,041099	0,171301	0,0030
BB10_99a	1,615286	0,026953	0,152308	0,001986	0,076801	0,000631	976,2	10,4	913,9	11,1	1116,0	16,3	18,1%	1116,0	16,3	1,615286	0,026953	0,152308	0,0019
BB10_98a	2,900080	0,102589	0,181095	0,005032	0,115881	0,002155	1381,9	26,4	1073,0	27,4	1893,6	33,1	43,3%	1893,6	33,1	2,900080	0,102589	0,181095	0,0050
BB10_97a	2,092054	0,033585	0,191332	0,002700	0,079122	0,000446	1146,2	11,0	1128,6	14,6	1175,2	11,1	4,0%	1175,2	11,1	2,092054	0,033585	0,191332	0,0027
BB10_96a	1,875628	0,050345	0,175413	0,004007	0,077374	0,000906	1072,5	17,6	1041,9	21,9	1130,8	23,2	7,9%	1130,8	23,2	1,875628	0,050345	0,175413	0,0040
BB10_95a	1,920658	0,046858	0,179799	0,003955	0,077299	0,000659	1088,3	16,2	1065,9	21,6	1128,9	16,9	5,6%	1128,9	16,9	1,920658	0,046858	0,179799	0,0039
BB10_94a	1,937584	0,034113	0,175242	0,002594	0,080008	0,000597	1094,2	11,7	1040,9	14,2	1197,2	14,7	13,1%	1197,2	14,7	1,937584	0,034113	0,175242	0,0025
BB10_93a	1,971569	0,033959	0,184003	0,002611	0,077535	0,000595	1105,8	11,5	1088,8	14,2	1135,0	15,2	4,1%	1135,0	15,2	1,971569	0,033959	0,184003	0,0026
BB10_92a	1,663993	0,025217	0,161475	0,002005	0,074569	0,000495	994,9	9,6	965,0	11,1	1056,9	13,3	8,7%	1056,9	13,3	1,663993	0,025217	0,161475	0,0020
BB10_91a	2,501371	0,085719	0,192670	0,004108	0,093945	0,002145	1272,4	24,6	1135,8	22,2	1507,0	42,5	24,6%	1507,0	42,5	2,501371	0,085719	0,192670	0,0041

BB10_90a	1,211092	0,019374	0,097081	0,001372	0,090272	0,000496	805,7	8,9	597,3	8,1	1431,3	10,4	58,3%	1431,3	10,4	1,211092	0,019374	0,097081	0,0013
BB10_89a	0,575215	0,0111348	0,072123	0,001070	0,057712	0,000615	461,4	7,3	448,9	6,4	518,8	23,2	13,5%	518,8	23,2	0,575215	0,0111348	0,072123	0,0010
BB10_88a	2,730112	0,046598	0,222194	0,0002829	0,089113	0,000816	1336,7	12,6	1293,5	14,9	1406,6	17,4	8,0%	1406,6	17,4	2,730112	0,046598	0,222194	0,0028
BB10_87a	1,999427	0,031487	0,180853	0,002265	0,080181	0,000598	1115,3	10,6	1071,6	12,4	1201,4	14,6	10,8%	1201,4	14,6	1,999427	0,031487	0,180853	0,0022
BB10_86a	1,613572	0,027771	0,152340	0,002172	0,076818	0,000580	975,5	10,7	914,1	12,1	1116,5	15,0	18,1%	1116,5	15,0	1,613572	0,027771	0,152340	0,0021
BB10_85a	1,363103	0,026613	0,127542	0,002032	0,077511	0,000705	873,2	11,4	773,8	11,6	1134,4	18,0	31,8%	1134,4	18,0	1,363103	0,026613	0,127542	0,0020
BB10_84a	1,848836	0,029200	0,169640	0,002277	0,078914	0,000499	1061,9	10,4	1010,1	12,5	1170,0	12,5	13,7%	1170,0	12,5	1,845836	0,029200	0,169640	0,0022
BB10_83a	1,809682	0,037490	0,160434	0,002767	0,081808	0,000759	1049,0	13,5	959,2	15,4	1240,9	18,1	22,7%	1240,9	18,1	1,809682	0,037490	0,160434	0,0027
BB10_82a	1,469993	0,037045	0,133538	0,002737	0,079837	0,000973	918,1	15,1	808,0	15,5	1193,0	23,9	32,3%	1193,0	23,9	1,469993	0,037045	0,133538	0,0027
BB10_81a	1,634460	0,028856	0,158937	0,002255	0,074583	0,000624	983,6	11,1	950,9	12,5	1057,3	16,7	10,1%	1057,3	16,7	1,634460	0,028856	0,158937	0,0022
BB10_80a	1,670907	0,036977	0,149473	0,002769	0,081073	0,000800	997,5	14,0	898,0	15,5	1223,2	19,3	26,6%	1223,2	19,3	1,670907	0,036977	0,149473	0,0027
BB10_79a	2,009792	0,028497	0,185710	0,002199	0,078488	0,000451	1118,8	9,6	1098,1	11,9	1159,3	11,3	5,3%	1159,3	11,3	2,009792	0,028497	0,185710	0,0021
BB10_78a	1,552458	0,027522	0,154169	0,002016	0,073247	0,000716	951,5	10,9	924,3	11,2	1020,8	19,7	9,5%	1020,8	19,7	1,552458	0,027522	0,154169	0,0020
BB10_77a	2,730251	0,043595	0,223798	0,002926	0,088739	0,000631	1336,7	11,8	1301,9	15,4	1398,5	13,6	6,9%	1398,5	13,6	2,730251	0,043595	0,223798	0,0029
BB10_76a	2,020121	0,032937	0,183028	0,002422	0,080284	0,000559	1122,3	11,0	1083,5	13,2	1204,0	14,6	10,0%	1204,0	14,6	2,020121	0,032937	0,183028	0,0024
BB10_75a	1,693307	0,025513	0,164611	0,002094	0,074821	0,000451	1006,0	9,6	982,3	11,6	1063,7	12,1	7,6%	1063,7	12,1	1,693307	0,025513	0,164611	0,0020
BB10_74b	1,656903	0,032199	0,158965	0,002273	0,075817	0,000823	992,2	12,2	951,0	12,6	1090,2	21,6	12,8%	1090,2	21,6	1,656903	0,032199	0,158965	0,0022
BB10_74a	3,261760	0,089946	0,167441	0,002764	0,141697	0,002672	1472,0	21,2	998,0	15,2	2248,1	32,2	55,6%	2248,1	32,2	3,261760	0,089946	0,167441	0,0027
BB10_73a	1,970358	0,030864	0,177409	0,002249	0,080787	0,000578	1105,4	10,5	1052,8	12,3	1216,3	14,0	13,4%	1216,3	14,0	1,970358	0,030864	0,177409	0,0022
BB10_72a	1,910041	0,035667	0,172695	0,002518	0,080451	0,000763	1084,6	12,4	1026,9	13,8	1208,1	18,6	15,0%	1208,1	18,6	1,910041	0,035667	0,172695	0,0022
BB10_71a	0,775718	0,014945	0,093106	0,001264	0,060603	0,000687	583,0	8,5	573,9	7,5	625,2	24,2	8,2%	625,2	24,2	0,775718	0,014945	0,093106	0,0012
BB10_70a	1,992194	0,049413	0,181235	0,003189	0,079957	0,001180	1112,9	16,6	1073,7	17,4	1195,9	28,8	10,2%	1195,9	28,8	1,992194	0,049413	0,181235	0,0031
BB10_69a	1,176050	0,018641	0,127248	0,001589	0,067227	0,000517	789,5	8,7	772,1	9,1	844,8	15,9	8,6%	844,8	15,9	1,176050	0,018641	0,127248	0,0015
BB10_68b	2,254601	0,026299	0,204869	0,001820	0,079995	0,000448	1198,2	8,2	1201,4	9,7	1196,9	11,0	-0,4%	1196,9	11,0	2,254601	0,026299	0,204869	0,0018
BB10_68a	2,183905	0,027049	0,197101	0,001899	0,080541	0,000470	1175,9	8,6	1159,7	10,2	1210,3	11,4	4,2%	1210,3	11,4	2,183905	0,027049	0,197101	0,0018
BB10_67a	1,883395	0,041521	0,175932	0,000302	0,077815	0,000898	1075,3	14,5	1044,8	16,6	1142,1	22,8	8,5%	1142,1	22,8	1,883395	0,041521	0,175932	0,0030
BB10_66a	1,623191	0,030936	0,156441	0,002568	0,075420	0,000582	979,2	11,9	937,0	14,3	1079,7	15,4	13,2%	1079,7	15,4	1,623191	0,030936	0,156441	0,0025
BB10_65a	1,992582	0,059585	0,164747	0,000325	0,087916	0,001795	1113,0	20,0	983,1	16,7	1380,6	38,7	28,8%	1380,6	38,7	1,992582	0,059585	0,164747	0,0030
BB10_64a	2,706607	0,063175	0,193714	0,0002718	0,010562	0,001624	1330,3	17,2	1141,5	14,7	1652,9	29,3	30,9%	1652,9	29,3	2,706607	0,063175	0,193714	0,0027

BB10_62a	4,857638	0,062412	0,311722	0,003226	0,113273	0,000641	1794,9	10,8	1749,2	15,8	1852,6	10,2	5,6%	1852,6	10,2	4,857638	0,062412	0,311722	0,0032
BB10_61a	1,741931	0,030504	0,165343	0,001819	0,076580	0,000875	1024,2	11,2	986,4	10,1	1110,3	22,7	11,2%	1110,3	22,7	1,741931	0,030504	0,165343	0,0018
BB10_60a	2,114372	0,032895	0,194348	0,002238	0,079081	0,000670	1153,5	10,7	1144,9	12,1	1174,2	16,7	2,5%	1174,2	16,7	2,114372	0,032895	0,194348	0,0022
BB10_59a	1,787619	0,022992	0,172800	0,001802	0,075197	0,000419	1041,0	8,3	1027,5	9,9	1073,8	11,1	4,3%	1073,8	11,1	1,787619	0,022992	0,172800	0,0018
BB10_58a	1,950310	0,031149	0,177947	0,002471	0,079667	0,000474	1098,6	10,7	1055,8	13,5	1188,8	11,7	11,2%	1188,8	11,7	1,950310	0,031149	0,177947	0,0024
BB10_57a	2,028888	0,026268	0,187791	0,001763	0,078533	0,000548	1125,2	8,8	1109,4	9,6	1160,4	13,8	4,4%	1160,4	13,8	2,028888	0,026268	0,187791	0,0017
BB10_56a	1,713854	0,037874	0,166257	0,002612	0,074931	0,000987	1013,7	14,1	991,5	14,4	1066,7	26,3	7,0%	1066,7	26,3	1,713854	0,037874	0,166257	0,0026
BB10_55a	1,6918124	0,031830	0,162155	0,002486	0,076122	0,000668	1007,8	11,9	968,7	13,8	1098,3	17,5	11,8%	1098,3	17,5	1,6918124	0,031830	0,162155	0,0024
BB10_54a	1,886943	0,027558	0,177308	0,001836	0,076780	0,000592	1076,5	9,6	1052,3	10,2	1115,5	15,3	5,7%	1115,5	15,3	1,886943	0,027558	0,177308	0,0018
BB10_53a	2,083413	0,028332	0,193311	0,001842	0,077757	0,000557	1143,4	9,3	1139,3	9,9	1140,7	14,2	0,1%	1140,7	14,2	2,083413	0,028332	0,193311	0,0018
BB10_52b	2,630866	0,039184	0,220378	0,002432	0,086129	0,000647	1309,3	10,9	1283,9	12,8	1341,1	14,4	4,3%	1341,1	14,4	2,630866	0,039184	0,220378	0,0024
BB10_52a	2,647821	0,037360	0,220810	0,002228	0,086514	0,000636	1314,0	10,3	1286,2	11,8	1349,7	14,1	4,7%	1349,7	14,1	2,647821	0,037360	0,220810	0,0022
BB10_50a	3,568817	0,053176	0,262924	0,002602	0,098147	0,000860	1542,6	11,7	1504,8	13,3	1589,2	16,3	5,3%	1589,2	16,3	3,568817	0,053176	0,262924	0,0026
BB10_49a	1,807564	0,026480	0,174608	0,001800	0,074854	0,000595	1048,2	9,5	1037,5	9,9	1064,6	15,9	2,5%	1064,6	15,9	1,807564	0,026480	0,174608	0,0018
BB10_48a	2,103451	0,041295	0,192759	0,002978	0,078905	0,000772	1149,9	13,4	1136,3	16,1	1169,7	19,3	2,9%	1169,7	19,3	2,103451	0,041295	0,192759	0,0029
BB10_47a	0,999498	0,068160	0,079342	0,002480	0,091088	0,005093	703,6	34,0	492,2	14,8	1448,4	102,9	66,0%	1448,4	102,9	0,999498	0,068160	0,079342	0,0024
BB10_46a	2,579763	0,037278	0,218596	0,002143	0,085534	0,000699	1294,9	10,5	1274,5	11,3	1323,1	15,8	3,7%	1323,1	15,8	2,579763	0,037278	0,218596	0,0021
BB10_45a	1,899475	0,039261	0,182238	0,002197	0,075366	0,001098	1080,9	13,7	1079,2	12,0	1078,3	29,0	-0,1%	1078,3	29,0	1,899475	0,039261	0,182238	0,0021
BB10_44a	2,072320	0,033466	0,177674	0,002073	0,084337	0,000741	1139,7	11,0	1054,3	11,3	1300,3	17,0	18,9%	1300,3	17,0	2,072320	0,033466	0,177674	0,0020
BB10_43a	1,917603	0,049361	0,177927	0,0003591	0,077929	0,001070	1087,2	17,0	1055,6	19,6	1145,1	27,1	7,8%	1145,1	27,1	1,917603	0,049361	0,177927	0,0035
BB10_42a	1,876514	0,028779	0,180354	0,001893	0,075233	0,000663	1072,8	10,1	1068,9	10,3	1074,7	17,6	0,5%	1074,7	17,6	1,876514	0,028779	0,180354	0,0018
BB10_41b	1,323894	0,019142	0,118418	0,001283	0,0808339	0,000565	856,2	8,3	721,5	7,4	1217,5	13,7	40,7%	1217,5	13,7	1,323894	0,019142	0,118418	0,0012
BB10_41a	1,894601	0,028644	0,175064	0,001707	0,078254	0,000721	1079,2	10,0	1040,0	9,4	1153,3	18,2	9,8%	1153,3	18,2	1,894601	0,028644	0,175064	0,0017
BB10_40a	1,992890	0,030417	0,185981	0,001863	0,077482	0,000710	1113,1	10,3	1099,6	10,1	1133,6	18,1	3,0%	1133,6	18,1	1,992890	0,030417	0,185981	0,0018
BB10_39a	0,695108	0,011522	0,084294	0,000764	0,059627	0,000695	535,9	6,9	521,7	4,5	590,1	25,1	11,6%	590,1	25,1	0,695108	0,011522	0,084294	0,0007
BB10_38a	1,744836	0,023721	0,170406	0,001515	0,074038	0,000579	1025,3	8,7	1014,3	8,3	1042,5	15,7	2,7%	1042,5	15,7	1,744836	0,023721	0,170406	0,0015
BB10_37a	2,090626	0,036612	0,197434	0,002231	0,076964	0,000856	1145,7	12,0	1120,3	22,0	-3,7%	1120,3	22,0	2,090626	0,036612	0,197434	0,0022		
BB10_36a	2,023964	0,037849	0,192151	0,002602	0,076559	0,000810	1123,6	12,6	1133,0	14,1	1109,7	21,0	-2,1%	1109,7	21,0	2,023964	0,037849	0,192151	0,0026

BB10_35a	2,024874	0,026264	0,185175	0,001705	0,079479	0,000512	1123,9	8,8	1095,2	9,3	1184,1	12,7	7,5%	1184,1	12,7	2,024874	0,026264	0,185175	0,0017
BB10_34a	1,928787	0,030367	0,177920	0,0002020	0,078794	0,000667	1091,1	10,5	1055,6	11,0	1167,0	16,7	9,5%	1167,0	16,7	1,928787	0,030367	0,177920	0,0020
BB10_33a	3,973394	0,076163	0,258542	0,004192	0,111703	0,000847	1628,8	15,4	1482,4	21,4	1827,3	13,7	18,9%	1827,3	13,7	3,973394	0,076163	0,258542	0,0041
BB10_32a	1,687465	0,026005	0,161737	0,001627	0,075833	0,000707	1003,8	9,8	966,4	9,0	1090,7	18,6	11,4%	1090,7	18,6	1,687465	0,026005	0,161737	0,0016
BB10_31b	2,759174	0,046473	0,229888	0,0002691	0,087236	0,000852	1344,6	12,5	1333,9	14,1	1365,7	18,7	2,3%	1365,7	18,7	2,759174	0,046473	0,229888	0,0026
BB10_31a	2,944537	0,050667	0,242652	0,0002793	0,088200	0,000926	1393,4	13,0	1400,5	14,5	1386,8	20,0	-1,0%	1386,8	20,0	2,944537	0,050667	0,242652	0,0027
BB10_30a	1,827463	0,048452	0,177133	0,0003553	0,074986	0,001219	1055,4	17,3	1051,3	18,3	1068,1	32,3	1,6%	1068,1	32,3	1,827463	0,048452	0,177133	0,0033
BB10_29a	2,041517	0,038531	0,187759	0,0002487	0,079029	0,000882	1129,5	12,8	1109,2	13,5	1172,9	21,9	5,4%	1172,9	21,9	2,041517	0,038531	0,187759	0,0024
BB10_28a	1,905568	0,036834	0,179528	0,0002430	0,076951	0,001003	1082,3	12,8	1064,4	13,3	1119,9	25,8	5,0%	1119,9	25,8	1,905568	0,036834	0,179528	0,0024
BB10_27a	2,104833	0,026398	0,190585	0,0001838	0,080150	0,000568	1150,4	8,6	1124,5	9,9	1200,7	13,9	6,3%	1200,7	13,9	2,104833	0,026398	0,190585	0,0018
BB10_26a	2,888298	0,036856	0,228789	0,0002276	0,091618	0,000647	1378,9	9,6	1328,2	11,9	1459,5	13,4	9,0%	1459,5	13,4	2,888298	0,036856	0,228789	0,0022
BB10_25a	1,488062	0,024308	0,137758	0,0001904	0,078405	0,000616	925,5	9,9	831,9	10,8	1157,2	15,5	28,1%	1157,2	15,5	1,488062	0,024308	0,137758	0,0019
BB10_24a	1,911150	0,034854	0,183216	0,0002209	0,075702	0,000974	1085,0	12,1	1084,5	12,0	1087,2	25,6	0,2%	1087,2	25,6	1,911150	0,034854	0,183216	0,0022
BB10_23a	1,855930	0,026052	0,163745	0,0001872	0,082257	0,000596	1065,5	9,2	977,6	10,4	1251,6	14,1	21,9%	1251,6	14,1	1,855930	0,026052	0,163745	0,0018
BB10_22a	1,722512	0,022183	0,157596	0,0001579	0,079322	0,000568	1017,0	8,2	943,4	8,8	1180,2	14,1	20,1%	1180,2	14,1	1,722512	0,022183	0,157596	0,0015
BB10_21a	1,859003	0,023414	0,168653	0,001743	0,079995	0,000498	1066,6	8,3	1004,7	9,6	1196,9	12,2	16,1%	1196,9	12,2	1,859003	0,023414	0,168653	0,0017
BB10_20a	1,986620	0,023535	0,189199	0,001694	0,076203	0,000518	1111,0	8,0	1117,0	9,2	1100,4	13,5	-1,5%	1100,4	13,5	1,986620	0,023535	0,189199	0,0016
BB10_19b	1,820001	0,023132	0,174802	0,001653	0,075562	0,000573	1052,7	8,3	1038,5	9,1	1083,5	15,1	4,2%	1083,5	15,1	1,820001	0,023132	0,174802	0,0016
BB10_19a	1,903254	0,020925	0,182267	0,0001443	0,075745	0,000508	1082,2	7,3	1079,4	7,9	1088,3	13,4	0,8%	1088,3	13,4	1,903254	0,020925	0,182267	0,0014
BB10_18a	2,031543	0,023276	0,187313	0,0001598	0,078673	0,000530	1126,1	7,8	1106,8	8,7	1163,9	13,3	4,9%	1163,9	13,3	2,031543	0,023276	0,187313	0,0015
BB10_17a	2,065163	0,024641	0,190375	0,0001619	0,078688	0,000591	1137,3	8,1	1123,4	8,8	1164,3	14,8	3,5%	1164,3	14,8	2,065163	0,024641	0,190375	0,0016
BB10_16a	2,883644	0,055279	0,226385	0,0002906	0,092397	0,001250	1377,6	14,4	1315,5	15,3	1475,6	25,4	10,8%	1475,6	25,4	2,883644	0,055279	0,226385	0,0029
BB10_15a	2,023871	0,026972	0,187407	0,0001703	0,078336	0,000701	1123,6	9,0	1107,3	9,2	1155,4	17,7	4,2%	1155,4	17,7	2,023871	0,026972	0,187407	0,0017
BB10_14a	1,923573	0,024204	0,182763	0,0001799	0,076346	0,000531	1089,3	8,4	1082,0	9,8	1104,2	13,9	2,0%	1104,2	13,9	1,923573	0,024204	0,182763	0,0017
BB10_13a	2,056715	0,027564	0,191326	0,0001768	0,077977	0,000695	1134,5	9,1	1128,6	9,6	1146,3	17,6	1,5%	1146,3	17,6	2,056715	0,027564	0,191326	0,0017
BB10_12a	1,901885	0,026458	0,181268	0,0001885	0,076108	0,000642	1081,7	9,2	1073,9	10,3	1097,9	16,8	2,2%	1097,9	16,8	1,901885	0,026458	0,181268	0,0018
BB10_11a	2,161396	0,041563	0,197875	0,0002415	0,079233	0,001120	1168,7	13,3	1163,9	13,0	1178,0	27,7	1,2%	1178,0	27,7	2,161396	0,041563	0,197875	0,0024
BB10_10a	2,173475	0,034529	0,196288	0,0002013	0,0803220	0,000915	1172,6	11,0	1155,3	10,8	1204,9	22,3	4,1%	1204,9	22,3	2,173475	0,034529	0,196288	0,0020
BB10_9a	2,097795	0,035141	0,194335	0,0002109	0,078303	0,000942	1148,1	11,5	1144,8	11,4	1154,6	23,7	0,8%	1154,6	23,7	2,097795	0,035141	0,194335	0,0021

BB10_8a	2,056452	0,022598	0,192531	0,001500	0,077479	0,000530	1134,4	7,5	1135,1	8,1	1133,5	13,5	-0,1%	1133,5	13,5	2,056452	0,022598	0,192531	0,0015
BB10_7a	2,091152	0,028499	0,173161	0,001729	0,087599	0,000742	1145,9	9,3	1029,5	9,5	1373,7	16,2	25,1%	1373,7	16,2	2,091152	0,028499	0,173161	0,0017
BB10_6a	2,124238	0,026283	0,194558	0,001697	0,079199	0,000629	1156,7	8,5	1146,0	9,1	1177,1	15,6	2,6%	1177,1	15,6	2,124238	0,026283	0,194558	0,0016
BB10_5a	1,925459	0,020174	0,185003	0,001418	0,075495	0,000467	1090,0	7,0	1094,3	7,7	1081,7	12,3	-1,2%	1081,7	12,3	1,925459	0,020174	0,185003	0,0014
BB10_4a	1,827121	0,018194	0,169236	0,001295	0,078314	0,000417	1055,2	6,5	1007,9	7,1	1154,9	10,5	12,7%	1154,9	10,5	1,827121	0,018194	0,169236	0,0012
BB10_3a	2,142333	0,026881	0,195261	0,001739	0,079586	0,000637	1162,6	8,6	1149,8	9,4	1186,7	15,7	3,1%	1186,7	15,7	2,142333	0,026881	0,195261	0,0017
BB10_2a	2,007828	0,023368	0,184872	0,001733	0,078781	0,000467	1118,2	7,9	1093,5	9,4	1166,6	11,7	6,3%	1166,6	11,7	2,007828	0,023368	0,184872	0,0017
BB10_1b	1,833481	0,041356	0,175769	0,002606	0,075666	0,001232	1057,5	14,7	1043,8	14,3	1086,2	32,3	3,9%	1086,2	32,3	1,833481	0,041356	0,175769	0,0026

Blaubeker Clast

Analysis #	Analysis name	Spot size (μm)	U conc. (ppm)	Ratios				rho:	Ages (Ma)										
				206Pb/238U	±2σ	207Pb/232U	±2σ		206Pb/238U	±2σ	207Pb/235U	±2σ	207Pb/206Pb	±2σ	207Pb/235U	±2σ%			
5	BBCI-01	35	143,3536938	0,24345023	0,0065538951	2,942617508	0,088647196	0,087662055	0,001315833	0,867028488	1404,59	32,97	2,35	1392,95	22,83	1,64	1375,16	28,87	2,10
7	BBCI-03	35	387,4133367	0,231700603	0,005964846	2,774190828	0,0808436136	0,086837616	0,001835989	0,8833383217	1343,36	31,22	2,32	1348,62	21,75	1,61	1356,96	26,34	1,94
8	BBCI-04	35	281,7022944	0,23332316	0,00617332	2,817690606	0,086810586	0,087623451	0,001381462	0,8859147516	1351,33	32,27	2,39	1360,25	23,09	1,70	1374,31	30,33	2,21
10	BBCI-06	35	242,1190097	0,245534828	0,006448507	2,993216547	0,089938762	0,088414554	0,001290681	0,874052073	1415,36	33,37	2,36	1405,90	22,87	1,63	1391,58	28,01	2,01
11	BBCI-07	35	157,022609	0,235013296	0,006540978	2,739870817	0,095773751	0,084554432	0,001788183	0,796221451	1360,68	34,14	2,51	1339,34	26,01	1,94	1305,41	41,08	3,15
12	BBCI-08	35	8,241656554	0,727917289	0,087912608	12,65245878	1,842255937	0,126064156	0,0102529102	0,829455617	3525,54	328,25	9,31	2654,13	137,86	5,19	2043,86	144,19	7,05
13	BBCI-09	35	130,428072	0,233874312	0,005972296	2,870641917	0,086694507	0,089021565	0,001433315	0,845563498	1354,73	31,20	2,30	1374,24	22,75	1,66	1404,69	30,38	2,20
17	BBCI-10	35	250,7773036	0,222570556	0,004861753	2,654472305	0,069124523	0,086498627	0,00122626	0,8358824831	1295,40	25,63	1,98	1315,89	19,21	1,46	1349,42	27,37	2,03
61	BBCI-100	35	190,9298829	0,221493603	0,003944999	2,603702755	0,056475382	0,085256783	0,001053416	0,8211412175	1289,72	20,82	1,61	1301,68	15,91	1,22	1321,45	23,98	1,82
62	BBCI-101	35	150,4311795	0,241503878	0,004315039	3,017917179	0,077382545	0,090633939	0,00151238	0,738041513	1394,47	22,40	1,61	1412,17	18,65	1,32	1438,99	31,81	2,21
63	BBCI-102	35	136,8841115	0,231346936	0,004364442	2,764591429	0,063014444	0,086669428	0,001108683	0,827667393	1341,51	22,85	1,70	1346,03	17,00	1,26	1353,22	24,68	1,82
64	BBCI-103	35	154,9465574	0,231087841	0,004429503	2,751601285	0,062059492	0,086558906	0,001103262	0,82410749	1340,15	22,49	1,68	1342,52	16,80	1,25	1346,30	24,67	1,83
65	BBCI-104	35	194,353267	0,224107096	0,004048949	2,670540323	0,061908574	0,086425571	0,001253373	0,779354554	1303,50	21,32	1,64	1320,34	17,13	1,30	1347,78	28,04	2,08
72	BBCI-108	35	185,9782805	0,223219958	0,003915656	2,649622962	0,060645385	0,086608942	0,001255054	0,768711062	1298,82	20,64	1,59	1314,54	16,82	1,28	1340,26	28,20	2,10
73	BBCI-109	35	146,5479576	0,238272738	0,003974819	2,908538102	0,06136256	0,088531766	0,001143456	0,790704621	1377,67	20,69	1,50	1384,13	15,94	1,15	1394,11	24,78	1,78
18	BBCI-111	35	148,168075	0,227766852	0,005102345	2,73142162	0,073806235	0,086975503	0,001314199	0,829393053	1322,74	26,79	2,03	1337,05	20,09	1,50	1360,02	29,12	2,14
74	BBCI-110	35	135,9753641	0,213178652	0,005022517	2,441724142	0,093424228	0,083071406	0,002503931	0,615764722	1245,69	26,69	2,14	1254,99	27,57	2,20	1270,97	58,86	4,63
4	BBCI-115	35	109,2578532	0,234278181	0,002693343	2,807443373	0,053793248	0,086911650	0,001330588	0,601325407	1356,84	14,10	1,04	1357,52	14,35	1,06	1358,61	29,51	2,17
5	BBCI-116	35	189,5590566	0,239784511	0,001853849	2,914970691	0,046689154	0,088168163	0,001236782	0,482693499	1385,53	9,64	0,70	1385,80	12,11	0,87	1386,22	26,94	1,94

6	BBCI-117	35	143.8316233	0.244232983	0.005414333	3,056336379	0,106301691	0,090760225	0,002432389	0,637584635	1408.62	2805	1,99	1421.82	26.62	1,87	1441.65	51.09	3,54
19	BBCI-112	35	116.4757024	0,243102666	0,00621253	2,952519418	0,090568142	0,0886363226	0,001496087	0,832708585	1403.07	32.21	2,30	1395.49	23.28	1,67	1383.93	32.64	2,36
9	BBCI-120	35	114.8010741	0,228776127	0,001646646	2,671817839	0,04613548	0,084702234	0,001329471	0,416832293	1328.04	8,64	0,65	1320.70	12.76	0,97	1308.80	30.47	2,33
10	BBCI-121	35	147.2640804	0,237097473	0,003349076	2,826898379	0,065035945	0,086473293	0,001570422	0,61394781	1371.55	17,45	1,27	1362.70	17.26	1,27	1348.85	35.06	2,60
18	BBCI-125	25	171.2405388	0,240170433	0,003835645	2,917193023	0,068503678	0,088093598	0,001516596	0,680095903	1387.54	19,94	1,44	1386.38	17.76	1,28	1384.60	33.07	2,39
19	BBCI-126	35	136.9108642	0,227891947	0,003727109	2,725783393	0,066060417	0,086748523	0,001551503	0,674828103	1323.40	19,57	1,48	1335.51	18.01	1,35	1354.98	34.50	2,55
20	BBCI-127	35	115.1154027	0,227517161	0,003368101	2,654359186	0,065366202	0,084527237	0,001507308	0,689671932	1322.66	20,31	1,54	1315.86	18.16	1,38	1304.78	34.64	2,65
21	BBCI-128	35	121.8490579	0,23842726	0,004249282	2,905020077	0,070391189	0,088367375	0,001450698	0,735515216	1378.47	22,12	1,60	1383.22	18,31	1,32	1390.55	31.51	2,27
22	BBCI-129	35	164.7758905	0,242474893	0,0003525399	2,965973626	0,069917103	0,088715445	0,001646444	0,61677306	1399.51	18,29	1,31	1398.95	17,90	1,28	1398.09	35.58	2,54
20	BBCI-13	35	268.8692164	0,241441239	0,005572634	2,903760969	0,085935474	0,087226439	0,001615734	0,779897428	1394.14	28,94	2,08	1382.89	22.36	1,62	1365.57	35.68	2,61
23	BBCI-130	35	180.4439702	0,233003572	0,005564676	2,785795204	0,081812469	0,086713233	0,001482	0,813218051	1350.18	29,09	2,15	1351.73	21.95	1,62	1354.20	32.97	2,43
24	BBCI-131	35	243.966445	0,237970023	0,005690753	2,920476888	0,084333583	0,089008247	0,001440708	0,828134094	1376.09	29,63	2,15	1387.23	21.85	1,57	1404.40	31.00	2,21
25	BBCI-132	25	96.400862522	0,228129316	0,0005873524	2,675093036	0,089592268	0,085046514	0,001821633	0,768751581	1324.64	30,83	2,33	1321.60	24.76	1,87	1316.67	41.54	3,15
26	BBCI-133	35	220.0953317	0,235441277	0,002575455	2,845766071	0,052182459	0,087662796	0,001290665	0,59608568	1362.91	13,43	0,99	1367.69	13.78	1,01	1375.17	28.31	2,06
30	BBCI-134	35	93.25627728	0,237618842	0,003159446	2,863596119	0,058885898	0,087403650	0,001371072	0,646592324	1374.26	16,46	1,20	1372.39	15.48	1,13	1369.48	30.19	2,20
31	BBCI-135	35	80.42152688	0,258251604	0,003791172	3,261497388	0,07495056	0,091595204	0,001619493	0,638811343	1480.84	19,42	1,31	1471.92	17,86	1,21	1459.08	33.62	2,30
32	BBCI-136	35	173.9426131	0,222973461	0,002691018	2,672150419	0,044290101	0,086917445	0,000987441	0,728144623	1297.53	14,18	1,09	1320.79	12.25	0,93	1358.73	21.90	1,61
33	BBCI-137	35	116.6393434	0,236302337	0,003167811	2,848512329	0,050759379	0,087227419	0,001026733	0,750982826	1367.40	16,52	1,21	1367.10	13,41	0,98	1366.62	22.70	1,66
34	BBCI-138	35	135.6107667	0,232419576	0,004164485	2,759027587	0,071372249	0,086095810	0,001606402	0,69652245	1347.12	21,78	1,62	1344.53	19.28	1,43	1340.40	36.06	2,69
35	BBCI-139	25	175.5985134	0,244962505	0,003857338	2,975433203	0,066417214	0,088804906	0,001298136	0,730191656	1412.40	19,97	1,41	1401.36	16,39	1,17	1384.62	28.30	2,04
21	BBCI-14	35	310.1282602	0,177605579	0,004511103	2,232108451	0,068341906	0,091150155	0,001553382	0,829572555	1053.85	24,69	2,34	1191.18	21,47	1,80	1449.81	32.55	2,25
36	BBCI-140	35	167.7662956	0,24971177	0,00406569	3,088418278	0,071959713	0,08969732	0,001495066	0,698756052	1436.99	20,97	1,46	1429.82	17,87	1,25	1419.16	31.87	2,25
37	BBCI-141	35	175.2141956	0,2414282518	0,003287192	3,007167072	0,062831892	0,0903920883	0,001431548	0,652147438	1393.32	17,07	1,23	1409.44	15,92	1,13	1433.89	30.22	2,11
39	BBCI-143	35	70.57078375	0,24955414	0,005013529	3,099455168	0,08692605	0,0900781183	0,001762747	0,716311615	1436.13	25,86	1,80	1432.56	21,53	1,50	1427.25	37.37	2,62
44	BBCI-144	35	179.7455489	0,23285706	0,002697577	2,797197429	0,052770751	0,087122923	0,001297254	0,614065013	1349.41	14,10	1,05	1354.79	14,11	1,04	1363.28	28,69	2,10
45	BBCI-145	35	283.7984879	0,241360243	0,002917811	2,944428203	0,047877067	0,088477727	0,000962011	0,7433548605	1393.72	15,15	1,09	1393.41	12,33	0,88	1392.95	20,86	1,50
46	BBCI-146	35	156.9247059	0,234196882	0,002747056	2,858679252	0,056338809	0,088528511	0,00140205	0,595174366	1356.41	14,35	1,06	1371.10	14,83	1,08	1394.05	30,38	2,18
47	BBCI-147	35	151.8785576	0,241467273	0,003150467	2,904040931	0,051411394	0,087225442	0,001043226	0,736987424	1394.28	16,36	1,17	1382.96	13,37	0,97	1365.55	23.05	1,69
49	BBCI-149	35	311.8567094	0,239297529	0,002674566	2,861278342	0,0485805016	0,086702369	0,001105329	0,659308355	1383.00	13,91	1,01	1371.78	12,76	0,93	1354.36	24.59	1,82
50	BBCI-150	35	119.4278515	0,241788204	0,002642969	2,89698341	0,08821169	0,086898416	0,002275741	0,385186943	1395.94	13,72	0,98	1381.13	21,42	1,55	1358.31	50,50	3,72
51	BBCI-151	35	228.7071759	0,236904136	0,00312926	2,877140157	0,052536969	0,088081987	0,001110516	0,723377562	1370.54	16,31	1,19	1375.94	13,76	1,00	1384.34	24.21	1,75
52	BBCI-152	35	75.242326132	0,098604971	0,001635544	0,822320952	0,028310374	0,060484265	0,001824793	0,481792853	166.21	9,60	1,58	609.34	15,78	2,59	621.02	65.12	10,49
57	BBCI-153	35	106.8451794	0,235982126	0,005005694	2,856492891	0,06868977	0,0877793	0,00099484	0,88263452	1365.63	26,11	1,91	1370.52	18,09	1,32	1378.16	21,79	1,58
58	BBCI-154	35	324.7789442	0,242336787	0,00470552	2,95677904	0,064724637	0,088439624	0,000896104	0,886515121	1399.05	24,42	1,75	1396.31	16,62	1,19	1392.12	19,44	1,40
59	BBCI-155	35	164.4044075	0,228940498	0,004679004	2,724207706	0,063573479	0,0868030923	0,000972167	0,875778276	1328.90	24,54	1,85	1335.08	17,33	1,30	1345.00	21,76	1,62
60	BBCI-156	35	81.74379371	0,252037665	0,005463832	3,11134116	0,091396763	0,089536093	0,001737834	0,738016211	1448.88	28,13	1,94	1435.50	22,58	1,57	1415.72	37,92	2,68
61	BBCI-157	35	128.93469	0,237374127	0,004620917	2,888575667	0,067338118	0,088170855	0,00134458	0,834244896	1372.99	24,07	1,75	1378.20	17,60	1,28	1386.28	24,71	1,78
63	BBCI-159	35	214.9587305	0,225768867	0,004642903	2,69697648	0,065340102	0,086445645	0,001160609	0,846942974	1312.24	24,42	1,86	1325.98	17,98	1,36	1348.23	24,92	1,85

23	BBCI-16	35	183,0776593	0,211425648	0,006460712	2,39982632	0,104366651	0,082322939	0,002547404	0,702652757	123,67	34,38	2,78	1242,55	31,18	2,51	1253,28	60,57	4,83
64	BBCI-160	35	103,0344094	0,2523185	0,005470318	3,153337334	0,093203458	0,090688017	0,001820757	0,733891254	1449,69	28,16	1,94	1445,82	22,79	1,58	1440,13	38,28	2,66
65	BBCI-161	35	126,8560541	0,221104364	0,004643236	2,592776981	0,077125347	0,085048483	0,001791759	0,705978514	1287,67	24,51	1,90	1298,60	21,80	1,68	1316,71	40,85	3,10
69	BBCI-162	35	44,52237945	0,241367786	0,006530575	2,938505466	0,091949891	0,088296995	0,001387962	0,864664107	1393,76	33,91	2,43	1391,89	23,71	1,70	1389,02	30,17	2,17
71	BBCI-164	35	441,1977469	0,236543081	0,005670587	2,854285544	0,07487537	0,087515684	0,000932186	0,913851652	1368,66	29,56	2,16	1369,94	19,73	1,44	1371,94	20,49	1,49
72	BBCI-165	35	192,8764881	0,251252489	0,005870818	3,148351195	0,083648746	0,090880671	0,00149328	0,879451666	1444,89	30,25	2,09	1444,60	20,48	1,42	1444,17	24,09	1,67
73	BBCI-166	35	120,0634366	0,235244117	0,005586506	2,843924894	0,074626619	0,087679503	0,000975803	0,90499426	1361,88	29,15	2,14	1367,21	19,72	1,44	1375,54	21,47	1,56
74	BBCI-167	35	230,11496691	0,21695941	0,005466756	2,494792436	0,096195639	0,083397811	0,002434113	0,653476866	1265,75	28,96	2,29	1270,52	27,96	2,20	1278,61	56,92	4,45
75	BBCI-168	35	182,4670099	0,231639315	0,005288086	2,777020969	0,069330636	0,086735939	0,000888624	0,912165623	1343,04	27,68	2,06	1347,55	18,67	1,39	1354,70	19,78	1,46
76	BBCI-169	35	133,3379185	0,250290784	0,006224564	3,1411986458	0,086583359	0,091045435	0,001080731	0,90246996	1439,93	32,09	2,23	1443,04	21,23	1,47	1447,63	22,60	1,56
24	BBCI-17	35	466,0657797	0,228072715	0,004957227	2,818045573	0,072800995	0,089613493	0,001251273	0,841349051	1324,35	26,02	1,96	1360,55	19,36	1,42	1417,37	26,70	1,88
77	BBCI-170	35	439,88923376	0,247360174	0,005669107	3,070484285	0,080379336	0,090027332	0,0011913975	0,87529576	1424,80	29,30	2,06	1425,36	20,06	1,41	1426,19	24,18	1,70
78	BBCI-171	35	193,0346254	0,239791359	0,005532697	2,905564748	0,07364258	0,087881155	0,000921812	0,910342731	1385,57	28,77	2,08	1383,36	19,15	1,38	1379,95	20,16	1,46
25	BBCI-178	35	113,33203657	0,231956783	0,006117346	2,722844518	0,09288854	0,085136245	0,001842323	0,773066178	1344,70	32,01	2,38	1334,71	25,34	1,90	1318,72	41,95	3,18
26	BBCI-179	35	126,853817	0,224991861	0,005379723	2,699642819	0,08770629	0,087023837	0,001915196	0,735780277	1308,16	28,31	2,16	1328,36	24,08	1,81	1361,09	42,41	3,12
30	BBCI-20	35	203,1258657	0,232606846	0,006532291	2,822855763	0,086283971	0,088016667	0,00162195	0,918758995	1348,10	34,16	2,53	1361,63	22,92	1,68	1382,92	23,18	1,68
31	BBCI-21	35	101,8861055	0,211890458	0,006167083	2,372691185	0,128085336	0,081213359	0,003692383	0,539150745	1238,84	32,80	2,65	1234,41	38,58	3,13	1226,69	89,38	7,29
32	BBCI-22	35	148,5894908	0,23426454	0,006476018	2,867311715	0,087439837	0,088752202	0,001144022	0,906314847	1356,77	33,82	2,49	1373,21	22,97	1,67	1398,88	24,71	1,77
33	BBCI-23	35	161,5129515	0,24353666	0,006882695	2,925177838	0,097045493	0,087113618	0,001513715	0,851684461	1405,01	35,68	2,54	1388,45	25,11	1,81	1363,08	33,47	2,46
34	BBCI-24	35	135,4868412	0,22952508	0,006549556	2,71981509	0,093656578	0,085942297	0,001653365	0,828847314	1331,97	34,34	2,58	1333,88	25,57	1,92	1336,95	37,25	2,79
35	BBCI-25	35	229,6973828	0,229505253	0,006981542	2,696168922	0,095534152	0,085206683	0,0015483121	0,858313592	1331,86	36,60	2,75	1327,41	26,25	1,98	1320,22	35,21	2,67
36	BBCI-26	35	227,7705757	0,226501701	0,00617342	2,731560675	0,081317356	0,087431027	0,001051751	0,914799325	1316,57	32,44	2,46	1337,08	22,14	1,66	1370,08	23,15	1,69
37	BBCI-27	35	125,8438303	0,229004459	0,006229743	2,757591966	0,0823468317	0,087305028	0,001086402	0,90933415	1329,55	32,67	2,46	1344,09	22,29	1,66	1367,31	23,96	1,75
44	BBCI-30	35	154,9098245	0,240924395	0,005889974	3,002868464	0,081156364	0,090393705	0,001069447	0,9001423197	1391,46	30,60	2,20	1408,35	20,69	1,47	1434,00	22,57	1,57
45	BBCI-31	35	155,9098337	0,215137138	0,005285949	2,497784729	0,143778287	0,08420509	0,004383301	0,426844103	1256,09	28,04	2,23	1277,39	41,76	3,28	1297,36	101,34	7,81
47	BBCI-33	35	136,9002823	0,217391518	0,005634902	2,658529433	0,076504558	0,088694686	0,00110866	0,90075693	1268,04	29,84	2,35	1317,01	21,24	1,61	1397,64	23,97	1,71
49	BBCI-35	35	271,4010173	0,238536906	0,0070419191	2,919409141	0,118445743	0,0887647254	0,002470371	0,773638028	1379,04	36,65	2,66	1386,95	30,69	2,21	1399,15	53,37	3,81
52	BBCI-38	35	267,4044115	0,230439834	0,00543192	2,798635764	0,078329823	0,088802193	0,001043317	0,893533627	1336,76	28,46	2,13	1355,17	19,74	1,46	1384,35	22,75	1,64
57	BBCI-39	35	323,3870823	0,221645294	0,002649684	2,62296651	0,046380595	0,085828777	0,001182737	0,676070376	1290,52	13,98	1,08	1307,10	13,00	0,99	1334,40	25,20	1,89
60	BBCI-42	35	300,022332	0,216532763	0,002533097	2,499714577	0,045308976	0,083726998	0,001589895	0,644870413	1263,49	13,41	1,06	1271,95	13,15	1,03	1286,28	26,97	2,10
61	BBCI-43	35	163,5847902	0,236813221	0,002174134	2,901753002	0,047769253	0,088869599	0,001214354	0,557689265	1370,06	11,33	0,83	1382,37	12,43	0,90	1401,42	26,18	1,87
63	BBCI-45	35	238,280889	0,227193037	0,0002434039	2,724434297	0,046102733	0,086972118	0,001139211	0,633114346	1319,73	12,79	0,97	1335,14	12,57	0,94	1359,94	25,24	1,86
64	BBCI-46	35	1202,779393	0,241465924	0,01020266	2,948967229	0,129138337	0,088575338	0,000994539	0,966580078	1394,27	53,07	3,81	1394,58	33,22	2,38	1395,06	21,53	1,54
65	BBCI-47	35	278,3286692	0,242940075	0,002676561	2,9222351575	0,05761367	0,087243288	0,001426347	0,5588336737	1401,92	13,88	0,99	1387,72	14,92	1,07	1365,94	31,49	2,31
69	BBCI-48	35	237,3459107	0,230505283	0,0002735508	2,784683511	0,057375323	0,087618071	0,001293765	0,626174892	1337,10	14,32	1,07	1351,44	14,15	1,05	1374,19	28,40	2,07
70	BBCI-49	35	157,7093929	0,242983387	0,003466139	3,054407728	0,072192402	0,091169337	0,001718121	0,60353796	1402,14	17,98	1,28	1421,34	18,08	1,27	1450,21	35,87	2,47

76	BBCL-55	35	205.7529428	0.253432972	0.003057638	2.907296884	0.059462837	0.08956139	0.001415109	0.634983634	1362.87	15.95	1.17	1383.81	15.45	1.12	1416.26	30.22	2.13
78	BBCL-57	35	113.3565445	0.229609878	0.003774637	2.752825199	0.0603833285	0.086053445	0.001262752	0.749456601	1332.41	19.79	1.49	1342.85	16.34	1.22	1359.53	27.99	2.06
4	BBCL-58	35	370.4151759	0.243870295	0.005987565	2.954383734	0.078273604	0.087863141	0.000874765	0.926708045	1406.74	31.03	2.21	1395.97	20.10	1.44	1379.56	19.14	1.39
6	BBCL-60	35	179.9385487	0.230112295	0.005672365	2.788037785	0.075868241	0.087873425	0.001012845	0.905863594	1335.04	29.73	2.23	1352.34	20.34	1.50	1379.79	22.15	1.61
7	BBCL-61	35	103.6821325	0.223060912	0.005565722	2.638855941	0.073402009	0.085800721	0.001054825	0.897027576	1297.99	29.33	2.26	1311.54	20.48	1.56	1333.77	23.78	1.78
8	BBCL-62	35	258.0461764	0.250147575	0.006410181	3.159034154	0.088516247	0.091591796	0.001038069	0.914545199	1439.19	33.05	2.30	1447.21	21.61	1.49	1459.00	21.55	1.48
9	BBCL-63	35	139.5011787	0.228259467	0.005789748	2.748661091	0.076906883	0.087224085	0.001031995	0.906420656	1325.49	30.39	2.29	1341.73	20.83	1.55	1367.73	22.75	1.66
10	BBCL-64	35	244.9467328	0.225905097	0.005626414	2.689284283	0.072062135	0.086339476	0.0008553467	0.929469715	1312.96	29.59	2.25	1325.51	19.84	1.50	1345.86	19.09	1.42
12	BBCL-66	35	342.9192365	0.228855365	0.006460482	2.738933781	0.081377004	0.0867799887	0.000804238	0.9520131438	1328.45	33.89	2.55	1339.09	22.10	1.65	1356.13	17.87	1.32
18	BBCL-68	35	188.5935593	0.22345274	0.003904436	2.565715051	0.0804643808	0.083276308	0.00216872	0.557160651	1300.05	20.57	1.58	1290.92	22.92	1.78	1275.77	50.80	3.98
19	BBCL-69	35	219.9382712	0.233154659	0.004566649	2.838302089	0.074975162	0.088290351	0.001564891	0.741471922	1350.97	23.87	1.77	1365.72	19.84	1.45	1388.88	34.03	2.45
20	BBCL-70	35	281.788208	0.247663398	0.004938726	3.098610345	0.08051705	0.090741063	0.001511757	0.767418416	1426.37	25.52	1.79	1432.35	19.95	1.39	1441.25	31.76	2.20
23	BBCL-73	35	161.8490591	0.228943083	0.004910528	2.675517673	0.088440895	0.084758752	0.002131813	0.6488874761	1328.91	25.76	1.94	1321.73	24.44	1.85	1310.10	48.83	3.73
25	BBCL-75	35	240.9281409	0.23395342	0.004028799	2.8387241484	0.06388905	0.08795155	0.001276192	0.76470502	1355.20	21.05	1.55	1365.44	16.91	1.24	1381.50	27.89	2.02
26	BBCL-76	35	163.1011667	0.243585229	0.005848262	3.0202038441	0.106583406	0.089980367	0.002324696	0.6507738932	1405.26	30.32	2.16	1413.20	26.91	1.90	1425.19	49.36	3.46
30	BBCL-77	35	295.7367968	0.209306469	0.003575195	2.499401965	0.070276689	0.086606837	0.001934306	0.667495833	1225.08	19.06	1.56	1271.86	20.39	1.60	1351.83	43.10	3.19
32	BBCL-79	35	152.2854402	0.233453811	0.004054508	2.7780365303	0.094757383	0.086383906	0.002333028	0.509634986	1352.44	21.19	1.57	1350.28	25.46	1.89	1346.86	56.64	4.21
34	BBCL-81	35	187.1880543	0.227140175	0.003225867	2.731138361	0.0552296	0.087206423	0.001255861	0.701951569	1319.45	16.94	1.28	1336.97	15.03	1.12	1365.13	27.73	2.03
35	BBCL-82	35	156.9199198	0.25683101	0.004048927	3.348210109	0.0882313125	0.094550510	0.002007496	0.592327203	1473.56	20.36	1.40	1492.37	20.61	1.38	1519.21	40.05	2.64
36	BBCL-83	35	155.8332308	0.216570344	0.0044832486	2.488015072	0.077436458	0.083320669	0.001970319	0.6501717326	1263.69	23.22	1.84	1268.55	22.55	1.78	1276.80	46.12	3.61
39	BBCL-86	35	188.7937789	0.227959763	0.004477803	2.726833788	0.07226417	0.086755935	0.001543244	0.741249621	1323.75	23.51	1.78	1335.80	19.69	1.47	1355.15	34.31	2.53
45	BBCL-88	35	197.0793974	0.221523791	0.002054539	2.650983195	0.05289756	0.086793125	0.001288066	0.668463125	1289.88	15.59	1.21	1314.92	14.71	1.12	1355.98	28.61	2.11
46	BBCL-89	35	186.4346616	0.227999951	0.002912211	2.739623875	0.050661402	0.087147634	0.00165342	0.690720704	1323.96	15.29	1.15	1339.28	13.76	1.03	1363.83	25.76	1.89
47	BBCL-90	35	418.7045096	0.239925906	0.003671353	2.928427334	0.057848424	0.088522982	0.00105907	0.774625825	1386.27	19.09	1.38	1389.29	14.95	1.08	1393.92	23.96	1.72
48	BBCL-91	35	377.8046539	0.232337194	0.004660715	2.823514555	0.060337535	0.088139384	0.00093148	0.88218753	1346.69	24.07	1.79	1361.80	16.83	1.24	1385.59	20.29	1.46
49	BBCL-92	35	237.6947478	0.227445198	0.00337811	2.712133859	0.0503339386	0.086483432	0.000962687	0.800202823	1321.05	17.74	1.34	1331.78	13.77	1.03	1349.08	21.49	1.59
51	BBCL-94	35	236.630996	0.234978412	0.003950347	2.883566468	0.066330249	0.089002203	0.001397373	0.730845635	1360.49	20.62	1.52	1377.62	17.34	1.26	1404.27	30.07	2.14
52	BBCL-95	35	183.3751066	0.229397288	0.004560095	2.66733058	0.076853385	0.084331003	0.001758915	0.689919356	1331.30	23.91	1.80	1319.45	21.28	1.61	1300.27	40.54	3.12
57	BBCL-96	35	157.1432873	0.23373127	0.003996685	2.831766977	0.058923479	0.087869584	0.001041758	0.82180612	1353.98	20.88	1.54	1363.99	15.62	1.14	1379.70	22.78	1.65
58	BBCL-97	35	332.5878743	0.223864388	0.006875471	2.616416298	0.127556179	0.084765770	0.003209383	0.629974191	1302.22	36.21	2.78	1305.26	35.83	2.74	1310.26	73.53	5.61

Kuibis Formation

Analysis name	Spot size (mm)	U conc. (ppm)	Ratios	$^{206}\text{Pb}/^{238}\text{U}$	$\pm 2\sigma$	$^{207}\text{Pb}/^{235}\text{U}$	$\pm 2\sigma$	$^{207}\text{Pb}/^{208}\text{Pb}$	$\pm 2\sigma$	$^{207}\text{Pb}/^{206}\text{Pb}$	$\pm 2\sigma$	Age (Ma)	rho:	Degree of concordance (%)	
GJ1	25														
KUL1_9	25	46	0.17871	0.00560	1,83371	0.08299	0.07442	0.00243	0.69	1060	31	1058	30	1053	66
KUL1_8	25	78	0.18434	0.00628	1,93551	0.07720	0,07115	0,0158	0.85	1091	34	1093	27	1099	42
KUL1_4	25	92	0.18468	0.00403	1,93412	0.05857	0.07596	0.00159	0.72	1092	22	1093	20	1094	42
KUL1_65	25	88	0.18633	0.00516	1,94813	0.06699	0.07583	0.00155	0.80	1101	28	1098	23	1091	41
KUL1_70	25	72	0.18764	0.00458	1,96363	0.08288	0.07590	0.00261	0.58	1109	25	1103	28	1092	69
KUL1_48r	25	71	0.18813	0.01301	1,98086	0.14239	0.07637	0.00150	0.96	1111	71	1109	49	1105	39
KUL1_15	25	55	0.19259	0.00578	2,06449	0.07323	0.07775	0.00147	0.85	1135	31	1137	24	1140	38
KUL1_48	25	61	0.19288	0.01060	2,04266	0.12513	0.07681	0.00208	0.90	1137	57	1130	42	1116	54
KUL1_39	25	65	0.19324	0.00883	2,06132	0,12093	0,07737	0,00285	0,78	1139	48	1136	40	1131	73
KUL1_69r	25	62	0.19486	0.00335	2,09372	0.06188	0.07793	0.00187	0.58	1148	18	1147	20	1145	48
KUL1_17r	25	48	0.19596	0.00753	2,08304	0.11831	0.07712	0.00322	0.68	1154	41	1143	39	1124	83
KUL1_47	25	51	0.19600	0.00968	2,07056	0,11874	0,07662	0,00224	0,86	1154	52	1139	39	1111	58
KUL1_49	25	49	0.19619	0.00890	2,10771	0.10956	0.07792	0.00197	0.87	1155	48	1151	36	1145	50
KUL1_55	25	54	0.19722	0.00998	2,12467	0.12468	0.07813	0.00232	0.86	1160	54	1157	41	1150	59
KUL1_44	25	79	0.19974	0.00925	2,23463	0.14916	0.08114	0.00390	0.69	1174	50	1192	47	1225	94
KUL1_17	25	74	0.20440	0.00743	2,27658	0.24260	0.08078	0.00809	0.34	1199	40	1205	75	1216	198
KUL1_69	25	64	0.20615	0.00490	2,3285	0.11485	0.08191	0.00354	0.48	1208	26	1221	35	1244	85
KUL1_45	25	63	0.21702	0.00945	2,50574	0.13667	0.08374	0.00225	0.80	1266	50	1274	40	1287	64
KUL1_3	25	326	0.35843	0.00636	6,05942	0,13093	0,12261	0,00151	0,82	1975	30	1984	19	1995	22
KUL1_74	25	163	0.35969	0.00867	5,99373	0,16158	0,12086	0,00146	0,89	1981	41	1975	23	1969	21
KUL1_68	25	119	0.36303	0.01811	6,10325	0.32374	0.12193	0.00220	0.94	1996	86	1991	46	1985	32
KUL1_40	25	71	0.36346	0.01775	6,18249	0.32623	0.12337	0.00246	0.93	1998	84	2002	46	2006	35
KUL1_57	25	216	0.36534	0.03293	6,24828	0.57295	0.12404	0.00210	0.98	2007	155	2011	80	2015	30
KUL1_64r	25	398	0.36961	0.01037	6,24930	0.21356	0.12263	0.00239	0.82	2027	49	2011	30	1995	35
KUL1_35	25	153	0.37281	0.01651	6,42724	0.29759	0.12504	0.00169	0.96	2043	78	2036	41	2029	24
KUL1_36	25	98	0.37282	0.03463	6,48043	0.62211	0.12607	0.00306	0.97	2043	163	2043	85	2044	43
KUL1_7	25	401	0.37396	0.01061	6,34814	0.19674	0.12312	0.00154	0.92	2048	50	2025	27	2002	22

KUI-1_6	25	237	0,37537	0,00667	6,57499	0,13985	0,12704	0,00149	0,84	2055	31	2056	19	2057	21	99,9
KUI-1_56	25	179	0,37721	0,01887	6,64177	0,34454	0,12770	0,00175	0,96	2063	88	2065	46	2067	24	99,8
KUI-1_38	25	149	0,37808	0,01957	6,66711	0,35245	0,12790	0,00138	0,98	2067	92	2068	47	2069	19	99,9
KUI-1_11	25	339	0,37877	0,01030	6,65433	0,19700	0,12742	0,00149	0,92	2070	48	2067	26	2063	21	100,4
KUI-1_34	25	129	0,37934	0,01946	6,65717	0,37207	0,12728	0,00282	0,92	2073	91	2067	49	2061	39	100,6
KUI-1_12	25	444	0,38174	0,01268	6,77588	0,24275	0,12874	0,00173	0,93	2084	59	2083	32	2081	24	100,2
KUI-1_41	25	369	0,38535	0,01633	6,87275	0,30081	0,12935	0,00141	0,97	2101	76	2095	39	2089	19	100,6
KUI-1_19	25	127	0,38802	0,01203	7,11934	0,24174	0,13307	0,00184	0,91	2114	56	2126	30	2139	24	98,8
KUI-1_58	25	72	0,38860	0,01059	7,00455	0,22006	0,13073	0,00205	0,87	2116	49	2112	28	2108	27	100,4
KUI-1_59	25	54	0,39146	0,01397	7,13063	0,28637	0,13211	0,00243	0,89	2130	65	2128	36	2126	32	100,2
KUI-1_62	25	456	0,39200	0,01258	7,01787	0,27974	0,12984	0,00307	0,80	2132	58	2114	35	2096	42	101,7
KUI-1_16	25	73	0,39278	0,01112	6,99358	0,22012	0,12914	0,00178	0,90	2136	51	2111	28	2086	24	102,4
KUI-1_54	25	507	0,39344	0,03277	7,23027	0,61782	0,13328	0,00254	0,97	2139	152	2140	76	2142	33	99,9
KUI-1_31	25	567	0,39495	0,01888	7,28289	0,38495	0,13374	0,00302	0,90	2146	87	2147	47	2148	39	99,9
KUI-1_27	25	305	0,39661	0,02310	7,28323	0,44574	0,13319	0,00250	0,95	2153	107	2147	55	2140	33	100,6
KUI-1_30	25	411	0,39831	0,02089	7,19459	0,38845	0,13100	0,00168	0,97	2161	96	2136	48	2112	23	102,4
KUI-1_30r	25	144	0,39972	0,01845	7,30324	0,34965	0,13251	0,00169	0,96	2168	85	2149	43	2132	22	101,7
KUI-1_29	25	108	0,39994	0,02186	7,35548	0,41511	0,13339	0,00188	0,97	2169	101	2156	50	2143	25	101,2
KUI-1_53	25	124	0,40013	0,03337	7,21310	0,63888	0,13074	0,00390	0,94	2170	154	2138	79	2108	52	102,9
KUI-1_10	25	239	0,40039	0,01161	7,46524	0,22310	0,13523	0,00151	0,93	2171	53	2169	28	2167	20	100,2
KUI-1_67	25	37	0,40135	0,00694	7,49889	0,17586	0,13351	0,00215	0,74	2175	32	2173	21	2171	28	100,2
KUI-1_14	25	357	0,40218	0,01225	7,28572	0,23668	0,13139	0,00148	0,94	2179	56	2147	29	2117	20	102,9
KUI-1_25	25	198	0,45820	0,02188	10,16410	0,51583	0,16089	0,00276	0,94	2432	97	2450	47	2465	29	98,6
KUI-1_32	25	340	0,46716	0,02513	10,26983	0,59769	0,15944	0,00354	0,92	2471	110	2459	54	2450	38	100,9
KUI-1_2	25	270	0,46893	0,00840	10,42809	0,22168	0,16129	0,00185	0,84	2479	37	2474	20	2469	19	100,4
KUI-1_42	25	84	0,47581	0,02538	10,63805	0,58666	0,16215	0,00228	0,97	2509	111	2492	51	2478	24	101,2
KUI-1_46	25	135	0,47779	0,02100	10,80378	0,50306	0,16400	0,00252	0,94	2518	92	2506	43	2497	26	100,8
KUI-1_66	25	120	0,50988	0,01203	12,56403	0,35512	0,17871	0,00278	0,83	2656	51	2648	27	2641	26	100,6
KUI-1_50	25	384	0,51532	0,02685	13,28768	0,75448	0,18701	0,00422	0,92	2679	114	2700	54	2716	37	98,6
KUI-1_28	25	120	0,51599	0,02565	13,09463	0,67285	0,18405	0,00240	0,97	2682	109	2686	49	2690	22	99,7
KUI-1_1	25	373	0,51721	0,01241	13,00235	0,39562	0,18233	0,00341	0,79	2687	53	2680	29	2674	31	100,5
KUI-1_21	25	175	0,51937	0,01791	13,29823	0,48541	0,18570	0,00222	0,94	2696	76	2701	34	2705	20	99,7
KUI-1_51	25	382	0,52000	0,02838	13,42375	0,74178	0,18223	0,00162	0,99	2699	120	2710	52	2718	14	99,3
KUI-1_23	25	175	0,52571	0,02203	13,40895	0,58817	0,18499	0,00240	0,96	2723	93	2709	41	2698	21	100,9
KUI-1_33	25	218	0,52882	0,02370	13,80439	0,69065	0,18933	0,00421	0,90	2736	100	2736	47	2736	37	100,0
KUI-1_20	25	89	0,53161	0,01702	13,97325	0,47885	0,19064	0,00233	0,93	2748	72	2748	32	2748	20	100,0
KUI-1_22	25	119	0,53448	0,01857	13,81035	0,52991	0,18740	0,00305	0,91	2760	78	2737	36	2720	27	101,5

KUL1_52r	25	99	0,54546	0,02691	14,57502	0,73632	0,19380	0,00210	0,98	2806	112	2788	48	2775	18	101,1
KUL1_52	25	70	0,54558	0,02998	14,68895	0,82227	0,19227	0,00208	0,98	2807	125	2795	53	2787	17	100,7
KUL1_13	25	127	0,55708	0,01766	16,09142	0,55088	0,20949	0,00270	0,93	2854	73	2882	33	2902	21	98,4
KUL1_63	25	281	0,57314	0,01444	16,62487	0,43871	0,21037	0,00165	0,95	2921	59	2913	25	2909	13	100,4
KUL1_18r	25	95	0,58399	0,01844	17,47399	0,58693	0,21627	0,00254	0,94	2973	75	2961	32	2953	19	100,7
KUL1_18	25	144	0,60289	0,01961	18,12152	0,63487	0,21800	0,00284	0,93	3041	79	2996	34	2966	21	102,5
KUL1_37	25	60	0,64055	0,03696	22,42652	1,32404	0,25393	0,00317	0,98	3191	145	3202	57	3209	20	99,4
KUL1_73	25	453	0,66223	0,00784	24,26186	0,34671	0,26572	0,00213	0,83	3276	30	3279	14	3281	13	99,8

Appendix F – EMPA data

Weight percent

Group : BSchulz01

Sample : AnProbe114

Page 1

No.	Na ₂ O	k ₂ O	MnO	TiO ₂	MgO	CaO	FeO	Cr ₂ O ₃	Al ₂ O ₃	V ₂ O ₃	SiO ₂	Total	Comment	Mineral
3	1,0904	0,4522	0,2887	0,3669	9,0580	12,0188	15,3163	0,0078	14,8847	0,0081	43,1981	96,6901	DMF-A-1	Amphibole
4	0,9311	0,3323	0,2656	0,3778	9,8926	11,4720	14,1170	0,0087	13,1918	0,0588	45,0019	95,6495	DMF-A-1-2	Amphibole
5	1,0856	0,4162	0,3007	0,3531	10,0889	11,9935	14,7371	0	13,7708	0,085	45,4005	98,2314	DMF-A-1-3	Amphibole
6	0,6284	0,1547	0,3105	0,1839	13,4061	12,1504	12,7913	0,0374	7,6597	0,0831	49,8456	97,2511	DMF-A-1-4	Amphibole
7	1,1419	0,5798	0,2971	0,3996	9,0626	11,3592	14,9958	0,0012	15,1361	0,0563	43,6156	96,6452	DMF-A-2-1	Amphibole
8	1,1261	0,3067	0,2951	0,3513	9,3310	11,9417	14,9437	0,0423	14,6478	0,0363	43,9145	97,1364	DMF-A-2-2	Amphibole
9	0,7364	0,2232	0,2497	0,2856	12,3021	12,0777	13,7579	0	9,6754	0,0009	48,7015	98,0104	DMF-A-2-3	Amphibole
10	1,0684	0,2648	0,2343	0,2827	9,5980	11,8530	14,8207	0,027	13,6116	0,0363	44,5317	96,3285	DMF-A-2-4	Amphibole
11	1,2094	0,4606	0,25	0,4906	9,2536	11,6169	14,9282	0,002	15,1145	0,0554	43,74	97,1212	DMF-A-3-1	Amphibole
12	1,2538	0,4179	0,1863	0,4869	9,1781	11,5633	14,9528	0,0321	15,1157	0,0627	43,5556	96,7952	DMF-A-3-2	Amphibole
13	1,2423	0,41	0,2313	0,5206	9,4755	11,5361	14,7938	0,0305	14,4628	0,02	44,1936	96,9165	DMF-A-3-3	Amphibole
14	1,2091	0,4308	0,2404	0,4531	9,2043	11,7286	14,8719	0,0896	15,1096	0,0581	43,7286	97,1783	DMF-A-3-4	Amphibole
15	1,1832	0,4697	0,2257	0,4888	9,3562	11,6766	14,4176	0	15,2383	0,0228	43,5548	96,6137	DMF-A-4-1	Amphibole
16	1,2909	0,3372	0,2096	0,3267	9,3537	11,5741	14,6028	0,0369	15,2358	0,0018	43,5439	96,9134	DMF-A-4-2	Amphibole
17	1,1802	0,5102	0,2212	0,6076	9,3371	11,6418	14,3271	0,0424	15,2772	0	43,4515	96,5962	DMF-A-4-3	Amphibole
18	1,0413	0,2929	0,5956	10,9926	8,2440	8,8136	21,2539	0,0136	11,8059	0,2849	33,7326	97,1210	DMF-A-4-4	Amphibole
19	1,2151	0,4382	0,2451	0,4648	9,6247	11,8617	14,6918	0,0063	15,1622	0,1223	44,6479	98,4801	DMF-A-5-1	Amphibole
20	1,1952	0,3799	0,1888	0,4072	9,7181	11,7909	14,2062	0	14,5161	0,1018	44,1185	96,6226	DMF-A-5-2	Amphibole
21	1,1604	0,3417	0,2118	0,4058	9,8164	11,6808	13,8990	0,0032	14,6976	0,0861	44,1812	96,4840	DMF-A-5-3	Amphibole
22	1,1666	0,4147	0,1808	0,4427	9,7767	11,9202	14,1496	0	14,8539	0,0238	44,3944	97,3285	DMF-A-5-4	Amphibole
23	1,1634	0,3157	0,1731	0,5224	10,7967	11,6240	13,9119	0,0564	13,152	0,0309	45,2216	96,9681	DMF-A-6-1	Amphibole
24	1,181	0,3311	0,196	0,5357	10,7508	11,6666	14,1832	0,1009	13,4701	0,0009	45,1759	97,5922	DMF-A-6-2	Amphibole
25	1,1837	0,3311	0,1163	0,4585	10,6755	11,6779	14,0992	0,0567	13,4118	0,0581	45,1071	97,0859	DMF-A-6-3	Amphibole
26	1,1266	0,3188	0,1344	0,4565	10,6378	11,6979	14,1261	0,0399	13,5972	0,0182	44,9202	97,0735	DMF-A-6-4	Amphibole
27	1,0406	0,3977	0,2576	0,5406	10,4164	11,9255	14,1355	0,0685	12,8405	0,0772	45,2505	96,9506	DMF-A-7-1	Amphibole
28	1,0743	0,484	0,269	0,549	9,5860	11,7186	14,9341	0,0301	14,6319	0,0354	44,0098	97,3221	DMF-A-7-2	Amphibole
29	1,092	0,4758	0,2817	0,4807	10,1156	11,9367	14,6667	0,0564	13,6626	0,0742	44,6845	97,5270	DMF-A-7-3	Amphibole
30	1,1209	0,4807	0,2883	0,4367	9,6247	11,7928	14,7912	0,0342	14,5502	0,0529	43,5518	96,7245	DMF-A-7-4	Amphibole
31	1,1791	0,4746	0,2823	0,5405	9,1701	11,6244	15,0420	0,1544	15,3164	0	43,8994	97,6832	DMF-A-8-1	Amphibole
32	1,1359	0,4747	0,3129	0,4677	9,0608	11,6336	14,7587	0,1188	15,231	0,01	43,5148	96,7189	DMF-A-8-2	Amphibole
33	1,2463	0,4672	0,3547	0,4679	9,1189	11,6170	14,8896	0,155	15,2115	0,0605	43,4913	97,0799	DMF-A-8-3	Amphibole

34	1,1939	0,4536	0,2472	0,3972	9,0301	11,6291	14,8725	0,1282	15,2958	0,0298	43,2269	96,5042	DMF-A8-4	Amphibole
36	0,9836	0,3546	0,2551	0,4186	10,851	11,9528	14,4724	0	13,1524	0,0521	46,1322	98,0019	DMF-T1-2	Titanite/Sphene
37	0	0,0089	0,0574	37,1389	0,0000	28,7859	0,5702	0,1001	2,371	0,656	31,4863	101,1747	DMF-T1-3	Titanite/Sphene
38	0	0	0,0175	38,1981	0,0000	28,8110	0,3473	0	1,9333	0,7818	31,1925	101,2815	DMF-T1-4	Titanite/Sphene
39	0,6394	0,0379	0,0225	0	0,0000	19,0010	0,0821	0	32,8794	0,01	44,8351	97,5233	DMF-T2-1	Titanite/Sphene
40	0,0042	0,0085	0,0636	38,0625	0,0000	28,7198	0,1658	0,02	2,1126	0,7482	31,1851	101,0903	DMF-T2-2	Titanite/Sphene
41	0	0	0,0797	37,6793	0,0000	29,1132	0,1431	0,0156	2,6759	0,6896	31,1809	101,5773	DMF-T2-3	Titanite/Sphene
42	0,0745	0,0432	0,0884	35,694	0,0000	27,8028	0,2064	0	2,2995	0,6944	30,4636	97,3668	DMF-T2-4	Titanite/Sphene
43	0	0	4,5078	0,0735	2,0720	9,2745	24,9579	0,0213	20,1691	0	38,0287	99,1048	DMF-A9-1	Cpx?
44	0	0,003	4,0897	0,1021	2,0949	8,7782	26,0995	0,028	20,3125	0	38,1837	99,6916	DMF-A9-2	Cpx?
45	0,0383	0,0047	3,6387	0,0828	2,0589	8,5752	26,6642	0	20,1073	0,0414	38,2193	99,4308	DMF-A9-3	Cpx?
46	0,0426	0,0114	3,3837	0,0153	2,1489	8,8307	27,4426	0,0534	20,4769	0	39,0018	101,4073	DMF-A9-4	Cpx?
47	1,1319	0,4196	0,2779	0,4054	9,6033	11,7507	14,5599	0,1805	14,6278	0,093	43,8048	96,8559	DMF-A10-1	Amphibole
48	1,1941	0,4192	0,2369	0,4249	9,5907	11,6099	14,1243	0,1429	14,6288	0,043	43,5621	95,9768	DMF-A10-2	Amphibole
49	1,2477	0,378	0,2776	0,4344	9,8913	11,4733	14,3815	0,0725	14,271	0,1529	44,0614	96,6416	DMF-A10-3	Amphibole
50	1,1695	0,4694	0,2048	0,4458	9,3091	11,6657	14,9123	0,0605	15,2552	0,0908	43,2254	96,8086	DMF-A10-4	Amphibole
51	0	0,0141	0,2293	0,1734	0,0663	23,3622	5,8393	0	26,876	0,1145	38,9373	95,6124	DMF-A11-1	Amphibole
52	1,2095	0,4337	0,2103	0,4288	9,1718	11,6322	14,8948	0,0296	15,6763	0,0406	43,6185	97,3461	DMF-A11-2	Amphibole
53	1,2224	0,4554	0,2216	0,4561	9,3868	11,6623	14,3070	0,0957	15,17	0,0937	43,74	96,8109	DMF-A11-3	Amphibole
54	1,2184	0,3727	0,2044	0,505	9,7315	11,6527	14,3607	0,0554	14,9019	0	44,5935	97,5962	DMF-A11-4	Amphibole
55	1,1854	0,3905	0,2296	0,5434	9,7410	11,7159	14,2016	0,1131	14,5792	0,041	43,7679	96,5086	DMF-A12-1	Amphibole
56	1,2422	0,4007	0,2127	0,4601	9,7960	11,6859	14,2445	0,0577	14,7861	0	43,7537	96,6396	DMF-A12-2	Amphibole
57	1,2153	0,4181	0,2472	0,4256	9,6339	11,8084	14,4676	0,0736	14,9148	0,0377	43,5271	96,7693	DMF-A12-3	Amphibole
58	1,1429	0,4313	0,249	0,5029	9,5559	11,7489	14,6001	0,1179	14,9841	0,0509	43,5515	96,9353	DMF-A12-4	Amphibole
59	0,009	0	4,8097	0,1601	2,2982	6,8282	27,0060	0,0946	20,3428	0,0081	38,1871	99,7437	DMF-A13-1	Cpx?
60	0,0047	0	5,0132	0,0573	2,2416	7,0256	27,0756	0,0146	20,1888	0,061	37,9224	99,6043	DMF-A13-2	Cpx?
61	0	0	4,1319	0,0319	2,1333	7,2833	27,3773	0	20,3519	0	38,2012	99,5108	DMF-A13-3	Cpx?
62	0	0	3,0261	0,0185	2,1753	7,7569	28,8152	0,0515	20,6227	0	38,3168	100,7630	DMF-A13-4	Cpx?
63	1,1876	0,3951	0,2659	0,7456	8,7934	11,5934	14,7129	0,083	16,0616	0,0953	42,0969	96,2307	DMF-A14-1	Amphibole
64	1,1046	0,4504	0,2028	0,4644	9,0595	11,7583	14,4578	0,0412	15,5171	0,0206	43,466	96,5428	DMF-A14-2	Amphibole
65	1,138	0,4589	0,2742	0,3034	9,2930	11,6567	14,8498	0	15,4803	0,0898	43,2931	97,0372	DMF-A14-3	Amphibole
66	1,133	0,4314	0,2464	0,5309	9,2772	11,6619	14,7999	0,0716	14,9269	0,0598	43,2934	96,4324	DMF-A14-4	Amphibole
67	0	0,0118	0,052	37,4042	0,0000	28,9142	0,2225	0,0055	2,3477	0,726	31,2033	100,8872	DMF-T3-1	Titanite
68	0	0,0056	0,1284	36,8563	0,0000	28,5825	0,2790	0	2,4272	0,8161	30,9375	100,0326	DMF-T3-2	Titanite
69	0	0	0,0631	37,6122	0,0000	28,7584	0,2618	0,0507	2,4544	0,7445	31,166	101,1111	DMF-T3-3	Titanite
70	0	0,0183	0,0515	37,5942	0,0000	28,8880	0,2345	0	2,3719	0,6753	31,0672	100,8929	DMF-T3-4	Titanite

A.E. Myhra

No.	Na ₂ O	K ₂ O	MnO	TiO ₂	MgO	CaO	FeO	Cr ₂ O ₃	Al ₂ O ₃	V ₂ O ₃	SiO ₂	Total	Comment	
71	0		0	0,0198	37,7834	0,0000	28,4901	0,1577	0,0159	1,9954	0,7143	31,1765	100,3531 DMF-I4-1	
72	0,0023		0,0124	0,0531	37,6246	0,0000	28,6236	0,2204	0,0004	2,0504	0,7866	30,9531	100,3269 DMF-I4-2	
73	0,017		0,0013	0,0298	36,5596	0,0000	28,5909	0,1881	0,0806	2,1368	0,7956	31,0676	99,8673 DMF-I4-3	
74	0	0,0137	0,0329	37,5692	0,0000	28,7741	0,2342	0,0551	2,3073	0,716	31,1231	100,8256 DMF-I4-4	Titanite	
Blaubeker Diamictite														
75	0	0	0,0956	0,5249	0,0000	0,0143	88,2701	0	0,0616	0,069	0,299	89,3345	DBD-M1-1	Magnetite
76	0	0,0064	0,0384	0,534	0,0000	0,0120	88,5045	0,0445	0	0,0974	0	89,2372	DBD-M1-2	Magnetite
77	0,0093	0	0,0111	0,2122	0,0000	0,0104	88,6724	0,0237	0,0969	0,0884	0	89,1244	DBD-M1-3	Magnetite
78	0,0164	0,1391	0,0496	0,4959	0,0000	0,0319	87,2110	0	0,4347	0,0948	0,8338	89,3072	DBD-M1-4	Magnetite
79	0	0,0195	0,0161	74,8132	0,0000	0,3054	22,6325	0,0147	0,0661	1,4445	0,157	99,4690	DBD-R1-1	Rutile
80	0	0,017	0,1964	91,6753	0,0303	0,3689	4,9638	0,0348	0,1147	1,8859	0,8067	100,0938	DBD-R1-2	Rutile
81	0,0298	0,0234	0,7755	76,2651	0,7663	3,5335	5,5833	0	0,4233	1,3406	1,1966	89,9394	DBD-R1-3	Rutile
82	0	0,0105	0	73,5222	0,0000	0,2097	15,5016	0	0,0887	1,2437	0,2225	90,8289	DBD-III-1	Ilmenite
83	0	0,0276	0,033	39,5552	0,0080	0,0346	52,5228	0,0281	0,2543	0,8015	0,6431	93,7082	DBD-III-2	Ilmenite
84	0,058	0,059	0,0139	46,1571	0,0000	0,0296	47,7798	0,04	0,0785	0,9233	0,3316	95,4377	DBD-III-3	Ilmenite
85	0	0	0,0129	58,3778	0,0000	0,0260	37,2593	0	0,0689	1,2001	0,0405	96,9855	DBD-III-4	Ilmenite
86	0	0	0,0375	0,025	1,7640	0,2576	71,5798	0	0	0	3,129	76,7929	DBD-M2-1	Magnetite, but intergrown or altered
87	0	0,4012	0,0361	0	1,4715	0,2663	71,5997	0,0154	2,0289	0	6,4317	82,2508	DBD-M2-2	Magnetite
88	0	0	0,0911	0	1,2829	0,2908	75,2164	0	0	0,0173	4,2067	81,1052	DBD-M2-3	Magnetite
89	0	0	0,0822	0	0,7316	0,3944	75,8111	0,0079	0	0,0211	4,9687	82,0171	DBD-M2-4	Magnetite
90	0,0159	0	0,044	0,9018	0,0000	0,0565	87,8883	0,0376	0	0,0836	0,6838	89,7115	DBD-M3-1	Magnetite
91	0	0,0053	0,0715	0,6148	0,0000	0,0403	87,2688	0,011	0,0084	0,0385	0,1622	88,2208	DBD-M3-2	Magnetite
92	0	0	0,1687	0,4374	0,0000	0,0137	87,9149	0,0481	0,0733	0	0,1637	88,8198	DBD-M3-3	Magnetite
93	0	0	0,1029	0	0,8931	0,4419	77,0390	0	0	0,081	3,9814	82,5393	DBD-II2-1	hematite, intergrowth
94	0,007	0,0147	0,1105	0	0,9317	0,3951	74,7801	0	0	0,0316	4,3462	80,6169	DBD-II2-2	Ilmenite
95	0,0042	0	0,0619	0,0373	1,0229	0,4192	74,9721	0,0413	0	0,012	4,8713	81,4422	DBD-II2-3	Ilmenite
96	0,0789	0,0209	0,1388	0,0048	0,9969	0,4553	74,7629	0,0287	0	0	4,7584	81,2257	DBD-II2-4	Ilmenite
97	0	0,0465	0	61,5866	0,0000	0,0148	34,9411	0	0,0413	1,1972	0,219	98,0465	DBD-II3-1	Ilmenite
98	0,0203	0,0571	0	59,4982	0,0000	0,0315	36,0614	0,0042	0,0025	1,1919	0,0109	96,8780	DBD-II3-2	Ilmenite
100	0,0048	0,0364	0,0006	7,3884	0,0000	0,0147	81,4232	0	0,5801	0,167	1,0141	90,6562	DBD-M4-1	Magnetite
101	0	0,0031	0,0341	2,8949	0,0000	0,0109	84,4728	0,0177	0,4961	1,016	0,8213	88,8325	DBD-M4-2	Magnetite
102	0,0221	0,0278	0,0191	5,9696	0,0770	0,0443	82,2335	0,0169	0,4773	0,1361	1,212	90,2314	DBD-M4-3	Magnetite
103	0,0508	0,0665	0,0336	2,0603	0,0711	0,0269	85,6982	0	0,262	0,0481	0,7099	88,9674	DBD-M4-4	Magnetite

Kuitbis No.	Na2O		K2O		MnO	TiO2	MgO	CaO	FeO	CeO3	Al2O3	V2O3	SiO2	Total	Comment
104	0	0,0156	0,0124	0	0,5806	0,5675	73,7135	0,0091	0	0,1634	3,8303	78,8924	FA-M1-1	Magnetite	
105	0,0413	0	0,004	0	0,6698	0,5222	73,8996	0	0	0,233	4,0125	79,2924	FA-M1-2	Magnetite	
106	0	0	0,0316	0	0,5626	0,6301	73,2979	0	0,0344	0,2229	3,6898	78,4494	FA-M1-3	Magnetite	
107	0,0787	0,0016	0	0	0,8174	0,5717	72,8783	0,0076	0,0141	0,2002	3,1809	77,7505	FA-M1-4	Magnetite	
108	0	0,0036	0,0373	100,413	0,2027	0,0476	0,2697	0,0952	0,1492	1,9664	0,351	103,5556	FA-R1-1	Rutile	
109	0,0664	0,0294	0,0204	45,5222	15,1539	0,0768	4,7712	0,0352	9,5113	0,897	14,5583	90,6422	FA-R1-2	Rutile	
110	0,02	0	0	90,5881	3,9268	0,0512	0,8071	0,1497	2,2051	1,7695	3,2384	102,7759	FA-R1-3	Rutile	
111	0,0477	0,0195	0,0056	74,9744	7,2645	0,0922	1,9815	0,0491	4,2157	1,4642	6,5483	96,6628	FA-R1-4	Rutile	
112	2,2331	0,0585	0,1519	0,7085	4,6693	0,8142	12,2039	0,0064	28,4803	0,0252	35,2566	84,6079	FA-Tu1-1	Tourmaline, add 10.5 wt% B2O3 to the sum	
113	2,2584	0,0654	0,1059	0,5046	4,7565	0,7411	12,2134	0	28,1158	0,0383	35,5248	84,3242	FA-Tu1-2	Tourmaline	
114	2,273	0,0715	0,1406	0,4865	4,6316	0,7580	12,1205	0	28,0484	0,0037	35,4553	83,9691	FA-Tu1-3	Tourmaline	
115	2,2466	0,0565	0,1832	0,5141	4,8120	0,7823	12,3317	0,0432	28,0556	0	35,9245	84,9496	FA-Tu1-4	Tourmaline	
116	0,0108	0,0118	0,0025	101,5202	0,0000	0,0312	0,2417	0,0438	0,0478	2,0679	0	103,9777	FA-R12-1	Rutile	
117	0	0	0,0211	100,2802	0,0000	0,0279	0,3524	0	0,0449	2,0289	0,0387	102,7041	FA-R2-2	Rutile	
118	0,07	0,0138	0	98,5488	0,0000	0,1204	0,5210	0	0,1864	2,1109	0,7798	102,3511	FA-R12-3	Rutile	
119	0	0,014	0,0037	100,5106	0,0000	0,0343	0,2712	0,0076	0,0529	2,0418	0,0849	103,0210	FA-R2-4	Rutile	
120	2,1596	0,0384	0,1372	0,6605	3,8441	0,5335	11,6539	0,0561	30,0746	0,0646	35,3964	84,6189	FA-Tu2-1	Tourmaline, add 10.5 wt% B2O3 to the sum	
121	2,0946	0,0431	0,1186	0,7708	3,8620	0,5563	11,4676	0,0162	30,0504	0	35,3588	84,3385	FA-Tu2-2	Tourmaline	
122	2,055	0,0195	0,0904	0,4944	4,4726	0,5238	10,4519	0	29,8596	0	35,6265	83,5937	FA-Tu2-3	Tourmaline	
123	2,1611	0,0324	0,114	0,8197	3,5961	0,5387	11,6528	0	29,9284	0,014	35,3976	84,2548	FA-Tu2-4	Tourmaline	
124	2,163	0,0277	0,025	0,926	4,6677	0,1932	8,9662	0,0721	31,0815	0,0677	36,1238	84,3139	FA-Tu3-1	Tourmaline	
125	2,082	0,0136	0,0601	0,8487	4,9511	0,3627	8,4582	0	31,4498	0,0699	35,9584	84,2545	FA-Tu3-2	Tourmaline	
126	2,013	0,0026	0,0812	0,8743	4,9936	0,3254	8,3413	0,0371	31,467	0,0961	36,2409	84,4725	FA-Tu3-3	Tourmaline	
127	2,0364	0,0254	0,0752	0,9408	4,9755	0,4941	8,9109	0,0466	31,0524	0,0412	35,8412	84,4397	FA-Tu3-4	Tourmaline	
128	2,0886	0,0122	0	1,0714	10,5361	0,5361	3,4742	0	28,5	0,108	37,572	84,5986	FA-Tu4-1	Tourmaline	
129	2,2078	0,0182	0,0772	0,9539	4,7657	0,1064	9,1272	0,0596	30,8892	0,0279	35,9702	84,2033	FA-Tu4-2	Tourmaline	
130	2,1664	0,063	0,0506	1,0848	4,7044	0,0967	8,9010	0,0165	30,8057	0,0781	36,2093	84,1766	FA-Tu4-3	Tourmaline	
131	2,1408	0,0405	0,079	0,9778	4,4094	0,1164	8,9942	0,0189	31,4813	0,0586	35,9854	84,3022	FA-Tu4-4	Tourmaline	
132	0,0358	0,0144	0	99,145	0,1561	0,0345	0,2546	0,0487	0,1437	2,0087	1,543	103,3845	FA-R13-1	Ti-on-V-correction: trueV203 wt%	

133	0	0	0	99,4426	0,0919	0,0121	0,4276	0	0,1999	2,0603	0,2254	102,4598	FA-Rt3-2	Rutile
134	0,0353	0,0011	0,031	99,0621	0,4871	0,0552	0,3473	0,0913	0,3934	2,05	0,5248	103,0786	FA-Rt3-3	Rutile
135	0	0,0043	0,0031	99,2503	0,5020	0,0614	0,2990	0,0278	0,3911	1,9292	0,6313	103,0995	FA-Rt3-4	Rutile
136	0	0,0887	0,1244	0,0012	0,5846	0,7472	73,6615	0,0633	0,4702	0,2025	4,632	80,5756	FA-M2-1	Magnetite
137	0,0211	0,2823	0	0	0,7126	0,7012	70,7201	0	0,8299	0,0748	4,7134	78,0554	FA-M2-2	Magnetite
138	0,0516	0,0132	0,0939	0,0198	0,5364	0,6917	75,3,038	0	0,4226	0,1663	4,4678	81,7705	FA-M2-3	Magnetite
139	0,0271	0,0059	0	0,0259	0,6758	0,8297	73,4055	0	0,4018	0,2612	3,0698	78,7026	FA-M2-4	Magnetite
140	0	0	0,0117	100,4336	0,0117	0,0404	0,1034	0,0554	0,0558	2,1287	0,1429	102,9837	FA-Rt3-1	Rutile
141	0	0,0093	0,0247	101,241	0,0000	0,0163	0,1783	0	0,061	2,1464	0	103,6770	FA-Rt3-2	Rutile
142	0	0,0013	0	101,0436	0,0000	0,0311	0,1616	0,1366	0,0449	2,1779	0,044	103,6410	FA-Rt3-3	Rutile
143	0	0,0122	0,0099	100,7261	0,0000	0,0442	0,0817	0,0719	0,0365	2,2441	0,0085	103,2351	FA-Rt3-4	Rutile
144	0	0,0051	0	100,9106	0,0000	0,0229	0,1436	0,0472	0	2,3548	0,1183	103,6025	FA-Rt5-1	Rutile
145	0	0	0,0265	100,2041	0,0000	0,0375	0,1396	0,0029	0,0523	2,205	0,1088	102,7767	FA-Rt5-2	Rutile
146	0	0,0149	0	102,4027	0,0000	0,0351	0,0152	0,0088	0,018	2,2587	0	104,7534	FA-Rt5-3	Rutile
147	0	0	0	101,9685	0,0395	0,0239	0,0790	0,0464	0,1109	2,3032	0,0088	104,5802	FA-Rt5-4	Rutile
148	1,7729	0,026	0,1235	0,171	0,8494	0,0617	13,6990	0,0119	31,6686	0	35,5279	83,9119	FA-Tu5-1	Tourmaline
149	1,7419	0,0482	0,0845	0,1105	0,8371	0,0809	13,5,507	0	31,9802	0	35,7521	84,1861	FA-Tu5-2	Tourmaline
150	1,6614	0,0421	0,148	0,1461	0,9112	0,0753	13,760	0	31,8886	0	35,6931	84,3418	FA-Tu5-3	Tourmaline
151	1,8014	0,0494	0,1044	0,058	0,9185	0,0710	13,8472	0,0039	31,7,389	0,0294	35,2763	83,8984	FA-Tu5-4	Tourmaline
152	0,0094	0,0206	0,0456	92,9544	0,0672	0,1163	0,2,264	0,0234	0,0895	1,9565	0,3511	98,8605	FA-Rt6-1	Rutile
153	0	0,0055	0,0018	100,2779	0,0000	0,0259	0,1672	0,0175	0,0505	1,9121	0	102,4584	FA-Rt6-2	Rutile
154	0,0102	0,0049	0	100,8139	0,0000	0,0466	0,1912	0,0585	0,0644	1,9141	0,0505	103,1543	FA-Rt6-3	Rutile
155	0,0231	0,0056	0,0424	101,9466	0,0000	0,0223	0,1935	0	0,0208	1,8953	0	104,1496	FA-Rt6-4	Rutile
156	1,6841	0,0389	0,1199	0,0783	0,8729	0,0697	13,7,276	0,0423	31,6634	0,0395	35,4377	83,7743	FA-Tu6-1	Tourmaline
157	1,6902	0,035	0,0891	0,1008	0,8838	0,0644	13,4310	0,0292	31,5,341	0	35,3357	83,2433	FA-Tu6-2	Tourmaline
158	1,7323	0,0381	0,099	0,1237	0,9514	0,1016	13,8234	0,0288	31,77	0,0423	35,2947	84,0052	FA-Tu6-3	Tourmaline
159	0	0,0018	0	0,0264	0,6531	0,5708	71,8776	0	0	0,3433	3,2302	76,7332	FA-M3-1	Magnetite
160	0,1035	0,0042	0,0145	0	0,6483	0,5916	73,4675	0,0492	0	0,3617	3,0759	78,3164	FA-M3-2	Magnetite
161	0,0341	0,0015	0	0	0,5841	0,5714	75,3,322	0	0	0,3884	3,4209	80,3325	FA-M3-3	Magnetite
162	0,0617	0,0049	0	0	0,8603	0,4289	71,3152	0,0423	0	0,2169	3,4567	76,3869	FA-M3-4	Magnetite
163	0,0089	0	14,5768	0,0694	0,2124	0,2897	27,9,651	0,0199	19,7802	0	36,9541	99,8764	FA-Tu7-1	Tourmaline
164	0	0,0113	14,2218	0,0341	0,1779	0,3403	28,0146	0,0607	19,8049	0,0112	36,9877	99,6445	FA-Tu7-2	Tourmaline
165	0,0178	0,0126	14,1746	0	0,2101	0,3048	28,3740	0	19,7947	0	37,0426	99,9313	FA-Tu7-3	Tourmaline
166	0	0	14,2951	0,005	0,1996	0,3295	27,9,862	0,0466	19,8909	0	36,9517	99,7046	FA-Tu7-4	Tourmaline

Numeres No.	Na2O	K2O	MnO	TiO2	MgO	CaO	FeO	C12O3	Al2O3	V2O3	SiO2	Total	Comment	
209	0	0,0035	0,0249	43,1745	0	25,5264	2,5987	0,0455	0,7326	1,004	27,8399	100,95	EMI391-T1-4	Titanite
211	0,1152	0	3,6399	0,0825	2,6359	8,4435	25,5261	0	20,5055	0,0519	38,0134	99,0139	EMI391-A1-2	Gamet
212	0,0229	0,015	3,647	0,062	2,8795	8,3131	26,3999	0,0069	20,4457	0,1148	37,9814	99,8882	EMI391-A1-3	Gamet
213	0,0748	0	3,3487	0,064	3,1288	8,2449	26,1427	0	20,2977	0,0656	37,8598	99,2227	EMI391-A1-4	Gamet
215	0,0503	0,2507	0,906	0,1143	10,9521	0,2556	20,5881	0,035	17,9734	0,0387	27,6183	78,7825	EMI391-M1-2	Magnetite
216	0	0,1007	5,4905	0	0,0067	84,6007	0,0601	0,0561	0,2355	0,1247	90,675	EMI391-M1-3	Magnetite	
217	0,0089	0,0066	0,2729	17,2213	0,2282	0,0091	73,5265	0,1003	0,2558	0,8678	0	92,4974	EMI391-M1-4	Magnetite
219	0,016	0,0114	0,4151	0,0245	7,8148	1,5959	29,6835	0	21,3664	0	38,5792	99,5068	EMI391-G2-2	Gamet
220	0,0066	0	0,4191	0,0313	7,4617	1,596	29,6585	0,0051	21,3517	0	38,4857	99,0157	EMI391-G2-3	Gamet
221	0	0,0022	0,0553	100,1922	0	0,049	0,2043	0,148	0,069	2,4684	0	103,1884	EMI391-R1-1	Rutile
222	0	0,0132	0,0206	100,584	0	0,0313	0,1547	0,0394	0,0804	2,4353	0,0197	103,3786	EMI391-R1-2	Rutile
223	0	0,0032	102,1024	0	0,0168	0,1466	0,0598	0,0929	2,4659	0	104,8876	EMI391-R1-3	Rutile	
224	0	0	0,309	45,9954	0,0504	0,0598	44,8878	0,0775	0,0583	1,0552	0,9488	93,4422	EMI391-M2-1	Magnetite
225	0,0066	0,0164	0,2625	16,8319	0,0052	0,0171	74,5226	0,0651	0,0143	0,6614	0	92,4031	EMI391-M2-2	Magnetite
226	0,0048	0,0107	0,0333	13,6982	0	0,0346	77,6005	0,038	0,0854	0,6237	0,0293	92,1585	EMI391-M2-3	Magnetite
227	0,0556	0	0,109	47,3494	0,0505	0,007	44,5595	0	0,0338	1,1175	0	93,2823	EMI391-M2-4	Magnetite
229	0,0124	0	1,6016	0	5,2639	3,1448	29,8102	0,0928	20,8298	0,0214	38,1393	98,9162	EMI391-G3-2	Gamet
230	0,0194	0	1,5918	0,0879	5,3365	3,1247	30,4746	0	21,0589	0,0373	38,3339	100,065	EMI391-G3-3	Gamet
231	0	1,6669	0	5,1778	3,1681	30,4972	0,0341	21,1699	0	38,2812	99,9952	EMI391-G3-4	Gamet	
232	0	0,0071	1,6366	0	5,1995	3,1871	30,5987	0	21,0729	0	38,3308	100,0227	EMI391-G3-5	Gamet
233	0	2,1363	0,0326	15,7769	0,308	0,0285	64,8912	0,0181	2,9326	0,3423	5,4542	91,9207	EMI391-M3-1	Magnetite
234	0	0,019	0	30,1305	0	0,0666	62,4526	0,0238	0,0837	0,6321	0,3359	93,7442	EMI391-M3-2	Magnetite
235	0,0535	0	0,0042	29,5146	0	0,0556	62,6004	0	0,4369	0,5633	0,4486	93,1371	EMI391-M3-3	Magnetite
236	0,0452	0,0112	0,0048	20,7556	0	0,0575	70,9896	0,0714	0,1717	0,4105	0,2617	92,7792	EMI391-M3-4	Magnetite
237	0,0017	0,0263	0,0909	14,9842	0	0	75,909	0	0,0092	0,5274	0	91,5487	EMI391-M4-1	Magnetite
238	0	0,0084	0,0712	11,4756	0	0,0115	80,2146	0,0578	0	0,5566	0	92,1957	EMI391-M4-2	Magnetite
239	0,2084	0	0,0282	22,1317	0	0,0359	68,7274	0,0241	0,0042	0,7151	0	91,875	EMI391-M4-3	Magnetite
240	0,0447	0	0	9,467	0	0,035	81,6598	0,1046	0,06	0,3268	0	91,6979	EMI391-M4-4	Magnetite
241	0,0238	0,0114	0,1395	11,892	0	0	79,8032	0	0,093	0,4122	0,0296	92,4047	EMI391-M4-5	Magnetite
242	0,0247	0,0151	0	103,0481	0	0,0219	0,6327	0,0367	0,0214	2,0328	0	105,8334	EMI391-R2-1	Rutile
243	0,0085	0	0	102,8665	0	0,0201	0,4006	0,0362	0,0226	2,1416	0	105,4961	EMI391-R2-2	Rutile
244	0	0,003	0,0366	102,283	0	0,0237	0,3682	0,082	0	2,0224	0	104,8189	EMI391-R2-3	Rutile
245	0	0,0021	0,1417	0	8,6865	0,7207	30,1729	0,0008	21,3739	0,027	38,8206	99,9462	EMI391-G4-1	Gamet

246	0	0	0,185	0,0197	8,6211	0,6778	30,4125	0	21,5722	0,0047	39,213	100,706	EMI391-C4-2	Garnet	
247	0	0,0028	0,2717	0,1254	8,7805	0,7642	30,0625	0	21,6407	0,0196	39,0922	100,7596	EMI391-C4-3	Garnet	
248	0,0093	0,0073	0,1502	0,0231	8,7496	0,744	30,2974	0,0218	21,7388	0,0271	39,2736	101,0422	EMI391-C4-4	Garnet	
249	0	0,0104	0,2091	0	8,6428	0,7715	30,1554	0,0468	21,7511	0,0711	39,5769	101,2351	EMI391-C4-5	Garnet	
250	0,022	0	0,0524	42,0005	0	26,8097	1,4062	0,0514	0,8363	0,8967	28,4194	100,4946	EMI391-T2-1	Titanite	
251	0	0	0,0471	40,817	0	26,8462	3,3011	0,0264	0,9431	0,746	28,4733	101,2002	EMI391-T2-2	Titanite	
252	0,0109	0,0015	0,0472	49,5062	0	18,6748	11,3366	0	0,8487	1,131	20,4842	102,0411	EMI391-T2-3	Titanite	
253	0	0,0058	0	41,6588	0,0062	27,7727	0,543	0,0142	0,7804	0,9552	29,5012	101,1875	EMI391-T2-4	Titanite	
254	0,0144	0,0165	0,0597	35,7754	0	28,7913	0,7479	0,0753	3,0759	0,7695	30,7779	100,1038	EMI391-T3-1	Titanite	
255	0,0367	0,0086	0,0775	36,0803	0	28,6583	0,7563	0,0297	3,0148	0,7836	30,3559	100,3048	EMI391-T3-2	Titanite	
256	0	0,0155	0,0433	37,4078	0	28,1223	0,7319	0	2,8229	0,7558	30,0301	99,9296	EMI391-T3-3	Titanite	
257	0	0,0037	0,021	35,4436	0	28,0051	0,7641	0	2,9995	0,7914	30,9397	99,2681	EMI391-T3-4	Titanite	
258	0	0,0053	0,0749	0,1291	0,0338	23,0011	9,2804	0	24,4271	0,0139	38,0529	95,0245	EMI391-G5-1	Garnet	
259	0	0,0001	0,1528	0,0716	0,0138	23,1929	9,5615	0	24,3833	0,0746	37,9154	95,366	EMI391-G5-2	Garnet	
260	0	0	0,1316	0,1251	0	23,1245	9,6009	0	24,4628	0,0678	38,0773	95,59	EMI391-G5-3	Garnet	
261	0,029	0,0152	0,1107	0,0921	0,0187	23,5414	9,3439	0,0277	24,5918	0,0541	38,3727	96,1973	EMI391-G5-4	Garnet	
262	0	0,0072	0,0219	102,4966	0	0,0144	0,1872	0,1572	0,0145	2,2111	0	105,1101	EMI391-R3-1	Rutile	
263	0,011	0	0,027	101,9242	0	0,0233	0,1601	0,2238	0,0411	2,2227	0	104,6332	EMI391-R3-2	Rutile	
264	0,0086	0	0,0208	0	101,9361	0	0,0228	0,1285	0,1694	0,0442	2,2561	0	104,5865	EMI391-R3-3	Rutile
265	0,0144	0	6,0909	0,0525	0,5821	9,7743	24,8062	0,024	19,8092	0,0585	36,9855	98,1976	EMI391-A2-1	Amphibole	
266	0,0862	0,0151	0	6,0949	0,0501	0,5402	10,0323	24,8483	0,0253	19,7677	0	37,1773	98,6734	EMI391-A2-2	Amphibole
267	0,0489	0,0059	6,0647	0	0,5997	9,9735	25,1641	0,0171	20,0093	0,0114	37,1483	99,0429	EMI391-A2-3	Amphibole	
268	0,0635	0	5,8417	0,0566	0,5544	9,9854	24,6971	0,1022	19,9495	0,056	37,3771	98,6835	EMI391-A2-4	Amphibole	
269	0,0643	0	5,8492	0,0625	0,5595	10,3144	24,5687	0	20,0183	0,0313	37,2625	98,7307	EMI391-A2-5	Amphibole	
270	0	0,0129	5,8734	0	0,6028	10,2729	25,1701	0	19,5556	0,0066	37,4497	98,9444	EMI391-A2-6	Amphibole	
271	0	0,0072	0	101,7337	0	0,0307	0,3297	0,059	0,0113	2,1223	0	104,2939	EMI391-R4-1	Rutile	
272	0	0	0,0117	101,8806	0	0,025	0,2085	0,0643	0,0316	2,1365	0	104,3582	EMI391-R4-2	Rutile	
273	0	0	0	101,1664	0	0,0061	0,2461	0,0313	0	2,2522	0	103,7021	EMI391-R4-3	Rutile	
274	0	0,0106	0,0662	36,7097	0	28,0409	1,1451	0,0242	1,6004	0,7638	30,0318	98,3927	EMI391-T4-1	Titanite	
275	0	0	0,0569	36,8391	0	27,853	1,1549	0,03	1,5718	0,7955	30,1082	98,4094	EMI391-T4-2	Titanite	
276	0,0023	0,0103	0,0238	37,4412	0	27,9811	0,9689	0	1,5566	0,7663	30,1434	98,8939	EMI391-T4-3	Titanite	
277	0	0	0,0992	37,0969	0	28,327	1,0409	0,0058	1,6149	0,8264	30,5801	99,5912	EMI391-T4-4	Titanite	
278	0,0495	0,0034	0,3529	0	6,8985	1,3522	31,023	0,0232	21,3669	0,0288	38,0456	99,138	EMI391-C6-1	Garnet	
279	0,0102	0,0064	0,3385	0,0306	6,8888	1,3652	31,1833	0,0563	21,1687	0,0353	38,1694	99,2527	EMI391-C6-2	Garnet	
280	0,0497	0,0043	0,3932	0,0191	6,9416	1,3678	31,3686	0,1071	21,3276	0	38,4012	99,9802	EMI391-C6-3	Garnet	
281	0,0258	0,0111	0,3722	0,0363	7,0648	1,3271	31,3474	0,0711	21,3329	0,0714	38,4723	100,1324	EMI391-C6-4	Garnet	
282	0,0112	0,0058	0,3594	0,0048	6,9027	1,333	31,0574	0,0526	21,2676	0,0056	38,4954	99,4955	EMI391-C6-5	Garnet	

283	0,0355	0	0,0405	101,3348	0	0,0215	0,2048	0,1144	0,0714	2,347	0,0355	104,2054	EMI391-R5-1	Rutile
284	0	0,0023	0,0128	101,8763	0	0,0109	0,1539	0,0597	0,0548	2,2923	0	104,463	EMI391-R5-2	Rutile
285	0	0,01	0,0238	101,6204	0	0,0142	0,1415	0,1152	0,0556	2,3045	0	104,2852	EMI391-R5-3	Rutile
286	0,0126	0,0119	0	102,4145	0	0,0072	0,0684	0,0559	0	2,297	0	104,8675	EMI391-R5-4	Rutile
287	0,0284	0,0132	0,0595	11,7028	0	0,013	79,3357	0,0752	0,0175	0,5648	0	91,8101	EMI391-M5-1	Magnetite
288	0,0136	0	0,1142	10,7411	0	0,0036	80,1143	0,0813	0	0,4913	0,0503	91,6097	EMI391-M5-2	Magnetite
289	0	0	0,4178	12,4443	0	0,0074	78,0781	0,0576	0,013	0,5978	0	91,6147	EMI391-M5-3	Magnetite
290	0	0	0,0463	11,4239	0	0,0126	79,963	0,0228	0	0,4381	0	91,9067	EMI391-M5-4	Magnetite
291	0,0127	0	0,5533	0,0679	8,4371	6,9423	22,9111	0,1011	21,2509	0,0153	39,0487	99,3404	EMI391-G7-1	Garnet
292	0,0554	0,0109	0,6268	0,12	8,4633	6,9355	22,885	0,046	21,3991	0	39,1666	99,7086	EMI391-G7-2	Garnet
293	0	0	0,5242	0,0376	8,4577	7,05	22,5405	0,0417	21,4577	0,0067	39,5334	99,6995	EMI391-G7-3	Garnet
294	0,0282	0	0,5269	0,0361	8,3243	6,9698	23,0679	0,0656	21,434	0	39,6594	100,1422	EMI391-G7-4	Garnet
295	0,0254	0	0	44,1213	0	24,5505	1,8087	0	1,2024	0,9302	26,8951	99,4836	EMI391-T5-1	Titanite
296	0,1224	0	0,1034	68,3984	0,0153	9,5792	6,9834	0	0,6106	1,3589	10,3255	97,4971	EMI391-T5-2	Titanite
297	0	0	0,0052	100,4084	0	0,3341	0,4019	0,1197	0,0113	2,0895	0,1146	103,4847	EMI391-T5-3	Titanite
298	0	0	0,0258	102,0019	0	0,4062	0,3325	0,0377	0,0378	2,1191	0	104,961	EMI391-T5-4	Titanite
299	0,0016	0	0,0119	37,0881	0	28,4814	0,2341	0	2,6118	0,8907	30,7502	100,076	EMI391-T5-5	Titanite
300	0	0	0,031	101,1652	0	0,0101	0,4777	0,0593	0,0297	2,1961	0,0331	104,0022	EMI391-R6-1	Rutile
301	0	0	0	100,9581	0	0,0031	0,4545	0,0233	0,0037	2,2028	0	103,6455	EMI391-R6-2	Rutile
302	0,0086	0	0,0175	101,3663	0	0,0324	0,5038	0,0799	0,0371	2,2358	0,0184	104,2998	EMI391-R6-3	Rutile
303	0	0,0122	0,0129	101,5042	0	0,0133	0,4437	0	0,0347	2,2071	0	104,2281	EMI391-R6-4	Rutile
304	0,0141	0,0058	0,6539	0,0548	4,4325	1,0552	34,7255	0,0402	20,8758	0,0364	37,5889	99,4831	EMI391-G8-1	Garnet
305	0	0	0,7029	0,0077	4,3973	1,0821	34,6836	0,0664	20,8609	0	37,8441	99,645	EMI391-G8-2	Garnet
306	0,0488	0	0,6019	0	4,4287	1,0731	34,8757	0	20,9733	0,046	37,9797	100,0272	EMI391-G8-3	Garnet
307	0	0,0186	0,6613	0,0688	4,3731	1,1551	35,1404	0,0555	21,0322	0	38,2232	100,7282	EMI391-G8-4	Garnet
308	0,0074	0	0,5601	0,0777	8,0946	2,6238	27,7807	0,035	21,4484	0,0459	38,8106	99,4842	EMI391-G9-1	Garnet
309	0	0,0175	0,5194	0,0679	8,2066	2,5855	27,9284	0,0281	21,7081	0	39,0995	100,1611	EMI391-G9-2	Garnet
310	0	0	0,5197	0	8,2256	2,5617	28,0028	0,1393	21,6087	0,0977	39,1074	100,2429	EMI391-G9-3	Garnet
311	0,0085	0,0063	0,5103	0	8,1814	2,5666	27,9823	0,0459	21,5953	0	39,2406	100,1372	EMI391-G9-4	Garnet
312	0,0087	0,0071	3,1992	0,0067	1,6786	2,1037	34,8976	0,0682	20,3703	0,0474	36,8337	99,2212	EMI391-G10-1	Garnet
313	0	0	3,2373	0	1,6786	2,1119	34,9174	0	20,6803	0	37,2029	99,8284	EMI391-G10-2	Garnet
314	0,019	0	3,2622	0	1,6494	2,357	34,7816	0	20,6879	0,0307	37,2529	100,0407	EMI391-G10-3	Garnet
315	0,0072	0,0054	3,3626	0,0451	1,5751	1,749	34,9379	0,0492	20,5032	0	37,2911	99,5258	EMI391-G10-4	Garnet

No.	Na ₂ O	K ₂ O	MnO	TiO ₂	MgO	CaO	FeO	Cr ₂ O ₃	Al ₂ O ₃	V ₂ O ₃	SiO ₂	Total	Comment
No.	Na ₂ O	K ₂ O	MnO	TiO ₂	MgO	CaO	FeO	Cr ₂ O ₃	Al ₂ O ₃	V ₂ O ₃	SiO ₂	Total	Comment
1	0	0.0063	0.5634	0.0735	10.4327	4.0535	23.1979	0	21.6266	0.017	39.3496	99.3205	alinstart1
2	0.0052	0.003	0.5874	0.0138	10.5444	4.0895	23.5473	0	21.741	0.0206	39.6474	100.1996	alinstart2
3	0	0	0.0025	0.0265	18.6408	25.7123	0.0051	0.0209	0.0098	0.0693	54.8865	99.3737	diospsstar1
4	0.0192	0.008	0.0232	0.1173	18.524	25.7264	0.0014	0	0	0	53.6419	98.0614	diospsstar2
	Na ₂ O	K ₂ O	MnO	TiO ₂	MgO	CaO	FeO	Cr ₂ O ₃	Al ₂ O ₃	V ₂ O ₃	SiO ₂	Total	Comment
	Matchless Zf												Mineral
5	0.0054	0.0029	0.0709	36.8458	0	28.7861	0.2432	0.017	2.3004	0.6465	30.3016	99.2198	L-ZFM-T1-1
6	0	0	0.0193	37.3821	0	29.0534	0.2152	0	2.244	0.6005	30.6241	100.1386	L-ZFM-T1-2
7	0	0.0077	0.0412	38.5194	0	28.6366	0.3758	0	1.5729	0.7749	30.3268	100.2553	L-ZFM-T2-1
8	0	0	0.0502	37.7761	0	28.6933	0.4402	0	1.6438	0.787	30.4113	99.8019	L-ZFM-T2-2
9	0.0301	0	0.0735	37.6226	0	28.8772	0.5142	0	1.5368	0.7319	30.5762	99.9625	L-ZFM-T2-3
10	0	0.0005	0.066	36.2651	0	29.0299	0.203	0	2.6062	0.575	30.4674	99.2131	L-ZFM-T3-1
11	0.0141	0.0105	0.0819	36.9076	0	28.826	0.1881	0.0297	2.3712	0.6025	30.8113	99.8429	L-ZFM-T3-2
12	0	0.0075	0.0348	37.6512	0	28.8479	0.1536	0	1.6843	0.7282	30.5703	99.6778	L-ZFM-T4-1
13	0	0.0102	0.034	37.5559	0	28.7835	0.1848	0.0084	1.7781	0.6722	30.0616	99.0918	L-ZFM-T4-2
14	0	0	0.0431	37.2699	0	28.8619	0.2418	0	2.3503	0.5563	30.7744	100.0977	L-ZFM-T5-1
15	0	0.0011	0.0279	36.9464	0	28.9511	0.2371	0	2.2658	0.6111	30.9339	99.9744	L-ZFM-T5-2
16	0.03	0	0.0518	37.6025	0	29.0222	0.2015	0.0157	2.132	0.6181	30.6697	100.3435	L-ZFM-T5-3
17	0	0	0.0426	37.1622	0	28.8501	0.2615	0.0455	2.2794	0.7619	30.1938	99.597	L-ZFM-T6-1
18	0.0184	0	0.0798	37.0783	0	28.9982	0.2255	0.0022	2.2823	0.6522	30.2057	99.5426	L-ZFM-T6-2
19	0.0403	0.0093	0.0153	37.2167	0	28.2667	0.225	0.0224	2.3362	0.5193	30.5916	99.2428	L-ZFM-T6-3
20	0.0156	0.0144	0.037	37.1301	0	28.3425	0.2541	0.0161	2.322	0.6147	30.5646	99.3111	L-ZFM-T6-4
21	0	0.0017	0.115	37.2247	0	28.9203	0.2418	0	2.2914	0.6522	30.5597	100.0568	L-ZFM-T7-1
22	0.0103	0.0103	0.0521	36.9712	0	28.2903	0.1817	0.0575	2.1902	0.6855	30.2047	98.6538	L-ZFM-T7-2
23	0	0	0.0706	36.8819	0	27.5295	0.1665	0.0049	2.1558	0.6553	30.7477	98.2122	L-ZFM-T7-3
24	0	0.0069	0.018	100.109	0	0.0263	0.4884	0	0.1088	1.685	0	102.4424	L-ZFM-R1-1
25	0.0091	0.0047	0.007	99.7459	0	0.0209	0.5875	0.0139	0.0082	1.7762	0	102.1734	L-ZFM-R1-2
26	0	0	0.0241	99.6007	0	0.0138	0.5184	0.069	0.0066	1.7807	0.0647	102.1374	L-ZFM-R1-3
27	0	0	0	98.6642	0	0.0149	0.726	0.0395	0.0465	1.8387	0	101.3298	Rutile
28	0.0535	0	0	100.4002	0	0.0217	0.4659	0.0149	0.0917	1.6468	0	102.6947	L-ZFM-R1-5
													take TiO ₂ as the sum, or subtract V ₂ O ₃
													take V ₂ O ₃ as the sum, or subtract TiO ₂
													take V ₂ O ₃ as the sum, or subtract Al ₂ O ₃
													take Al ₂ O ₃ as the sum, or subtract V ₂ O ₃

29	0,0131	0	0	100,1384	0	0,007	0,3994	0	0,0799	1,7704	0	102,4082	L-ZfM-R1-6	Rutile	take TiO2 as the sum, or subtract V203
30	0,0039	0,0093	0,0414	37,1997	0	28,8687	0,1679	0,0215	2,1918	0,7604	30,4417	99,7063	L-ZfM-T8-1	Titanite	
31	0	0,0049	0,0279	37,2028	0	28,7931	0,1873	0,0416	2,1213	0,7289	30,469	99,5768	L-ZfM-T8-2	Titanite	
32	0	0	0,0556	36,577	0	28,3481	0,2033	0	2,2013	0,7612	30,1548	98,3013	L-ZfM-T8-3	Titanite	
33	0,0225	0	0,127	36,9545	0	28,3314	0,2415	0,0295	2,2686	0,7044	30,5533	99,4327	L-ZfM-T8-4	Titanite	
34	0,0173	0	0,0593	36,6024	0	28,6847	0,2729	0,0102	2,3548	0,5423	30,0141	98,558	L-ZfM-T9-1	Titanite	
35	0	0,01	0,0898	36,4803	0,0029	28,8336	0,2121	0	2,4852	0,5318	30,2192	98,8649	L-ZfM-T9-2	Titanite	
36	0,0346	0	0,0105	36,9593	0	28,7538	0,2646	0,0031	2,4647	0,6617	30,2849	99,4172	L-ZfM-T9-3	Titanite	
37	0,0548	0,0034	0,0966	36,759	0	29,0051	0,1514	0	2,3955	0,5488	30,3782	99,3928	L-ZfM-T9-4	Titanite	
38	0	0	0,0682	36,8265	0	28,873	0,2084	0,0253	2,5769	0,5812	30,6194	99,7789	L-ZfM-T9-5	Titanite	
39	0	0	0,0669	37,1121	0	27,8874	0,2768	0,0417	2,5116	0,5533	31,2103	99,6601	L-ZfM-T9-6	Titanite	
40	0	0	0,0647	33,7047	0	26,2871	0,14	0	2,144	0,5457	37,8284	100,7146	L-ZfM-T9-7	Titanite	
41	0	0,0026	0,0527	36,7756	0	28,8889	0,2618	0,0432	2,2196	0,5692	31,807	100,6206	L-ZfM-T10-1	Titanite	
42	0,0366	0	0,0507	37,1757	0	29,2891	0,1989	0	2,3788	0,6315	31,8046	101,5659	L-ZfM-T10-2	Titanite	
43	0,0093	0	0,0305	36,6489	0	27,8627	0,1815	0,039	2,2513	0,6087	30,7116	98,3435	L-ZfM-T11-1	Titanite	
44	0,0004	0	0,0292	36,8709	0	28,691	0,1783	0	2,2974	0,5468	29,7621	98,3761	L-ZfM-T11-2	Titanite	
45	0,0173	0,0101	0,0689	36,6763	0	28,9951	0,2875	0,0143	2,4044	0,5418	30,3708	99,3865	L-ZfM-T11-3	Titanite	
46	0,011	0,0074	0,1412	36,6245	0	28,6325	0,2535	0	2,2973	0,5455	30,3016	98,8145	L-ZfM-T11-4	Titanite	
47	0	0,0047	0	99,726	0	0,0214	0,4401	0,0206	0,0838	1,6655	0	101,9621	L-ZfM-R2-1	Rutile	take TiO2 as the sum, or subtract V203
48	0	0,0095	0	100,4917	0	0,0363	0,4827	0,0691	0,0507	1,7294	0	102,8694	L-ZfM-R2-2	Rutile	take TiO2 as the sum, or subtract V203
49	0	0	0,0042	99,9134	0	0,0241	0,3861	0,0561	0,0035	1,7099	0	102,0973	L-ZfM-R2-3	Rutile	take TiO2 as the sum, or subtract V203
50	0	0,0102	0,0133	99,5639	0	0,0199	0,6294	0,0618	0,0786	1,655	0	102,0321	L-ZfM-R2-4	Rutile	take TiO2 as the sum, or subtract V203
51	0	0,0095	0,0477	37,4589	0	28,8845	0,1799	0,0368	2,0777	0,6798	30,9209	100,2957	L-ZfM-T12-1	Titanite	
52	0	0,0081	0,1097	37,0832	0	28,978	0,2669	0,0041	2,182	0,5975	30,8414	100,0709	L-ZfM-T12-2	Titanite	
53	0,0068	0	0,0746	36,2812	0	28,1944	0,2744	0,0119	2,0467	0,6621	32,907	100,4591	L-ZfM-T12-3	Titanite	
Auburez Zf															
54	0	0,0061	0,0042	99,5202	0	0,0408	0,181	0,1687	0,0492	1,7315	0,029	101,7307	L-ZfA-R1-1	Rutile	take TiO2 as the sum, or subtract V203
55	0	0,0216	0,0215	99,6572	0	0,0323	0,1056	0,0374	0,0914	1,6352	0	101,6022	L-ZfA-R1-2	Rutile	take TiO2 as the sum, or subtract V203
56	0	0	0	100,6474	0	0,024	0,1785	0	0,0253	1,5514	0,0262	102,4528	L-ZfA-R2-1	Rutile	take TiO2 as the sum, or subtract V203
57	0,0256	0,0001	0,0071	101,4381	0	0,0286	0,1488	0,0424	0,0241	1,668	0	103,3828	L-ZfA-R2-2	Rutile	take TiO2 as the sum, or subtract V203
58	0	0	0,0219	100,8937	0,0026	0,0247	0,0877	0,0185	0,0475	1,598	0	102,6946	L-ZfA-R2-3	Rutile	take TiO2 as the sum, or subtract V203
59	0,0271	0	0,0362	37,2775	0	28,9201	0,8685	0	1,5665	0,8172	30,6217	100,1348	L-ZfA-T1-1	Titanite	
60	0	0,0098	0,0487	37,2676	0	28,8451	0,9153	0	1,5329	0,7472	30,7253	100,0919	L-ZfA-T1-2	Titanite	

61	0	0	0,0518	70,442	0	0,3744	24,5519	0,0449	0,3266	1,184	1,0039	97,9795	L-ZfA-T2-1	Ilmenite?
62	0	0,0039	0,0843	61,0022	0,1968	0,2931	29,488	0,0369	0,8322	0,9508	2,9455	95,8337	L-ZfA-T2-2	Ilmenite?
63	0	0,0076	0,0795	63,8645	0,0293	0,4609	29,9002	0	0,293	1,1172	0,8182	96,5704	L-ZfA-T2-3	Ilmenite?
64	0	0,0221	0,0327	70,9024	0,167	0,3428	22,5636	0	0,7248	1,2318	3,5576	99,5448	L-ZfA-T2-4	Ilmenite?
65	0,0353	0,0068	0,03	38,6324	0	28,3269	0,5893	0	1,0377	0,7135	30,2168	99,5887	L-ZfA-T3-1	Titanite
66	0,0338	0,0098	0,0006	38,5345	0	27,7326	0,5721	0,0601	1,1069	0,6429	30,0219	98,7152	L-ZfA-T3-2	Titanite
67	0,0148	0,0117	0,0861	37,7855	0	28,3354	0,6972	0,0664	1,3225	0,7537	30,4637	99,5337	L-ZfA-T3-3	Titanite
68	0	0,0105	0,0818	37,9273	0	28,1032	0,5287	0	1,216	0,699	30,119	98,7565	L-ZfA-T3-4	Titanite
69	0,0269	0	0,0404	34,5422	0	26,4967	0,8881	0,0374	1,1941	0,6897	25,0377	88,9532	L-ZfA-T4-1	Titanite
70	0,0045	0,0181	0,0707	35,4248	0	28,2851	1,3787	0	2,1005	0,7471	31,0299	99,0594	L-ZfA-T4-2	Titanite
71	0,0093	0,0068	0,0517	34,6907	0	27,5604	1,6445	0	2,3545	0,7372	30,3625	97,4176	L-ZfA-T4-3	Titanite
72	0	0,0031	0,0472	36,3117	0	28,5709	0,9753	0,0097	2,3614	0,6892	30,3475	99,3213	L-ZfA-T5-1	Titanite
73	0	0,0033	0,0438	36,1285	0	28,7083	0,9039	0,0475	2,366	0,6878	30,5556	99,4451	L-ZfA-T5-2	Titanite
74	0	0	0,0506	35,4387	0	28,9776	0,9484	0,054	2,3914	0,6438	30,6299	99,1344	L-ZfA-T5-3	Titanite
75	0,0004	0,0074	0,0338	38,0659	0	28,0863	0,4082	0,0252	0,9755	0,5879	29,3221	97,5127	L-ZfA-T6-1	Titanite
76	0,0039	0,005	0,0723	39,2233	0	28,1412	0,435	0	1,0203	0,6605	30,0363	99,5978	L-ZfA-T6-2	Titanite
77	0	0	0,0459	38,3042	0	28,1931	0,444	0	1,0453	0,6439	31,1088	99,7852	L-ZfA-T6-3	Titanite
78	0,0189	0,0023	0	99,9015	0	0,0307	0,087	0,0382	0,0319	1,8554	0	101,9659	L-ZfA-R2-1	Rutile
79	0,0256	0,0021	0,0331	99,5614	0	0,0222	0,0776	0	0,0199	1,7253	0	101,4672	L-ZfA-R2-2	Rutile
80	0	0	0	100,7336	0	0,0172	0,0757	0,0696	0,0117	1,6438	0	102,5516	L-ZfA-R2-3	Rutile
81	0	0,0073	0,0011	100,9266	0	0,0247	0,0822	0,0421	0,0493	1,6505	0	102,7838	L-ZfA-R2-4	Rutile
82	0,1336	0,0417	0,0061	92,934	0,1221	0,2106	0,7463	0	0,6727	1,4998	2,4332	98,8051	L-ZfA-R3-1	Rutile
83	0	0,036	0,0006	100,5084	0	0,0511	0,0708	0,0485	0,0298	1,6437	0,0653	102,4542	L-ZfA-R3-2	Rutile
84	0	0,0145	0,0422	100,5546	0	0,0421	0,0568	0,0162	0,0617	1,6034	0	102,4315	L-ZfA-R3-3	Rutile
85	0	0	0,0509	38,866	0	28,314	0,5907	0,0057	0,631	0,8457	30,185	99,4489	L-ZfA-T7-1	Titanite
86	0	0	0,0514	39,2405	0	28,6499	0,4089	0,0825	0,8351	0,7029	30,4838	100,4454	L-ZfA-T7-2	Titanite
87	0	0,0018	0,0505	39,2985	0	28,8273	0,3743	0,076	0,7982	0,7098	30,287	100,4234	L-ZfA-T7-3	Titanite
89	0,0289	0,0127	0	98,8346	0	0,2204	0,4362	0,032	0,0883	1,7515	0,6666	101,4712	L-ZfA-R4-2	Rutile
90	0	0	0	0,5366	0	0,5649	0,0102	0	0,0374	0,0161	0,8701	2,0353	L-ZfA-T8-1	Titanite
91	0	0,0042	0,0677	38,1948	0	28,6693	0,5507	0	1,3309	0,7249	30,3607	99,9032	L-ZfA-T8-2	Titanite
92	0,0284	0,0007	0,0375	38,0255	0	28,7	0,6811	0,0363	1,2905	0,6731	30,4764	99,9495	L-ZfA-T8-3	Titanite

Klein Aub Mf

93	0,0419	0	0,0257	30,7041	0,0135	31,8009	1,4616	0	3,6694	0,5826	21,0283	89,3228	B-A-MfS-T1-1	Titanite	
94	0	0,0254	0,0816	40,0994	0,7412	22,5237	4,0951	0,0075	4,3528	0,7172	26,044	98,6925	B-A-MfS-T1-2	Titanite	
95	1,9643	0,0426	0,1029	1,0091	2,655	0,2243	11,5558	0	32,6812	0,0809	35,1469	85,443	B-A-MfS-Tul-1	Tourmaline	Tur-add 10.5 wt% B2O3
96	2,0749	0,0575	0,0989	0,9874	2,9381	0,2173	11,3669	0,0011	32,8294	0,0124	35,0606	85,6445	B-A-MfS-Tul-2	Tourmaline	Tur-add 10.5 wt% B2O3
97	0,0204	0,0073	0,0154	43,0894	0	19,8332	10,6162	0	3,0074	0,8231	21,4464	98,8488	B-A-MfS-T2-1	Titanite	
98	0	0	0,0028	33,5609	0	23,8552	10,6642	0,0425	3,6005	0,5903	25,7636	98,08	B-A-MfS-T2-2	Titanite	
99	0,0339	0	0,0094	46,1405	0	21,6942	4,4424	0	2,9581	0,905	23,486	99,6695	B-A-MfS-T2-3	Titanite	
100	0	0	0,0541	0,1983	0	0,0148	88,5227	0,0272	0,0875	0,1464	0,0984	89,1494	B-A-MfS-M1-1	Magnetite	
101	0	0	0,0492	0,2265	0	0,0229	88,2668	0,0438	0,0473	0,2541	0,0481	88,9599	B-A-MfS-M1-2	Magnetite	
102	0	0,2462	0,0703	16,5918	0,0874	0,0691	69,7933	0,073	1,1995	1,2433	1,5501	90,9224	B-A-MfS-M2-1	Magnetite	
103	0,0885	0,0156	0,0327	11,5491	0	0,0738	76,3852	0,013	0,3402	1,28	0,3508	90,1289	B-A-MfS-M2-2	Magnetite	
104	0	0,0849	0,0612	61,0796	0,1954	0,1312	31,3595	0	0,5181	1,1073	0,974	95,5112	B-A-MfS-M11-1	Ilmenite	
105	0,0034	0	0,119	35,2775	0	0,0399	59,3372	0	0	0,6666	0,0594	95,503	B-A-MfS-M11-2	Ilmenite	
106	0	0,0113	0,0249	63,4357	0	0,0182	30,5691	0,0039	0,047	1,2954	0,1724	95,6679	B-A-MfS-M11-3	Ilmenite	
107	0	0,0204	0,0778	5,9512	0,0341	0,0358	82,6847	0,066	0,3951	0,4166	0,3573	90,039	B-A-MfS-M12-1	too many FeO for ilmenite, maybe titanio-magnetite or titanio-hematite	
108	0,0173	0,2847	0,0519	4,09	1,4044	0,1104	78,7809	0	2,2772	0,4209	3,4082	90,8407	B-A-MfS-M12-2	too many FeO for ilmenite, maybe titanio-magnetite or titanio-hematite	
109	0,0581	0,0994	0,0822	6,0138	0	0,0643	80,927	0,036	0,681	0,3835	0,7724	89,1177	B-A-MfS-M12-3	too many FeO for ilmenite, maybe titanio-magnetite or titanio-hematite	
110	0	0	0,1006	10,6142	0	0,0617	77,3716	0,0998	0,7503	0,4393	0,1403	89,5778	B-A-MfS-M12-4	too many FeO for ilmenite, maybe titanio-magnetite or titanio-hematite	
111	0	0	0,071	37,8502	0	28,0675	0,6985	0	1,2368	0,62	30,1826	98,7266	B-A-MfS-T3-1	Titanite	
112	0	0,0382	0,1104	37,4689	0	28,0985	0,8805	0	1,2873	0,6762	30,0088	98,5688	B-A-MfS-T3-2	Titanite	
113	0,0358	0,2599	0,3574	2,4631	0,0598	0,0887	73,4121	0,0083	0,6033	0,0752	2,7911	80,1547	B-A-MfS-M3-1	Magnetite	
114	0	0,7545	0,0517	17,4735	0,4449	0,0547	66,6665	0	3,1531	0,3196	4,1764	93,0949	B-A-MfS-M3-2	Magnetite	
115	0	0,6713	0,0411	8,1968	0,2796	4,2503	68,6948	0	2,9277	0,2255	8,3008	93,5879	B-A-MfS-M3-3	Magnetite	
116	0	0,3033	0,0199	8,6174	0	4,612	69,1148	0	1,3075	0,2493	6,5194	90,7436	B-A-MfS-M3-4	Magnetite	
117	0,0416	0,023	0,0225	46,3789	0,0707	15,3694	3,3193	0	1,35	1,0218	16,661	84,2582	B-A-MfS-T4-1	Titanite	
118	0	0,0047	0,0737	37,2167	0	27,7838	1,5597	0	1,0342	0,6921	29,9086	98,2735	B-A-MfS-T4-2	Titanite	
119	2,4448	0,7492	0,0677	0,9181	6,0079	0,7626	12,5469	0,0223	27,71697	0,0558	37,5558	88,3062	B-A-MfS-Tu2-1	Tourmaline	
122	0,0103	0,0276	0	35,7949	0,5418	23,4595	5,4495	0,1191	4,5989	0,8367	27,1238	97,9621	B-A-MfS-T5-2	Titanite	
124	0,0097	0,0175	0,0734	31,2884	0	0,0643	59,6097	0	0,0983	0,6379	0,7775	92,5767	B-A-MfS-M5-2	Magnetite	
125	0,0174	0,0138	0,2199	34,5828	0	0,0558	57,232	0	0	0,64	0,159	92,9207	B-A-MfS-M5-3	Magnetite	
129	0,031	0,157	0,0124	33,385	0,0919	26,6632	1,2093	0,0325	2,7594	0,7037	34,2657	99,3111	B-A-MfS-T6-2	Titanite	
130	0	0,2698	0,1955	33,7516	0,0573	28,292	1,8673	0	3,0604	0,6232	30,8787	98,9958	B-A-MfS-T6-3	Titanite	

131	0,117	0,0821	0,0884	1,051	0,0685	0,1401	83,4692	0,0498	0,6588	0,0486	2,018	87,7915	B-A-MIS-M6-1	Magnetite
132	0,0065	0,5481	0,1147	0,9953	0,1244	0,0758	81,5237	0,1094	1,5709	0,0636	3,7381	88,8705	B-A-MIS-M6-2	Magnetite
133	0,0613	0,0735	0,0661	1,0227	0,1262	0,1089	83,8198	0	0,5857	0,0537	2,4283	88,3462	B-A-MIS-M6-3	Magnetite
134	0	0,06	0,048	2,6259	0	0,0546	85,5286	0	0,2408	0,3024	0,6432	89,5035	B-A-MIS-M7-1	Magnetite
135	0,0088	0,3458	0,0935	3,3	0,2114	0,0497	81,5454	0	1,4263	0,5628	2,1279	89,6716	B-A-MIS-M7-2	Magnetite
136	0,0505	0,081	0,1351	2,4938	0,8577	0,1063	83,9817	0,0873	0,8559	0,239	1,6838	90,5741	B-A-MIS-M8-1	Magnetite
137	0	0,0132	0,043	6,7978	0,076	0,0787	80,6488	0,4489	0,7122	0,5792	0,3211	89,7189	B-A-MIS-M8-2	Magnetite
138	0,0549	0,0119	0,0728	11,0522	0,0328	0,0583	75,0695	0,3131	1,668	0,8076	0,2883	89,4294	B-A-MIS-M8-3	Magnetite
139	0	0,0078	0,0225	78,9629	0	7,7387	1,3734	0	0,2054	1,5751	7,4263	97,3121	B-A-MIS-M7-1	Titanite
140	0	0,0124	0	61,5541	0	17,953	0,9343	0,0337	0,2974	1,1246	19,2092	101,1187	B-A-MIS-M7-2	Titanite
141	0,0419	0	0,0098	82,8455	0	8,4004	1,0444	0,0409	0,2311	1,7292	8,5774	102,9206	B-A-MIS-M7-3	Titanite
142	0	0	0,0305	66,1089	0	13,7658	4,11	0,0671	0,2932	1,2335	14,8519	100,4609	B-A-MIS-M7-4	Titanite
143	2,5602	0,0449	0,2424	0,373	0,3761	0,0517	16,2767	0	30,4881	0,0108	34,9325	85,3564	B-A-MIS-M7-5	Tourmaline
144	2,6163	0,0686	0,2272	0,369	0,3084	0,0322	16,4184	0,0384	30,6281	0,0555	34,9148	85,6769	B-A-MIS-M7-6	Tourmaline
145	2,5427	0,0611	0,2191	0,3182	0,3481	0,0514	16,5896	0	30,6558	0,0018	35,1743	85,9621	B-A-MIS-M7-3	Tourmaline
146	2,5564	0,0789	0,2459	0,277	0,3043	0,0328	16,432	0	30,6305	0	34,9213	85,4881	B-A-MIS-M7-4	Tourmaline
147	1,8853	0,0038	0,051	0,3	8,981	1,4122	3,9487	0,0695	31,1363	0,0424	36,7912	84,6214	B-A-MIS-M7-4	Tourmaline
148	1,8844	0,0108	0	0,3562	8,4615	1,3868	3,8875	0,0333	31,9523	0,0198	36,6687	84,6613	B-A-MIS-M7-4	Tourmaline
149	1,8807	0,0036	0,0171	0,291	8,4147	1,364	3,9629	0,05	31,8173	0	36,7009	84,5022	B-A-MIS-M7-4	Tourmaline
150	2,0293	0,0024	0	0,1006	8,64	1,1862	3,7008	0,0726	32,0664	0	36,7703	84,5686	B-A-MIS-M7-4	Tourmaline
151	1,9575	0,0156	0,0118	0,4385	8,8723	1,3367	4,0651	0,0444	31,2181	0	36,8841	84,8441	B-A-MIS-M7-4	Tourmaline
152	1,9478	0,0008	0,0117	0,3082	8,6095	1,335	3,9989	0,0152	31,8356	0	36,7406	84,8183	B-A-MIS-M7-4	Tourmaline
153	1,9692	0,0006	0,0176	0,2903	8,8413	1,2997	3,8652	0,0643	30,9301	0,0392	36,6	83,9229	B-A-MIS-M7-4	Tourmaline
154	0,0051	0	0,0369	0,5159	0	0,0455	87,8584	0	0,0013	0,0578	0,1946	88,7175	B-A-MIS-M9-1	Magnetite
155	0,0988	0,0087	0,1036	0,4494	0	0,0402	88,1359	0,0031	0	0,0731	0,2215	89,1343	B-A-MIS-M9-2	Magnetite
156	0,0581	0,0098	0	1,6299	0	0,0231	87,5968	0	0	0	0,1104	89,4281	B-A-MIS-M9-3	Magnetite
157	0,0325	0,1245	0	33,5161	0,1457	27,4186	2,2178	0	3,2622	0,6473	29,9376	97,3023	B-A-MIS-M7-8-1	Titanite
158	0,0389	0,2784	0,0445	32,0764	1,0562	26,6807	1,5429	0	4,3355	0,666	31,122	97,8415	B-A-MIS-M7-8-2	Titanite
159	0	0,2079	0,1966	28,2348	2,7325	23,302	3,47	0,0409	7,3961	0,8395	29,3339	95,7542	B-A-MIS-M7-8-3	Titanite
160	0,0121	0,3318	0,0719	31,1519	1,3768	26,3326	1,9075	0,0344	4,6701	0,9762	31,1921	98,0574	B-A-MIS-M7-8-4	Titanite
161	0,0087	0,0544	0,0273	34,0529	0,0704	28,2567	0,5598	0,0453	3,9916	1,3062	30,786	99,1593	B-A-MIS-M7-8-5	Titanite
162	0,0246	0,0077	0,5059	12,1998	0	0,0403	78,5816	0,1954	0	0,36	0	91,9153	B-A-MIS-M10-1	Magnetite
163	0	0,0059	0,2354	8,7168	0	0,0367	80,4198	0,2068	0	0,259	0	89,8804	B-A-MIS-M10-2	Magnetite
164	0	0	0,491	13,995	0,2596	0,0523	74,9063	0,2062	0,2237	0,4024	0,3552	90,8885	B-A-MIS-M10-3	Magnetite

Aubures_Mf

165	0	0	0.3338	1,3002	0	0.0889	86.1209	0,0461	0.3253	0.0935	0.2399	88.5486	B-A-MfA-M1-1	Magnetite
166	0	0,0122	0,2864	2,4641	0,1171	0,1492	85.0151	0,0397	0,3616	0,1461	0,506	89.0975	B-A-MfA-M1-2	Magnetite
167	0	0	0,219	1,32	0	0,0522	85.7623	0,0405	0,306	0,1591	0,3417	88.2008	B-A-MfA-M1-3	Magnetite
168	0	0,0186	0,5675	7,441	0,0055	0,0938	79.6192	0,0511	0,1614	0,1317	0,3341	88.4239	B-A-MfA-M1-4	Magnetite
169	0	0	0,3902	4,1291	0	0,0661	82.6348	0,0469	0,2728	0,1189	0,2683	87.9271	B-A-MfA-M1-5	Magnetite
170	0	0,0057	0,0195	0,0858	0	0,03	88.0722	0,0249	0,0003	0,071	0,1588	88.4682	B-A-MfA-M2-1	Magnetite
171	0,0218	0	0,0218	0,0856	0	0,0226	87.1048	0,0067	0,0446	0,1011	0,5162	87.9252	B-A-MfA-M2-2	Magnetite
172	0	0,0003	0,0075	0,0541	0	0,0077	88.0525	0,0642	0	0,0768	0	88.2631	B-A-MfA-M2-3	Magnetite
173	0	0,0323	0	0,0528	0,2653	0,0324	86.7303	0,0602	0,2457	0,0906	0,8892	88.3988	B-A-MfA-M2-4	Magnetite
174	0,0052	0	0,2875	4,642	0,0347	0,0751	82.9878	0,0843	0,8316	0,3383	0,322	89.6085	B-A-MfA-M3-1	Magnetite
175	0	0,0822	0,2982	4,821	0,0783	0,0499	81.9362	0,1456	0,9866	0,2344	0,8832	89.5156	B-A-MfA-M3-2	Magnetite
176	0	0,0083	0,327	7,5092	0,0422	0,0588	79.9271	0,0738	0,9343	0,3997	0,2361	89.5165	B-A-MfA-M3-3	Magnetite
177	0,0565	0,1784	0,3932	4,8732	0,3818	0,0711	80.7027	0,1331	1,6181	0,3716	1,5691	90.3378	B-A-MfA-M3-4	Magnetite
178	0,0271	0,0393	0,2577	5,756	0,0998	0,0606	81.6483	0,1236	0,9172	0,3645	0,4811	89.7752	B-A-MfA-M3-5	Magnetite
179	0,0056	0	0,0962	37.8316	0	28.1272	0,9271	0,0412	1,4226	0,7645	30.0333	99.2493	B-A-MfA-T1-1	Titanite
180	0	0,0054	0,1284	37.7183	0	28.1755	0,852	0,0074	1,3523	0,7498	30.4093	99.3984	B-A-MfA-T1-2	Titanite
181	0,0288	0,0002	0,1809	0,2182	0	0,0021	87.852	0,055	0,1458	0,2988	0,0984	88.8802	B-A-MfA-M4-1	Magnetite
182	0,0509	0	0,0864	0	0	0,0149	88.1604	0	0,1239	0,2844	0,1123	88.8332	B-A-MfA-M4-2	Magnetite
183	0	0,0048	0,1149	0,1737	0	0,0153	87.1822	0,0187	0,1081	0,3148	0,0315	87.964	B-A-MfA-M4-3	Magnetite
184	0	0	0,0663	0,1671	0	0,0209	88.5894	0,0107	0,0615	0,262	0	89.1779	B-A-MfA-M4-4	Magnetite
185	0	0	0,1004	1,1176	0	0,0608	85.7081	0,0189	0,1249	0,0492	0,2609	87.4408	B-A-MfA-M5-1	Magnetite
186	0	0,0996	0,0909	0,3679	0	0,0419	85.7374	0	0,3384	0	0,708	87.3841	B-A-MfA-M5-2	Magnetite
187	0	0,0067	0,1413	36.5537	0	28.1281	1,2939	0,0139	1,5599	0,7544	30.2835	98.7154	B-A-MfA-T2-1	Titanite
188	0	0	0,0695	36.9126	0	28.4959	1,2017	0,0139	1,5644	0,6691	30.4578	99.3849	B-A-MfA-T2-2	Titanite
189	0,0764	0	0,0778	36.1405	0	28.0959	1,3137	0	1,5655	0,7275	29.6932	97.6905	B-A-MfA-T2-3	Titanite
190	0,0194	0,188	0,147	35,025	0,1297	27,3362	2,1425	0,0404	2,0196	0,6896	30.0377	97.7751	B-A-MfA-T2-4	Titanite
191	0	0	0,0977	36.979	0	28.3052	0,9715	0,0034	1,2556	0,657	30.0683	98.3377	B-A-MfA-T2-5	Titanite
192	1,3522	0,003	0,0511	0,1523	7,7532	0,3092	3,1553	0,0413	33.2773	0	36.9426	83.0375	B-A-MfA-Tul-1	Tourmaline
193	2,1999	0,0699	0,1207	0,3652	6,7109	0,7985	7,8036	0,0403	30,5005	0,0323	35,3974	84.0392	B-A-MfA-Tul-2	Tourmaline
194	2,1481	0,0522	0,0993	0,4124	6,7089	0,7569	7,8574	0,0421	30,3719	0,049	35,4419	83,9401	B-A-MfA-Tul-3	Tourmaline
195	0	0	0,0178	36.9189	0	28.7914	1,3225	0,0351	1,2446	0,7879	30,5886	99.7068	B-A-MfA-T3-1	Titanite
196	0,0226	0,0006	0,0227	36.9809	0	28.7592	1,3689	0,1784	1,3177	0,8824	30,645	100.1784	B-A-MfA-T3-2	Titanite

197	0	0	0,005	36.7777	0	28.8341	1,5188	0,0938	1.2637	0.8267	30.625	99.9448	B-A-MfA-T3-3	Titanite
198	0.0422	0	0,073	37.2303	0,0021	28.5106	1,5245	0,0367	1.2685	0.7826	29.9231	99.3936	B-A-MfA-T3-4	Titanite
199	0	0	0,097	0,0209	0	0,0231	89.4846	0	0	0.1606	0,0047	89.7909	B-A-MfA-M6-1	Magnetite
200	0.0117	0,006	0,095	0,0789	0	0,0194	88.4475	0,0834	0	0.2647	0.4075	89.4141	B-A-MfA-M6-2	Magnetite
201	0	0	0,2337	0,207	0	0,0319	87.8262	0,0632	0,0667	0.1984	0,1656	88.7927	B-A-MfA-M6-3	Magnetite
202	0	0	0,2459	0,4722	0	0,0469	87.4358	0,0424	0,0978	0,1393	0.2732	88.7535	B-A-MfA-M6-4	Magnetite
203	0.0346	0,0022	0,1097	0,2187	0	0,0285	85.4917	2,6779	0	0.3192	0,1536	89.0361	B-A-MfA-M7-1	Magnetite
204	0	0	0,0205	0,1021	0	0,023	86.1364	2,6295	0	0.3024	0,0286	89.2425	B-A-MfA-M7-2	Magnetite
205	0.0324	0,0108	0,0954	0,1372	0	0,0272	85.4069	2,5647	0	0,298	0,0309	88.5935	B-A-MfA-M7-3	Magnetite
206	0	0,0075	0,0891	0,1018	0	0,01	86.3876	2,6536	0	0.2195	0,0889	89.558	B-A-MfA-M7-4	Magnetite
207	0,033	0,0062	0,0467	0,0776	0	0,0747	85.9844	2,4946	0	0,315	0,0337	89.0659	B-A-MfA-M7-5	Magnetite
208	0,0231	0,0383	0,0026	28.4887	1,054	22.8299	0,8565	0,021	5,3157	0,5428	33.5482	92.7208	B-A-MfA-T4-1	Titanite
209	0,0394	0,0353	0,0097	43.6156	0,4335	20.2553	0,88	0,0364	3,3743	0,8267	27.1525	96.6587	B-A-MfA-T4-2	Titanite
210	0,0029	0	0,0065	36.1333	0,1961	26.4962	0,6974	0,0057	2,8598	0,7537	31,0145	98.1661	B-A-MfA-T4-3	Titanite
211	0,0244	0,0143	0,1419	0,229	0	0,0091	87.6102	0,0763	0,3847	0,2429	0,1292	88.3662	B-A-MfA-M8-1	Magnetite
212	0	0	0,0717	0,1494	0	0,0125	88.1989	0,0266	0,2411	0,2459	0,0371	88.9832	B-A-MfA-M8-2	Magnetite
213	0	0	0,0337	0,1769	0	0,0151	87.8751	0,0186	0,2582	0,2124	0	88.59	B-A-MfA-M8-3	Magnetite
214	0	0,0214	0,0723	0,1416	0	0,0254	88.2377	0,0726	0,2988	0,1591	0,0492	89.0781	B-A-MfA-M8-4	Magnetite

Holgat Fm

No.	Na2O	K2O	MnO	TiO2	MgO	CaO	FeO	Cr2O3	Al2O3	NiO	SiO2	Total	Comment	
113	2,3405	0,0204	0,0152	0,6896	8,1506	0,7508	6,9972	0	27.9535	0	35.3608	82.2786	N-Mf-Tu1-1	add 10.5 wt% B2O3
114	1,9885	0,0455	0,0346	0,7064	6,1679	0,3858	7,2143	0	31,0761	0,0488	35.2035	82.8714	N-Mf-Tu1-2	add 10.5 wt% B2O3
115	1,8279	0,0476	0,0577	0,6867	5,1267	0,4837	7,2958	0,0619	32.4855	0,1217	35,0296	83.2248	N-Mf-Tu1-3	add 10.5 wt% B2O3
117	1,8518	0,0512	0,0218	0,8665	4,491	0,3888	8,13	0	32.9839	0	35,0703	83.8553	N-Mf-Tu2-2	add 10.5 wt% B2O3
118	1,8391	0,0381	0,0663	0,809	4,5366	0,3322	7,909	0	32,7327	0	35,1446	83.4076	N-Mf-Tu2-3	add 10.5 wt% B2O3
120	1,7752	0,025	0,0061	0,6708	6,6756	0,5217	4,6662	0,0347	33,1883	0,0963	35,9652	83.6231	N-Mf-Tu3-2	add 10.5 wt% B2O3
121	1,8183	0,0197	0,0073	0,5355	6,5824	0,5015	4,713	0,0029	33,5275	0	36,0369	83,745	N-Mf-Tu3-3	add 10.5 wt% B2O3
122	1,8211	0,0188	0,0266	0,4887	6,3217	0,4713	4,6489	0,0743	33,0344	0	35,7416	82,6474	N-Mf-Tu3-4	add 10.5 wt% B2O3
123	1,6994	0,0211	0,0153	0,2393	6,2835	0,501	5,0766	0	33,5006	0	35,9838	83,3226	N-Mf-Tu3-5	add 10.5 wt% B2O3
125	0	0,0615	0,032	99,0778	0	0,043	0,5507	0,0055	0	0	0,1337	99,9042	N-Mf-R1-2	Rutile olk
126	0,0262	0,8688	0,0972	77,3431	0,4618	0,0638	0,8892	0	2,3393	0	18,6269	100,7163	N-Mf-R1-3	rutile-quartz mix
128	1,8755	0,4432	0,058	0,7604	5,9268	0,3668	5,9171	0,0132	32,6169	0	36,2229	84,2008	N-Mf-Tu4-2	add 10.5 wt% B2O3
129	2,0692	0,0594	0	0,7942	6,5173	0,3447	6,1917	0,0682	31,8209	0	35,8359	83,7015	N-Mf-Tu4-3	add 10.5 wt% B2O3
130	1,8898	0,4233	0,0623	0,698	5,8983	0,3222	6,0514	0	32,4378	0	36,3677	84,1508	N-Mf-Tu4-4	add 10.5 wt% B2O3
131	0,0356	0,2552	0,0091	96,9047	0,0157	0,011	0,5493	0,1095	0,2418	0,0025	0,631	98,7659	N-Mf-R2-1	
132	0	0,0393	0,0097	97,6822	0	0,0091	0,8049	0,0379	0	0	0	98,5831	N-Mf-R2-2	
133	0	0,0656	0	96,2591	0	0,0032	0,6187	0,0707	0,0733	0	1,5409	98,6315	N-Mf-R2-3	

134	2.0669	0.0335	0.1102	0.4247	4.1533	0.0915	8.4671	0	32.8588	0.0158	35.8155	84.0373	N-Mf-Tu5-1	add 10.5 wt% B2O3
135	2.0096	0.0293	0.1088	0.2716	4.2015	0.0805	8.374	0	32.7868	0.1198	35.7233	83.7052	N-Mf-Tu5-2	add 10.5 wt% B2O3
136	1.9444	0.0329	0.0702	0.5858	4.4088	0.0906	8.3615	0	32.7569	0	35.6928	83.9439	N-Mf-Tu5-3	add 10.5 wt% B2O3
137	2.0247	0.0112	0.0109	0.5777	4.2623	0.0849	8.6605	0.0049	32.6528	0	35.7213	84.1031	N-Mf-Tu5-4	add 10.5 wt% B2O3
138	1.7004	0.0177	0.0043	0.9199	4.5893	0.5941	7.9916	0.0016	32.5788	0.0786	34.9601	83.4364	N-Mf-Tu6-1	add 10.5 wt% B2O3
139	1.6189	0.0375	0.0263	0.9703	4.3949	0.5193	7.807	0.0606	33.0894	0.0766	35.1541	83.7549	N-Mf-Tu6-2	add 10.5 wt% B2O3
140	1.7435	0.0307	0.0372	0.944	4.5694	0.5391	7.8771	0	33.2985	0.1075	34.546	83.693	N-Mf-Tu6-3	add 10.5 wt% B2O3
141	1.7634	0.029	0.0448	0.8838	4.6673	0.5606	7.6193	0.0227	32.9483	0.0415	34.2362	82.8201	N-Mf-Tu6-4	add 10.5 wt% B2O3
142	1.6745	0.018	0.0115	1.3333	4.9375	0.715	8.0615	0.0456	31.6825	0	35.2887	83.7716	N-Mf-Tu7-1	add 10.5 wt% B2O3
143	1.648	0.0023	0.0157	1.0392	4.9562	0.6858	7.8584	0.0459	32.4006	0	35.2107	83.8628	N-Mf-Tu7-2	add 10.5 wt% B2O3
144	1.6488	0.0064	0.0031	1.2199	5.0719	0.6981	7.8868	0.0148	32.167	0	35.3951	84.1119	N-Mf-Tu7-3	add 10.5 wt% B2O3
145	0	0	0.0352	91.9404	1.1267	0.0665	1.7225	0.0206	1.2494	0.1243	1.5823	97.868	N-Mf-R3-1	
146	0	0.5181	0.0101	91.2286	0.758	0.1189	0.9183	0.037	1.624	0	3.2891	98.5021	N-Mf-R3-2	
147	0.0032	0.0395	0	97.6675	0.447	0.0737	0.8421	0.0071	0.4383	0.0785	0.4642	100.0611	N-Mf-R3-3	
148	1.5602	0.0561	0.0064	0.8249	5.1621	1.1347	8.0861	0.1773	32.4839	0	34.3115	83.8032	N-Mf-Tu8-1	add 10.5 wt% B2O3
149	1.6294	0.0255	0.0382	0.9152	5.0749	1.1093	7.7567	0.1546	32.1786	0.0385	34.2107	83.1316	N-Mf-Tu8-2	add 10.5 wt% B2O3
150	1.5916	0.0272	0.0243	0.7752	5.0966	1.0536	8.0173	0.1774	32.2852	0.0005	34.5002	83.5356	N-Mf-Tu8-3	add 10.5 wt% B2O3
151	1.547	0.046	0.007	0.8371	5.1041	1.0707	7.8169	0.0795	32.3344	0.1146	34.6034	83.5627	N-Mf-Tu8-4	add 10.5 wt% B2O3
152	1.3907	0.0132	0.0455	0.3767	4.8336	0.6452	7.7964	0.0692	33.1725	0	35.097	83.44	N-Mf-Tu8-5	add 10.5 wt% B2O3
153	1.4236	0.03	0.0058	0.4439	4.7578	0.6524	7.8059	0.0835	32.9519	0	35.0882	83.2443	N-Mf-Tu8-6	add 10.5 wt% B2O3
154	1.8214	0.0168	0.0051	0.6645	4.5245	0.6388	8.9951	0	31.9743	0.01	35.5295	84.18	N-Mf-Tu9-1	add 10.5 wt% B2O3
155	1.7345	0.0121	0.0251	0.6402	4.6091	0.621	9.0502	0	32.2784	0	35.2656	84.2332	N-Mf-Tu9-2	add 10.5 wt% B2O3
156	1.9284	0.0322	0.0527	0.7493	4.6678	0.5437	9.47	0.0377	31.4176	0.1105	35.0224	84.0323	N-Mf-Tu9-3	add 10.5 wt% B2O3
157	1.9691	0.0366	0.0438	0.6286	5.3427	0.5712	7.7085	0.1153	32.2354	0.0446	35.197	83.8828	N-Mf-Tu10-1	add 10.5 wt% B2O3
158	1.8224	0.0557	0.0466	0.6049	6.5766	0.5818	7.5523	0.0642	31.5538	0	35.6056	84.4644	N-Mf-Tu10-2	add 10.5 wt% B2O3
159	1.9103	0.0227	0.0461	0.5995	5.5375	0.5759	7.6999	0.0372	32.4549	0	35.1893	84.0643	N-Mf-Tu10-3	add 10.5 wt% B2O3
160	1.8715	0.0521	0.0766	0.6475	5.4521	0.5675	7.8985	0.066	32.1278	0	35.061	83.8206	N-Mf-Tu10-4	add 10.5 wt% B2O3
161	0.0544	0.088	0	69.8457	0.012	0.0393	0.359	0.0104	0.2081	0	28.9026	99.5195	N-Mf-R4-1	
162	0	0.1352	0.0012	97.3102	0	0.0513	0.7217	0	0.2842	0	0.6188	99.1226	N-Mf-R4-2	
163	0	0.2561	0	89.7654	0.0277	0.0541	0.6385	0.0384	0.72	0.0986	0.6434	98.0328	N-Mf-R4-3	
164	1.6454	0.0232	0.0293	0.9084	5.7823	0.8187	6.6348	0.0276	32.3422	0	35.2477	83.4596	N-Mf-Tu11-1	add 10.5 wt% B2O3
165	1.6189	0.0121	0.0398	0.5013	5.5114	0.6036	6.7047	0.0489	33.0991	0	35.2526	83.3984	N-Mf-Tu11-2	add 10.5 wt% B2O3
166	1.6203	0.0023	0	0.6229	5.4417	0.5086	6.7493	0	32.9291	0	35.3171	83.1913	N-Mf-Tu11-3	add 10.5 wt% B2O3
167	0.0117	0.4263	0.0253	92.5012	0.4151	0.0653	0.9504	0.1177	1.4652	0.0005	2.4459	98.4246	N-Mf-R5-1	
168	0	0.2336	0	93.6697	0.5968	0.07	1.098	0.0786	1.1273	0	1.7763	98.6503	N-Mf-R5-2	
169	0.0077	0.096	0.0043	95.8654	0.343	0.2238	0.7761	0.141	0.5877	0	0.8825	98.9565	N-Mf-R5-3	
170	1.7693	0.0462	0.0143	0.8044	6.0433	0.984	7.704	0.0325	31.5004	0	34.6068	83.5052	N-Mf-Tu12-1	add 10.5 wt% B2O3
171	1.8061	0.0259	0.0118	0.705	6.0247	1.0441	7.8597	0.0683	31.41	0.0591	34.6435	83.6582	N-Mf-Tu12-2	add 10.5 wt% B2O3
172	0.0009	0	0	98.939	0	0.0541	0.5287	0.0576	0.0251	0	0	99.6054	N-Mf-R6-1	
173	0	0.0057	0	97.977	0	0.0703	0.5624	0.1647	0.0405	0	0	98.8206	N-Mf-R6-2	
174	1.8377	0.0185	0.0112	0.8497	6.3586	0.7695	6.252	0.1444	31.9206	0	35.1113	83.2735	N-Mf-Tu13-1	add 10.5 wt% B2O3
175	1.8795	0.0295	0.0199	0.9797	6.3275	0.8813	6.0813	0.1742	32.2742	0	34.785	83.4321	N-Mf-Tu13-2	add 10.5 wt% B2O3
176	1.9694	0.0264	0	1.0268	6.2005	0.8167	6.1307	0.1621	32.2352	0.041	34.9235	83.5323	N-Mf-Tu13-3	add 10.5 wt% B2O3
177	1.9518	0.0231	0.0056	0.5087	6.8848	0.9949	7.5492	0	30.8605	0	35.2315	84.0101	N-Mf-Tu14-1	add 10.5 wt% B2O3
178	1.9759	0.0423	0.0156	0.5778	6.7951	1.0601	7.577	0.0276	30.9906	0.0102	35.132	84.2074	N-Mf-Tu14-2	add 10.5 wt% B2O3
179	1.9463	0.023	0.0306	0.5211	6.8044	1.06	7.93	0	31.1073	0	35.5546	84.9773	N-Mf-Tu14-3	add 10.5 wt% B2O3

180	2.0729	0,109	0,0119	0,391	7,469	0,7883	6,7242	0,0272	30,7414	0	35,5714	83,9063	N-MfTu4-4	add 10.5 wt% B2O3
181	2.0249	0,0491	0,0081	0,5386	6,825	1,0609	7,6347	0	30,7695	0	35,0075	83,9183	N-MfTu4-5	add 10.5 wt% B2O3
182	1.8339	0,0355	0,0193	1,0539	5,3493	0,6225	7,5661	0,0606	32,7327	0,0749	35,2699	84,6196	N-MfTu5-1	add 10.5 wt% B2O3
183	1.8408	0,0362	0,0231	1,107	5,2695	0,6358	7,2166	0	32,762	0	35,065	83,956	N-MfTu5-2	add 10.5 wt% B2O3
184	1,9482	0,0087	0,0543	0,7787	5,2894	0,4627	7,8511	0,0159	32,5209	0,0938	35,6888	84,7125	N-MfTu5-3	add 10.5 wt% B2O3
186	1,6906	0,0199	0,0381	0,6912	5,1202	0,6705	7,284	0,0142	33,118	0,1138	35,2138	83,9743	N-MfTu6-1	add 10.5 wt% B2O3
187	1,8264	0,0251	0,0568	0,7531	5,248	0,6455	7,7691	0,0314	33,0668	0,104	35,558	85,0842	N-MfTu6-2	add 10.5 wt% B2O3
188	1,6994	0,0216	0,0143	0,7892	5,2455	0,6466	7,4518	0	32,9968	0	35,4974	84,3626	N-MfTu6-3	add 10.5 wt% B2O3
189	1,749	0,0539	0,0405	0,9481	5,059	0,9748	7,418	0,0021	32,5663	0	34,6726	83,4843	N-MfTu7-1	add 10.5 wt% B2O3
190	1,7441	0,0363	0,0044	1,0166	5,0848	0,9289	7,7691	0,0154	32,7756	0	34,6851	84,0603	N-MfTu7-2	add 10.5 wt% B2O3
191	2,0625	0,0316	0	0,203	5,0005	0,1685	7,0773	0	33,4667	0,0118	35,48	83,5019	N-MfTu7-3	add 10.5 wt% B2O3
192	2,0528	0,0107	0,0168	0,3176	5,1255	0,1463	6,9036	0,0262	33,2575	0,059	35,6536	83,5746	N-MfTu7-4	add 10.5 wt% B2O3
193	0,0404	0,0866	0,0351	93,5685	0,0395	0,0388	0,5926	0,0764	0,2322	0,095	4,3811	99,1862	N-MfR7-1	
194	0,0175	0,1138	0,0259	97,3999	0,0096	0,0427	0,512	0,0845	0,284	0	0,4225	98,9134	N-MfR7-2	
195	0,0004	0,0872	0,0043	94,8793	0,3311	0,0515	0,8515	0,07	0,5553	0,003	2,0316	98,8652	N-MfR7-3	